SEISMICITY AND CRUSTAL STRUCTURE STUDIES OF SOUTHERN CALIFORNIA: TECTONIC IMPLICATIONS FROM IMPROVED EARTHQUAKE LOCATIONS

Thesis by

Edward John Corbett

In Partial Fulfillment of the Requirements

for the Degree of

Doctor of Philosophy

California Institute of Technology

Pasadena, California

1984

(Submitted January 5, 1984)

Dedicated to:

Mom and Dad.

ACKNOWLEDGMENTS

First of all I would like to thank all the professors who made my education at the Caltech Seismological Laboratory possible. I am grateful to Clarence Allen for his patient guidance as my research advisor and for serving on my thesis committee. His thorough reviews and effective criticism contributed greatly to the quality of this thesis. I would like to thank Dave Harkrider for being an understanding academic advisor and for serving as chairman of my thesis committee. Carl Johnson was my mentor of sorts. He got me started in seismicity studies and was a constant source of advice along the way. Carl designed, and still oversees, the CEDAR system, which made this thesis possible, and he gave me plentiful assistance in accessing and utilizing the CEDAR data, as well as helpful reviews of my writing. I am grateful to Kerry Sieh for stimulating discussions over the years, and for serving on my thesis committee. I am especially grateful to Kerry and his wife Laurie for their support during the difficult early years at Caltech. I thank Don Helmberger for reviewing an early draft of Chapter 4, for serving on my thesis commitee, and for his reflections on refractions, synthetics, and running pass-patterns. I thank Hiroo Kanamori for continued encouragement, his insightful reviews of my work, and for serving on my thesis committee. I am grateful to Rob Clayton for the use of his VAX computer (on which this thesis was printed and which performed the data analysis for Chapter 4), as well as his patient advice on programming. I wish to thank Lee Silver for our stimulating discussions of the tectonics and structure of southern California. And I will never forget Bernard Minster for his support and encouragement during my early years at Caltech.

Secondly, I would like to thank all those at outside institutions whose effort helped me to progress. I thank Leon Teng, Tom Henyey, and John McRaney for providing data from the USC seismic network for the 1978 Santa Barbara earthquake. I am especially grateful to Ken Piper, at USC, who assisted me greatly with these data, as well as provided me with the USC data for the 1981 Santa Barbara Island earthquakes and the Catalina quarry blast. At UCSB, I would like to thank Barbara Bogaert and Bill Prothero for data regarding the UCSB seismic refraction line and critical review of Chapter 2. I am also indebted to Barry Keller for providing data from his offshore explosions, his reviews of my work, and lively geological discussions over the years. I want to thank the following individuals at the U.S. Geological Survey, Menlo Park, for their reviews, help, and encouragement: Ralph Archuleta, Rob Cockerham, Ed Cranswick, Gary Fuis, Dave Hill, Paul Spudich, and Randy White. On the island of Catalina, I would like to thank Steve Dickey for bringing the Catalina explosion to the attention of the U.S. Geological Survey. I also thank the owners and employees of the quarry for their cooperation in timing the blast.

I will always remember all of my friends from the staff and students of the Seismo Lab. Their hard work and their smiles made my education a pleasure. I am especially grateful to Tom Hearn for reviewing parts of my thesis and our many discussions of crustal structure. I thank Jim Pechmann for his review of Chapter 2 and our hours of seismological shooting-the-bull, and for field assistance, along with Ronan Le Bras, on some cold autumn nights at Mammoth. Gladys Engen and Terry Wallace provided computer programs and taught me how to make synthetics for quarry blasts, and I also thank Terry for reviews and discussions. I thank Karen McNally for her encouragement and support on my early projects, in particular on Borrego Mountain. I want to thank my "we're all in this together" compatriots at the Lab for their willingness to share their experience in seismology and programming, including John

Cipar, John Ebel, Jeff Given, Dave Hadley, Marianne Walck, and John Louie. One of our great resources is the U.S. Geological Survey staff at Caltech. I especially thank Tom Heaton, Doug Given, Chuck Koesterer, and Vic Lamanuzzi for a week of valuable field experience in Mammoth. I also thank Doug and Chuck for "catching" the Catalina quarry blast in the field. Most of the data used in this thesis were analyzed by members of the CEDAR crew and I thank them: Kate Hutton, leader, Riley Geary, Ann Blanchard, Kathy Watt, Barbara Reed, Susan Green, Peter German, Doug Given, and Gary Gutierrez. I thank Dee Page for helping with all the little details needed to keep my work moving. I thank Dorothy Coy for mothering me, and all the students, through the Caltech graduate process. I would like to thank Linda Rosenthal for typing a early draft of Chapter 2. And I am especially grateful to Elizabeth Wood for typing much of this thesis onto the VAX. Her prompt service greatly expedited my progress. I thank Laszlo Lenches for his assistance in preparing figures.

And finally, I want to thank all my friends at the Seismo Lab for being such good sports, be it at football, softball, and skiing. I thank Marianne Walck for being manager of the Tremors, and Eric Chael for being the "world's best roommate" for four years. I am especially grateful for my many friends out at UCLA, at the Newman Center, and the Sailing Club, for providing wholesome diversions from my studies, especially Jim McCauley and Dan & Lisa. For being special friends, I thank Patsy and Sharon. And last, but not least, I thank the skipper and the crew of *Cardinal Sin.*

This research was supported by:

U.S. Geological Survey contract 14-08-0001-21209,

U.S. Geological Survey contract 14-08-0001-19268,

U.S. Geological Survey contract 14-08-0001-19270,

U.S. Geological Survey contract 14-08-0001-16719,

U.S. Air Force Office of Scientific Research contract F49620-81-C-0008,

California Division of Mines and Geology agreement 5-3098.

ABSTRACT

This thesis consists of studies of: 1) the 1978 Santa Barbara earthquake and its aftershocks; 2) the depth distribution of seismicity in the Transverse Ranges; 3) crustal-velocity structure of the Continental Borderlands derived from explosion data; 4) the 1981 Santa Barbara Island earthquake and its aftershocks; and 5) earthquake location procedures, in particular the calibrated master-event technique.

The 5.1 M_L Santa Barbara earthquake of 13 August 1978 occurred at 22^h 54^m 52.8^s GMT. The epicenter was located 3 km southeast of Santa Barbara at 34° 23.9' N latitude and 119° 40.9' W longitude with a focal depth of 12.7 km. The mainshock was followed between 13 August and 30 September by 373 aftershocks that were located with the Caltech-USGS array. The aftershock zone extended 12 km west-northwest from the epicenter and was 6 km wide in the north-south direction, and it had a very clear temporal development. During the first 20 minutes of activity, all the aftershocks were located in a cluster 7 km west-northwest of the mainshock epicenter. During the next 24 hours the aftershock zone grew to 11 km in the west-northwest direction and 4 km in the north-south direction. During succeeding weeks the zone extended to 12 by 6 km. This temporal-spatial development relative to the mainshock epicenter may indicate that the initial rupture propagated 7 km unilaterally to the west-northwest, and the initial rupture plane may have been considerably smaller than that of the eventual aftershock zone. This smaller area suggests that the stress drop may have been significantly greater than that derived from the area of the final aftershock zone.

In cross-section, the aftershock hypocenters outline a nearly horizontal plane (dipping 15° or less) at 13-km depth. The mainshock focal mechanism indicates north-northeast/south-southwest compression and vertical extension. The preferred fault plane strikes N 80° W and dips 26° NNE, indicating north-over-south thrusting with a component of left-lateral movement. Focal mechanisms for 40 aftershocks also indicate compression in the general north-south direction. For most of these events, the north-dipping nodal plane dips between 7° and 45°, with most dipping 25° or more, which is significantly steeper than the plane delineated by the hypocenters themselves. These observations are consistent with a tectonic model in which much of the slip during the Santa Barbara earthquake occurred on a nearly horizontal plane. The aftershocks then might represent movement on a complex series of imbricate thrust faults that flatten into the plane of primary slip. Hence, the Santa Barbara earthquake may be taken as evidence for mid-crustal horizontal shearing in the western Transverse Ranges.

To further test the decollement hypothesis, Caltech catalog locations were reviewed to determine the depth distribution of earthquakes in the Transverse Ranges. Only events with ERH < 1 km and ERZ < 2 km were utilized. These were scrutinized further with a numerical test of location procedures to test the reliability of the Caltech catalog quality assignments. These tests confirmed location qualities within 40 km of the east-west axis of the Transverse Ranges, but cast doubt on locations to the north and south.

The bottom of the seismogenic zone is clearly deepest along the southern front of the Transverse Ranges, with the deepest earthquakes occurring in the Pt. Mugu-Malibu area and under San Gorgonio Pass. Seismic activity is noticeably shallower north and east of the San Andreas fault than it is across the fault to the southwest. The seismogenic zone is thinnest in the southern Mojave Desert and at the east end

of the Transverse Ranges. The seismicity of the western Transverse Ranges is typified by several north-dipping planar structures that correlate with the aftershock zones of recent earthquakes. The eastern Transverse Ranges are typified by ubiquitous seismicity extending from the surface down to the floor of the seismogenic zone. The San Bernardino Mountains are underlain by a well-defined bottom of the seismogenic zone that dips southward from 5-km depth under the Mojave Desert to 15-km depth where it intersects the San Andreas fault. South of the San Andreas fault, seismic activity deepens abruptly to as much as 22-km depth. The most intense seismicity is localized in the San Gorgonio Pass between the north and south branches of the San Andreas fault. This study falls short of the solving the decollement question, but it does add more intriguing evidence to the puzzle.

A large quarry explosion detonated on Catalina Island produced clear signals at stations throughout southern California. Data from near-shore and island stations were utilized to derive velocity structure by the slope-intercept method. A 5.2-km/sec layer underlain by a 6.3-km/sec refractor was typically observed in most azimuths. A 7.8-km/sec Moho refraction was observed at ranges beyond 120 km. The interpretation is that the crustal refractor is at 5.5-km depth and the Moho is at 22-km depth. The upper crustal layer is significantly faster (5.5 km/sec) and thinner (2.5 km) under Catalina Island. An early P_n arrival and possible Moho reflections observed at San Nicolas Island may constrain the Moho to be an average of 2 km shallower in the direction west from Catalina. This velocity structure was successfully used to improve the locations of the 1981 Santa Barbara Island earthquakes.

The Santa Barbara Island earthquake occurred at 15:50:50 GMT on September 4, 1981, at 30° 40.9' N and 119° 3.6' W, and registered 5.3 M_L. Aftershocks exhibited a clear northwest-southeast alignment that coincides with the northeast-facing escarpment of the submarine Santa Cruz-Catalina ridge. This alignment also

coincides with a mapped bedrock fault which is herein referred to as the Santa Cruz-Catalina fault. Focal mechanisms of the mainshock and the 3 largest aftershocks consistently show right-lateral strike slip on a northwest-trending plane, with possibly a component of dip slip. Aftershock depths show a near-vertical fault plane. The aftershock zone was initially 6 km long or less, and was concentrated southeast of the mainshock, suggesting unilateral rupture. The aftershock zone grew bilaterally to 15-km length after 24 hours to 21 km after 10 days, and to 35 km long after several months. This behavior may be interpreted in terms of an asperity model.

This seismic activity suggests strike-slip motion on the Santa Cruz-Catalina fault, with Santa Monica basin being displaced southeastward relative to points west. Structural complexities at the northwest and southeast ends of this fault suggest that the Santa Monica basin and Catalina Island are behaving as a coherent block pulling away from the Transverse Ranges, with extension at the northwest corner of the basin and compression to the south at the Catalina escarpment. Thus the Santa Monica basin may have formed as a triangular gap opening up between Peninsular Ranges blocks and the Transverse Ranges along the lines of the model of Luyendyk *et al.* (1980).

Nearly all earthquake location programs use Geiger's (1912) method of least squares. This rigorous statistical method assumes that all the data are of equal quality and the only source of error is in measuring arrival times. This is not generally true of real earthquake data, which has led to a number of attempts at improvement. One of the most common modifications is data weighting of three types: quality weighting, distance weighting, and residual weighting. Programs that use all three must be used carefully to avoid feedback between weighting routines, with residual weighting being the worst cause of feedback. Station corrections are used to correct for systematic velocity variations and permit higher precision relative locations. The two

most popular relative location methods are Joint Hypocenter Determination (JHD) and the master-event technique. The locations in Chapters 2 and 5 were performed with a modification termed the calibrated master event (CME) method. First, an intermediate-sized event is calibrated (preferably by explosion data) to achieve the best possible absolute location. Then, the residuals and hypocenter of this master event are used for establishing station delays and starting location, respectively, for relocating the seismicity of interest. Case histories of previous location attempts document the improvement attained with the CME method.

TABLE OF CONTENTS

Chapter 1

INTRODUCTION

This thesis is basically the summation of 4 different seismological studies. They all involved earthquake location as a means or as an end, and they all addressed seismological and tectonic problems of southern California.

Chapter 2 is a study of the 1978 Santa Barbara earthquake and its aftershocks, already published by Corbett and Johnson (1982). The study greatly benefited from the timely research of two other institutions. Seismologists at the University of Southern California (USC) installed four ocean-bottom seismometers in the epicentral area the day before the earthquake. Marine geophysicists at the University of California, Santa Barbara, (UCSB) ran a seismic refraction profile just south of the epicenter one month before the event. The data from these two studies yielded well-constrained, calibrated master-event locations of two months of Santa Barbara seismicity. One of the results was detailed information about the temporal development of the aftershock zone. These results raised seismological questions about asperities and stress drops, and questioned the standard practice of using the first 24 hours of aftershocks to define the rupture plane. This chapter also addressed the tectonic question of the southern California decollement suggested by others (Leon Silver, oral comm.; Hadley and Kanamori, 1978; Yeats, 1981). The aftershock zone and focal mechanisms suggested a low-angle rupture zone that may be part of this often-suggested mega-shear.

In order to evaluate further the decollement hypothesis a systematic search of the Caltech catalog was undertaken in Chapter 3. The quality of catalog locations is

highly variable and the standards are listed in Table 1-1.

Table 1-1. Event Quality in the Caltech Catalog

Quality	Maximum Errors		
	RMS (sec)	ERH (km)	ERZ (km)
A	.15	1.	2.
B	.3	2.5	5.
C	.5	5.	-
D	greater than the above		
E	ERH>90 km or fewer than 3 stations		

As indicated by the table, A-quality events are the only ones precise enough to use for conclusions that depend on earthquake depths, and hence only these quality-A events were considered. A numerical test was performed to evaluate the A-quality designation. It revealed that in the area of densest station coverage, along the axis of the Transverse Ranges, quality-A events were probably at least as reliable as the error bars indicate. Thus the A-quality catalog locations may be used for tectonic conclusions within 40 km of the 34th parallel. Ironically, the evidence for a decollement was weakest in the western Transverse Ranges. In the eastern Transverse Ranges, however, the seismogenic zone had a well defined lower limit that dips gently southward and is suggestive of structural control. The preliminary results have been informally presented (Corbett and Hearn, 1981).

The impetus of Chapters 4 and 5 was to study the Santa Barbara Island earthquakes commencing in September 1981. Interest in the offshore area had been stimulated by the Santa Barbara study in Chapter 2, and there was a (mistaken) idea of finding low-angle structures offshore. The study of the 1981 earthquakes was aided by a well-timed explosion at a quarry on Catalina in November 1981. The arrival-time data from the explosion were studied in Chapter 4. This study added new constraints to the Continental Borderland crustal structure (Corbett, 1983) and was successful in providing a velocity model appropriate for locating earthquakes in

Chapter 5.

In Chapter 5, the Santa Barbara Island earthquakes were relocated with a calibrated master event. The aftershock locations and focal mechanisms revealed that the earthquakes were the result of slip on a strike-slip fault similar to the other right-lateral faults west of the San Andreas fault. This fracture is the westernmost well-documented active fault in the southern California Continental Borderland; it is herein referred to as the Santa Cruz-Catalina fault after the name of the northwest-trending submarine ridge that it bounds. An attempt is made to interpret this fault in terms of the present tectonic environment, and a suggestion is made as to what happens at the juncture between the Transverse Ranges and Peninsular Ranges provinces.

Chapter 6 summarizes what I have learned about precise earthquake locations during the last few years. Earthquake location methods and their limitations are discussed. Some examples are given of the results of erroneous assumptions in preliminary studies that were corrected for in the improved locations presented in other chapters. Finally, the calibrated master-event method, as used in this thesis, is defined.

The research undertaken in this thesis would not have been possible but for the timely inception of the Caltech Earthquake Detection and Recording System (CEDAR) at the time I entered my studies at Caltech. In the preceding years, the timing of earthquakes was a considerable task. From the inception of the Seismological Laboratory up until the 1970's, accurate timing of earthquakes was a continual problem due to inadequate clocks, mechanical recording drums, and the limited resolution of ink and photographic records. With the improved media of film and magnetic tape, the accuracy problem was largely solved, but the timing of numerous events remained a tedious task. The digital acquisition system implemented in CEDAR removed much of

the tedium and further improved the precision of timing. One of the beauties of the CEDAR system is that all records are made on the same computer-controlled time base. Hence, earthquake locations are always possible, even when radio time-code is lost. And this also eliminated one of the other sources of error in previous systems: human measurement error. Even the highest resolution analog tape playbacks are limited by stretch in the paper, ink-line thickness, and the rectitude of rulers. The CEDAR system routinely produces data with an accuracy of .02 sec., which allows earthquake location precision of hundreds of meters, instead of kilometers. I say "precision" because the timing accuracy now greatly exceeds our knowledge of the detailed velocity structure. Nevertheless, I was able to employ these precise locations to explore tectonic and seismological questions in the detail that is really necessary for meaningful conclusions.

Chapter 2

THE SANTA BARBARA, CALIFORNIA EARTHQUAKE OF AUGUST 13, 1978

INTRODUCTION

On the afternoon of 13 August 1978, the Santa Barbara area was shaken by a magnitude 5.1 M_L earthquake which caused moderate damage. The epicenter was located just offshore, 3 km southeast of Santa Barbara, with a hypocentral depth of nearly 13 km. The event was preceded by two foreshocks and was followed by over 300 aftershocks that were locatable using the Caltech-USGS seismographic network. This earthquake has been previously studied by Lee *et al.* (1978), but their locations for the mainshock and aftershocks are systematically 4 km southwest of our locations. This discrepancy is probably due to a strong contrast between the velocity structure in the Santa Barbara Channel and that on the mainland. We feel we have successfully corrected for that factor in this study.

Two fortunate circumstances allowed us to obtain high quality locations for the mainshock and many of its aftershocks. First, University of Southern California (USC) seismologists began deploying ocean bottom seismographs (OBS) in the Santa Barbara Channel on the day before the earthquake, and four of them were in operation when the earthquake occurred (Henyey *et al.*, 1978). These stations were located almost directly above the activity and provided excellent data for controlling focal depths. Second, one month before the earthquake, a group from the University of California at Santa Barbara (UCSB) shot a seismic refraction line in the Santa Barbara

Channel (Crandall *et al.*, 1979) and the arrival times at the onshore stations allowed us to calibrate the network for the velocity gradient in the Santa Barbara region. These two data sets greatly enhanced the location accuracy of the mainshock and aftershocks, which enabled us to delineate the source mechanism involved in the Santa Barbara earthquake.

The work described in this chapter was done in conjunction with Carl E. Johnson and has been recently published as Corbett and Johnson (1982). Johnson's main contribution was in designing and running the Caltech Earthquake Detection and Recording (CEDAR) system (Johnson, 1979), which was the source of most of the data used in this study. He also produced the data tape of arrival times and first motions for the 376 earthquakes studied in this chapter. Johnson also wrote the location program that I used and gave me considerable guidance on how to use it properly and not introduce systematic biases into the locations. My contribution was to do the earthquake locations, calculate their focal mechanisms, interpret the results, and write the manuscript. My writing, of course, benefited greatly from the many suggestions by Johnson.

Geologic Setting

The Santa Barbara earthquake occurred in the western portion of the Transverse Ranges of southern California (fig. 2-1). This province is typified by geologically young mountain ranges and deep sedimentary basins that trend east-west, cutting across the northwest-southeast grain of most other geologic structures in California. The western Transverse Ranges include the Santa Ynez Mountains, located just north of Santa Barbara, the 700-m-deep Santa Barbara Channel, and the Channel Islands. The geologic structure of the western Transverse Ranges is dominated by east-trending reverse faults, such as the Santa Ynez, Red Mountain, North

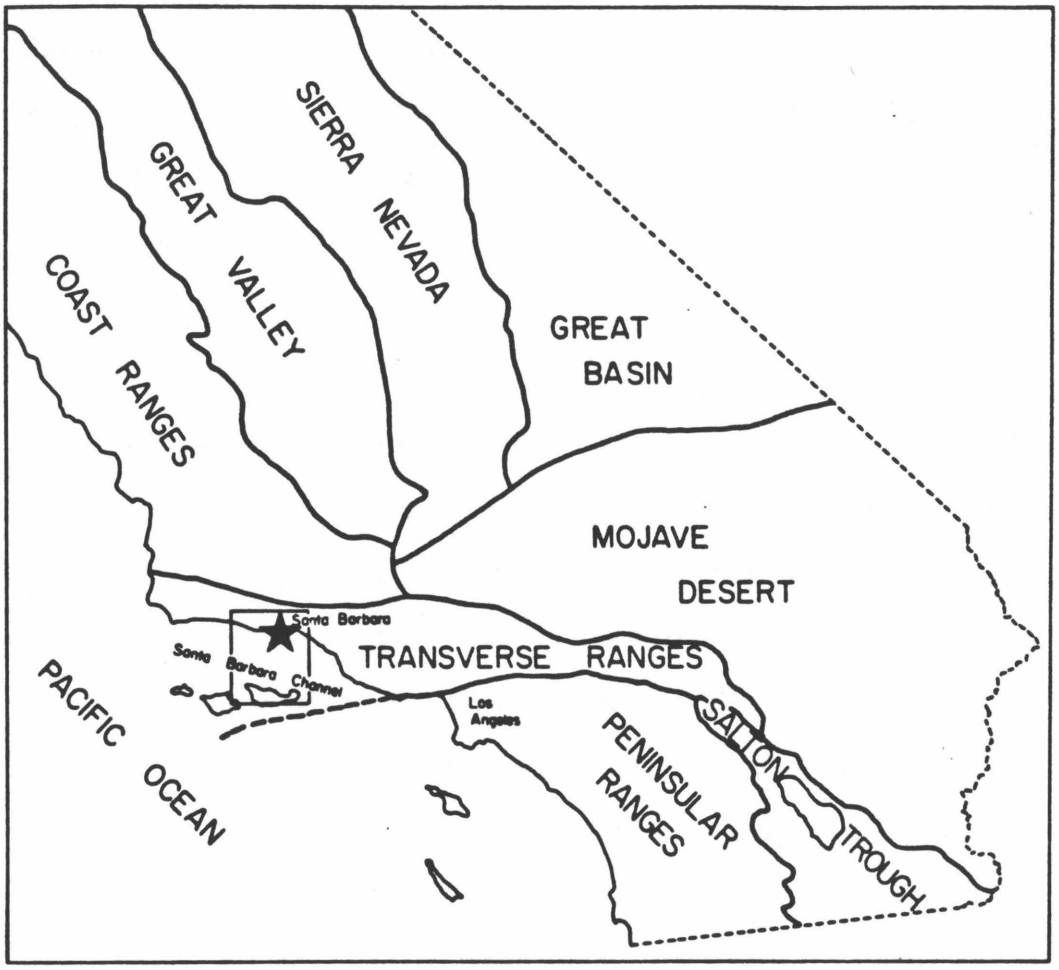

Figure 2-1. Map showing geomorphic provinces of southern California and location of Santa Barbara earthquake (star). Box outlines area of this study.

Channel Slope-Pitas Point-Ventura, Mid-Channel, and Santa Cruz Island-Anacapa Faults; all of these show signs of Quaternary activity (Yerkes *et al.*, 1980; Jennings, 1975). The recency of deformation is attested to by marine terraces, 45,000 to 2,500 years in age, which indicate local average uplift rates of 3-6 m per thousand years over this period (Yerkes and Lee, 1979). Indeed, the Santa Barbara region is tectonically a very active region, and hence the occurrence of the Santa Barbara earthquake is not surprising.

Previous Seismicity

The Santa Barbara area is typified by abundant seismicity which has been previously studied by Hamilton *et al.* (1969), Sylvester *et al.* (1970), Lee and Vedder (1973), and Lee *et al.* (1979). These previous workers have shown that the seismicity is spatially diffuse and often occurs in swarms such as that in 1968 (Sylvester *et al.*, 1970). The seismic energy release apparently occurs by thrust movements on east-striking, north-dipping faults, which is in agreement with mapped geology in the region (Vedder *et al.*, 1969; Lee *et al.*, 1979). Of recent interest is a swarm that occurred in the Santa Barbara Channel beginning in late March 1978 and continued sporadically through July 1978 (Whitcomb *et al.*, 1979). The swarm was located 25 km southeast of the August 1978 activity and was at the site of the small shock that preceded the 13 August mainshock by four hours.

VELOCITY MODEL AND LOCATION PROCEDURES

Previous Velocity Models

Previous seismicity studies (Lee and Vedder, 1973; Lee *et al.*, 1979) have used the regional crustal velocity model of Healy (1963). It consists of 3 layers over a half space and was derived for a northwest-southeast line that passed along the California coast 50 km east of Santa Barbara. The preliminary study of this earthquake (Lee, *et al.*, 1978) used a modification of this model that subdivided the upper two layers into seven layers to better approximate the velocity profile in the Santa Barbara Channel. Wallace *et al.* (1981) derived a velocity structure by inversion of the strong-motion records generated by the earthquake that was basically the same as that used by Lee *et al.* (1978). Most recently, Crandall *et al.* (1979) have determined the velocity structure of the eastern end of the Santa Barbara Channel from a seismic refraction profile. In contrast to all the above-mentioned models, they found that both the high-velocity lower crust and the Moho are 5 km shallower than has been previously observed. In addition they observed a 7-km-thick cover of low-velocity sediments. Evidently there is a dramatic change in the crustal structure between the onshore and offshore parts of the Santa Barbara region. This means that modeling the velocity structure as horizontal layers for the purpose of earthquake location computations will be, at best, difficult.

UCSB Seismic Refraction Line

Since the explosions used in the Crandall *et al.* (1979) refraction study were detectable on the Caltech-USGS network, these were the best data to test the above-mentioned velocity models. On July 16, 1978, the R.V. Ellen B. Scripps, sailing from east to west along 34° 18.5'N. latitude, fired 10 shots (locations shown in fig.

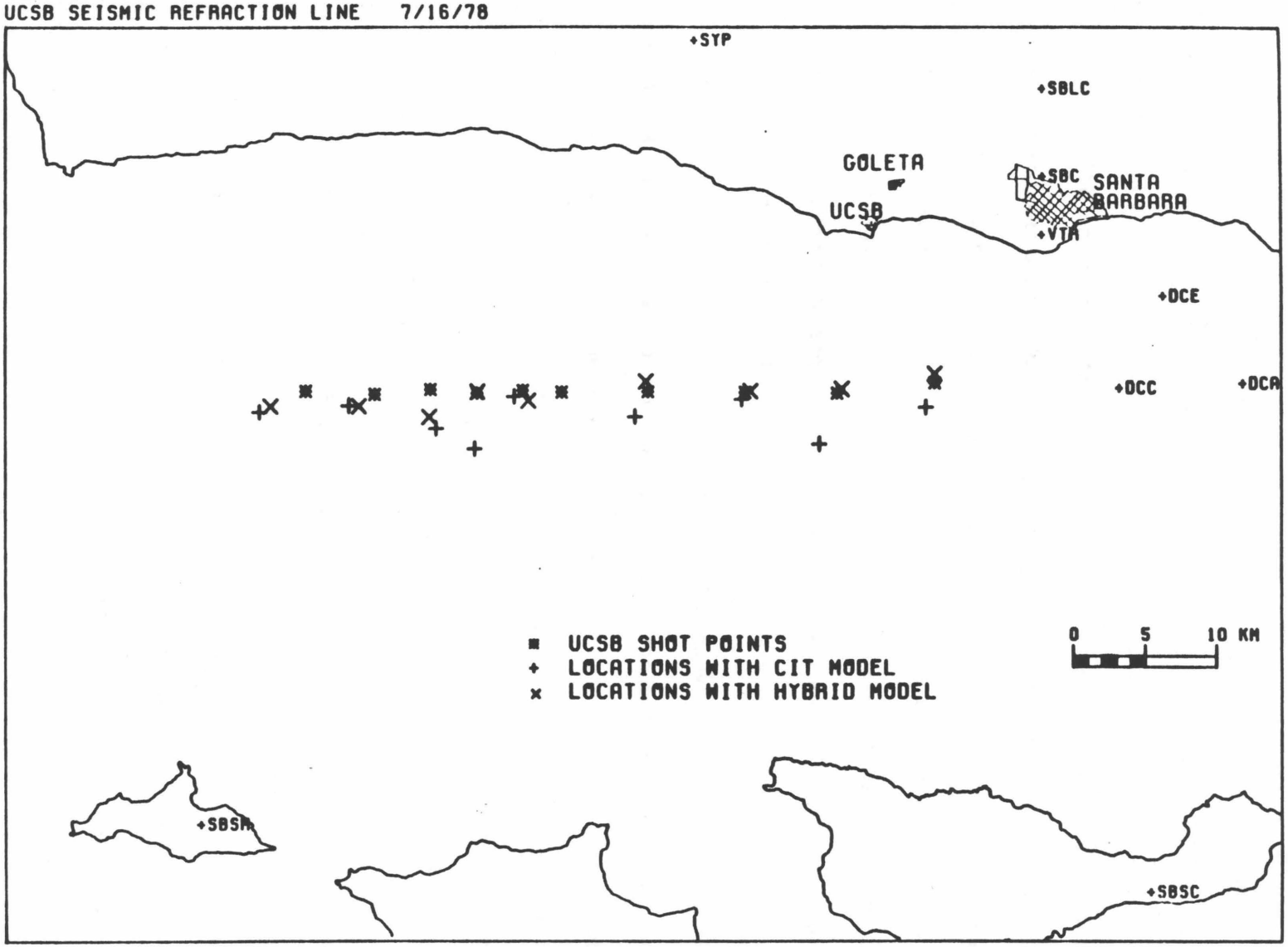

Figure 2-2. Map comparing actual locations of shot points in UCSB seismic refraction line with calculated locations using Caltech's standard southern California velocity model and hybrid model of this study.

2-2). Of these, 9 could be reread from the Caltech archive magnetic tapes. The seismograms were retimed for 17 of the closest stations, which were 25 to 150 km from the shot points. The arrivals at the quiet stations were timed to an accuracy of .02 sec. The seismograms from the noisy stations (SBSC and SBSM in particular) were filtered with a 10-Hz low pass filter which allowed the arrivals to be picked out from the noise more precisely. The filter was tested on seismograms from some of the quieter stations and it was shown that arrival times were delayed, but by not more than .04 sec. Thus, it is believed that all arrivals, even those at the noisy stations, were picked to an accuracy of .10 sec. A few S-arrivals were observed, but only rarely. Consequently only P-wave first arrivals were used in this study.

All four of the above-mentioned velocity models as well as the Caltech Southern California model were tested with this data set using the location program QED1 written by Johnson (1979). The explosions were first located using no station delays and a depth of 0.5 km (average water depth along the traverse). In general, the results were poor, with the epicenters locating 1-5 km from the given explosion locations, usually biased towards the southwest, with the mislocation problem getting worse towards the east end of the line (i.e. the area of interest). The results of using the Caltech Southern California Model are indicated by the crosses in figure 2-2. Of the 5 models, Healy's (1963) model located the explosions most accurately. It was, however, only marginally better, and gave large origin time errors (> +1 sec). Not surprisingly, the Crandall *et al.* (1979) model gave the best fit to origin times.

Next, an iterative process was used whereby station delays were determined from fixed locations. The locations and origin times of the shots were fixed to those given by UCSB, which reduced the number of useful events from nine to seven. The P-residuals for each station were considered, and the median value was taken as the P-delay for that station. These station delays were then used in a freed solution to

try and relocate the explosions. This method worked well for all velocity models, with most computed locations within 2 km of their true locations, and many within 0.5 km. Again, Healy's (1963) model relocated the explosions most accurately. However, this necessitated using large positive station delays (1-2 sec.) for 11 out of the 17 stations, indicating that this velocity profile does not adequately model the thick sedimentary pile in the eastern Santa Barbara Channel. On the other hand, the Crandall *et al.* (1979) structure appears to best model the travel times, since it requires small P-delays (< +-.15 sec.) for 4 out of the 5 stations around the perimeter of the channel. Unfortunately, this model does the poorest job of relocating the explosions, and indicates a systematic bias as one moves from east to west along the refraction line. The relocations are shifted 1.5 km to the northeast at the east end of the line, unshifted near the center, and shifted 3 km southwest at the west end of the line. This effect may come from a systematic change in velocity structure along the axis of the channel, but it could also be caused by decreasing azimuthal control towards the west. Among other things, this exercise shows the difficulty of locating events within the Santa Barbara Channel using stations outside of the channel.

Hybrid Velocity Model

Although the Crandall *et al.* (1979) velocity structure is probably the one that is most appropriate within the Santa Barbara Channel, onshore there is a much thinner cover of low-density sediments. The higher-velocity Moho and lower crust decpen rapidly, so Healy's (1963) model is probably more appropriate there. This is apparent in looking at the results of the above-mentioned attempt to fit the Crandall *et al.* (1979) model to the data. Stations beyond 70 km are required to have large positive residuals, indicating that the velocity model is too fast for the observed travel times. This discrepancy comes from the fact that the model would predict crossover to

lower crust and Moho velocities for stations beyond 70 km, which is not observed. Since these more distant stations are reached by rays that travel deeper and travel more of their path in onshore crust than offshore crust, it was deemed appropriate to use a hybrid model that consists of Healy's (1963) model in the lower crust, and of the Crandall *et al.* (1979) model in the upper crust. This model is tabulated in Table 2-1.

Table 2-1. Hybrid Velocity Model

P-wave velocity (km/sec)	Depth of top of layer (km)
1.7	0.0
2.2	0.5
3.23	1.2
4.9	3.1
6.4	7.3
7.0	16.6
8.0	26.1

Determination of Station Delays

This model was used in the manner described above to determine P-delays and to relocate the explosions. As shown in figure 2-2, the 4 events at the east end of the line were located within 0.5 km of their given locations. The other 5 appear to get more and more biased to the south and west as one moves west. P-delays obtained for this model are listed in the middle column of Table 2-2. Stations located on north and northeast azimuths, such as ABL, BCH, and SBCC still have large positive delays, which indicates that velocities of this model are still not slow enough along these azimuths. Since the area of interest, however, is at the east end of the UCSB seismic refraction line, it is felt that this model locates the explosions to satisfactory accuracy.

Table 2-2. Station Delays Relative to Hybrid Model

Station	P-delay (seconds) UCSB seismic refraction line	Master Event 2311 13 August
ABL	0.71	----
BCH	1.05	1.00
BMT	----	1.30
CAM	0.32	0.41
CRG	----	1.77
ECF	0.43	0.35
FTC	----	0.39
KYP	-1.10	-0.82
PKM	0.42	0.41
PYR	0.25	0.63
RYS	0.58	0.44
SAD	----	-0.55
SBCC	0.78	0.92
SBCD	0.84	0.25
SBLC	-0.13	0.01
SBLG	-0.08	-0.92
SBLP	-0.14	-0.24
SBSC	-0.70	-1.11
SBSM	0.02	-1.14
SIP	-0.07	-0.01
SYP	-0.12	-0.21
YEG	----	1.52
VTR	-0.09*	-0.09
DCA	0.35*	0.34
DCC	0.12*	0.09
DCE	0.06*	0.08

* delays derived from first 12 hr of aftershocks rather than UCSB seismic refraction line

This velocity model and set of station delays is a good starting model for locating the Santa Barbara earthquake sequence. It is, however, not completely appropriate because the P-delays are derived for surface shots and not for an earthquake at depth. Consequently, it was necessary to use this starting model to pick a master event, which would in turn be used to locate the mainshock and aftershocks in the manner described by Johnson and Hadley (1976).

Because the 4 USC stations (VTR, DCE, DCC, and DCA) had not yet been installed when the UCSB seismic line was run, we were not able to determine station delays for these OBS's. In trying to choose possible master events, it was observed

that the location solutions were unstable without the data from these 4 key stations, and it was not possible to evaluate which master events were better than the others. Consequently, we had to derive station delays for the 4 USC stations to use in the starting model. We did this by locating the mainshock and first 12 hours of aftershocks using the hybrid model with delays, but without letting the OBS's constrain the solution. When an appropriate starting location was used, 47 events located reasonably well (ERZ < 2 km). The OBS station residuals for these best events were reviewed, and the median values were selected as the P-delays. These are tabulated at the bottom of the second column in Table 2-2. Thus, we have a set of unconstrained P-delays for the Caltech-USGS stations around the Santa Barbara Channel and the USC stations in the channel to use as a starting model for locating the Santa Barbara activity.

Selection of Master Event

We located the mainshock and aftershocks with this model and picked A-quality and B-quality events larger than magnitude 2.5 for consideration as possible master events. This step also gave us the averages, standard deviations, and medians of the P-residuals for all of the stations. We then used this statistical information to evaluate each possible master event. From these, we selected 6 candidate master events, the mainshock and 5 aftershocks, on the criterion that they gave consistent station residuals for the most stations, including the 11 key stations in and around the channel. During this process, we observed that the residuals varied noticeably along the aftershock zone. In particular, as one moves from the mainshock location to the northwest, the residuals at SBSM and SBSC become more negative by 0.2 sec over a distance of only 6 km. This was observed for many of the possible master events and is hence believed to be systematic, further reflecting the velocity

gradient in this area. This change is sufficient to appreciably affect the earthquake locations. Experimentation with the six candidate master events revealed that using the mainshock as a master event would cause earthquake locations ~ 1 km southwest of those that would result from selecting a master event that was located at the northwest end of the aftershock zone. At this point, we picked the aftershock that occurred at 2311 GMT on 13 August as the master event, because it was the one most centrally located within the aftershock zone. We used the residuals from this aftershock as station delays, according to the master event technique (Gardner, 1964; Johnson and Hadley, 1976), and located all 376 events using the location program QED1, the hybrid velocity model (Table 2-1), and the set of P-delays indicated in the third column of Table 2-2. The calculated location parameters are listed in Table 2-3.

EARTHQUAKE LOCATIONS

Mainshock

The Santa Barbara mainshock occurred on 13 August 1978 at 22^h 54^m 52.8^s GMT. Our hypocentral location is 34° 23.9'N latitude and 119° 40.9'W longitude (fig. 2-3) with a depth of 12.7 km. Due to the problems in modeling velocity, we conservatively estimate that the epicenter and depth may both be in error by as much as 2 km. Note that this location is 6 km north-northeast of that reported by Corbett and Johnson (1978) and 4.5 km northeast of the location reported by Lee *et al.* (1978). It is in better agreement with Bogaert *et al.* (1978) and Henyey *et al.* (1978), who initially reported the epicenter to be closer to the Santa Barbara coastline.

Table 2-3 Santa Barbara Seismicity Aug-Sept 1978

YEAR	MO	DA	HR	MN	SEC	LATITUDE	LONGITUDE	DEPTH	MAG	GAP	NSTA	Q	RMS	ERH	ERZ	
1978	8	1	18	26	45.51	34 56.53	118 12.74	12.29		0	5	E	0.00	99.0	99.0	
1978	8	7	12	12	6.01	34 26.32	119 39.73	12.16	1.9	207	7	E	0.00	99.0	99.0	
1978	8	13	19	2	25.92	34 16.70	119 28.69	7.78	2.4	89	46	C	0.18	4.0	99.0	FORESHOCK?
1978	8	13	22	54	52.84	34 23.92	119 40.88	12.68	5.1	63	111	A	0.08	0.3	0.3	MAINSHOCK
1978	8	13	23	1	1.20	34 26.10	119 44.37	12.77	2.4	81	32	A	0.06	0.6	0.4	
1978	8	13	23	1	33.07	34 26.61	119 46.14	10.93		210	11	C	0.07	2.7	1.7	
1978	8	13	23	2	46.12	34 26.23	119 44.35	11.93	2.6	65	29	A	0.08	0.9	0.8	
1978	8	13	23	3	10.00	33 38.31	118 18.68	12.29		0	2	E	0.00	99.0	99.0	
1978	8	13	23	2	7.26	34 25.97	119 44.56	12.29		360	2	E	0.00	99.0	99.0	
1978	8	13	23	4	14.31	34 25.85	119 44.24	12.17		174	12	A	0.02	0.7	0.3	
1978	8	13	23	6	19.44	34 26.03	119 44.39	12.33	2.6	69	25	A	0.04	0.3	0.2	
1978	8	13	23	6	57.90	34 26.27	119 44.63	11.39	2.3	108	19	A	0.08	0.9	0.7	
1978	8	13	23	7	30.60	34 26.33	119 44.95	11.98	2.3	63	26	A	0.03	0.2	0.2	
1978	8	13	23	8	27.66	34 25.97	119 44.80	12.29	2.8	64	25	A	0.06	0.3	0.3	
1978	8	13	23	9	21.31	34 26.00	119 44.79	12.29	2.3	185	15	B	0.07	1.5	0.9	
1978	8	13	23	10	33.50	34 25.86	119 43.25	11.49	2.4	117	12	B	0.05	1.0	0.9	
1978	8	13	23	10	52.36	34 25.01	119 47.88	11.55		249	5	E	0.00	99.0	99.0	
1978	8	13	23	11	2.25	34 25.98	119 44.55	12.29	3.4	64	28	A	0.00	0.0	0.0	MASTER EVENT
1978	8	13	23	11	8.87	34 25.84	119 44.68	11.41	3.4	116	21	A	0.03	0.6	0.9	
1978	8	13	23	12	47.13	34 26.25	119 45.64	12.27		123	6	E	0.03	99.0	99.0	
1978	8	13	23	13	10.63	34 26.82	119 45.19	12.29		278	2	E	0.00	99.0	99.0	
1978	8	13	23	13	16.26	34 26.27	119 45.50	11.78		100	15	B	0.03	1.8	1.4	
1978	8	13	23	13	29.42	34 25.95	119 44.57	12.29		242	3	E	0.00	99.0	99.0	
1978	8	13	23	15	2.96	34 25.78	119 44.39	12.49	3.0	64	27	A	0.04	0.2	0.2	
1978	8	13	23	16	42.72	34 25.48	119 44.12	11.87	2.1	119	16	A	0.06	0.8	0.5	
1978	8	13	23	18	10.53	34 24.53	119 42.09	12.65	2.4	77	23	A	0.09	0.8	0.6	
1978	8	13	23	18	33.19	34 25.14	119 39.69	9.77	2.9	78	16	D	0.44	6.8	9.0	
1978	8	13	23	18	57.45	34 25.26	119 42.85	12.25	2.8	62	21	A	0.02	0.2	0.2	
1978	8	13	23	19	42.62	34 25.16	119 43.19	12.51	2.6	189	9	E	0.02	99.0	99.0	
1978	8	13	23	19	51.91	34 24.81	119 41.93	9.62		136	6	E	0.01	99.0	99.0	
1978	8	13	23	20	9.57	34 25.97	119 44.57	12.29		360	2	E	0.00	99.0	99.0	
1978	8	13	23	22	5.08	34 24.99	119 41.18	12.19		112	12	B	0.06	1.1	0.9	
1978	8	13	23	22	10.21	34 25.98	119 44.30	12.29	2.2	201	18	E	0.01	99.0	48.2	
1978	8	13	23	22	47.71	34 26.62	119 48.38	12.14	2.3	301	3	E	0.00	99.0	99.0	
1978	8	13	23	22	51.08	34 24.89	119 41.34	12.59	2.5	91	14	A	0.02	0.3	0.3	
1978	8	13	23	23	8.96	34 26.67	119 47.85	11.89	2.8	294	3	E	0.00	99.0	99.0	
1978	8	13	23	23	26.37	34 26.39	119 45.22	12.15	3.2	83	18	A	0.04	0.2	0.2	
1978	8	13	23	23	54.27	34 25.61	119 42.89	11.67	3.2	105	16	A	0.03	0.4	0.4	
1978	8	13	23	25	26.66	34 25.13	119 41.89	12.25	2.5	124	7	B	0.01	1.4	0.9	
1978	8	13	23	28	36.97	34 23.58	119 41.24	11.69	2.2	125	16	A	0.05	0.5	0.4	
1978	8	13	23	29	7.82	34 25.98	119 45.50	12.26		263	8	E	0.05	99.0	99.0	
1978	8	13	23	30	21.23	34 26.21	119 46.31	12.14	2.0	175	16	A	0.02	0.3	0.2	
1978	8	13	23	30	47.33	34 26.58	119 47.01	12.15	2.2	69	21	A	0.03	0.2	0.2	
1978	8	13	23	31	45.28	34 24.42	119 41.74	12.48	2.3	104	18	A	0.03	0.3	0.3	
1978	8	13	23	31	23.93	34 24.71	119 48.18	12.29		262	6	E	0.02	99.0	99.0	
1978	8	13	23	34	26.95	34 26.35	119 45.27	13.57	2.3	65	18	A	0.04	0.3	0.2	
1978	8	13	23	35	14.38	34 24.52	119 41.77	12.52		97	9	A	0.03	0.9	0.7	
1978	8	13	23	35	54.16	34 26.09	119 45.19	12.66	2.5	129	20	A	0.03	0.3	0.3	
1978	8	13	23	36	38.09	34 26.17	119 44.64	10.72	1.9	199	13	C	0.09	3.1	1.9	
1978	8	13	23	36	44.50	34 25.98	119 46.05	12.06	2.1	189	14	A	0.03	0.8	0.5	
1978	8	13	23	40	3.12	34 26.44	119 45.20	12.32	2.3	64	24	A	0.03	0.2	0.2	
1978	8	13	23	40	53.92	34 26.55	119 46.35	11.83		228	7	E	0.00	99.0	99.0	
1978	8	13	23	41	17.24	34 26.95	119 44.64	11.78		183	10	E	0.08	99.0	99.0	
1978	8	13	23	47	7.61	34 25.65	119 41.01	12.32	1.9	171	14	A	0.02	0.3	0.3	
1978	8	13	23	47	30.84	34 25.06	119 42.98	12.09		265	5	E	0.01	99.0	99.0	
1978	8	13	23	50	32.87	34 25.74	119 39.28	12.29	1.9	144	8	E	0.41	99.0	99.0	
1978	8	13	23	51	48.57	34 26.31	119 45.22	12.38	2.0	129	16	A	0.02	0.2	0.2	
1978	8	13	23	52	16.85	34 24.49	119 42.69	12.34	2.1	143	19	A	0.02	0.3	0.3	
1978	8	13	23	54	52.83	34 26.45	119 46.99	12.44	2.7	66	31	A	0.05	0.2	0.3	
1978	8	13	23	55	18.98	34 25.28	119 41.07	12.27	2.4	100	18	A	0.02	0.2	0.2	
1978	8	13	23	56	3.68	34 26.30	119 46.54	11.86	2.5	65	28	A	0.04	0.2	0.3	
1978	8	14	0	9	1.88	34 26.40	119 46.87	11.71	2.0	184	11	E	0.03	99.0	99.0	
1978	8	14	0	14	1.83	34 25.67	119 45.41	12.43	2.5	117	28	A	0.06	0.3	0.3	
1978	8	14	0	21	14.01	34 26.65	119 46.85	12.24	2.6	118	27	A	0.07	0.4	0.4	
1978	8	14	0	22	15.45	34 25.97	119 44.57	12.29		360	1	E	0.00	99.0	99.0	
1978	8	14	0	21	42.20	34 22.84	119 38.02	11.44		355	2	E	0.00	99.0	99.0	
1978	8	14	0	22	15.08	34 26.73	119 46.08	8.89		223	4	E	0.00	99.0	99.0	
1978	8	14	0	22	25.51	34 24.64	119 44.48	13.44	2.1	208	11	C	0.19	2.7	1.9	
1978	8	14	0	28	22.16	34 25.73	119 45.43	12.26	2.3	66	23	A	0.03	0.2	0.2	
1978	8	14	0	35	39.06	34 26.74	119 46.55	11.22	2.0	86	20	A	0.03	0.3	0.3	
1978	8	14	0	36	11.69	34 24.67	119 41.73	12.26		266	6	E	0.00	99.0	99.0	
1978	8	14	0	36	44.13	34 25.65	119 45.43	12.68	2.6	117	21	A	0.05	0.3	0.5	
1978	8	14	0	40	11.40	34 25.97	119 44.60	12.40	2.4	83	23	A	0.02	0.1	0.1	
1978	8	14	0	41	11.80	34 25.60	119 45.55	12.29		268	3	E	0.00	99.0	99.0	
1978	8	14	0	42	18.09	34 25.54	119 45.07	12.67	2.2	138	27	A	0.04	0.4	0.2	
1978	8	14	0	46	18.78	34 23.84	119 40.96	11.21	2.0	113	20	A	0.12	0.8	0.8	
1978	8	14	0	48	54.02	34 25.54	119 44.72	12.83	2.3	151	25	A	0.04	0.3	0.2	
1978	8	14	0	49	36.96	34 25.97	119 44.56	12.29		360	1	E	0.00	99.0	99.0	
1978	8	14	0	49	47.24	34 25.97	119 44.57	12.29		360	2	E	0.00	99.0	99.0	
1978	8	14	0	58	59.02	34 25.24	119 41.19	12.51	1.8	108	16	A	0.04	0.5	0.4	
1978	8	14	1	2	35.61	34 25.47	119 41.34	12.50	3.1	65	37	A	0.03	0.1	0.1	
1978	8	14	1	3	41.99	34 25.99	119 42.44	14.08	2.3	240	7	E	0.02	99.0	99.0	
1978	8	14	1	3	58.60	34 23.60	119 41.06	11.29	1.8	179	9	A	0.00	0.5	0.4	
1978	8	14	1	12	23.51	34 26.33	119 46.73	12.24	2.2	141	22	A	0.03	0.2	0.3	
1978	8	14	1	15	46.00	34 26.59	119 45.46	11.94	1.8	147	13	A	0.04	0.8	0.5	
1978	8	14	1	15	41.20	34 25.97	119 44.57	12.29		0	6	E	0.00	99.0	99.0	
1978	8	14	1	18	59.17	34 26.31	119 45.70	12.59	2.7	65	30	A	0.02	0.1	0.1	
1978	8	14	1	19	41.27	34 26.39	119 45.11	12.02	2.1	158	12	B	0.03	1.8	1.2	
1978	8	14	1	22	17.76	34 25.55	119 43.67	12.40	2.2	126	17	A	0.05	0.6	0.4	
1978	8	14	1	22	48.75	34 26.09	119 43.42	11.49		185	4	E	0.00	99.0	99.0	
1978	8	14	1	23	57.23	34 27.09	119 46.06	12.04	2.6	219	8	C	0.02	3.1	2.2	
1978	8	14	1	24	4.65	34 22.25	119 42.06	10.92	2.8	81	20	A	0.13	0.9	0.7	
1978	8	14	1	24	56.43	34 25.79	119 44.86	10.99		222	6	E	0.03	99.0	99.0	
1978	8	14	1	25	19.04	34 22.16	119 43.13	6.78		212	10	A	0.01	0.3	0.2	
1978	8	14	1	28	2.11	34 26.35	119 46.22	12.29	2.5	241	10	E	0.00	99.0	99.0	
1978	8	14	1	29	49.99	34 26.34	119 45.48	12.21	2.0	129	19	A	0.02	0.3	0.3	
1978	8	14	1	30	25.84	34 26.38	119 45.18	12.41	2.1	112	16	B	0.05	1.5	1.3	
1978	8	14	1	47	6.34	34 25.02	119 41.36	12.15	2.1	121	15	B	0.05	1.9	1.9	
1978	8	14	1	47	36.57	34 25.97	119 44.57	12.29		360	1	E	0.00	99.0	99.0	
1978	8	14	1	47	6.50	34 25.97	119 44.57	12.29		0	9	B	0.00	1.4	1.5	
1978	8	14	1	54	51.84	34 25.37	119 41.52	12.71	1.7	232	16	E	0.01	99.0	99.0	
1978	8	14	1	58	49.77	34 25.34	119 46.29	12.43	2.3	66	23	A	0.05	0.7	0.7	
1978	8	14	2	1	45.35	34 26.45	119 44.88	12.19	2.3	64	22	A	0.02	0.2	0.2	
1978	8	14	2	2	8.02	34 26.54	119 45.12	12.29	2.0	275	8	E	0.00	99.0	99.0	
1978	8	14	2	5	19.70	34 25.42	119 44.92	12.61	2.2	65	28	A	0.04	0.4	0.3	
1978	8	14	2	5	16.12	34 25.97	119 44.57	12.29	2.6	0	9	E	0.00	99.0	99.0	
1978	8	14	2	12	54.69	34 26.36	119 46.92	11.76	2.1	169	16	A	0.02	0.3	0.3	
1978	8	14	2	19	24.99	34 25.97	119 44.57	12.29		360	2	E	0.00	99.0	99.0	
1978	8	14	2	19	33.41	34 25.19	119 41.77	12.92	1.9	175	15	A	0.03	0.7	0.6	
1978	8	14	2	28	57.38	34 25.38	119 43.59	12.73	2.8	64	35	A	0.03	0.1	0.1	
1978	8	14	2	36	4.03	34 26.70	119 43.98	12.04	2.0	235	11	E	0.03	99.0	99.0	
1978	8	14	2	36	18.90	34 25.97	119 44.56	12.29		360	2	E	0.00	99.0	99.0	
1978	8	14	2	39	9.41	34 26.56	119 44.94	12.32	2.0	116	13	A	0.02	0.5	0.4	
1978	8	14	2	41	46.72	34 25.58	119 43.20	12.23	2.4	198	15	A	0.01	0.6	0.4	
1978	8	14	2	42	35.09	33 23.31	120 14.69	12.29		0	2	E	0.00	99.0	0.0	
1978	8	14	2	48	6.74	34 26.14	119 44.85	12.29	1.8	298	6	E	0.00	99.0	99.0	
1978	8	14	2	48	31.88	34 25.97	119 44.57	12.29		360	1	E	0.00	99.0	99.0	
1978	8	14	2	58	54.06	34 25.28	119 46.03	12.07	2.4	196	12	E	0.01	99.0	99.0	
1978	8	14	2	59	21.17	34 26.13	119 46.07	9.40	1.7	282	5	E	0.00	99.0	99.0	
1978	8	14	2	59	45.23	34 25.97	119 44.57	12.29		360	1	E	0.00	99.0	99.0	
1978	8	14	3	15	56.30	34 25.97	119 44.57	12.29		360	2	E	0.00	99.0	99.0	
1978	8	14	3	27	37.30	34 23.22	119 41.91	13.15	2.3	236	8	E	0.01	99.0	99.0	
1978	8	14	3	33	59.25	34 25.93	119 44.57	12.29	2.0	267	10	E	0.02	99.0	99.0	
1978	8	14	3	35	34.50	34 25.87	119 43.81	12.29	1.8	118	14	E	0.03	99.0	99.0	
1978	8	14	3	42	53.79	34 26.36	119 46.10	12.03	1.9	116	18	A	0.02	1.0	0.7	
1978	8	14	3	43	22.85	34 25.97	119 44.57	12.29		360	2	E	0.00	99.0	99.0	

Table 2-3 Santa Barbara Seismicity Aug-Sept 1978

YEAR	MO	DA	HR	MN	SEC	LATITUDE	LONGITUDE	DEPTH	MAG	GAP	NSTA	Q	RMS	ERH	ERZ
1978	8	14	3	43	28.13	34 25.97	119 44.56	12.29		360	1	E	0.00	99.0	99.0
1978	8	14	4	0	53.37	34 25.28	119 42.78	12.86	2.7	53	49	A	0.03	0.1	0.1
1978	8	14	4	9	11.86	34 26.11	119 44.97	12.55	1.7	238	13	E	0.03	99.0	99.0
1978	8	14	4	13	48.90	34 23.27	119 41.58	11.29	2.1	235	11	A	0.01	0.6	0.7
1978	8	14	4	14	6.09	34 26.22	119 47.34	12.06		346	3	E	0.00	99.0	99.0
1978	8	14	5	9	40.98	34 25.28	119 42.60	12.78	2.4	54	32	A	0.03	0.2	0.2
1978	8	14	5	22	42.51	34 25.09	119 41.89	12.38	2.8	61	36	A	0.04	0.2	0.2
1978	8	14	6	17	21.93	34 25.42	119 43.80	12.50	1.6	237	12	E	0.01	99.0	99.0
1978	8	14	6	33	27.23	34 25.79	119 42.55	12.29	2.4	57	29	A	0.04	0.2	0.2
1978	8	14	7	1	19.21	34 25.89	119 43.50	7.67	2.5	113	24	A	0.06	0.3	0.5
1978	8	14	7	3	15.84	34 25.59	119 43.46	12.52	2.5	63	28	A	0.04	0.2	0.2
1978	8	14	7	9	3.18	34 26.51	119 44.25	12.44	1.7	173	9	E	0.02	99.0	99.0
1978	8	14	7	45	51.14	34 26.26	119 46.32	12.29	2.5	65	24	A	0.03	0.2	0.2
1978	8	14	7	47	55.27	34 26.83	119 45.41	13.10	2.3	63	29	A	0.02	0.2	0.2
1978	8	14	7	54	53.30	34 26.14	119 45.93	12.29	2.3	67	30	A	0.03	0.2	0.3
1978	8	14	7	55	31.88	34 25.97	119 44.56	12.29		360	4	E	0.00	99.0	99.0
1978	8	14	8	31	20.90	34 26.09	119 45.49	11.58	2.0	183	15	A	0.03	0.4	0.3
1978	8	14	8	46	51.92	34 26.43	119 45.44	10.54	2.9	64	56	A	0.05	0.2	0.3
1978	8	14	9	32	28.43	34 25.23	119 42.71	12.33	2.3	63	27	A	0.03	0.2	0.2
1978	8	14	9	52	56.29	34 26.09	119 46.90	11.90	1.9	116	17	A	0.04	0.5	0.7
1978	8	14	10	14	6.10	34 26.54	119 46.84	11.96	1.9	116	14	A	0.04	0.4	0.5
1978	8	14	10	22	25.34	34 26.23	119 45.95	12.27		183	11	B	0.02	1.7	1.5
1978	8	14	10	22	29.59	34 25.99	119 47.85	13.95	2.0	189	20	A	0.03	0.9	0.9
1978	8	14	10	22	26.02	34 25.97	119 44.57	12.29		0	11	A	0.00	0.3	0.7
1978	8	14	10	25	13.12	34 25.71	119 44.16	12.48	2.3	64	31	A	0.06	0.5	0.6
1978	8	14	10	41	21.72	34 27.58	119 47.97	10.43	1.8	112	12	B	0.08	1.1	1.6
1978	8	14	10	54	1.75	34 26.41	119 46.22	11.84	1.9	131	20	A	0.02	0.2	0.2
1978	8	14	11	21	54.55	34 26.44	119 45.07	11.99	2.3	63	28	A	0.03	0.2	0.2
1978	8	14	12	24	34.55	34 17.43	119 42.78	11.73	1.7	140	17	C	0.19	3.4	3.6
1978	8	14	12	25	2.36	34 25.97	119 44.57	12.29		360	2	E	0.00	99.0	99.0
1978	8	14	12	43	10.63	34 26.36	119 45.28	12.18	1.9	116	18	A	0.02	0.2	0.2
1978	8	14	12	45	33.41	34 25.79	119 45.77	12.86	1.8	170	18	A	0.02	0.3	0.3
1978	8	14	12	53	42.66	34 25.60	119 44.21	12.34	2.7	64	42	A	0.06	0.3	0.3
1978	8	14	12	53	28.20	34 26.04	119 44.04	12.72	2.6	117	20	A	0.04	0.6	0.6
1978	8	14	13	20	31.71	34 26.51	119 43.35	13.20	2.0	116	14	A	0.04	0.6	0.6
1978	8	14	13	34	35.67	34 26.02	119 42.99	12.51	2.0	118	18	A	0.05	0.6	0.6
1978	8	14	13	58	5.30	34 26.45	119 45.39	12.24	1.9	123	11	A	0.02	0.5	0.5
1978	8	14	14	33	17.26	34 25.30	119 42.63	12.70	2.0	63	18	A	0.04	0.4	0.5
1978	8	14	15	10	11.72	34 27.21	119 38.23	11.96		341	2	E	0.00	99.0	99.0
1978	8	14	15	10	13.08	34 25.91	119 45.33	13.37	2.2	113	21	A	0.05	0.8	0.8
1978	8	14	15	10	53.30	34 25.97	119 44.56	12.29	1.9	360	2	E	0.00	99.0	99.0
1978	8	14	15	31	52.68	34 26.50	119 45.89	11.81	1.9	142	12	E	0.01	99.0	99.0
1978	8	14	15	37	21.50	34 26.37	119 44.76	12.67	2.1	180	15	E	0.01	99.0	99.0
1978	8	14	16	9	0.89	34 27.14	119 45.86	11.94		239	5	E	0.00	99.0	99.0
1978	8	14	16	9	47.10	33 20.79	119 48.91	12.29		0	3	E	0.00	99.0	0.0
1978	8	14	16	9	52.71	34 27.21	119 45.47	12.29		285	2	E	0.00	99.0	99.0
1978	8	14	16	11	38.51	34 25.97	119 44.57	12.29		360	1	E	0.00	99.0	99.0
1978	8	14	16	55	1.24	34 20.94	119 48.84	13.22	2.5	78	25	A	0.10	0.6	1.0
1978	8	14	17	3	58.95	34 26.34	119 43.48	14.64	2.2	118	7	E	0.03	99.0	99.0
1978	8	14	17	4	10.61	34 26.51	119 44.86	12.23	2.3	116	21	A	0.02	0.4	0.2
1978	8	14	17	21	31.99	34 26.75	119 43.68	9.63	2.3	116	16	A	0.03	0.5	0.5
1978	8	14	17	26	57.59	34 22.07	119 49.02	10.45	2.4	120	23	B	0.15	1.6	2.8
1978	8	14	17	27	35.08	34 25.78	119 43.83	12.56	2.2	64	18	A	0.06	0.8	0.8
1978	8	14	18	35	39.57	34 26.28	119 45.83	12.06	1.7	183	13	A	0.01	0.6	0.5
1978	8	14	19	0	3.00	34 26.34	119 46.32	11.99	2.1	65	23	A	0.02	0.3	0.3
1978	8	14	19	0	44.87	34 25.97	119 44.56	12.29		360	2	E	0.00	99.0	99.0
1978	8	14	19	34	53.71	34 25.77	119 43.41	12.30	1.6	180	9	E	0.02	99.0	99.0
1978	8	14	19	35	27.30	34 25.97	119 44.56	12.29		360	1	E	0.00	99.0	99.0
1978	8	14	19	34	53.06	34 25.97	119 44.57	12.29		0	2	E	0.00	99.0	99.0
1978	8	14	19	50	54.39	34 25.97	119 44.57	12.29		360	2	E	0.00	99.0	99.0
1978	8	14	20	22	52.77	34 25.97	119 43.25	12.39	1.9	118	14	B	0.03	1.2	0.8
1978	8	14	20	25	44.94	34 26.08	119 45.75	12.29		335	3	E	0.00	99.0	99.0
1978	8	14	20	25	53.85	34 25.97	119 44.57	12.29		360	2	E	0.00	99.0	99.0
1978	8	14	20	26	5.50	34 25.97	119 44.57	12.29		360	2	E	0.00	99.0	99.0
1978	8	14	21	5	31.73	34 25.37	119 43.86	12.33	1.7	178	12	E	0.02	99.0	99.0
1978	8	14	21	5	56.55	34 20.03	119 48.96	12.24		219	7	E	0.18	99.0	99.0
1978	8	14	21	13	10.83	34 26.44	119 47.03	11.65	1.7	184	11	E	0.01	99.0	99.0
1978	8	14	21	13	32.94	34 25.97	119 44.56	12.29		360	2	E	0.00	99.0	99.0
1978	8	14	23	58	33.58	34 26.42	119 45.11	12.29		324	5	E	0.00	99.0	99.0
1978	8	15	0	22	59.36	34 25.97	119 44.56	12.29		360	1	E	0.00	99.0	9.4
1978	8	15	0	32	39.96	34 25.97	119 44.57	12.29		360	2	E	0.00	99.0	99.0
1978	8	15	1	18	36.01	34 27.38	119 47.18	12.55	2.1	242	12	B	0.02	1.6	0.7
1978	8	15	1	19	34.04	34 26.29	119 44.76	12.31	2.1	265	5	E	0.01	99.0	99.0
1978	8	15	2	28	18.47	34 25.41	119 42.64	12.12	2.1	114	14	A	0.03	0.6	0.5
1978	8	15	4	26	9.24	34 21.45	119 48.50	7.50	1.8	155	12	E	0.06	99.0	99.0
1978	8	15	4	37	13.77	34 22.12	119 49.44	8.26	2.3	120	17	D	0.19	9.8	99.0
1978	8	15	4	37	48.96	34 21.54	119 47.37	10.92	2.2	127	11	E	0.10	99.0	99.0
1978	8	15	5	40	17.05	34 25.60	119 41.05	12.54	2.2	106	16	A	0.02	0.6	0.5
1978	8	15	6	25	57.86	34 21.65	119 48.67	12.88	2.4	122	22	A	0.10	0.8	1.0
1978	8	15	7	0	52.50	34 25.97	119 44.57	12.29		360	2	E	0.00	99.0	9.4
1978	8	15	8	14	11.65	34 26.17	119 44.06	12.70	1.7	119	15	B	0.04	1.9	1.5
1978	8	15	9	58	32.54	34 26.09	119 45.48	12.56	2.4	64	36	A	0.03	0.2	0.2
1978	8	15	12	9	25.56	34 25.77	119 43.95	12.29	2.1	114	15	E	0.03	99.0	99.0
1978	8	15	13	7	56.57	34 25.97	119 44.56	12.29		360	2	E	0.00	99.0	99.0
1978	8	15	15	52	46.23	34 26.16	119 44.99	12.42	2.2	64	18	A	0.02	0.1	0.1
1978	8	15	17	16	43.35	34 25.28	119 42.80	12.44	2.2	90	21	A	0.02	0.2	0.2
1978	8	15	18	48	31.34	34 25.68	119 44.48	12.29		316	7	E	0.06	99.0	99.0
1978	8	15	19	1	42.96	34 21.54	119 48.52	12.35	2.2	155	8	E	0.01	99.0	99.0
1978	8	15	19	1	40.66	34 25.97	119 44.57	12.29		0	8	E	0.00	99.0	99.0
1978	8	16	0	39	34.23	34 25.53	119 43.81	12.33	2.2	81	20	A	0.06	0.6	0.5
1978	8	16	1	47	4.02	34 26.09	119 43.53	12.36	1.7	118	9	E	0.02	99.0	99.0
1978	8	16	1	57	12.77	34 25.87	119 43.46	12.59	2.0	235	9	E	0.02	99.0	99.0
1978	8	16	4	24	29.85	34 23.49	119 41.47	12.17	2.2	127	22	A	0.06	0.8	1.1
1978	8	16	5	31	6.88	34 17.14	119 41.94	12.29	2.5	77	26	B	0.17	1.0	1.1
1978	8	16	7	43	35.34	34 26.33	119 44.98	12.37	2.0	116	15	A	0.02	0.3	0.3
1978	8	16	8	10	54.15	34 21.64	119 47.63	8.47	2.0	146	12	E	0.07	99.0	99.0
1978	8	16	8	57	57.63	34 21.04	119 47.90	8.77	2.2	149	15	D	0.05	7.1	99.0
1978	8	16	9	57	28.85	34 23.24	119 41.44	11.29	2.2	65	25	A	0.09	0.6	0.6
1978	8	16	10	43	37.90	34 25.89	119 43.63	12.66	1.9	113	20	B	0.06	1.2	1.1
1978	8	16	10	55	17.20	34 26.61	119 44.13	13.55	1.9	117	18	A	0.02	0.6	0.4
1978	8	16	11	40	28.44	34 25.51	119 43.85	12.43	2.7	64	52	A	0.04	0.3	0.2
1978	8	16	12	45	13.97	34 22.99	119 42.21	12.11		237	7	E	0.02	99.0	99.0
1978	8	16	13	35	12.09	34 26.35	119 46.30	12.51	3.3	65	44	A	0.04	0.2	0.2
1978	8	16	13	36	10.80	34 27.57	119 45.72	12.29	2.5	291	4	E	0.00	99.0	99.0
1978	8	16	15	36	58.50	34 26.39	119 44.30	12.29	2.3	130	8	E	0.02	99.0	99.0
1978	8	16	19	12	39.85	34 26.08	119 43.84	12.29	1.7	220	5	E	0.00	99.0	99.0
1978	8	16	21	45	13.87	34 25.97	119 44.56	12.29		360	2	E	0.00	99.0	9.4
1978	8	17	2	0	9.47	34 26.90	119 42.25	10.92	2.2	259	10	E	0.01	99.0	99.0
1978	8	17	2	58	6.42	34 26.19	119 47.41	13.38	2.6	66	31	A	0.06	0.3	0.3
1978	8	17	4	48	25.94	34 25.54	119 43.37	12.29	1.8	235	18	A	0.01	0.5	0.3
1978	8	17	8	44	4.01	34 25.97	119 44.57	12.29		360	2	E	0.00	99.0	99.0
1978	8	17	8	53	37.33	34 23.34	119 41.81	11.65	2.0	129	19	A	0.04	0.9	1.0
1978	8	17	11	40	5.87	34 26.15	119 44.37	9.73	1.7	180	11	A	0.01	0.5	0.5
1978	8	17	12	52	8.65	34 25.47	119 44.28	12.42	2.4	128	28	A	0.02	0.1	0.1
1978	8	17	15	57	42.96	34 26.78	119 45.93	12.29		312	4	E	0.00	99.0	99.0
1978	8	17	18	2	46.66	34 26.05	119 44.67	11.94	2.1	86	16	E	0.04	99.0	99.0
1978	8	17	18	30	27.00	34 25.96	119 44.92	11.80	2.0	129	11	E	0.01	99.0	99.0
1978	8	17	19	32	3.99	34 25.13	119 42.43	11.93	2.2	181	7	E	0.00	99.0	99.0
1978	8	17	21	40	6.36	34 26.74	119 44.55	12.29		216	3	E	0.00	99.0	99.0
1978	8	17	21	52	59.51	34 25.08	119 44.58	12.03	2.0	185	16	E	0.01	99.0	99.0
1978	8	17	21	53	35.07	34 25.97	119 44.56	12.29		360	1	E	0.00	99.0	99.0
1978	8	17	23	28	15.36	34 24.66	119 41.40	11.74	2.2	122	18	A	0.03	0.6	0.7
1978	8	18	0	31	13.48	34 26.31	119 44.58	12.02	1.8	237	11	E	0.01	99.0	99.0
1978	8	18	1	55	6.49	34 26.38	119 45.99	12.51	2.2	67	20	A	0.03	0.2	0.2
1978	8	18	2	24	22.30	34 26.67	119 44.58	12.83	2.2	79	15	A	0.05	0.6	0.6
1978	8	18	2	24	40.79	34 25.97	119 44.57	12.29	2.0	360	8	E	0.00	99.0	99.0

Table 2-3 Santa Barbara Seismicity Aug-Sept 1978

YEAR	MO	DA	HR	MN	SEC	LATITUDE	LONGITUDE	DEPTH	MAG	GAP	NSTA	Q	RMS	ERH	ERZ
1978	8	18	2	52	50.72	34 26.03	119 43.67	12.47	1.8	124	10	B	0.02	1.1	0.8
1978	8	18	7	18	51.79	34 25.88	119 44.00	12.58	2.2	81	28	A	0.03	0.2	0.2
1978	8	18	8	16	34.57	34 26.24	119 43.71	12.45	1.8	124	18	B	0.05	1.0	0.8
1978	8	18	8	53	46.02	34 26.15	119 45.67	12.18	1.8	178	16	B	0.02	1.0	0.8
1978	8	18	11	17	5.99	34 26.01	119 43.76	12.26	1.7	118	15	C	0.09	3.0	2.7
1978	8	18	11	54	51.03	34 26.29	119 46.09	12.06	2.1	117	16	A	0.02	0.3	0.3
1978	8	18	13	20	59.67	34 26.15	119 44.51	12.75	1.9	149	10	E	0.01	99.0	99.0
1978	8	18	16	12	49.52	34 26.22	119 47.36	12.01	2.3	66	19	A	0.03	0.3	0.4
1978	8	18	18	40	1.62	34 25.90	119 43.63	12.16	2.3	113	16	A	0.02	0.8	0.6
1978	8	18	22	17	58.84	34 25.60	119 44.21	12.34	1.9	183	11	B	0.03	2.0	1.5
1978	8	18	23	37	7.72	34 25.99	119 45.08	12.53	1.9	183	16	B	0.06	1.8	1.1
1978	8	18	23	37	1.10	34 25.97	119 44.57	12.29	1.7	0	6	E	0.00	99.0	99.0
1978	8	18	23	37	41.82	34 25.97	119 44.57	12.29		360	1	E	0.00	99.0	99.0
1978	8	19	0	0	30.10	34 26.51	119 45.63	12.12	2.2	116	15	E	0.04	99.0	99.0
1978	8	19	1	52	31.43	34 27.19	119 46.12	12.78	1.8	178	10	E	0.01	99.0	99.0
1978	8	19	14	59	42.60	34 25.97	119 44.57	12.29		360	2	E	0.00	99.0	99.0
1978	8	19	14	59	40.98	35 49.86	119 17.57	12.29	2.3	360	17	E	0.00	99.0	99.0
1978	8	19	16	17	35.86	34 25.22	119 42.71	12.22	2.0	113	16	A	0.02	0.3	0.3
1978	8	19	22	22	28.54	34 26.00	119 44.84	12.36	1.8	185	10	E	0.02	99.0	99.0
1978	8	19	22	49	0.84	34 25.84	119 43.06	12.22	1.7	235	12	E	0.01	99.0	99.0
1978	8	19	22	56	22.85	34 25.61	119 43.85	12.87	1.8	237	12	E	0.01	99.0	99.0
1978	8	20	2	9	58.34	34 26.27	119 46.60	12.06	2.3	116	25	A	0.02	0.4	0.4
1978	8	20	4	4	52.87	34 25.73	119 43.72	12.69	2.1	181	15	A	0.02	0.9	0.6
1978	8	20	13	14	55.54	34 25.16	119 42.76	12.12	2.2	63	25	A	0.03	0.3	0.3
1978	8	20	16	20	58.59	34 25.50	119 46.56	11.98	1.9	118	18	B	0.04	1.3	1.6
1978	8	20	20	15	46.47	34 25.68	119 44.43	12.57	3.1	65	37	A	0.04	0.2	0.2
1978	8	20	23	21	53.30	34 25.81	119 44.31	12.35	1.8	182	16	B	0.01	1.1	0.8
1978	8	21	0	4	52.37	34 24.79	119 43.07	12.68	1.9	128	14	E	0.02	99.0	99.0
1978	8	21	0	6	37.84	34 25.20	119 42.81	12.49	1.8	185	10	E	0.02	99.0	99.0
1978	8	21	7	34	7.30	34 26.11	119 47.22	11.93	1.9	186	13	E	0.01	99.0	99.0
1978	8	21	7	41	19.28	34 26.21	119 47.32	12.23	2.6	66	35	A	0.04	0.3	0.4
1978	8	21	8	10	7.53	34 26.34	119 46.38	12.01	1.8	184	15	E	0.01	99.0	99.0
1978	8	21	13	32	36.57	34 25.42	119 42.00	12.99	1.9	115	18	A	0.04	0.6	0.6
1978	8	21	17	17	57.51	34 25.88	119 43.61	12.50	1.8	118	13	E	0.01	99.0	99.0
1978	8	21	18	56	29.86	34 21.30	119 48.15	8.86	2.1	155	14	E	0.03	99.0	99.0
1978	8	21	19	23	5.29	34 21.42	119 48.83	13.77	2.0	127	6	E	0.01	99.0	99.0
1978	8	21	19	37	18.17	34 20.94	119 34.55	13.64		265	5	E	0.00	99.0	99.0
1978	8	21	22	54	2.73	34 21.56	119 48.40	9.83	2.1	155	11	E	0.05	99.0	99.0
1978	8	22	3	28	12.98	34 27.47	119 46.38	12.84	1.7	177	14	E	0.02	99.0	99.0
1978	8	22	5	16	18.91	34 25.01	119 43.22	12.67	1.5	236	10	E	0.00	99.0	99.0
1978	8	22	17	32	23.11	34 25.41	119 48.49	11.74	2.1	255	12	E	0.02	99.0	99.0
1978	8	22	22	17	2.84	34 25.97	119 44.56	12.29		360	2	E	0.00	99.0	99.0
1978	8	23	4	25	10.00	34 26.67	119 44.02	7.26	2.0	176	13	B	0.03	1.4	0.7
1978	8	23	9	59	1.22	34 25.87	119 44.50	12.58	2.3	64	25	A	0.03	0.4	0.4
1978	8	23	13	25	32.19	34 26.18	119 45.88	12.08	2.4	65	18	A	0.03	0.3	0.4
1978	8	23	13	26	9.44	34 26.07	119 45.79	11.90	2.1	65	15	A	0.03	0.5	0.5
1978	8	23	14	29	17.46	34 25.97	119 44.57	12.29		360	1	E	0.00	99.0	99.0
1978	8	23	14	29	37.19	34 25.88	119 45.21	12.29		270	3	E	0.00	99.0	99.0
1978	8	23	16	17	11.65	34 28.13	119 44.14	13.18	1.9	139	9	E	0.01	99.0	99.0
1978	8	23	23	44	6.42	34 27.10	119 41.40	12.29	1.9	230	10	E	0.00	99.0	99.0
1978	8	24	0	17	13.14	34 27.74	119 46.75	12.49	2.3	64	22	A	0.05	0.5	0.5
1978	8	24	2	29	51.84	34 25.97	119 44.57	12.29		360	1	E	0.00	99.0	99.0
1978	8	24	2	36	56.67	34 26.17	119 45.59	12.40	2.4	66	23	A	0.02	0.2	0.2
1978	8	24	13	37	31.42	34 26.81	119 44.55	13.33	2.1	116	13	B	0.04	1.1	0.9
1978	8	25	5	37	7.22	34 26.06	119 47.35	11.94	2.0	187	7	E	0.01	99.0	99.0
1978	8	25	9	27	57.95	34 25.36	119 44.18	12.36	1.9	183	11	E	0.02	99.0	99.0
1978	8	25	12	20	43.61	34 28.79	119 52.85	11.73	2.1	130	11	E	0.06	99.0	99.0
1978	8	25	17	43	27.23	34 26.83	119 45.93	13.93	2.0	124	8	E	0.01	99.0	99.0
1978	8	26	3	40	53.03	34 26.12	119 44.15	12.71	1.8	262	13	E	0.02	99.0	99.0
1978	8	26	16	26	38.42	34 26.86	119 46.37	13.09	2.7	64	27	A	0.05	0.4	0.4
1978	8	26	23	38	49.16	34 21.79	119 43.46	6.94	1.7	251	14	E	0.06	99.0	99.0
1978	8	28	0	44	37.06	34 22.46	119 40.83	13.01	2.1	235	11	E	0.03	99.0	99.0
1978	8	28	2	47	53.60	34 27.64	119 45.90	12.42	1.7	238	7	E	0.01	99.0	99.0
1978	8	28	8	39	49.36	34 22.81	119 42.14	11.64	1.9	237	11	E	0.02	99.0	99.0
1978	8	28	9	33	1.38	34 25.76	119 43.41	12.45	2.3	113	24	A	0.03	0.3	0.3
1978	8	28	22	58	21.82	34 26.92	119 47.01	12.72	1.9	190	8	E	0.02	99.0	99.0
1978	8	29	3	18	53.65	34 25.32	119 42.56	12.38	2.1	175	18	A	0.04	0.5	0.5
1978	8	29	3	57	49.81	34 27.32	119 46.31	12.50	1.7	178	9	E	0.02	99.0	99.0
1978	8	29	5	47	9.77	34 25.47	119 44.42	12.51	2.0	179	13	B	0.03	1.8	1.6
1978	8	29	6	4	49.06	34 26.34	119 44.70	13.89	2.8	64	34	A	0.04	0.3	0.3
1978	8	29	8	46	39.58	34 26.27	119 43.71	7.39	2.1	117	15	D	0.06	9.4	99.0
1978	8	29	10	51	45.33	34 26.98	119 47.11	13.66	2.6	114	22	A	0.03	0.3	0.3
1978	8	29	15	28	57.05	34 26.94	119 45.65	13.00	2.0	239	7	E	0.02	99.0	99.0
1978	8	29	17	20	54.12	34 26.88	119 40.98	12.36	1.9	171	12	E	0.03	99.0	99.0
1978	8	29	19	3	58.44	34 25.79	119 44.41	12.29	2.2	118	10	E	0.03	99.0	99.0
1978	8	29	23	6	58.37	34 26.45	119 44.69	12.29	2.3	63	28	A	0.05	0.6	0.6
1978	8	30	1	23	5.54	34 26.19	119 44.83	12.26	1.9	126	12	A	0.02	0.7	0.5
1978	8	30	10	54	36.11	34 28.26	119 46.13	12.72	2.0	126	11	E	0.02	99.0	99.0
1978	8	31	13	11	23.78	34 25.48	119 43.51	10.36	2.1	237	13	E	0.15	99.0	99.0
1978	8	31	16	37	6.49	34 13.28	119 43.74	20.17	2.5	90	32	A	0.08	0.5	0.8
1978	8	31	22	0	5.31	34 25.97	119 44.57	12.29		360	2	E	0.00	99.0	99.0
1978	9	1	8	15	59.85	34 26.82	119 46.49	12.18	2.0	176	7	E	0.00	99.0	99.0
1978	9	1	13	17	14.14	34 21.38	119 24.16	10.86	2.0	208	11	E	0.05	99.0	99.0
1978	9	1	22	32	35.66	34 27.08	119 46.47	13.45	2.1	114	10	E	0.03	99.0	99.0
1978	9	1	22	57	55.32	34 26.62	119 44.11	13.63		119	7	E	0.04	99.0	99.0
1978	9	2	7	6	25.40	34 27.37	119 46.75	12.49	1.9	120	18	E	0.06	99.0	99.0
1978	9	3	10	11	17.50	34 23.11	119 41.81	9.42	2.1	145	13	A	0.02	0.3	0.9
1978	9	3	15	25	4.92	34 26.22	119 44.43	12.29	2.0	144	7	E	0.02	99.0	99.0
1978	9	3	18	37	10.31	34 26.45	119 43.94	12.56	2.0	119	12	E	0.01	99.0	99.0
1978	9	4	3	26	7.05	34 26.50	119 46.45	13.23	2.1	169	15	A	0.01	0.4	0.3
1978	9	5	5	38	7.51	34 25.73	119 42.93	12.13	2.2	168	18	A	0.03	0.6	0.5
1978	9	5	8	6	17.77	34 12.93	119 42.60	19.49	2.8	88	31	A	0.11	0.7	1.1
1978	9	5	14	35	24.23	34 25.81	119 44.52	12.29	2.1	118	12	E	0.04	99.0	99.0
1978	9	5	20	19	50.43	34 25.65	119 43.73	11.59	2.3	80	23	A	0.06	0.5	0.5
1978	9	6	18	57	40.46	34 27.02	119 47.24	10.90	2.2	127	13	A	0.05	0.8	1.1
1978	9	7	1	0	11.67	34 25.57	119 41.08	12.29	2.3	58	26	A	0.04	0.3	0.3
1978	9	7	12	32	30.17	34 23.35	119 57.46	15.13		149	8	E	0.22	99.0	99.0
1978	9	7	19	0	20.02	34 26.16	119 43.73	13.20	2.5	124	36	A	0.04	0.2	0.2
1978	9	7	23	23	2.60	34 25.47	119 41.72	13.56	2.0	233	9	E	0.03	99.0	99.0
1978	9	8	23	35	23.80	34 25.56	119 41.33	12.70	1.9	177	8	E	0.04	99.0	99.0
1978	9	10	15	28	41.16	34 28.37	119 46.48	11.84	2.5	79	23	A	0.05	0.5	0.4
1978	9	11	4	19	38.19	34 27.74	119 45.83	11.76	2.2	131	24	A	0.06	0.4	0.4
1978	9	11	11	51	30.01	34 27.79	119 44.88	12.10	2.0	285	9	E	0.02	99.0	99.0
1978	9	11	18	27	38.82	34 25.08	119 46.49	11.13	1.9	190	9	E	0.00	99.0	99.0
1978	9	12	11	57	54.74	34 28.11	119 45.02	14.28	3.4	112	74	A	0.09	0.5	0.4
1978	9	14	1	7	4.61	34 11.12	119 37.09	15.33	2.2	162	11	A	0.04	0.7	0.7
1978	9	15	11	39	27.54	34 25.97	119 44.56	12.29		360	2	E	0.00	99.0	28.7
1978	9	15	14	33	39.48	34 26.31	119 43.62	13.26	2.0	78	14	A	0.03	0.8	0.6
1978	9	16	1	31	51.39	34 26.50	119 46.19	14.56	2.0	286	12	E	0.00	99.0	99.0
1978	9	16	9	19	49.84	34 25.92	119 46.78	11.75	1.8	186	12	E	0.01	99.0	99.0
1978	9	16	9	48	2.77	34 22.44	119 42.05	10.50	2.8	116	33	A	0.09	0.5	0.6
1978	9	16	9	49	15.68	34 24.09	119 42.86	12.69	1.8	276	8	E	0.00	99.0	99.0
1978	9	16	13	59	50.02	34 25.97	119 44.57	12.29	2.6	0	29	D	0.00	26.9	26.9
1978	9	16	13	59	45.05	34 27.24	119 44.61	12.28		304	6	E	0.02	99.0	99.0
1978	9	17	15	7	53.79	34 25.97	119 44.57	12.29		360	1	E	0.00	99.0	99.0
1978	9	18	1	38	30.19	34 26.27	119 45.32	12.50	2.4	65	28	A	0.08	0.8	0.6
1978	9	20	4	18	44.95	34 25.08	119 41.39	12.06	2.3	61	27	A	0.06	0.5	0.4
1978	9	22	3	5	3.18	34 29.89	119 44.57	12.29	2.2	307	5	E	0.03	99.0	99.0
1978	9	22	14	57	18.53	34 26.46	119 43.16	13.35	1.8	249	6	E	0.00	99.0	99.0
1978	9	23	17	40	40.50	34 26.36	119 40.76	5.31	2.0	204	12	E	0.04	99.0	99.0
1978	9	24	2	4	26.90	34 26.63	119 44.07	10.26	3.5	113	78	A	0.06	0.3	0.4
1978	9	26	0	2	38.47	34 26.83	119 45.50	12.34	1.9	179	10	E	0.00	99.0	99.0
1978	9	26	14	36	14.53	34 25.86	119 44.36	12.29	1.9	252	3	E	0.00	99.0	99.0
1978	9	28	15	36	1.92	34 26.27	119 43.68	13.16	2.0	178	16	B	0.04	1.4	1.0
1978	9	28	21	23	52.59	34 26.21	119 45.94	12.11	1.8	183	13	E	0.00	99.0	99.0
1978	9	29	11	6	25.42	34 26.55	119 47.78	12.13	2.0	120	19	A	0.02	0.4	0.4
1978	9	30	1	35	10.11	34 26.14	119 45.50	12.31	1.8	183	12	E	0.01	99.0	99.0

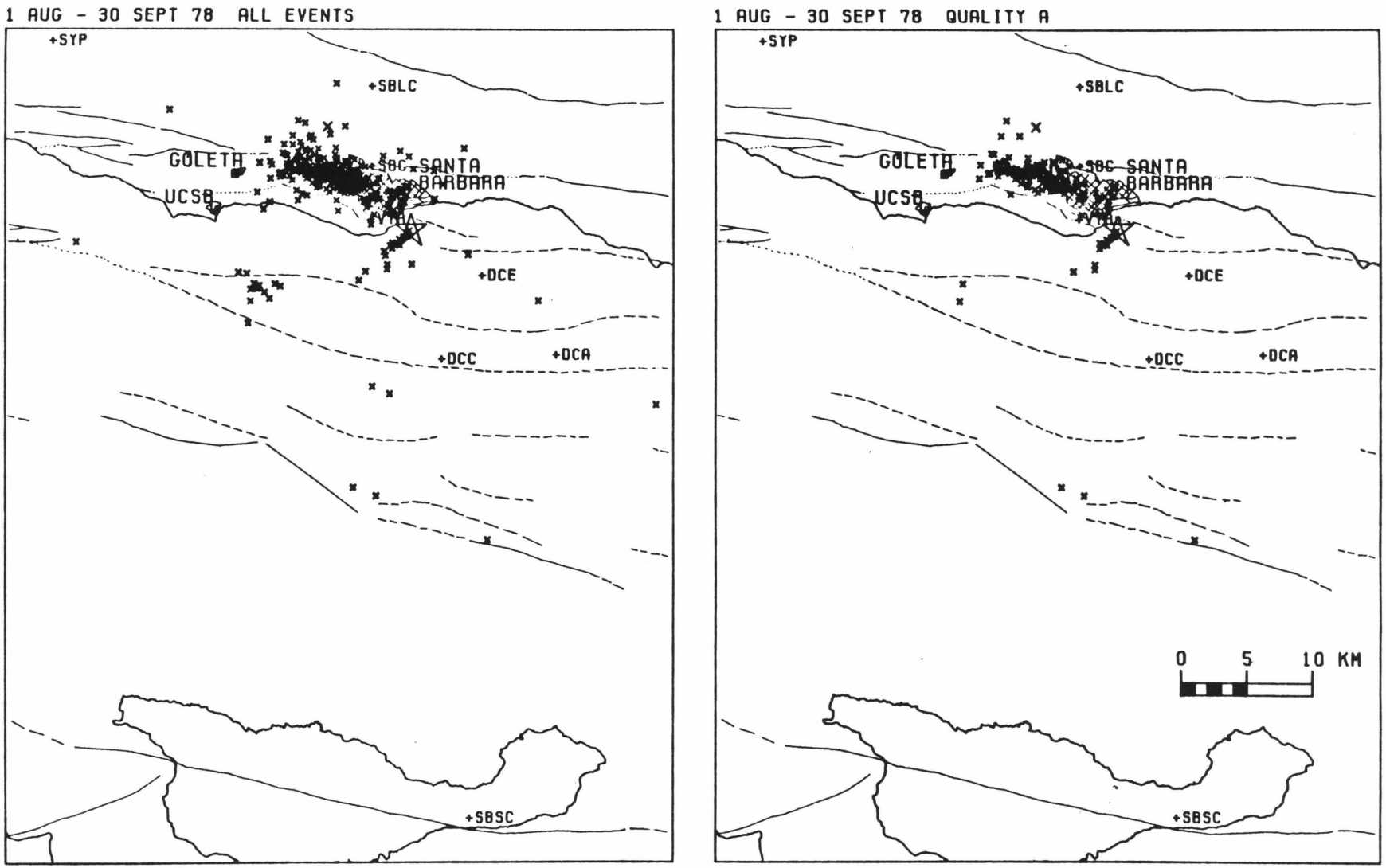

Figure 2-3. Maps showing location of epicenters for August and September 1978: a) all locations; b) A-quality locations. Star is mainshock. Small x's are events of less than magnitude 3. Large x's are of magnitude 3-3.5. +'s mark stations. Light, broken lines are faults after Yerkes *et al.* (1980).

Foreshocks

A search of Caltech-USGS network data for the two weeks prior to the mainshock disclosed only two events that might be considered to be foreshocks. On 7 August at 1212 GMT, a magnitude 1.9 M_L event occurred under Santa Barbara. Its calculated location is 5 km northeast of the mainshock (fig. 2-3a) with a depth of 12 km in a spot that is nearly absent of subsequent aftershocks. This event, however, was poorly recorded, and its location may be in error. The other event occurred at 1902 GMT on 13 August, 4 hours before the Santa Barbara earthquake. It was located 23 km southeast of the mainshock epicenter (fig. 2-3a) at 8 km depth, and it had a magnitude of 2.4 M_L. Its location is of interest because it is at a spot where there was considerable swarm activity in the preceding months, and there may be some causal relationship between the swarm activity, this foreshock, and the Santa Barbara earthquake. Most of the swarm activity occurred from March 27 to April 15, but there was further sporadic activity in this same spot during late April, mid-June, and mid-July. The 13 August "foreshock" was the only event to occur here in all of August and September, and thus may have been the final shock of the swarm activity. In fact, the complete shutoff of activity in this area after 13 August may actually be more significant than the "foreshock" itself.

Aftershock Locations

The data allowed us to locate 376 events (fig. 2-3a). These include 2 foreshocks, the mainshock, and 373 aftershocks that occurred between 1 August and 30 September 1978. Of these locations, 159 were of quality A (fig. 2-3b). We feel that the relative accuracy of the quality-A events is 0.5 km in both the horizontal and vertical directions, but due to possible errors in velocity modeling, the absolute inaccuracy may be as much as 2 km.

As can be seen in figure 2-3, a couple of features disappear when we look at the higher quality data. The cluster of events located 10 km southwest of the main aftershock zone is evidently due to location errors. Double checking the computer solutions for these events revealed that most of them were E-quality locations that were systematically mislocated. The two events that remain in figure 2-3b evidently are accurately located. There are also two events located southeast of the mainshock in figure 2-3a that suggest a lineation between the foreshock and the mainshock. Checking their solutions indicates that these are also poor locations. High residuals at stations to the east indicate that both these events are probably located within the main aftershock zone. Since there are a sufficient number of A-quality locations to delineate all the features of the aftershock zone, we will use only these highest quality locations in further discussion, so as not to confuse the issue with potentially inaccurate locations.

The aftershock location pattern had a very clear and intriguing development with time, as shown in figure 2-4. The most noticeable feature is that nearly all of the aftershocks were located north and west of the mainshock epicenter, and the great bulk of them were located between 4 and 10 km northwest of the epicenter. All of the first recorded aftershocks, between 2300 and 2315 GMT, occurred in a cluster 7 km northwest of the mainshock. Between 2315 and 2330 GMT, aftershocks began to fill in the zone between the mainshock epicenter and the initial cluster. Between 2330 and 2400 GMT the aftershock zone spread 3 km northward from the mainshock and also extended another 4 km west from the initial cluster. During the following 24 hours of 14 August GMT, aftershocks further filled in the zone outlined during the first hour's activity, with a noticeable lack of activity in the spot occupied by the initial cluster. There was also relatively little activity between this point and the mainshock epicenter, especially after 0600 GMT. Also, between 0000 and 0600

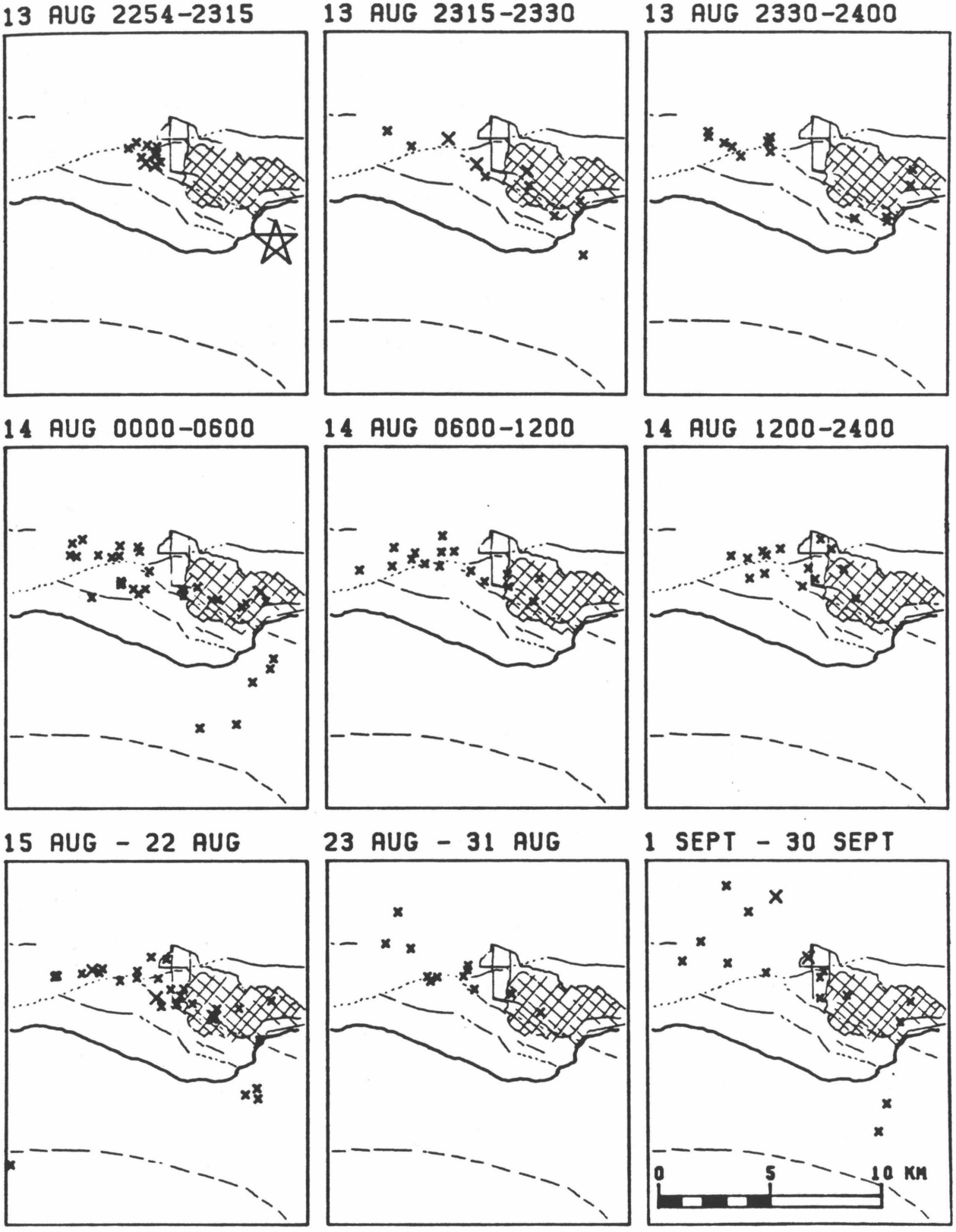

Figure 2-4. Maps showing temporal development of aftershock zone. Symbols as in fig. 2-3.

GMT, a new feature began to develop as aftershocks began to occur southwest of the mainshock epicenter. Four out of these five events occurred during a 40-minute period between 0046 and 0126 GMT and show a very clear migration away from the mainshock epicenter toward the southwest and toward the surface (fig. 2-5a). During the following few days, aftershock activity began to die off, but it continued to occur in the two zones outlined in the first 25 hours of activity. During the following weeks, activity died down even further, until it was averaging one detectable event per day by the end of September. A few of these latter events occurred up to 2 km farther north than the previously outlined aftershock zone. The most significant of these was a magnitude 3.4 aftershock that occurred on 12 September, 2 km north of and 2 km deeper than the previous activity.

The hypocentral distribution of the aftershocks can be seen in the cross-sections (fig. 2-5) and the stereo pair (fig. 2-6). These both show that most of the aftershocks outline a roughly rectangular structure that is nearly horizontal extending 11 km in the west-northwest direction and 4 km in the north-northeast direction. Contrary to normal expectations, there is less resolution of structure in the cross-dip cross-section (fig. 2-5a) than in the cross-strike cross-section (fig. 2-5b). This is due in part to the unusually shallow dip of the aftershock zone and in part due to the fact that the aftershock zone shallows slightly in the west-northwest direction, causing the apparent upward scatter in the N 15° E cross-section (fig. 2-5a). The stereo plot (fig. 2-6) makes this quite evident.

The cross-sections also show the distribution of the aftershocks that trend southwest from the mainshock epicenter. They are systematically shallower to the south-southwest and faintly suggest a structure that dips ~ 55° to the north-northeast. This "structure" projects to the surface near the trace of the North Channel Slope-Pitas Point Fault as mapped by Yerkes *et al.* (1980) (fig. 2-3).

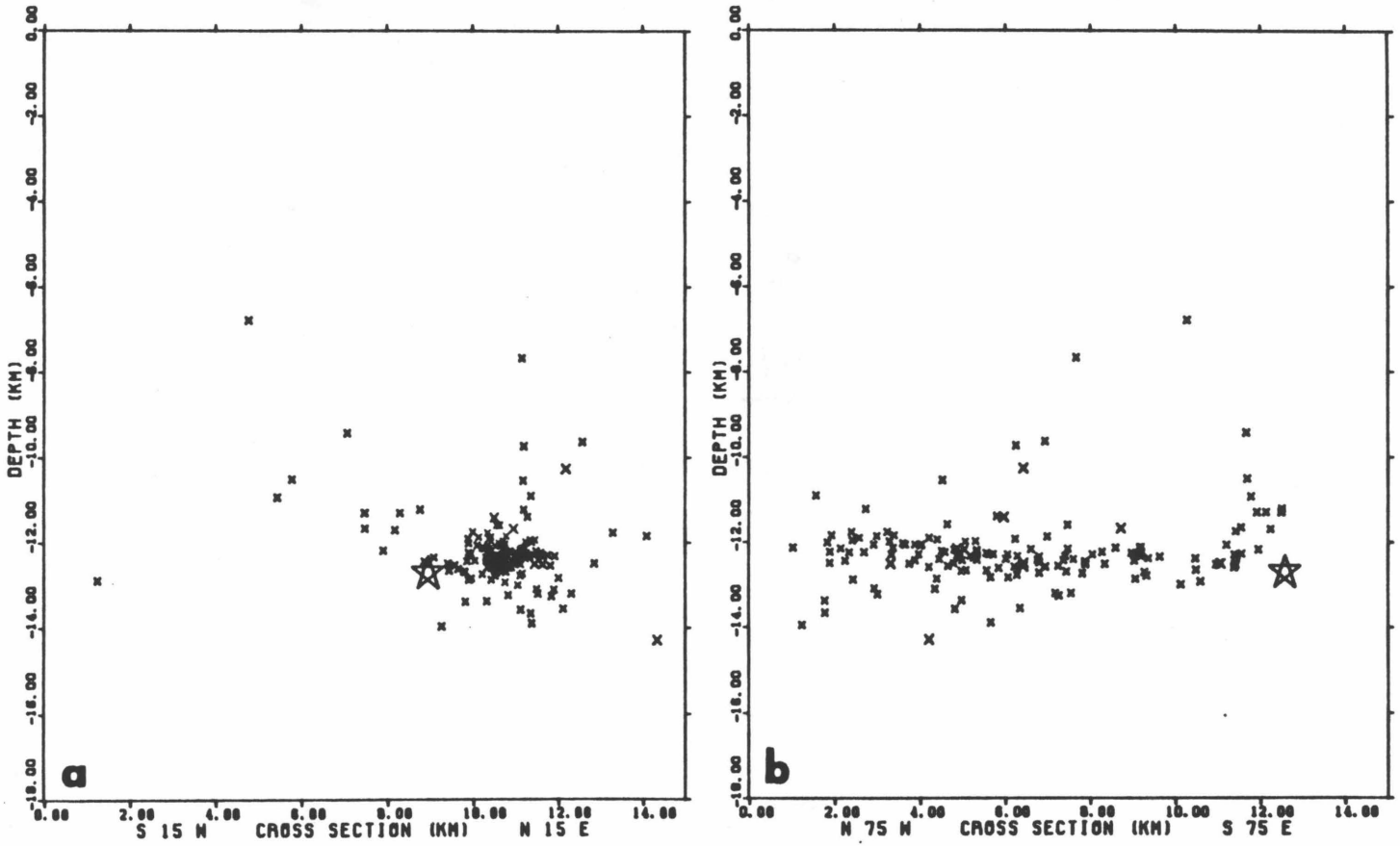

Figure 2-5. a) SSW-NNE and b) WNW-ESE cross-sections of hypocentral locations. Star is mainshock. Small x's are events of less than magnitude 3, larger x's are events of magnitude 3-3.5.

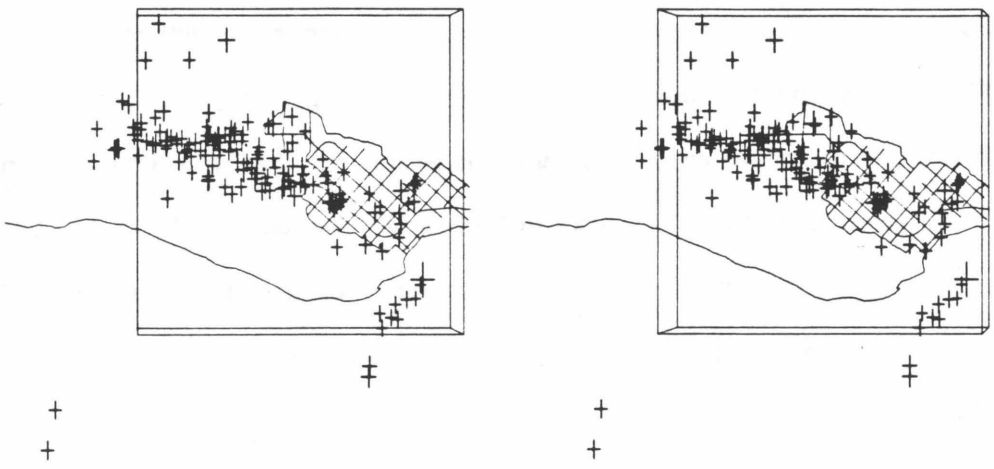

Figure 2-6. Stereographic plot of mainshock and aftershocks showing 3-D distributions of hypocenters. Crosses are scaled linearly to magnitude: mainshock is the largest cross in the southeast corner. For scale, the box is 10 x 10 km and extends to 10 km depth.

Yerkes *et al.* (1980) indicate that this fault is a reverse fault that strikes N 70° W (at this point) and dips 70° N (25 km W of this point), and has undergone movement in Quaternary time. Using these few aftershocks to tie a surface structure to activity at 13 km depth is admittedly risky, but the geometry is interesting and suggestive.

Interpretation of Aftershock Distribution

The high resolution of the locations, and the timing of the mainshock and aftershocks, allow us to make unusually precise statements about the rupture process. The location of the mainshock epicenter in the southeast corner of the aftershock zone (fig. 2-3) strongly suggests unilateral rupture towards the northwest. The clustering of all aftershocks 7 km west-northwest of the mainshock during the first 20 minutes (fig. 2-4) then apparently marks the extent of primary rupture. The gradual increase in the aftershock zone length to 10 km during the first hour may indicate growth of the initial rupture surface through aseismic slip and aftershocks. The northeast-southwest extent of the initial ruptured surface is not so clearly determined, but it may be as narrow as 1 km, as indicated by the width of the initial cluster; or it may be as wide as 4 km, as indicated by the aftershock zone width after 1 hour. By the end of the first 25 hours, an area of 4 km by 11 km was clearly outlined. By the end of September, the aftershock zone had grown ~ 60% to 6 km by 12 km (fig. 2-4f). This observation of rupture-plane growth with time illustrates the dangers of using overall aftershock zones to determine the size of the initial fault rupture planes.

We feel that the initial rupture may have involved as little as 7 km^2 and may have been as large as 28 km^2. An estimate based on the whole aftershock zone would have given 44 to 72 km^2 of ruptured area, which could lead to an under-

estimation of stress drop for the Santa Barbara earthquake. We have calculated theoretical stress drops for these fault dimensions (fig. 2-7), according to the formulation of Kanamori and Anderson (1975), for a circular fault (Keilis-Borok, 1959). We have used this geometry in spite of our knowledge that this was primarily a dip-slip event, because there was a significant component of strike-slip motion, and the difference in the geometric factor for different fault types is relatively small ($\sim$ 1.3) compared to the other uncertainities in the problem. We have used the seismic moments of 1.1 x 10^{25} dyne-cm (from WWSSN short- and long-period records) and 3.6 x 10^{24} dyne-cm (from strong-motion records) computed by Wallace *et al.* (1981). This discrepancy in seismic moments is interesting, and may be partly explained by Ebel *et al.* (1980), who derived the time function for this event. The time function has a pair of high-amplitude spikes during the first 2 seconds which are followed by a low-amplitude tail out to 6-seconds duration. This may indicate that the event started as a fast (or high stress drop) event that ruptured the first 5-7 km of the fault plane, but then continued as a slow (or low stress drop) event over the remainder of the fault plane (Ebel, personal communication). Thus the strong-motion records may represent only the high-frequency, early part of the event.

As figure 2-7 shows, the smaller fault area and the larger moment would give an unusually high value for stress drop ($\sim$ 1400 bars). We consider this only as an extreme possibility, especially since it would require an unrealistically large displacement ($\sim$ 5 m) for a magnitude 5 earthquake. Figure 2-7 was intended to show the variation in stress drop with fault area chosen (which depends on when one picks the aftershock zone). But it also shows that the average stress drop for the whole Santa Barbara sequence decreased as a function of time. (We may neglect the seismic moment of the aftershocks, since 373 magnitude-3 events contribute about 1 x 10^{23} dyne-cm, i.e. < 3% of the total moment). Since we prefer the smaller fault areas for

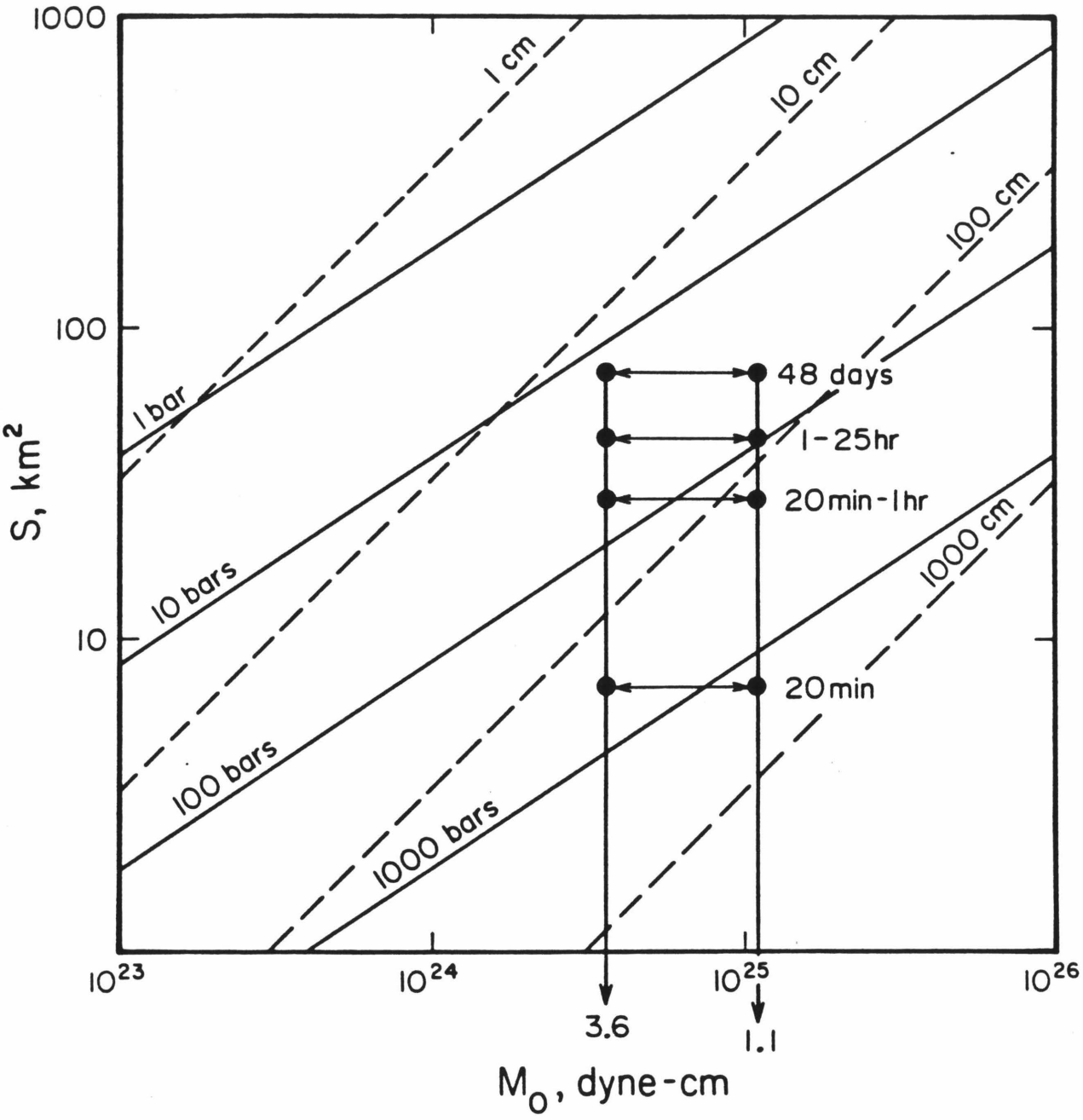

Figure 2-7. Plot of seismic moment, M_o, versus area of aftershock zone, S, at different times after the mainshock. Seismic moments of 3.6×10^{24} (strong-motion) and 1.1×10^{25} dyne-cm (WWSSN) were calculated by Wallace *et al.* (1981). Slanted lines indicate average stress drop (solid) and average displacement (dashed) for a circular fault model.

the size of the initial rupture plane, this implies that the initial rupture may have had about a meter of displacement and a stress drop of hundreds of bars. Then the fault plane may have grown by small displacement, low stress drop activity (creep?) in the surrounding area.

It is interesting to note the holes in the aftershock pattern -- the gaps that appear between the mainshock and the main body of aftershocks. These holes appear either when we consider just the quality-A locations or all of the locations (fig. 2-3). It has been suggested by Wallace *et al.* (1981) that the fault breakage was rough, with several asperities. They interpret the acceleration records to indicate that the later asperities were probably located 3 km and 5 km northwest of the mainshock epicenter, which corresponds reasonably well with the locations of areas of few aftershocks. Another asperity zone is identified by the aftershocks during the first 15 minutes. Apparently this was an area of stress concentration where the fault rupture either changed in character or temporarily stopped. In either case, this stuck patch had been broken through by aftershocks by 20 minutes after the mainshock. During the 3 days following the mainshock this patch was noteworthy for its absence of aftershocks (fig. 2-4). A few events occurred in this spot between 17 August and 24 August, but the area became completely quiescent after that date.

The temporal development of the fault plane and the holes in the aftershock pattern suggest an asperity model for the rupture process. We feel that most of the energy released in the 5.1 M_L mainshock was radiated from a few relatively small areas of the aftershock zone (probably < 10 km ^{2}) of high shear stress (possibly hundreds of bars). Then, in the ensuing hours and days, the fault extended into surrounding areas of low stress. The asperities, having once been broken through are then areas of few aftershocks, either because of total stress relaxation or because they still have more strength than the surrounding plane. So the aftershocks may be

a better indication of where new rupture is occurring than where the main rupture was. This phenomenon has been observed elsewhere: Ebel (1980) suggested that the short-period energy in the Borrego Mountain earthquake of 1968 was radiated from two asperities with a few hundred bars of stress drop. And these asperity zones correspond to areas of few aftershocks.

This feature may be common to many earthquakes but may have not been observed for a number of reasons. Perhaps when the asperities are broken the rupture plane extends into areas of low stress very quickly, -- in a matter of minutes. Another reason is that earthquakes seldom happen where there is good station coverage. Usually, portable seismographs are not installed in the epicentral region until hours or days after activity has started. Hence, the details of locations during the first few minutes of aftershocks are usually lost. The accuracy of our locations would not have been possible except for the great good fortune of having 4 seismographs installed in the epicentral region the day before the earthquake.

EARTHQUAKE MAGNITUDES

The Pasadena magnitude for the Santa Barbara earthquake was 5.1 M_L (Whitcomb and Hutton, 1978) and was based on readings from 18 Wood-Anderson seismographs with good agreement between readings. Berkeley reported a magnitude of 5.7 M_L, also based on Wood-Anderson readings. Magnitudes of 5.5 m_b and 5.6 M_S were reported in the Preliminary Determination of Epicenters (PDE). The discrepancy between the Pasadena M_L and the PDE readings is consistent with the observation that the WWSSN records showed a factor of 3 larger seismic moment than did the strong-motion records (Wallace *et al.*, 1981). The discrepancy in reported local magnitudes may be due in part to a directivity effect. The aftershock distribution suggests that the rupture propagated unilaterally towards the northwest,

which is away from most of the Pasadena stations and towards the Berkeley stations. Still this is a surprisingly strong directivity effect for such a small fault, but this may argue in favor of the fault plane being quite narrow.

Magnitudes for aftershocks were calculated by Richter's method if they were large enough to be seen on the Pasadena Wood-Anderson instruments, and are reported in Whitcomb *et al.* (1979). Magnitudes for the smaller aftershocks were calculated by the coda-amplitude method described by Johnson (1979). The magnitudes for the first week of activity are plotted in figure 2-8. As can be seen, almost all of the energy was released in the mainshock, as no aftershocks even approached it in size. Most of the aftershocks were of magnitude 3 or less, and no aftershock was larger than 3.5 M_L.

FOCAL MECHANISMS

Focal mechanisms for the mainshock, foreshock, and aftershocks were derived using P-wave first motions. Take-off angles were calculated from the same velocity model used in the locations, and the data were analyzed with the computer program FOCPLT written by Whitcomb and Garmany (Whitcomb, 1973). This program assumes a double couple and checks all possible solutions (with a resolution of 3.5°) to minimize the number of "stations in error". The results are plotted on an equal-area projection. The program worked well for most events, but for some poorly constrained solutions, we input nodal planes that better fit the data.

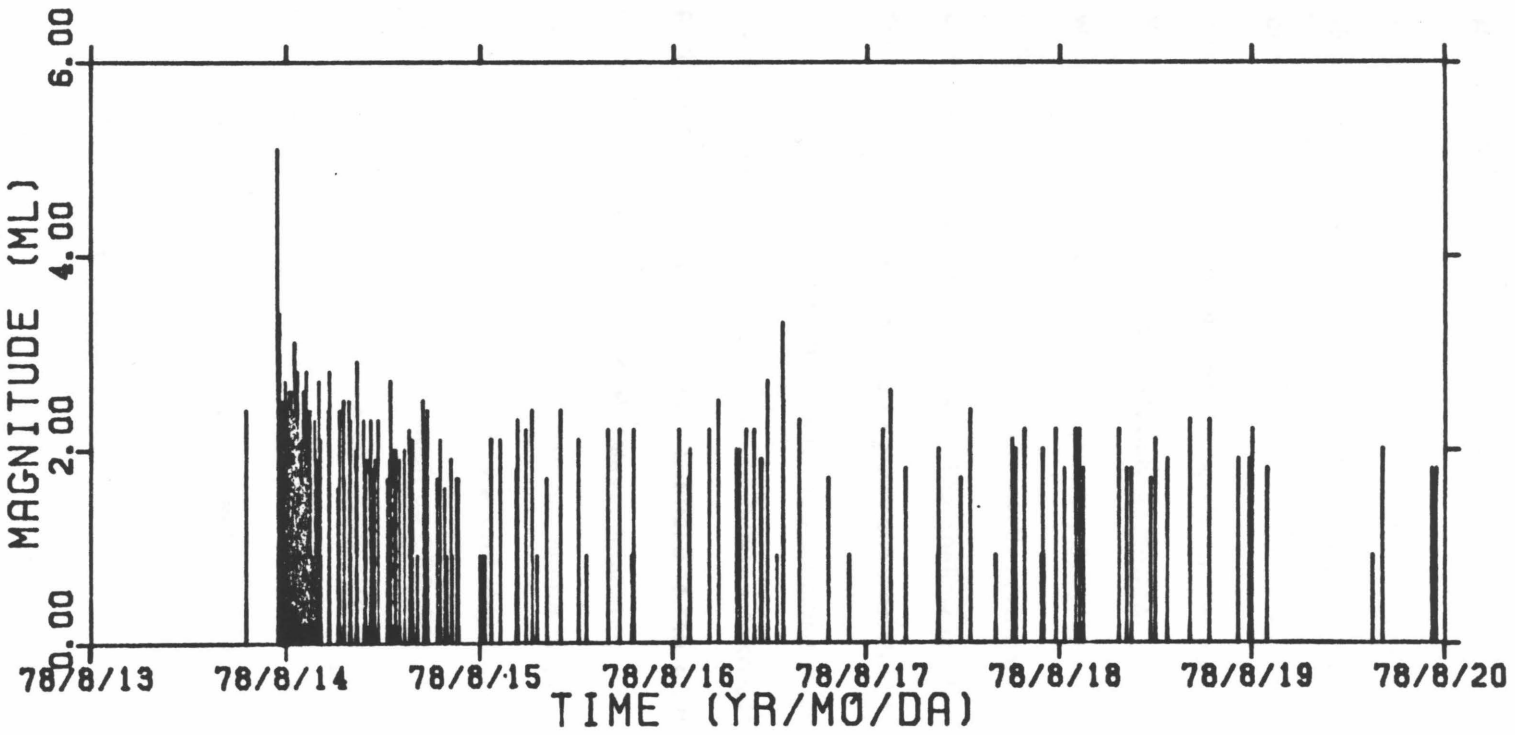

Figure 2-8. Plot of magnitudes of foreshock, mainshock, and aftershocks of the Santa Barbara earthquake versus time, for the first week of activity.

Mainshock

The focal mechanism for the mainshock (fig. 2-9) is very well constrained, using first-motion data from the USC OBS's, Berkeley stations (R. Miller, personal communication), and the Caltech-USGS southern California network. The fault-plane solution has one nodal plane dipping shallowly to the north (strike 280°, dip 26°, slip angle 57°), and the other dipping steeply southwest (strike 135°, dip 69°, slip angle 105°), with the quadrant between them being compressional. In either case, the mechanism is indicative of compression in the north-northeast-south-southwest direction with a component of strike-slip motion. The shallow north-dipping plane is preferred as the fault plane, based on its close agreement with the aftershock distribution.

Because of the above-mentioned problems in modeling velocity, we have some concern that we may not have calculated take-off angles completely accurately, particularly in the N-S direction. Stations to the south, such as SBSC and SBSM, typically have large negative P-delays, indicating that the apparent velocity in this direction is somewhat faster than our hybrid model would predict. This means that take-off angles in this direction are probably lower than the model predicts. Conversely, stations to the north, such as CRG, BCH, SBCC, and YEG have large positive P-delays. Consequently, apparent velocities are somewhat slower, and north-going take-off angles are probably somewhat greater (i.e., more horizontal) than the model predicts. Since the shallow north-dipping plane is principally controlled by the stations CRG, SBSC, BCH, YEG, and SBCC, this nodal plane may be dipping at a shallower angle than we have calculated here.

During the process of testing velocity models for location, we also tested them to see how they influenced the mainshock focal mechanism. It was noticed that models containing many layers, such as the Lee *et al.* (1978) location model (9 layers) and Wallace's *et al.* (1981) model (10 layers) also gave a shallower dip to

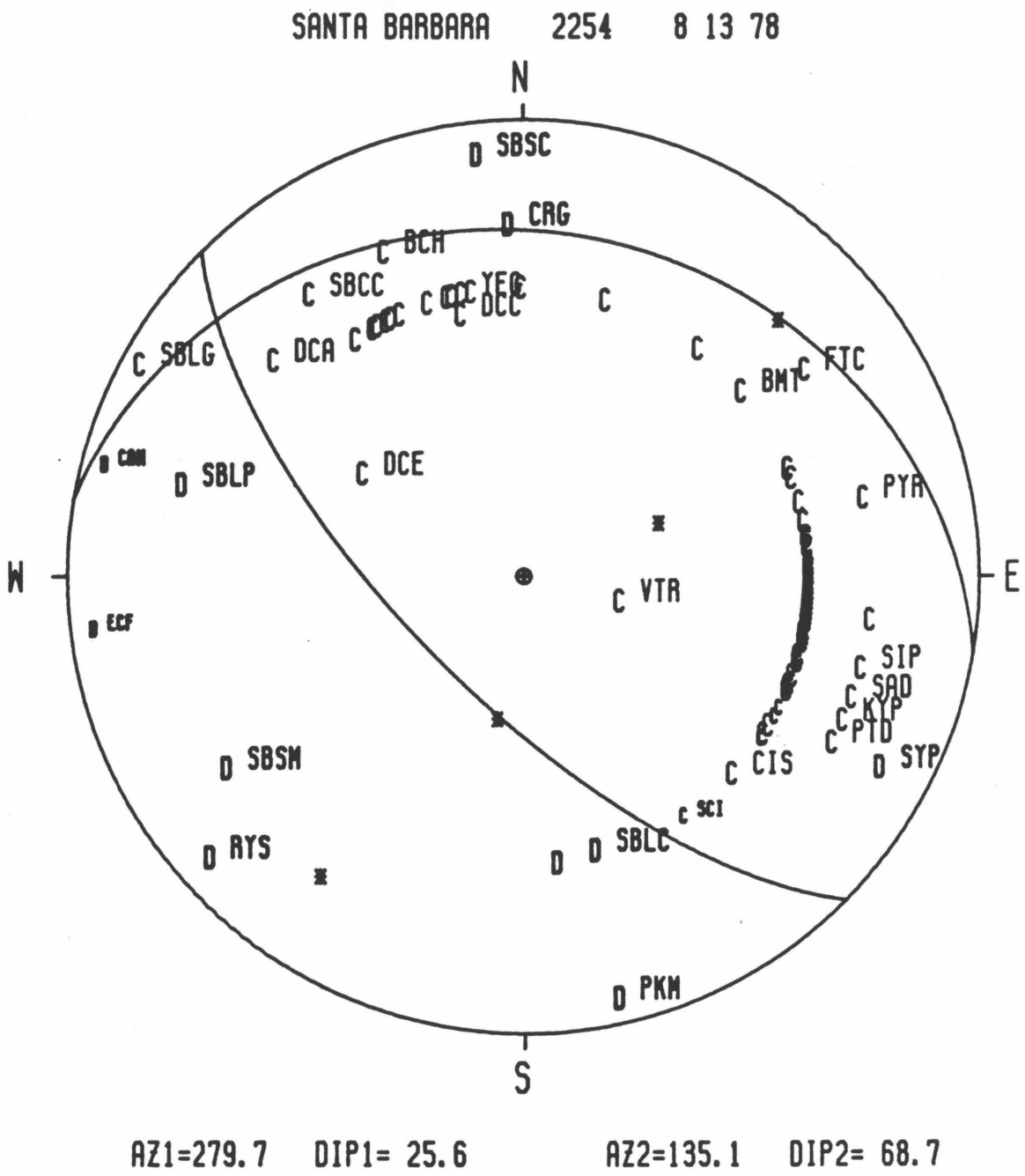

Figure 2-9. Focal mechanism of the Santa Barbara mainshock. Equal-area, lower hemispheric projection. C's are compressions, D's are dilation. 3-letter designations are nearby stations.

the nodal plane. These more smoothed velocity models may better simulate the curvature of the ray paths from the source.

Foreshock

The focal mechanism of the foreshock that occurred 4 hours before the mainshock is shown in figure 2-10a. As can be seen, it is nearly identical to the mainshock and also indicates north-northeast-south-southwest thrusting with a component of strike-slip, in spite of being located some 23 km southeast of the mainshock. The mechanism is fairly well constrained and has one nodal plane dipping at 36° in the north-northwest direction and the other dipping 61° in the south-southwest direction. We cannot say with confidence which plane is preferred as there is no other activity located in the area.

Aftershocks

We were able to derive reliable focal mechanisms for 46 aftershocks. We consider 24 of these solutions to be well constrained (generally more than 14 first motions and no contradictions), 20 to be fairly constrained (fewer first motions and some contradictions), and 2 to be poorly constrained. These are plotted on the maps in figure 2-11. Almost all of the mechanisms (40) indicate thrust movement, with the direction of thrusting varying between west-northwest and east-northeast. For most of these events, the northward-dipping nodal plane dips at 25° to 45°, in general agreement with the mainshock focal mechanism. A typical example of one of these solutions is shown in figure 2-10b.

Of particular interest are the few focal mechanisms that may indicate very low-angle thrusting. There are 5 in the principal aftershock zone that have a north-dipping plane with dips ranging from 7° to 15°. All 5 of them occur along the northern

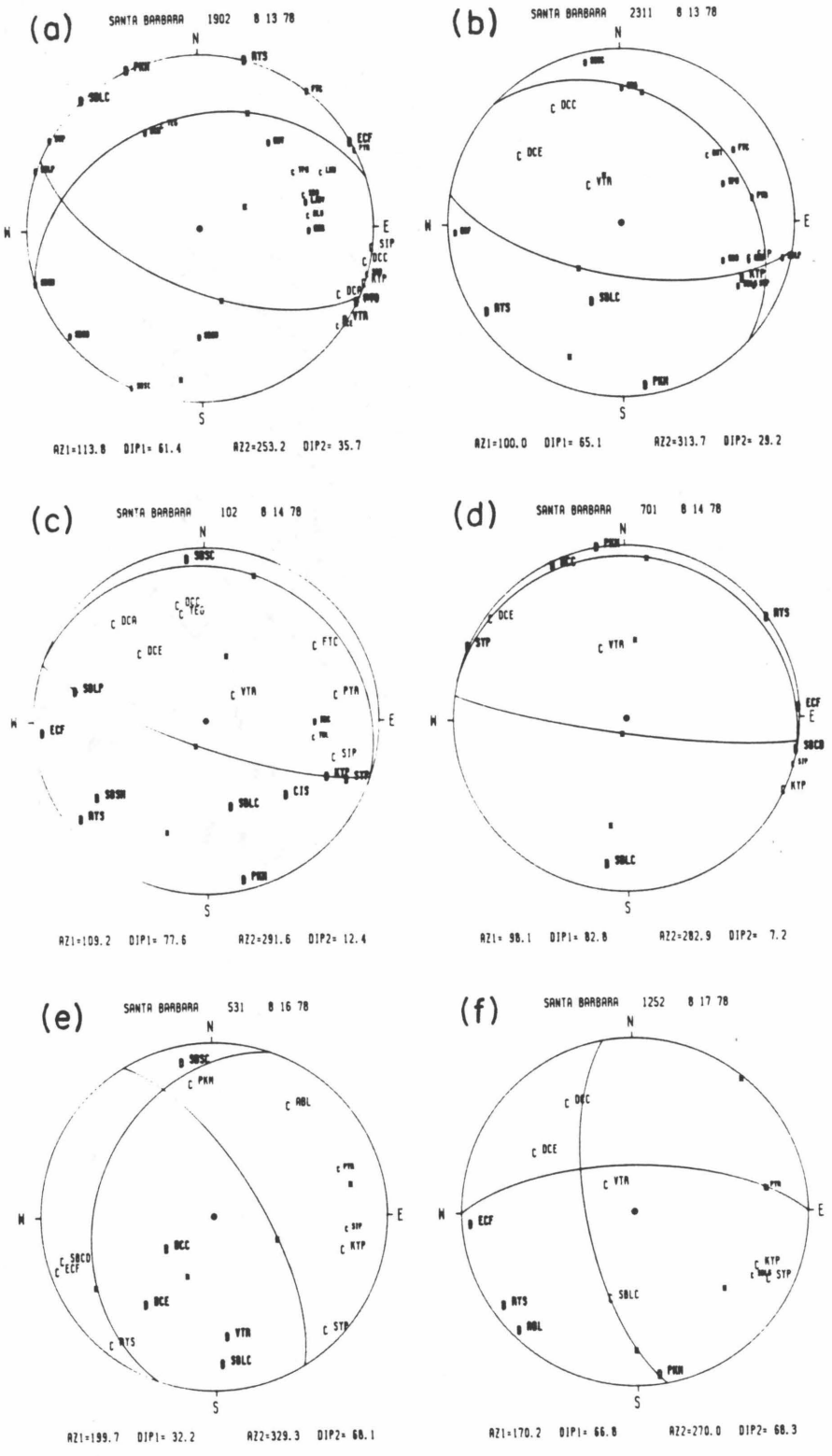

Figure 2-10. Focal mechanism of foreshock and some typical aftershocks. Same projection and symbols as in fig. 9.

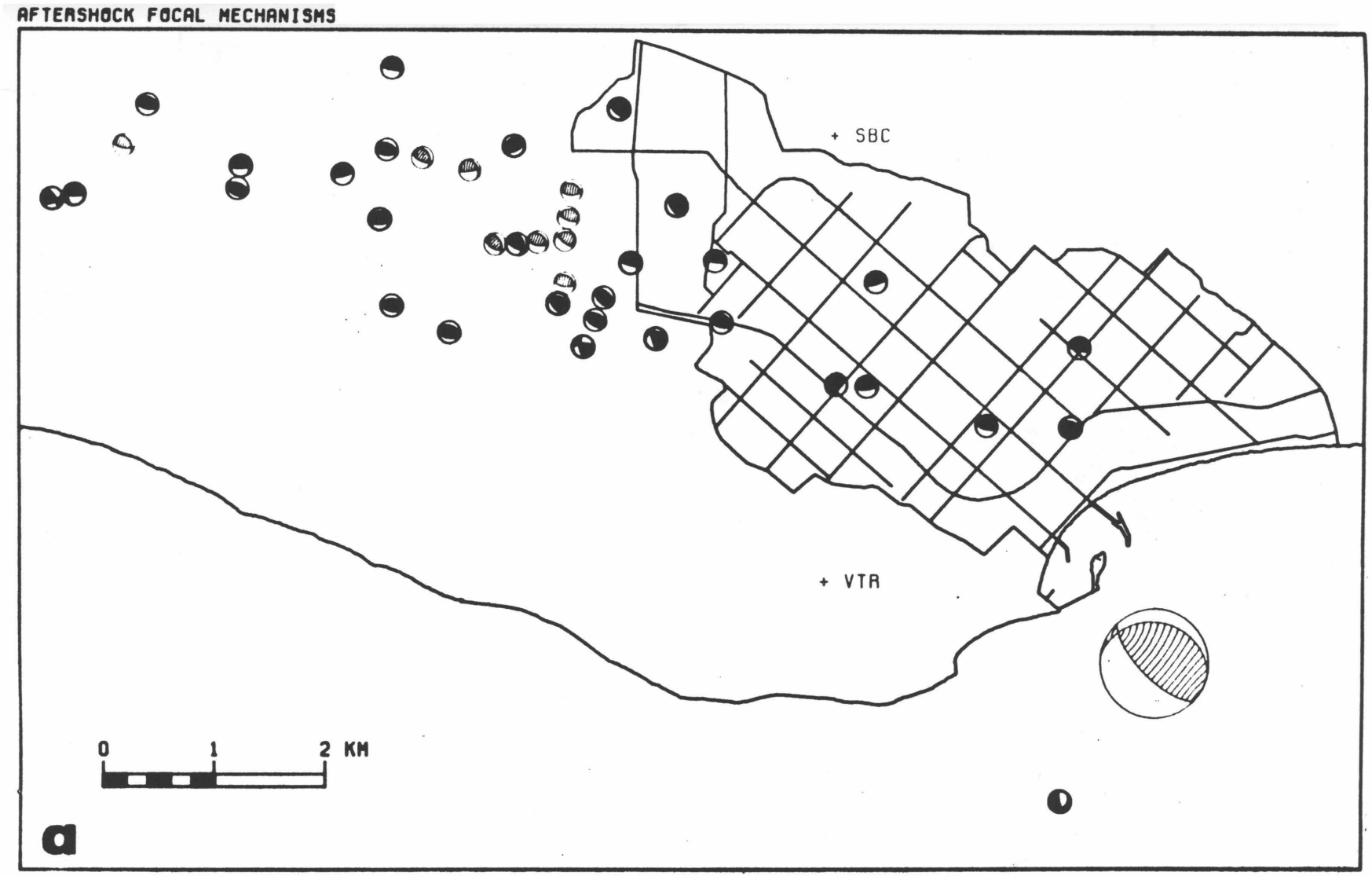

Figure 2-11a. Large-scale map showing mainshock and aftershock focal mechanisms located at their epicenters. Light-colored events occurred on August 13-14, dark-colored events, August 15 - September 30.

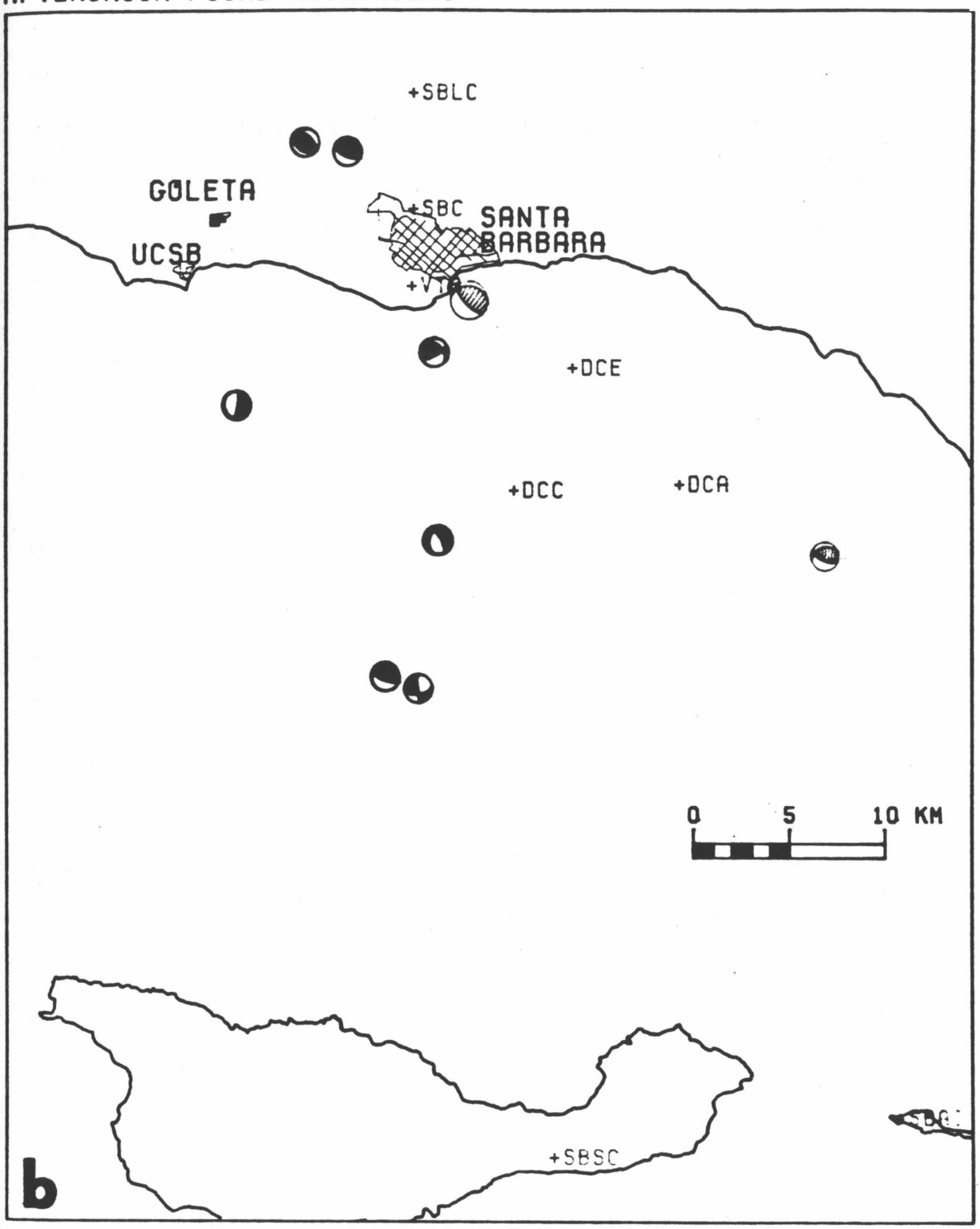

Figure 2-11b. Small-scale map showing mainshock, foreshock, and aftershocks that would not be shown in figure 2-11a.

edge of the aftershock zone between the mainshock epicenter and the initial aftershocks (compare fig. 2-4 and fig. 2-11a). These are the only events we could find that exhibit a possible fault plane with a dip as low as that seen in the aftershock cross-sections (fig. 2-5). These events occurred at 102, 633, 701, and 747 GMT on 14 August, and at 718 GMT on 18 August. Typical mechanisms of this group are shown in figures 2-10c and 2-10d. Two of these mechanisms are well constrained (102 and 701); two are fairly constrained (633 and 718); and one is fair to poorly constrained (747).

There are 6 focal mechanisms that are not thrust: 3 normal and 3 strike-slip (see fig. 2-11). Five of these 6 occurred relatively closely together in time, between 1655 GMT on 14 August and 1252 GMT on 17 August (i.e. on 3 days out of the 48-day aftershock period we considered). This was immediately after a rather sudden decrease in the rate of aftershock occurrence (see fig. 2-8). So these "different" mechanisms may be related to a change in the mode of stress release at this time.

The normal mechanisms occurred first -- at 1655 GMT on 14 August, and at 531 and 957 GMT on 16 August. All three mechanisms indicate east-west extension, although one (1655, 14 August) has one plane so nearly horizontal (9° WSW) that it could be considered to indicate more horizontal shearing than extension, if that nodal plane is the fault plane. One of the normal mechanisms is shown in figure 2-10e.

The normal events were followed by two of the strike-slip events on 17 August, at 257 and 1252 GMT (fig. 2-10f). They were both located along the southern edge of the main aftershock zone (fig. 2-11a). The third strike-slip event occurred at 806 GMT on 5 September, 20 km south of the main aftershock zone (fig. 2-11b), at a depth of 19 km, making it one of the deepest events observed in this study. All three strike-slip events are compatible with horizontal compression in the north-northeast-south-southwest direction.

The significance of these "different" focal mechanisms is uncertain. During the 3-day period in which the 5 non-thrust events occurred, there were also 3 thrust events observed, as well as numerous other events that were too small to study for focal mechanisms. Three of these six "different" events are located significantly south of the main aftershock zone (fig. 2-11b), and hence are outside the area for which the original velocity modeling was intended. Thus there could be some error in these fault plane solutions. Looking at the first-motion plots, however, it would take a radically different velocity model to get a thrust mechanism out of the distribution of first motions seen in plots such as figure 2-10e.

DISCUSSION

Mode of Faulting

The mainshock focal mechanism clearly indicates that the Santa Barbara earthquake was the result of reverse faulting. We prefer the nodal plane that dips 26° to the north as the fault plane since it most closely corresponds with the strike and dip of the aftershock hypocentral distribution. This dip, however, is somewhat greater than the dip of the aftershock zone itself (15° or less) (fig. 2-5a). The discrepancy may be due in part to the difficulties of velocity modeling in this area. Most of the aftershocks have north-dipping nodal planes dipping at least 25° and ranging as high as 45°, which is significantly steeper than the plane suggested by the cross-sections. These planes are shown in cross-section in figure 2-12. Our suggestion is that this pattern indicates a complex series of imbricate thrust faults. A zone of imbricate thrusting has been previously observed nearby in a similar tectonic environment: along the south front of the Transverse Ranges near Pt. Mugu (Stierman and Ellsworth, 1976). In our case, the dip of these imbricate faults may shallow with

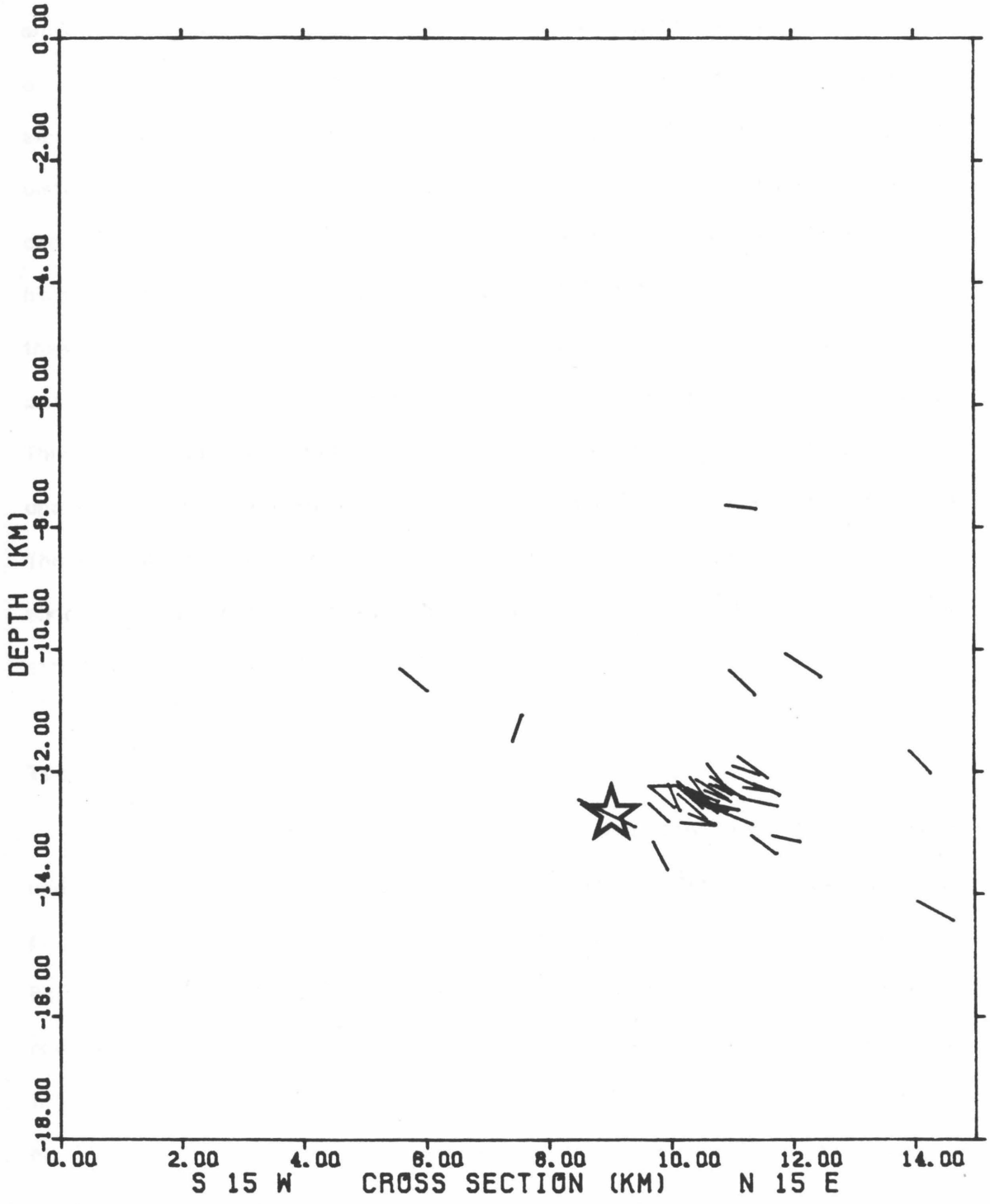

Figure 2-12. SSW-NNE cross-section showing orientations of preferred planes from mainshock and aftershock focal mechanisms. Mainshock is indicated by the star.

depth into a more nearly horizontal structure. In figure 2-12 there is a slight hint of such curved fault planes. This suggestion should be viewed with some caution, however, since the relative location accuracy of the events is only about 0.5 km. It seems clear, however, that the planes shown in figure 2-12 represent some sort of distributed shear. The north-south spread of these planes is not some artifact of choosing the wrong cross-section projection, but the result of the aftershock zone being at least 2 km wide along most of its length (see fig. 2-11a). The reason why these aftershock planes do not outline a single plane may be because the first-motion fault plane solutions show how the ruptures initiate but not how they progress. Thus we are suggesting that for many of the aftershocks the rupture initiated at the upper end of the imbricate thrust faults and propagated northward and downward. The few flat focal mechanisms that occurred along the northern edge of the aftershock zone then might be events that initiated at the north edge of the low-angle structure and propagated southward.

Tectonic Implications

One possible interpretation of our results is that the Santa Barbara area is underlain by a very low-angle thrust fault. Its complete extent is unknown, but if we project this structure upward at a dip of 15°, it would surface 48 km south of Santa Barbara, near Santa Cruz Island. This island is bisected by a known active fault; however, it is steeply dipping and its offset is evidently left-lateral rather than thrust (Jennings, 1975; Weaver, 1969; Patterson, 1978). It is unduly speculative, however, to project a fault plane over such a large distance without any other supporting data. The Santa Barbara Channel is in fact cut by many steeper north-dipping reverse faults (Yerkes *et al.*, 1980) that are apparently active, and it is probably more likely that the low-angle structure curves upward into one or more of these.

Haxel and Dillon (1978) hypothesize that a large area of southern California is allocthonous and is underlain by Pelona-Orocopia schist. They suggest that the allocthon was emplaced during Paleocene or Late Cretaceous time along a single thrust fault that is extensive under the Transverse Ranges and the Mojave Desert. Campbell *et al.* (1966) have reported Miocene detachment faults that surface in the Santa Monica Mountains and Yeats (1983) has identified 3 levels of Quaternary detachment in the Ventura area. Several workers have expressed the idea that a low-angle mega-thrust system may be presently active under the Transverse Ranges. Thatcher (1976) used a low-angle thrust fault to successfully model vertical displacements preceding the 1971 San Fernando earthquake. The Palmdale uplift (Castle *et al.*, 1976) may have been caused by aseismic slip of a low-angle thrust fault (Rundle, 1978; Rundle and Thatcher, 1980). Recent changes in horizontal compression across the San Andreas fault have been modeled as a horizontal southward-propagating dislocation under the Transverse Ranges, south of Palmdale (Savage *et al.*, 1981).

Hadley and Kanamori (1978) have suggested that the central Transverse Ranges are underlain by a shallowly north-dipping structure and that the San Gabriel Mountains are behaving as a decollement. They cite as evidence a pair of focal mechanisms indicating low-angle thrust at 12 km depth in the San Fernando region. Yeats (1981) has suggested that this detachment structure is extensive under the Transverse Ranges and comes to the surface in a zone of reverse faults that extends from Banning Pass to the Santa Barbara Channel region, where it appears as the Red Mountain and Pitas Point faults near Ventura. Yerkes *et al.* (1980) map the north-dipping Pitas Point fault westward across the channel to other active structures in the western Santa Barbara Channel. The Santa Barbara earthquake may have been the result of slip on such a structure, and the overlying crust here may

also be a decollement.

CONCLUSIONS

We have calibrated seismographic stations in the Santa Barbara region from a seismic refraction line shot by UCSB (Crandall *et al.*, 1979), to obtain a model appropriate for earthquake locations near Santa Barbara. We have used this model to locate the 13 August 1978 Santa Barbara earthquake and all of its aftershocks to 30 September 1978. These locations suggest unilateral rupture directed towards the west-northwest followed by progressive growth of the fault plane with time. Hypocentral distribution and focal mechanisms for these events indicate that the earthquake was probably caused by thrust movement on a low-angle north-dipping structure 13 km under Santa Barbara. These observations suggest a tectonic model in which the western Transverse Ranges are being deformed by horizontal southward movement of the upper crust along a mid-crustal detachment surface.

Chapter 3

The Depth of the Seismic Zone in the Transverse Ranges of Southern California

Introduction

An intriguing question for many geologists and seismologists is: What lies under southern California? The idea that southern California is underlain by some sort of decollement has been suggested by several authors (e.g. Hadley and Kanamori, 1978; Yeats, 1981). The geologic structure in southern California is clearly different than in northern and central California. From the Mendocino Fracture zone south, the boundary between the North American plate and the Pacific plate is the fairly simple strike-slip regime of the San Andreas fault system. The transform boundary at the surface is in many places only as wide as the main strand of the San Andreas fault (< 1 km) and at most is 60 km wide where it includes two major branch faults in the San Francisco Bay area. South of latitude 35° N, however, the character of the boundary changes drastically. Here we have a 250-km-wide zone of compressional tectonics (the Transverse Ranges), and south of this, an equally wide zone of active strike-slip faulting (the Peninsular Ranges). This is undoubtedly related to the fact that the San Andreas fault takes a big bend to the east between latitude 35° and 34° N, and the plate boundary moves 120 km inland. But it is unclear whether this change in structure is caused by the Big Bend or vice versa. The wide zone of strike-slip faulting may imply that the crust is weaker here and/or the zone of brittle deformation is thinner than it is further north. In addition there is now some evidence that the

Transverse Ranges may have been rotated a large amount, independently of surrounding structures (Luyendyk *et al.*, 1980).

Since 1977, the CEDAR system has been operating at Caltech and recording high-quality data from a dense network of seismographs. Consequently the Caltech earthquake catalog has been growing at the rate of about 20,000 events per year. Those close to the data have long noticed that earthquakes do not occur below a relatively shallow depth (10-20 km) in southern California. In addition, this lower limit to the seismicity is consistently deeper along the southern front of the Transverse Ranges than elsewhere in southern California (Hearn, oral comm.). Some have suggested that the above-mentioned detachment surface may mark the lower limit of seismic activity in this region, which in other parts of the world has been interpreted as the transition from brittle to ductile crust (Meissner and Strehlau, 1982). Hence it was decided to use the Caltech catalog for a preliminary look at what the depth of earthquakes might say about the hypothesis of decollement.

There are many dangers inherent in using catalog locations, mainly because they are produced from large amounts of data that are processed by routine methods which were not intended for this kind of study. In addition, since the seismicity is so shallow, it is difficult to constrain depth unless there is a station directly above the activity. In light of these problems, only the A-quality events in the catalog were used. A-quality implies that the standard errors in the epicenter are less than 1 km, and the standard errors in depth are less than 2 km. In addition a numerical experiment was done to try to duplicate the standard location procedures used by the CEDAR system to test how well it really does locate events, and to see if quality-A locations are as good as claimed. The strategy in this chapter will be first to present the data, and second to discuss some of the problems in the catalog-location process.

This work was done initially in conjunction with fellow graduate student Tom Hearn. He did the original work of making earthquake-depth contour maps from the catalog, and we both noticed the correlation between deeper events and the south front of the Transverse Ranges. He also noticed that the bottom of the seismic zone appeared to "daylight" in the Mojave Desert and at the east end of the Transverse Ranges. I carried this work further with a more thorough search of the Caltech catalog and the initial results were presented by Corbett and Hearn (1981). For that study, Hearn helped prepare the synthetic earthquake location plots that tested the CEDAR location procedures. The maps, cross-sections, and histograms are my own work.

Previous Suggestions

Materials and Structures. Whatever underlies southern California is of course controlled by the geologic history of the region. From Mesozoic up until mid-Oligocene time, the Pacific Coast was characterized by an Andean-type subduction complex (Atwater, 1970). At that time, 30 million years ago, the East Pacific Rise began to impinge on the coast, and the subduction gradually began to give way to the transform faulting that we see today. During the previous period of subduction, oceanic rocks of the Pelona schist may have been thrust under southern California along a shallowly dipping zone as suggested by Haxel and Dillon (1978). They further suggest that the Pelona schist is extensive under southern California and that the overlying crust is allocthonous. It is inferred that the Pelona schist is possibly more ductile than the granites in the upper crust, and the upper crust may be behaving as a detached plate. Such detachment structures are not unknown in southern California. For example, an extensive mid-Tertiary detachment structure has been intensively studied in the desert of southeastern California (Davis *et al.*, 1980; Frost *et al.*,

1981; Frost and Martin, 1982). To the west, Miocene detachment faults in the Santa Monica Mountains have been mapped in the field by Campbell *et al.* (1966). And Quaternary detachment faults at depth in the Ventura Basin have been documented by Yeats (1983).

Seismicity and Seismic Velocities. Hadley and Kanamori (1978) have noted events at the bottom of the San Fernando aftershock zone with focal mechanisms that may be interpreted as representing horizontal shearing at 12-km depth. Following this, Pechmann's (1983) study of focal mechanisms in the central Transverse Ranges included some events that had horizontal nodal planes. Later, Corbett and Johnson (1982) observed a near horizontal aftershock zone at 13 km depth for the 1978 Santa Barbara earthquake. They also derived a few focal mechanisms that may indicate sub-horizontal shearing. Along the south front of the Santa Monica Mountains, focal mechanisms for aftershocks of the 1973 Pt. Mugu earthquake possibly indicate a broad zone of imbricate faulting between 12- and 17-km depth (Stierman and Ellsworth, 1976). This might be typical of the upper plate above a decollement. Gutenberg (1951) postulated a low-velocity zone in the lower crust on the basis of data from large quarry blasts. Hadley and Kanamori (1979) have derived an S-wave velocity structure for the southern Mojave and central Transverse Ranges which indicates a low-velocity zone between 10 and 20 km depth.

Models. Thatcher (1976) used a low-angle thrust fault successfully to model vertical displacements preceding the 1971 San Fernando earthquake. Rundle (1978) and Rundle and Thatcher (1980) have suggested that the Palmdale Bulge was caused by aseismic slip of a low-angle thrust fault. Savage *et al.* (1981) have modeled changes in horizontal compression across the San Andreas fault during 1979 as a horizontal southward-propagating dislocation under the Transverse Ranges. Luyendyk *et al.* (1980) have tried to explain apparent rotations of paleomagnetic

vectors in Miocene volcanics with a model that rotates the whole Transverse Ranges by 90° in a clockwise direction. They, however, fail to address the question of what happens at the bottom of this block. If they are correct, the amount of rotation must either gradually decrease downward through a ductile transition zone, or detachment must occur at some level.

The Study

The study area considered herein is shown in figure 3-1, along with all the data: 5800 quality-A earthquakes that occurred between June 1977 and September 1981. The principal features of the seismicity are the east-west trend through the Transverse Ranges, and the high seismicity trend along the San Jacinto fault and southeast into the Imperial Valley. The next few figures show how the seismicity pattern changes for different depth cutoffs. Figure 3-2 shows all the A-quality events deeper than 5 km. The main difference from the previous figure is a thinning of seismicity northeast of the San Andreas fault in the southern Mojave Desert and the eastern Transverse Ranges. Below 10 km (figure 3-3), the seismicity in the southern Mojave Desert and eastern Transverse Ranges thins dramatically, and seismicity starts to decrease noticeably in other regions. Below 15 km (fig. 3-4) there is virtually no activity northeast of the San Andreas fault, and very little activity elsewhere. What remains is a trend of deep activity at the southern front of the mountains, and along the San Jacinto fault southeast toward the Imperial Valley. There are only 8 events deeper than 20 km (fig. 3-5), 4 in the western Transverse Ranges and 4 in the San Gorgonio Pass area.

Another way to look at these data is with a histogram of the number of events versus depth (fig. 3-6a) and log moment vs. depth (fig. 3-6b). In figure 3-6a it is obvious that the great bulk of the activity is shallow (< 6 km) and tapers off at 20

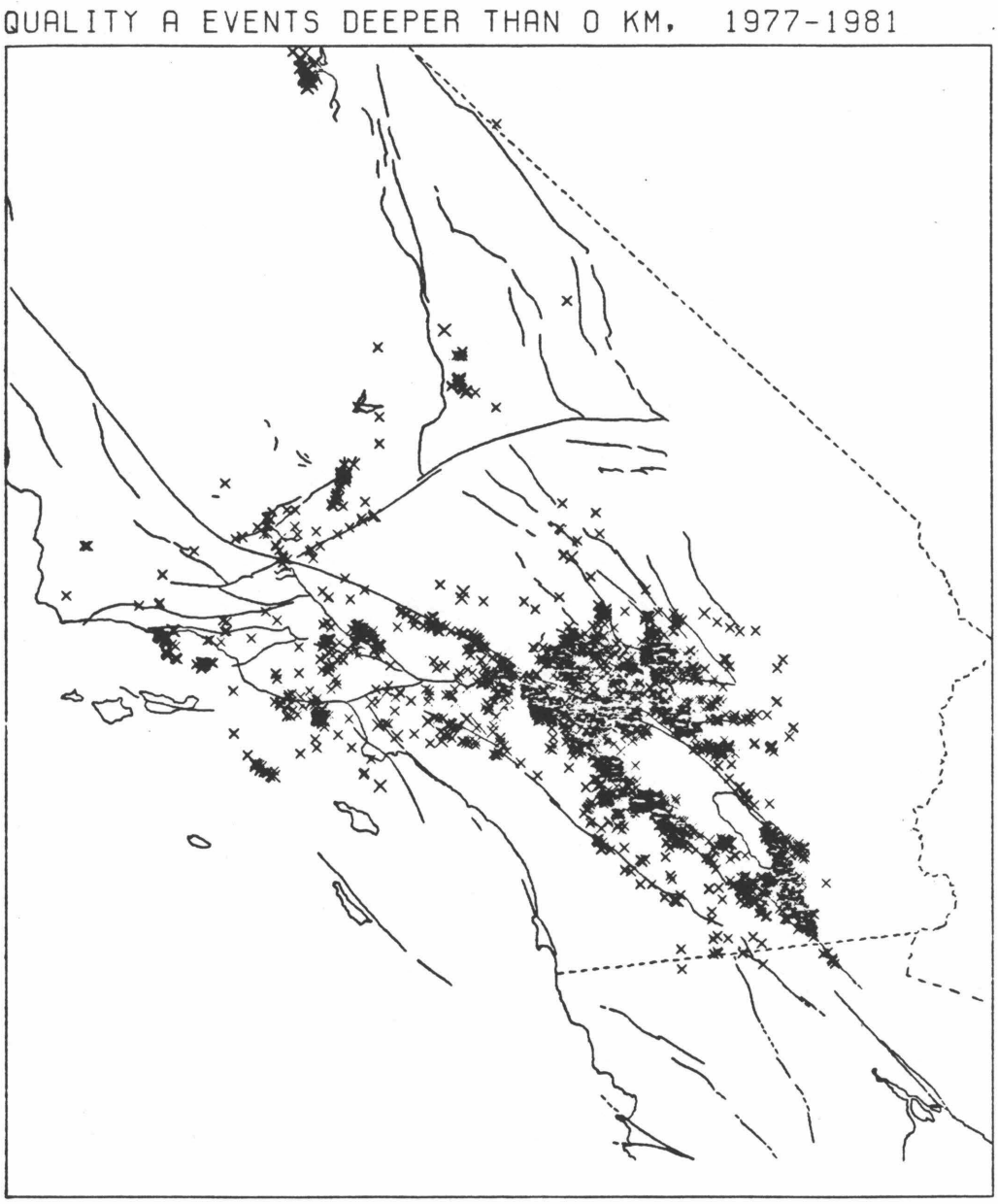

Figure 3-1. Map of study area showing all data used: 5800 quality-A earthquake locations from the Caltech catalog.

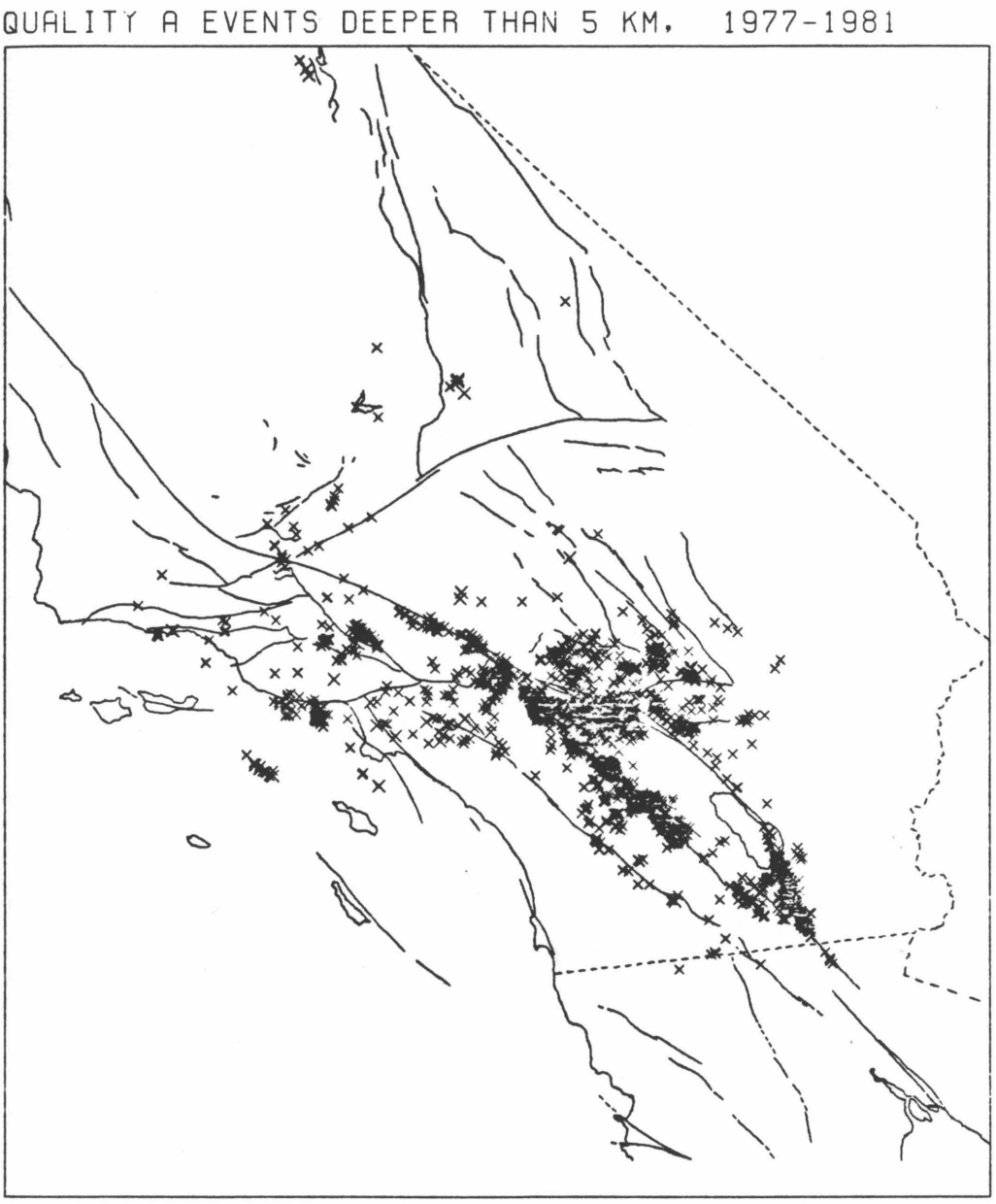

Figure 3-2. Map of all earthquakes deeper than 5 km.

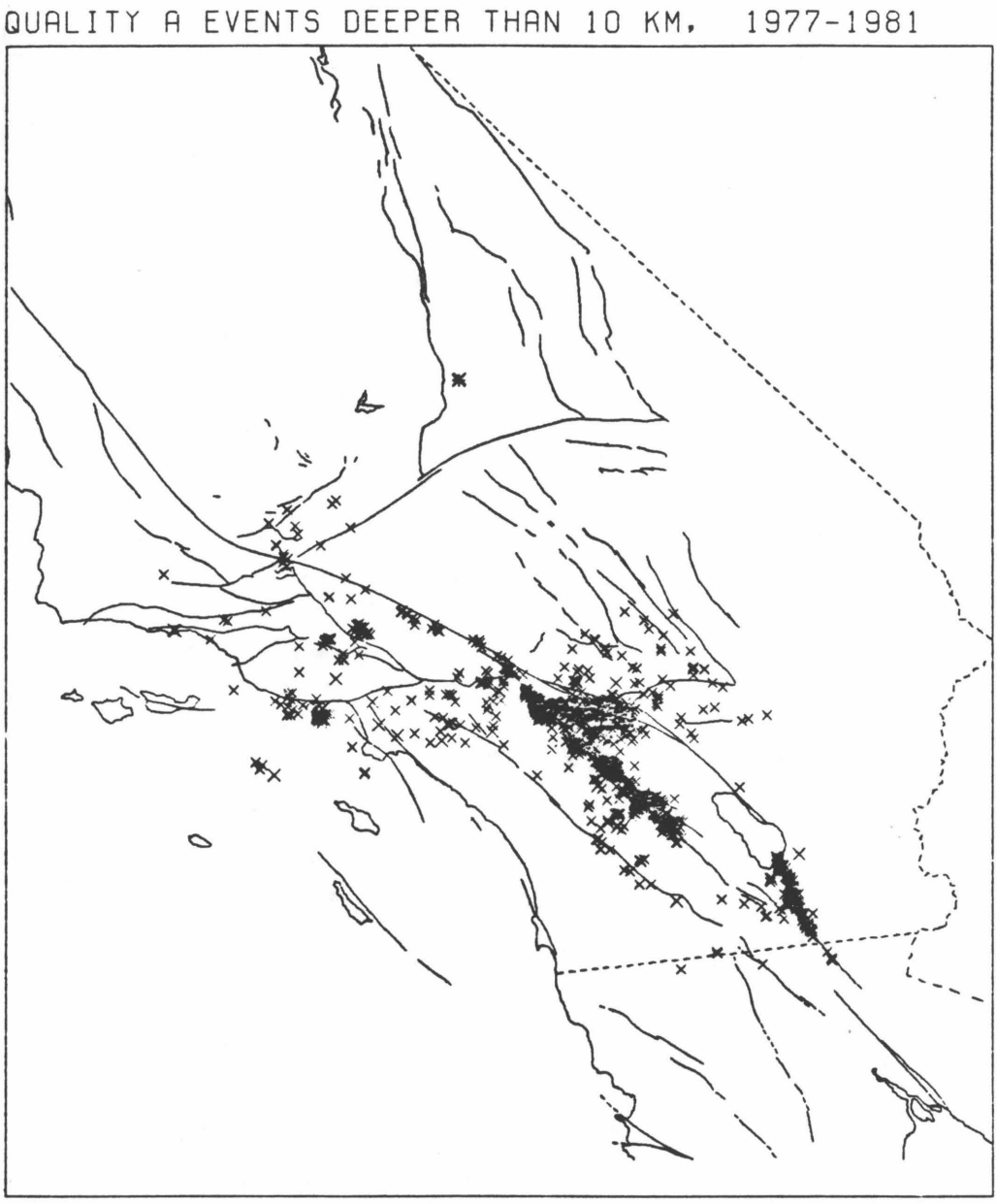

Figure 3-3. Map of all earthquakes deeper than 10 km.

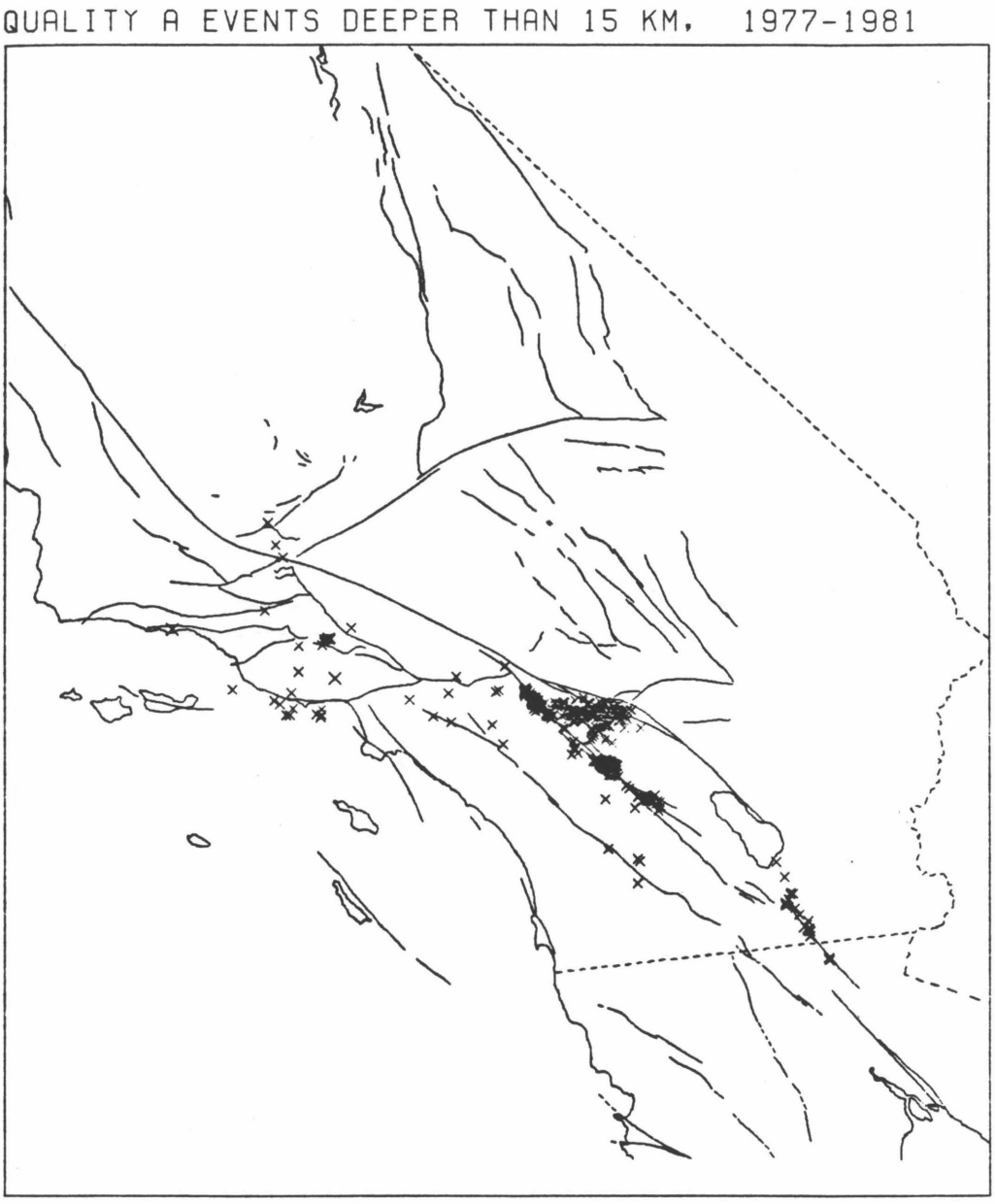

Figure 3-4. Map of all earthquakes deeper than 15 km.

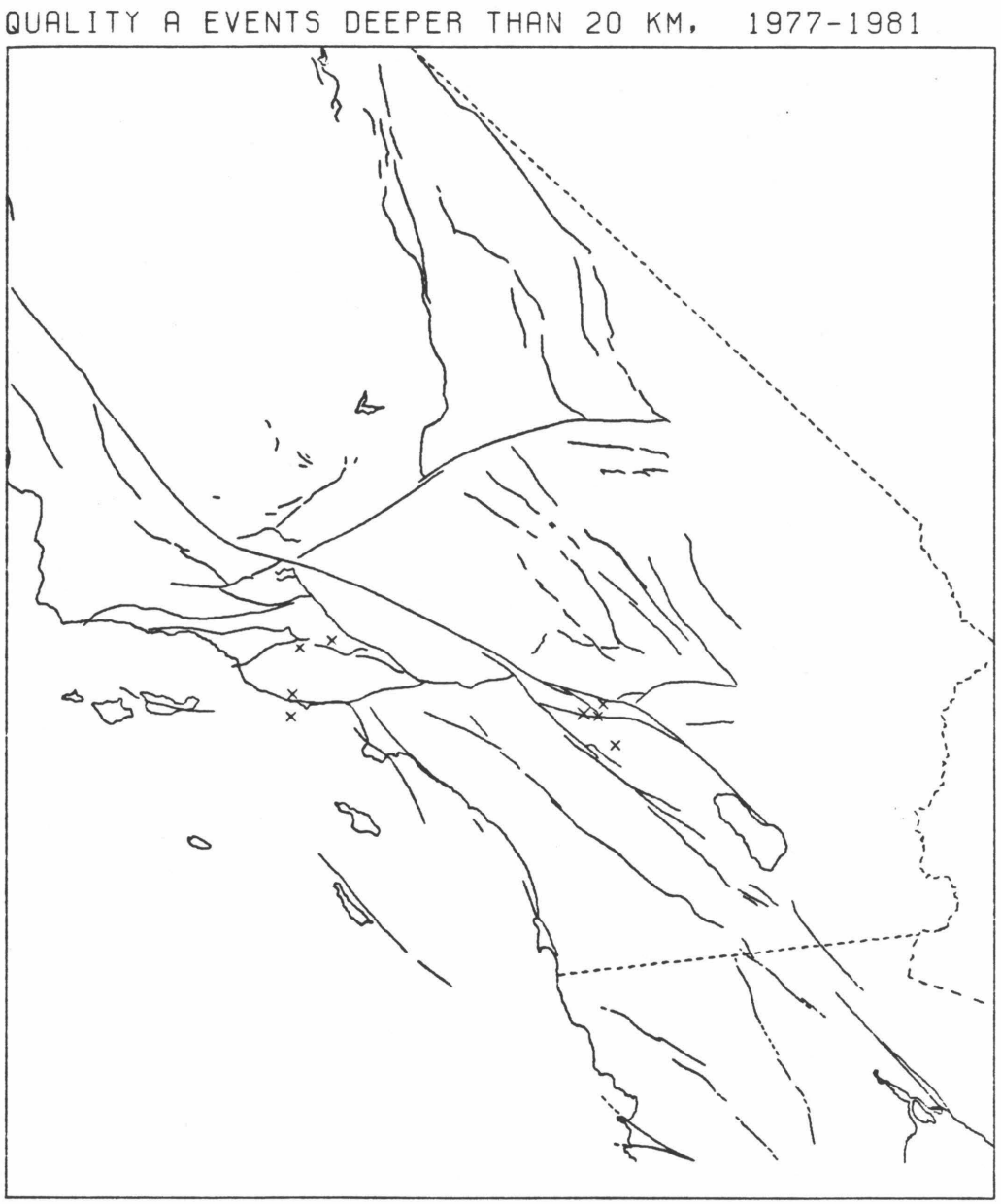

Figure 3-5. Map of all earthquakes deeper than 20 km.

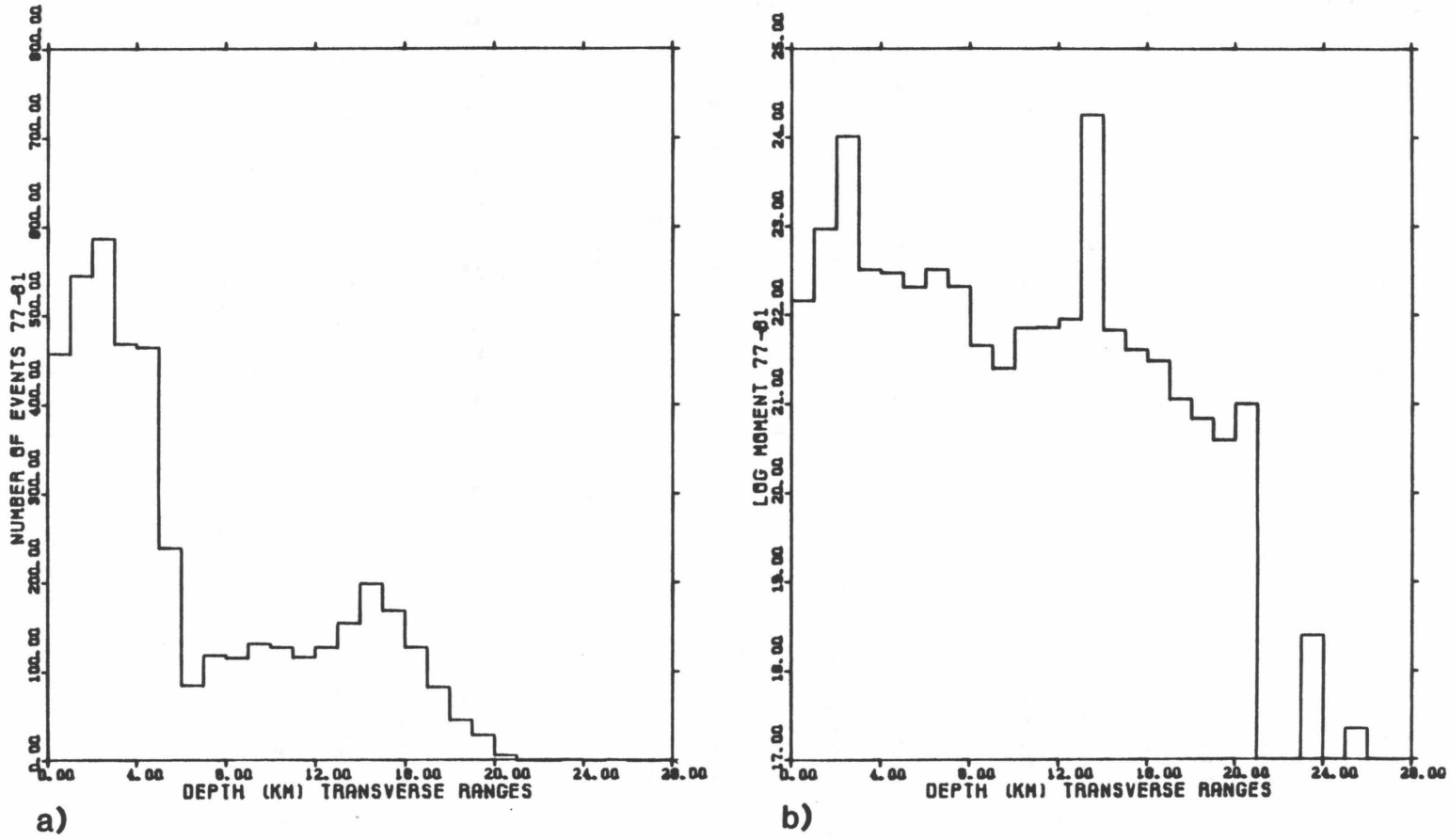

Figure 3-6. Histograms of seismic energy release at different depths. a) number vs. depth, b) moment vs. depth.

km depth. The log-moment diagram shows a similar trend--a systematic decrease in energy release with depth. Peaks at 3 km and 13 km are evidently related to single events. If we cut the study area in two, along a line corresponding to the San Andreas fault, a slightly different picture emerges. The western Transverse Ranges (figure 3-7) show earthquakes down to 20 km depth, with a rather variable energy release vs. depth. In figure 3-8, for the eastern Transverse Ranges and the area northeast of the San Andreas fault, most of the energy release is shallow with a very steep drop off. There is only one event below 12 km.

Next will be presented a series of north-south cross-sections through the Transverse Ranges proceeding from west to east, using no vertical exaggeration. Figures 3-9 through 3-16 will alternately show map views of sections of the Transverse Ranges followed by their accompanying 4 cross-sections. On the map views the locations of the 4 cross-sections are indicated as well as the 34th parallel, which is the reference-axis for the cross-sections.

Cross-Sections through the Transverse Ranges

Western Transverse Ranges. In figure 3-9, the four cross-sections sample seismic activity in the Santa Barbara Channel and Continental Borderland. Figure 3-10a intersects possible north-dipping structures south of Santa Barbara. Figure 3-10b indicates a possible north-dipping structure in the eastern Santa Barbara Channel. Figure 3-10c shows a weak hint of north dip under the mountains north of Ventura. On figure 3-10d activity at x=-40 km is the 1981 Santa Barbara Island activity, which exhibits a diffuse pattern. Depth control here is poor and it is questionable if these events are truly quality-A. At x=0 km we see the aftershock zone of the 1973 Pt. Mugu earthquake. There are scattered events down to 20 km, but no obvious pattern is seen.

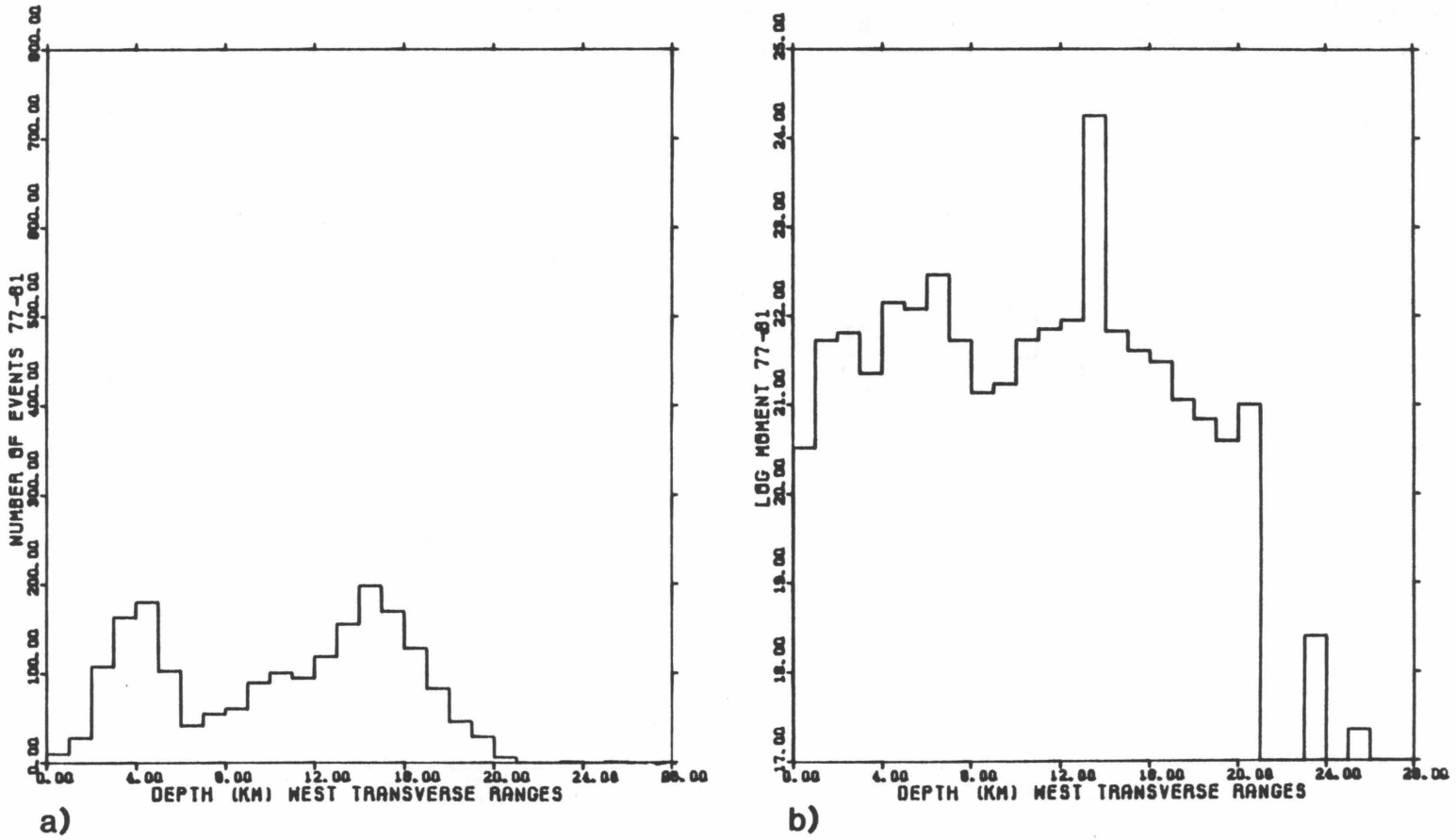

Figure 3-7. Histograms for all events located in the Transverse Ranges southwest of the San Andreas Fault. a) number vs. depth, b) moment vs. depth.

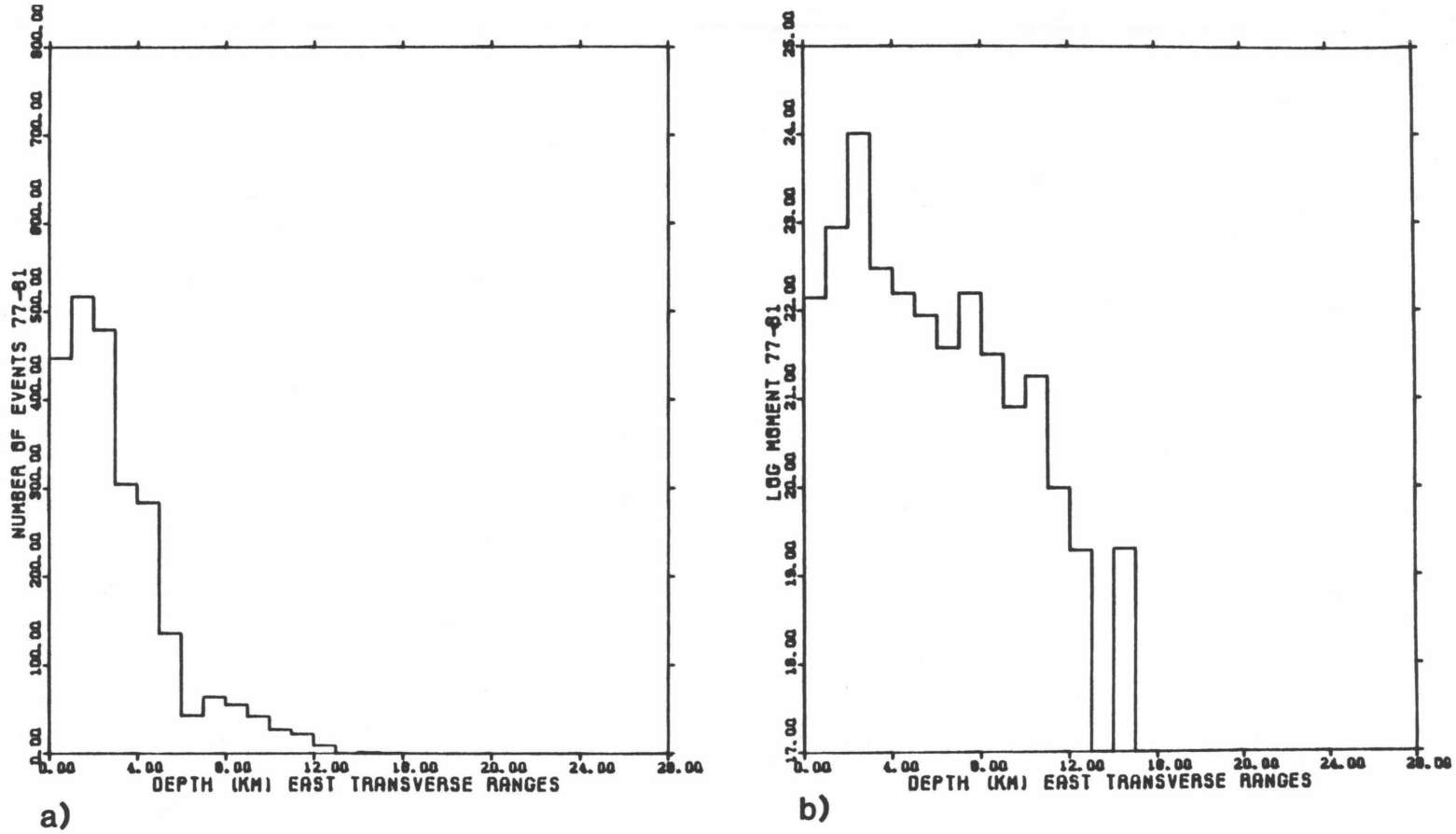

Figure 3-8. Histograms for all events located in the Transverse Ranges northeast of the San Andreas Fault. a) number vs. depth, b) moment vs. depth.

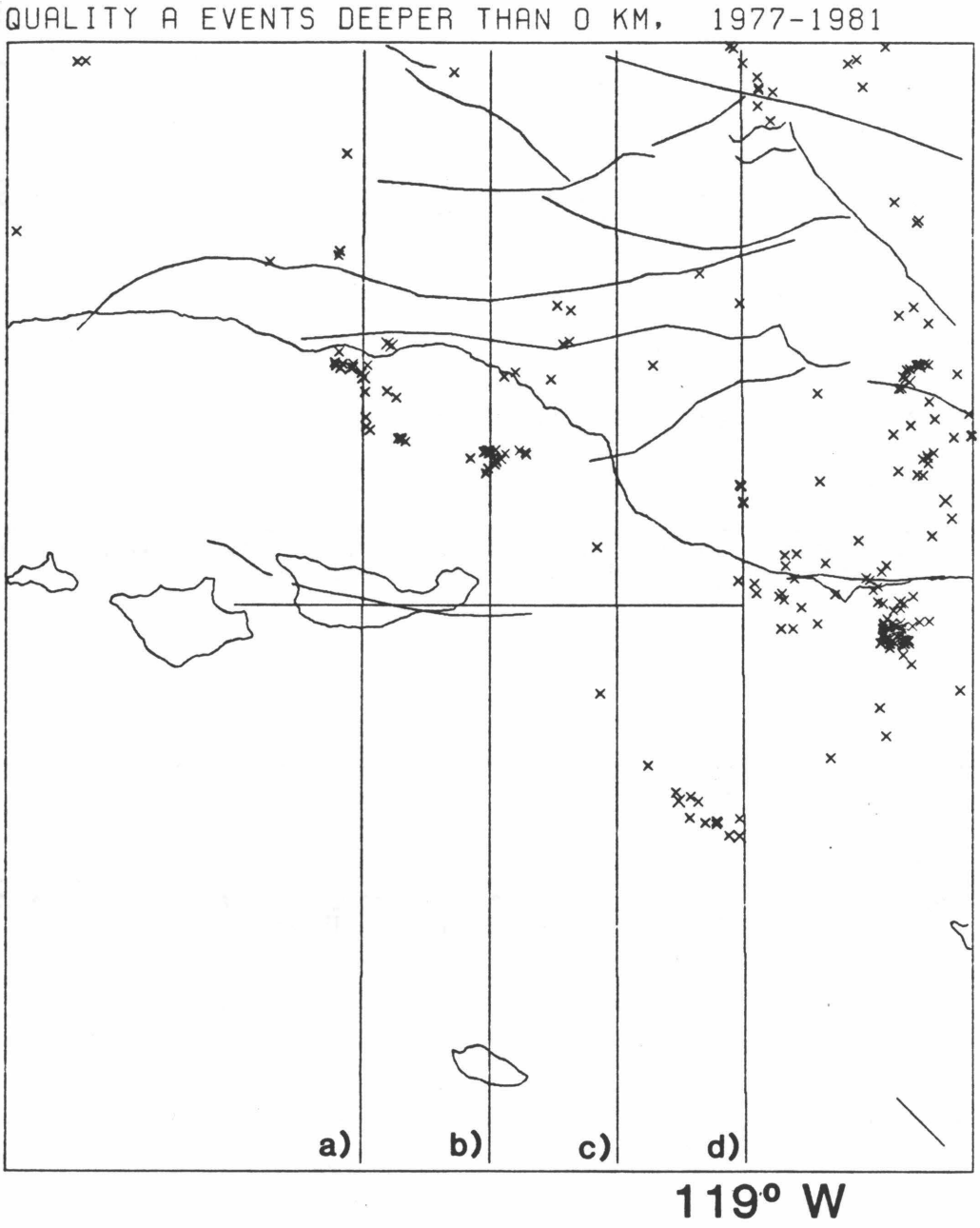

Figure 3-9. Map of seismicity in the western Transverse Ranges. Vertical lines show cross-sections in figure 3-10. Jagged lines are faults from Jennings (1975).

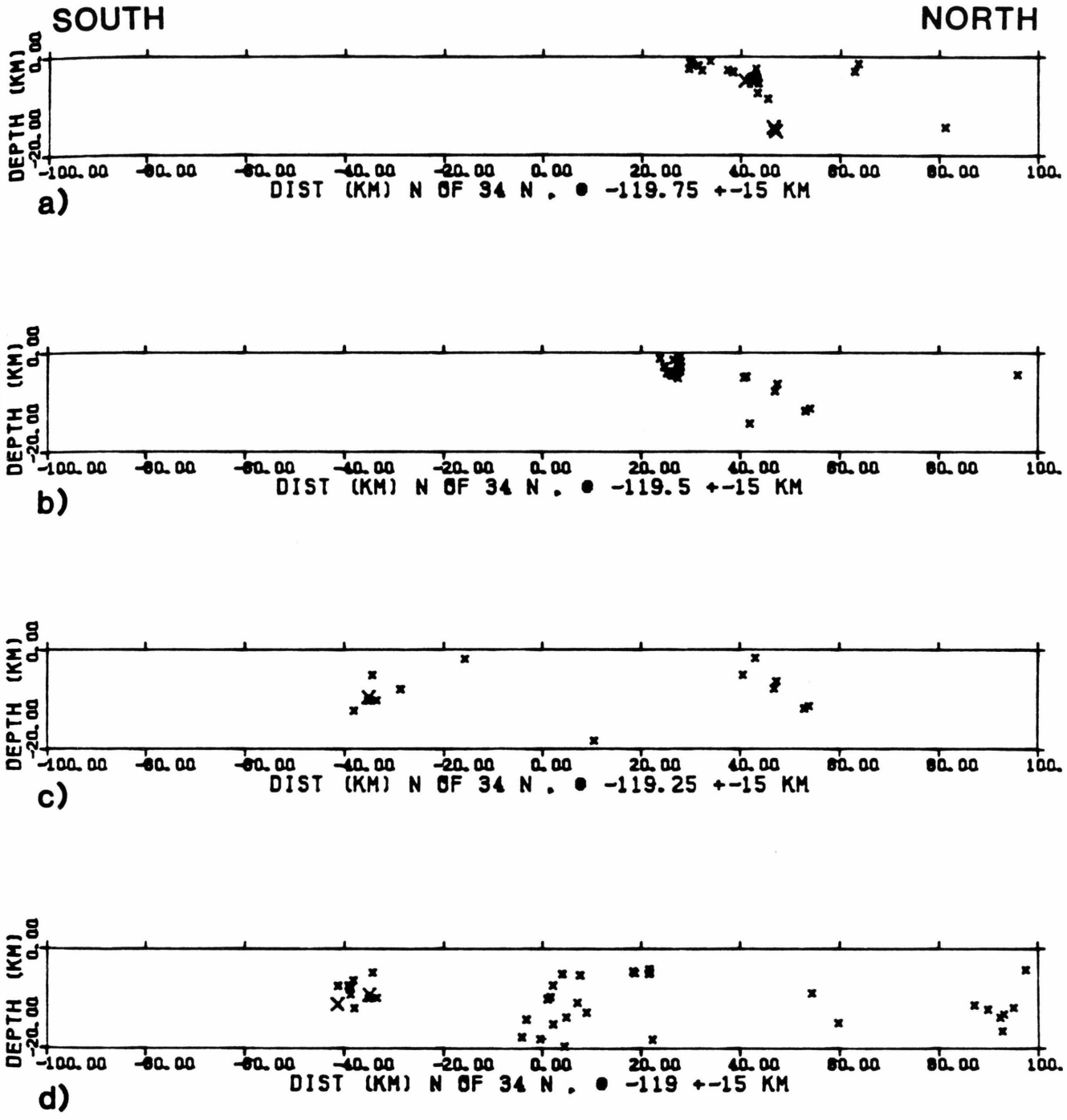

Figure 3-10. South to north cross-sections of figure 3-9. No vertical exaggeration.

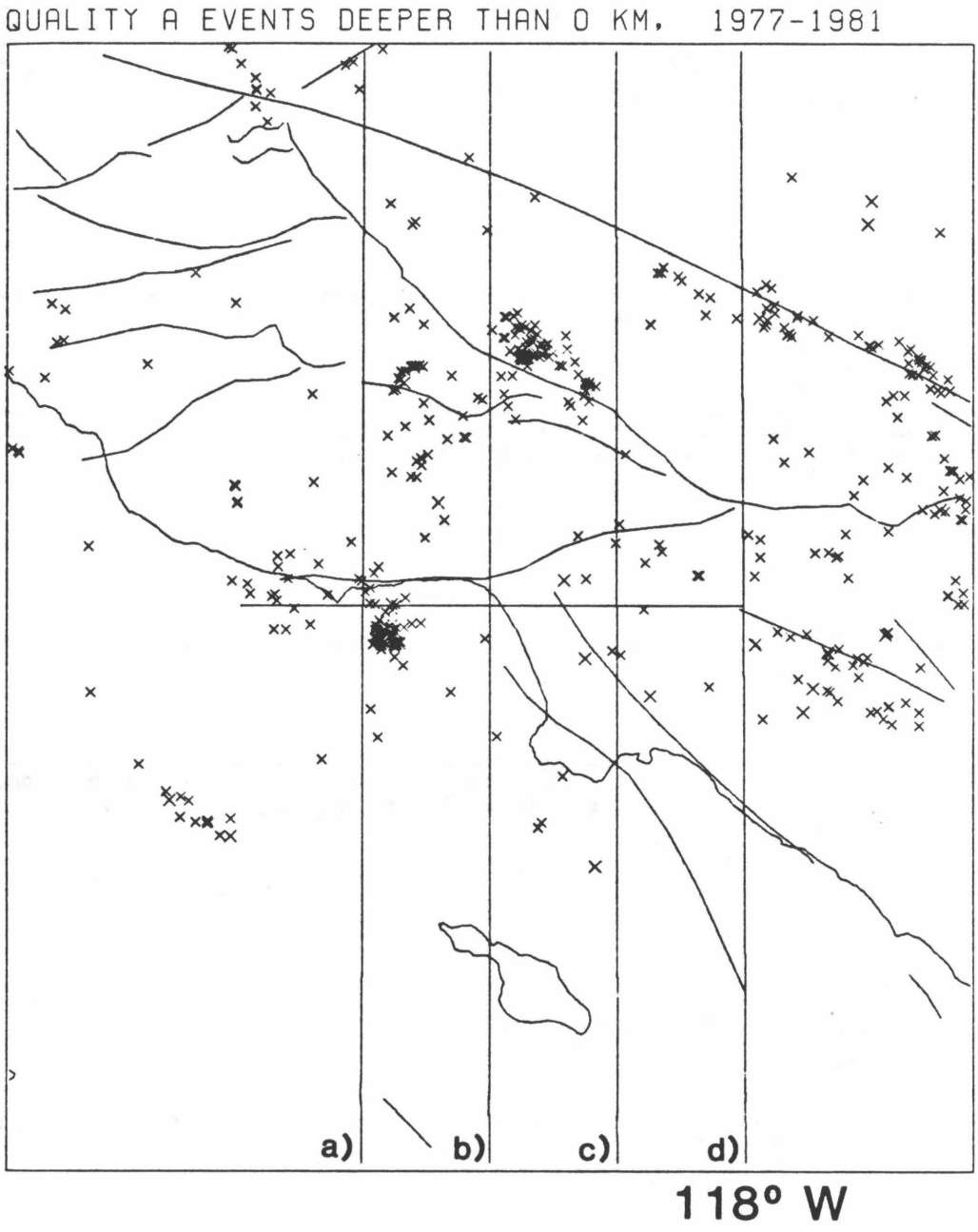

Figure 3-11. Map of seismicity in the west-central Transverse Ranges. Vertical lines show cross-sections in figure 3-12.

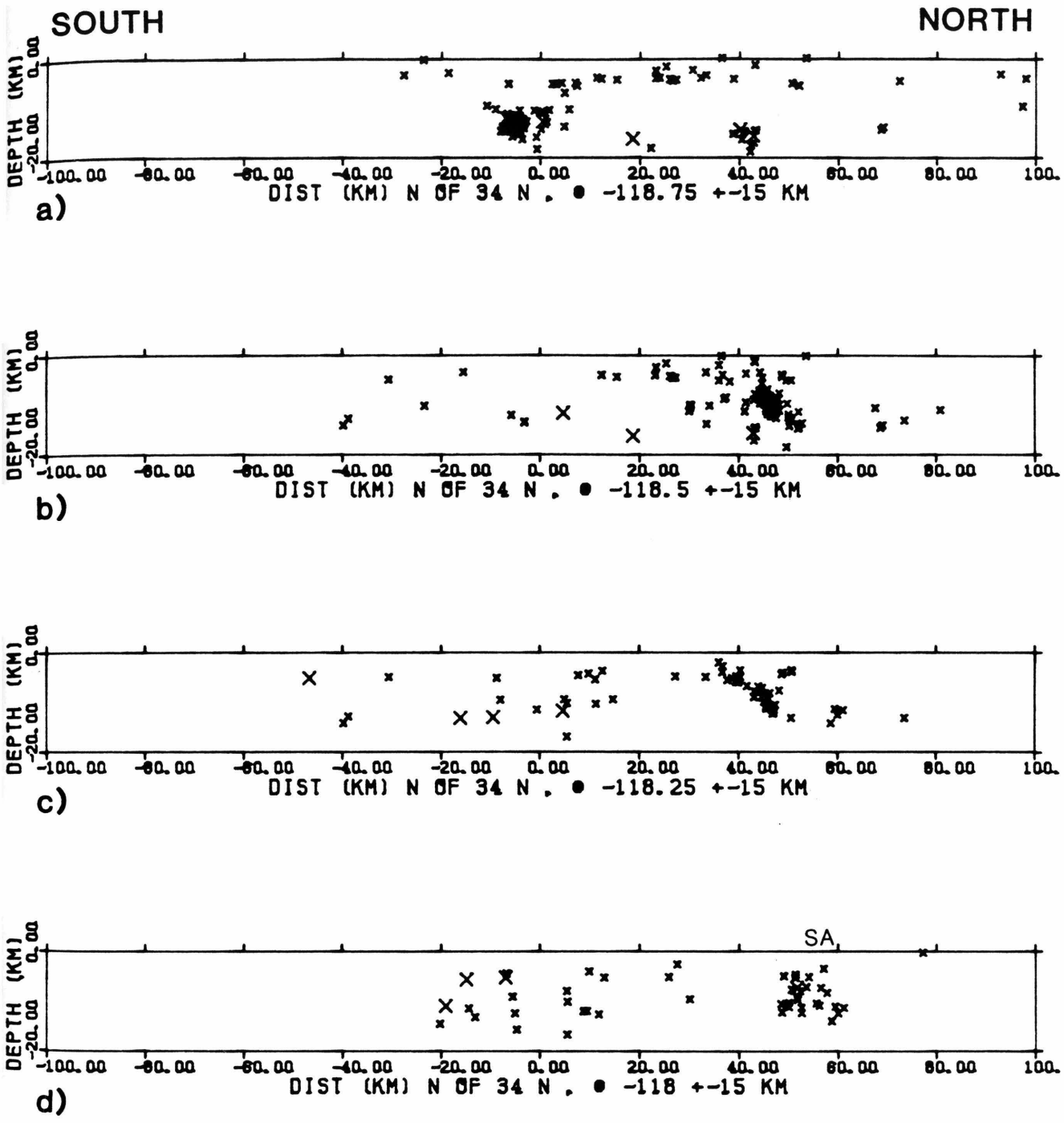

Figure 3-12. South to north cross-sections of figure 3-11. No vertical exaggeration. SA indicates where section croses the San Andreas fault.

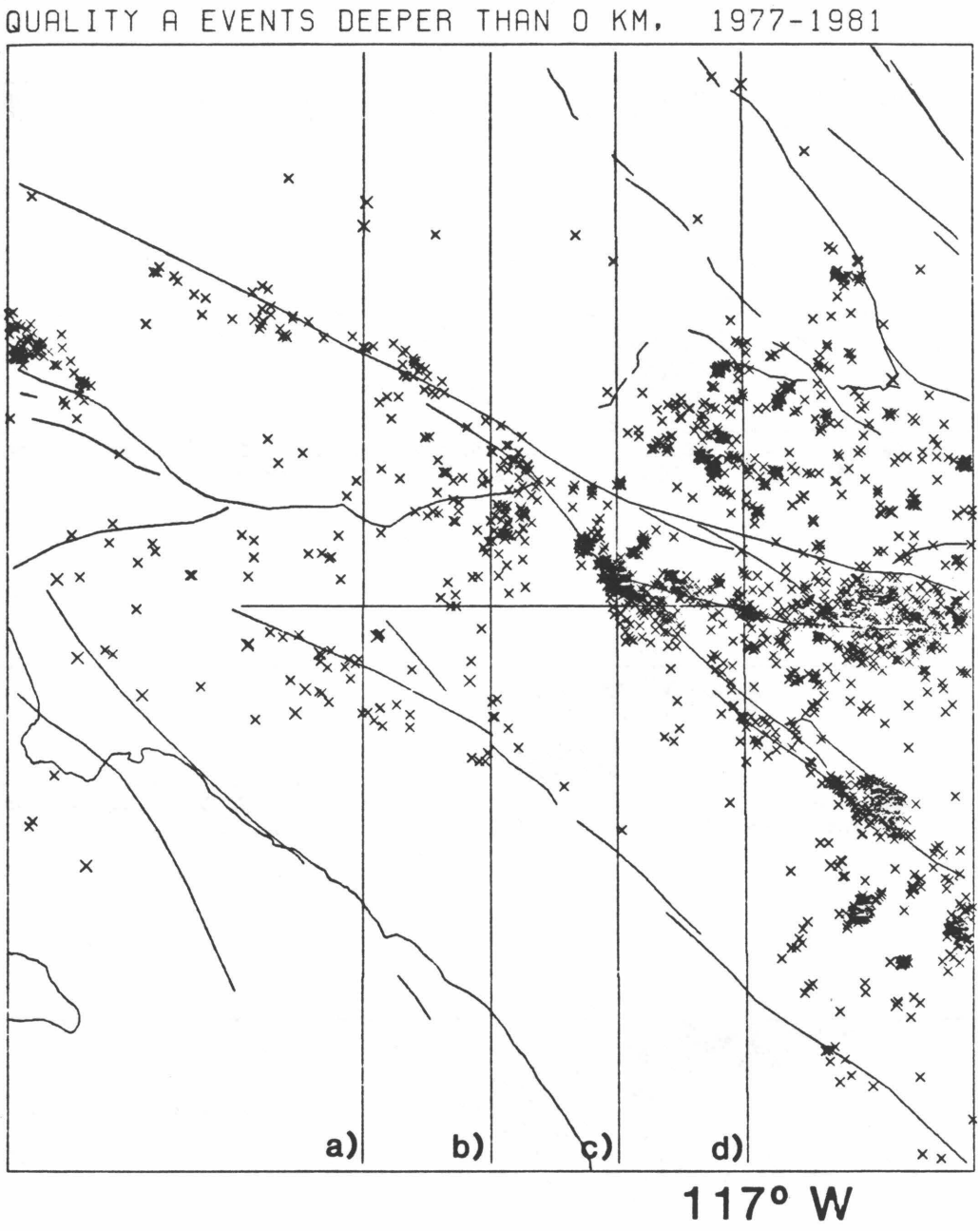

Figure 3-13. Map of seismicity in the east-central Transverse Ranges. Vertical lines show cross-sections in figure 3-14.

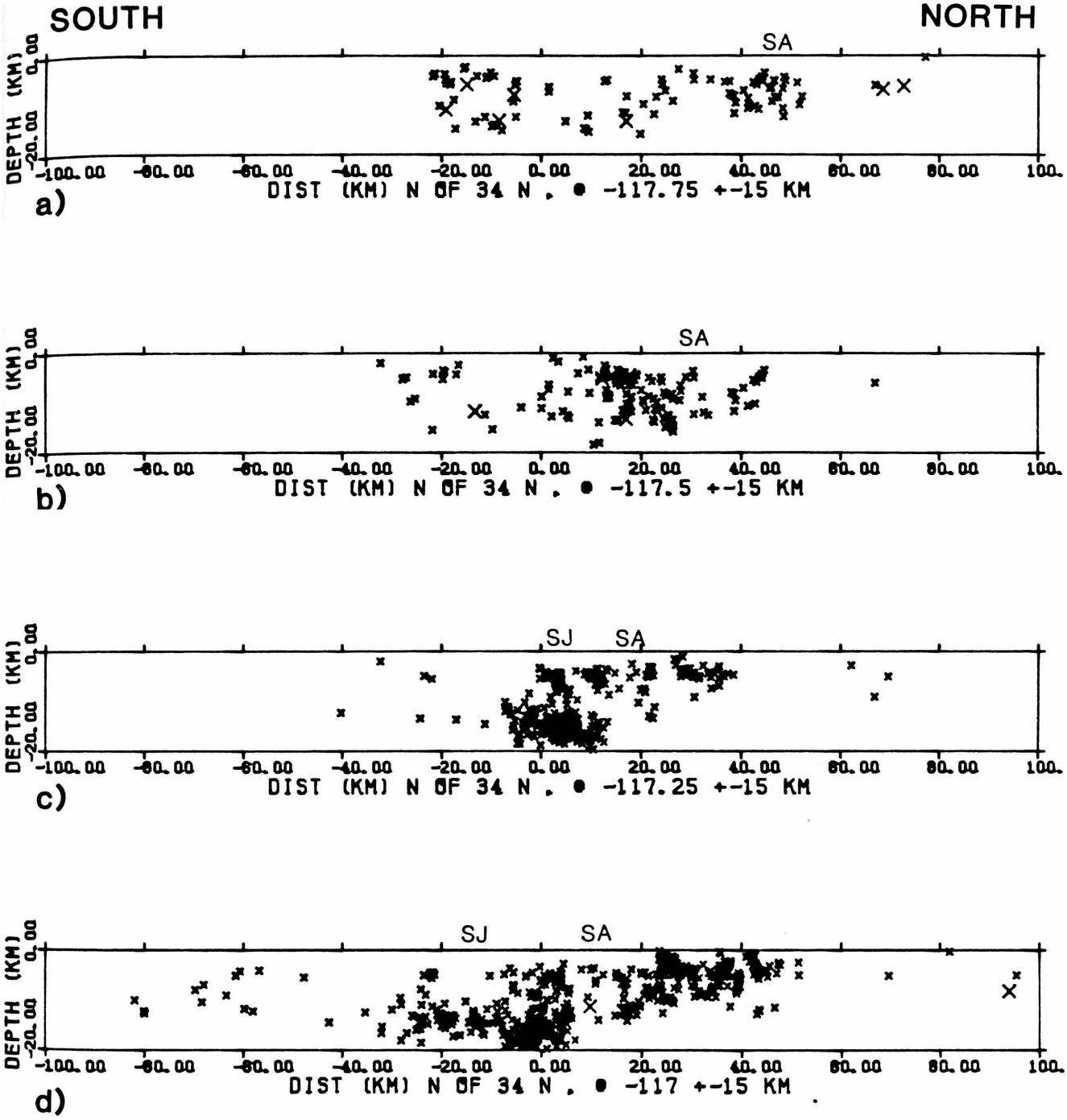

Figure 3-14. South to north cross-sections of figure 3-13. No vertical exaggeration. SA indicates where section croses the San Andreas fault. SJ: San Jacinto fault.

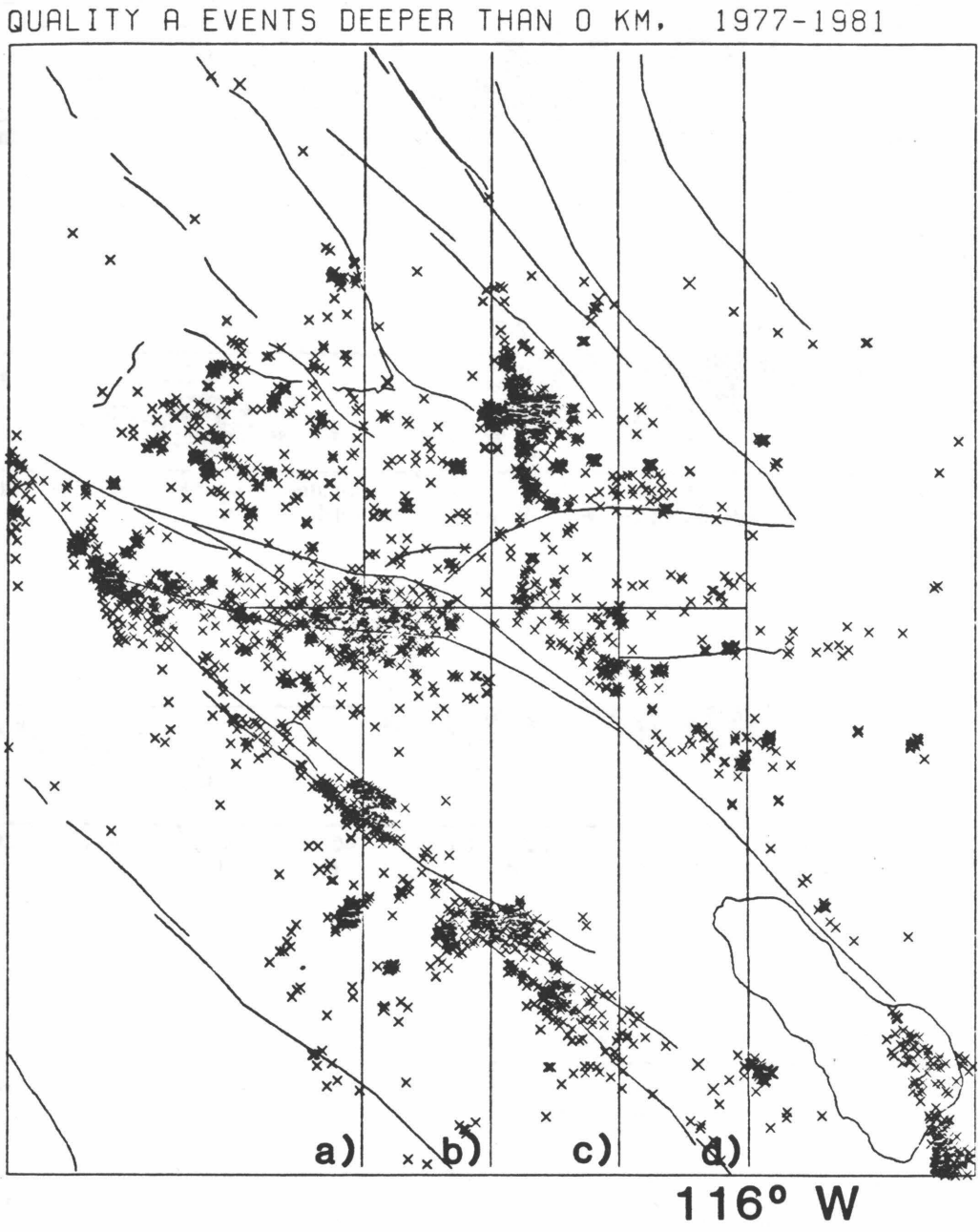

Figure 3-15. Map of seismicity in the eastern Transverse Ranges. Vertical lines show cross-sections in figure 3-16.

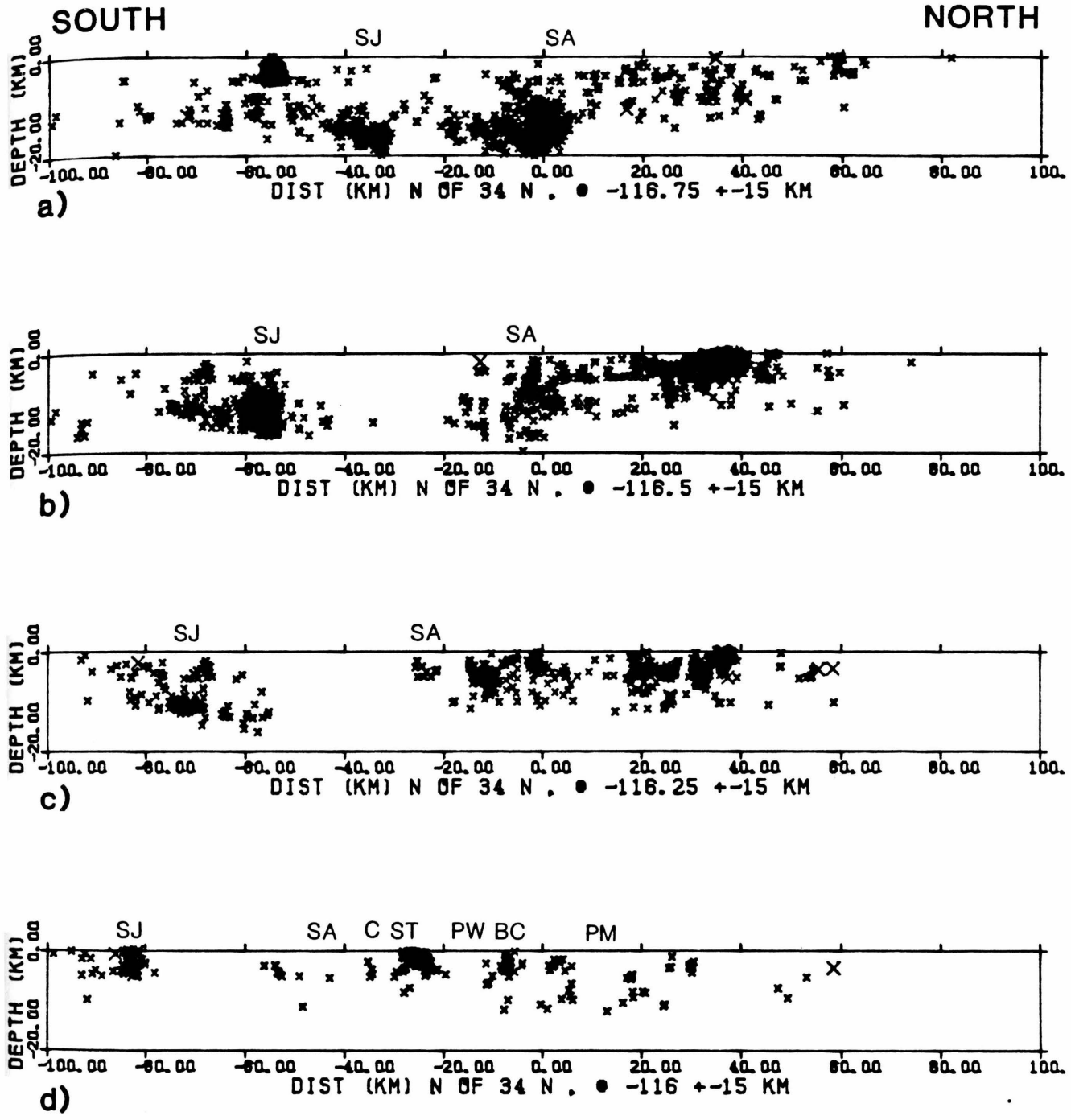

Figure 3-16. South to north cross-sections of figure 3-15. No vertical exaggeration. SJ: San Jacinto fault; SA: San Andreas fault; C: Chiriaco fault; SM Smoke Tree Wash fault; PW: Porcupine Wash fault; BC: Blue Cut fault; PM: Pinto Mountain fault.

West-central Transverse Ranges. The next four cross-sections (figure 3-11) primarily show activity near Malibu, the mountains north of San Fernando, and the Los Angeles Basin. Figure 3-12a primarily shows the New Year's Day, 1979, Malibu sequence. No structure is apparent, but there is activity down to 20 km, which is deep for southern California. Some of the scatter may be due to problems with locations at that time (Kate Hutton, oral comm.). Figure 3-12b samples the west end of the aftershock zone of the 1971 San Fernando earthquake and gives some hint of a northerly dip. Figure 3-12c crosses the east end of the San Fernando aftershock zone and shows a clear 45° N dip. Scattered deep to shallow activity is also apparent in the Los Angeles Basin. Figure 3-12d illustrates scattered activity in the eastern Los Angeles Basin and on the San Andreas fault near Palmdale. No pattern is apparent.

East-central Transverse Ranges. The next four cross-sections (fig. 3-13) sample activity from west of Cajon Pass, east through San Bernardino to San Gorgonio Pass. Figure 3-14a shows the eastern San Gabriel Mountains and eastern San Gabriel Valley. There is no clear structure, but there is a slight hint of events becoming shallower to the north. Figure 3-14b crosses through Cajon Pass. There is no apparent structure, but events are shallowing towards the north. Figure 3-14c shows activity under the western San Bernardino Mountains and the San Bernardino Valley. Shallowing towards the north is even more apparent. Activity is noticeably deeper south of the San Andreas fault. Figure 3-14d shows a most definite shallowing toward the north, with a clear lower limit to the seismicity under the San Bernardino Mountains. The San Andreas fault crosses at x=5 km and apparently marks the north edge of the deep (20 km) seismicity in the San Gorgonio Pass area near Banning.

Eastern Transverse Ranges. On figure 3-15 the last 4 cross-sections show activity in San Gorgonio Pass, in Homestead Valley, and east toward the southeastern

Mojave Desert. Figure 3-16a again shows the seismic zone shallowing to the north under the eastern San Bernardino Mountains, and as well as activity in the San Andreas fault zone in San Gorgonio Pass and along the San Jacinto fault 40 km farther south. Figure 3-16b shows deep activity along the San Jacinto fault, San Andreas fault, and shallow activity of the Homestead Valley earthquakes of 1979 (x=35 km). In figure 3-16c activity dies out southwest of the San Andreas fault, and is less than 10 km deep north of the San Andreas fault. Activity becomes shallower along the San Jacinto fault. The easternmost cross-section (figure 3-16d) shows activity on the several east-trending left-lateral faults east of the San Andreas fault. Seismicity along the southern San Jacinto fault is evidently quite shallow (< 5 km). The San Andreas fault is noticeably quiet.

Recent Seismicity. Since this study was initially completed, seismicity has of course continued throughout southern California. To verify that the pattern has not changed in the interim, the Caltech catalog was re-searched for the time period from October 1981 to August 1983. This search was carried out for the most intriguing area: the San Bernardino Mountains. Figure 3-17 shows that the overall seismicity pattern for the last two years is essentially the same as for the previous four (figure 3-15). The main difference is that the seismicity is thinner, reflecting the shorter time period. Also the Homestead Valley aftershock zone has died down to background level. In cross-section (fig. 3-18), the region also looks the same as before (fig. 3-14d). Note that the cross-section includes a slightly wider area that is equivalent to the whole width of the San Bernardino Mountains. There are fewer events, but deep seismicity south of the San Andreas fault and a south-dipping bottom to the seismic zone are still apparent.

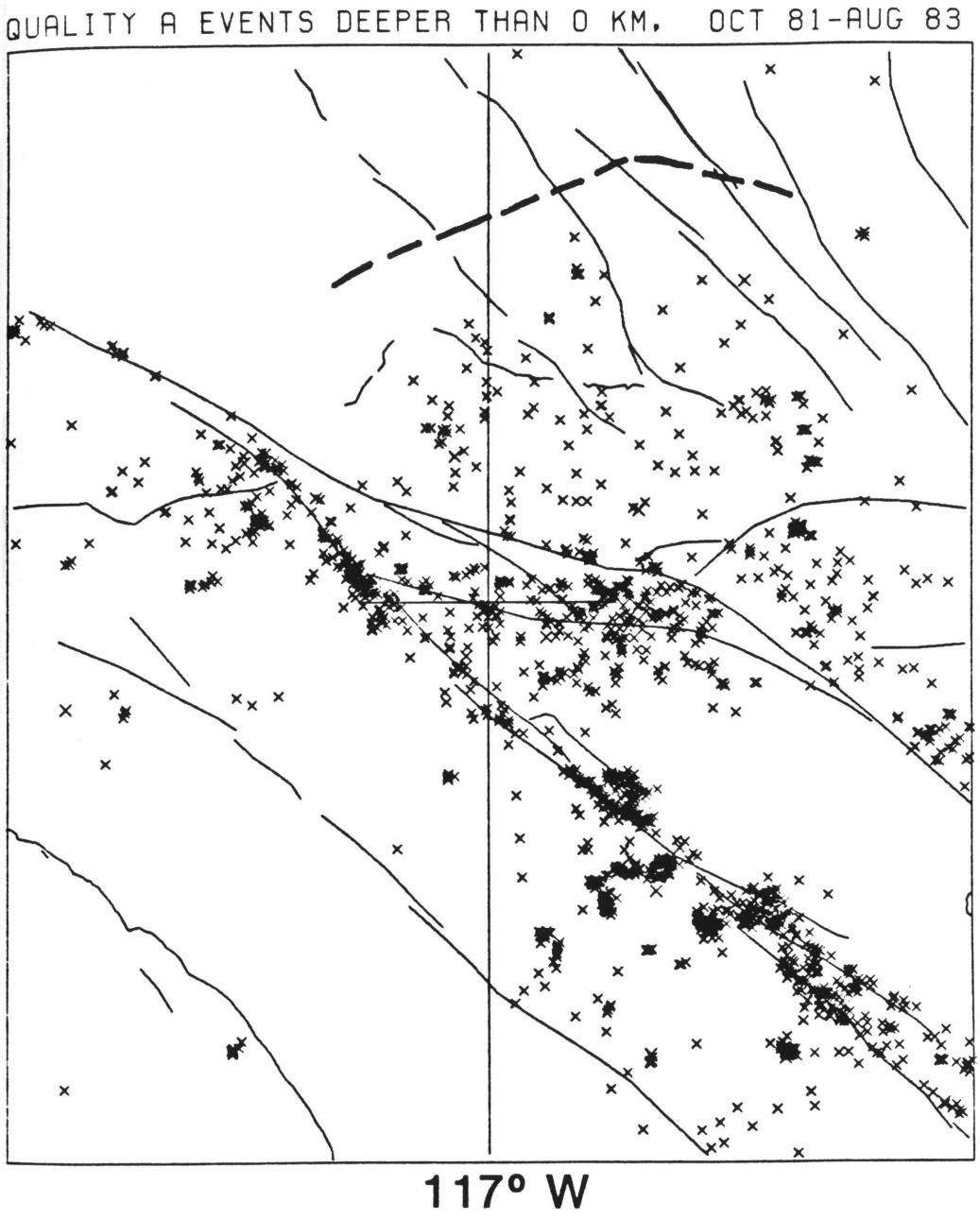

Figure 3-17. Map of seismicity of the Transverse Ranges in the vicinity of the San Bernardino Mountains, October 1981 to August 1983. Vertical line shows cross-section in figure 3-18. Horizontal line shows width of projection. Heavy dashed line shows surface projection of the base of the seismogenic zone, based on northward projection from figures 3-14c and d, 3-16a and b, and 3-18.

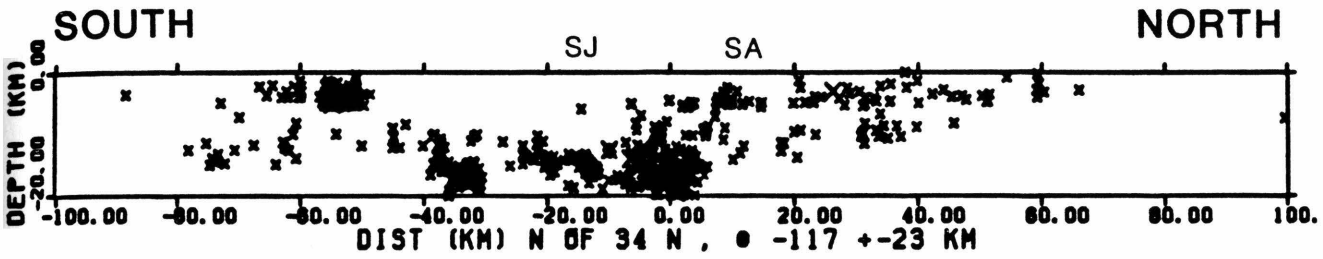

Figure 3-18. South to north cross-section of figure 3-18. No vertical exaggeration. Same as figure 3-14d, except for later time period, and wider zone.

Accuracy of Locations

There are a number of potential problems in this data set that should be mentioned. First, it should be noted that the overall seismicity pattern (fig. 3-1) looks remarkably similar to the pattern of station distribution (fig. 3-19). Undoubtedly, the heavy concentration of stations through the Transverse Ranges and throughout the Imperial Valley is partly responsible for the large numbers of well-located events in these regions. It must be remembered, however, that the stations were in fact installed where the highest activity had historically occurred. The histograms of number vs. depth (fig. 3-6) also may show an artifact of velocity structure. The standard Caltech location procedure uses a starting location of 5 km and the velocity model indicated by table 3-1.

Table 3-1. Caltech Velocity Model

P-velocity (km/sec)	Depth (km)
5.5	0.0
6.3	5.5
6.7	16.0
7.8	37.0

Evidently, events can artifically concentrate just above 5 and 16 km, robbing the surrounding ± 2 km, and still qualify as A-quality. In this light, it was decided to test one of the cross-sections numerically to see how much it is influenced by station distribution and velocity model. I chose the section shown in figure 3-14d, since it seems to be the most provocative.

To test the effect of station distribution, a grid of "earthquakes" was designed on 5-km centers (fig. 3-20a) and theoretical travel times were calculated for about a dozen nearby stations. The travel times were then used to locate the artificial events to see how many would locate as quality-A. When only P-times were used, all the

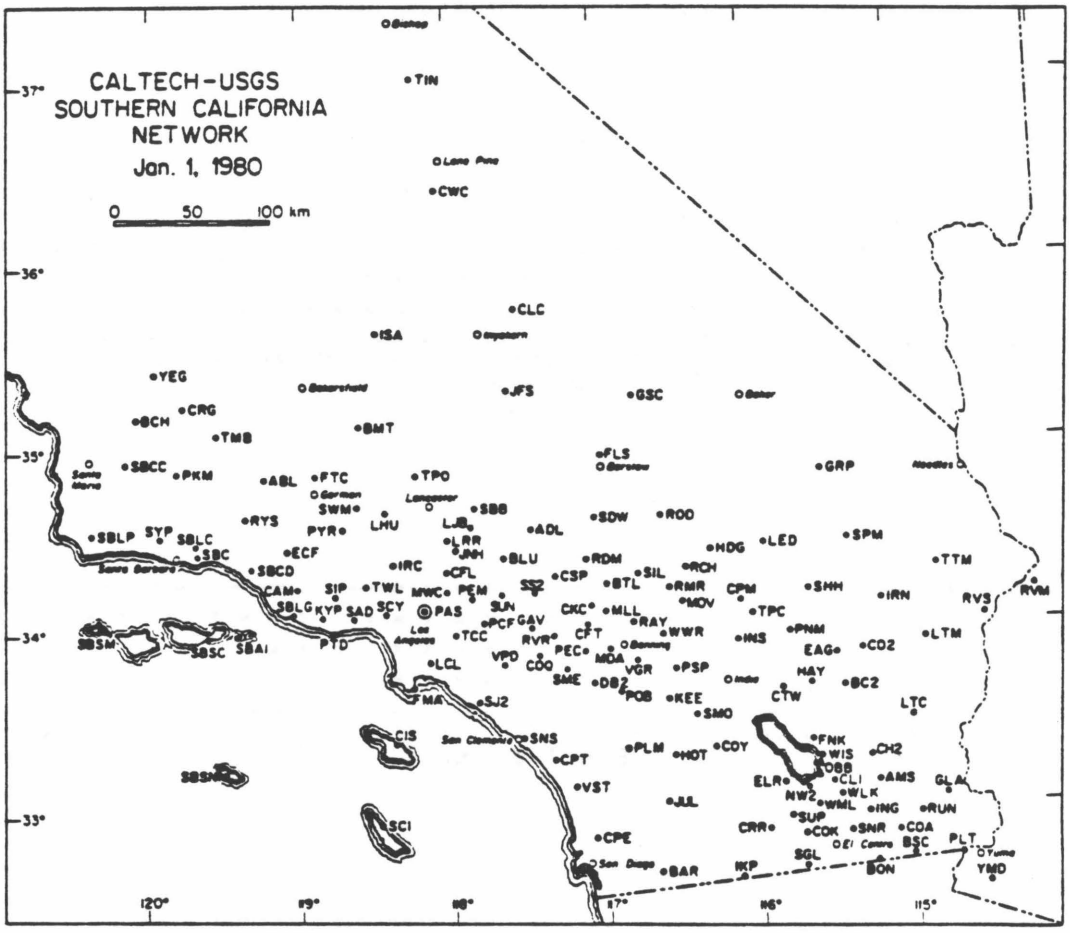

Figure 3-19. Map of Southern California Array for Research on Local Earthquakes and Teleseisms (SCARLET).

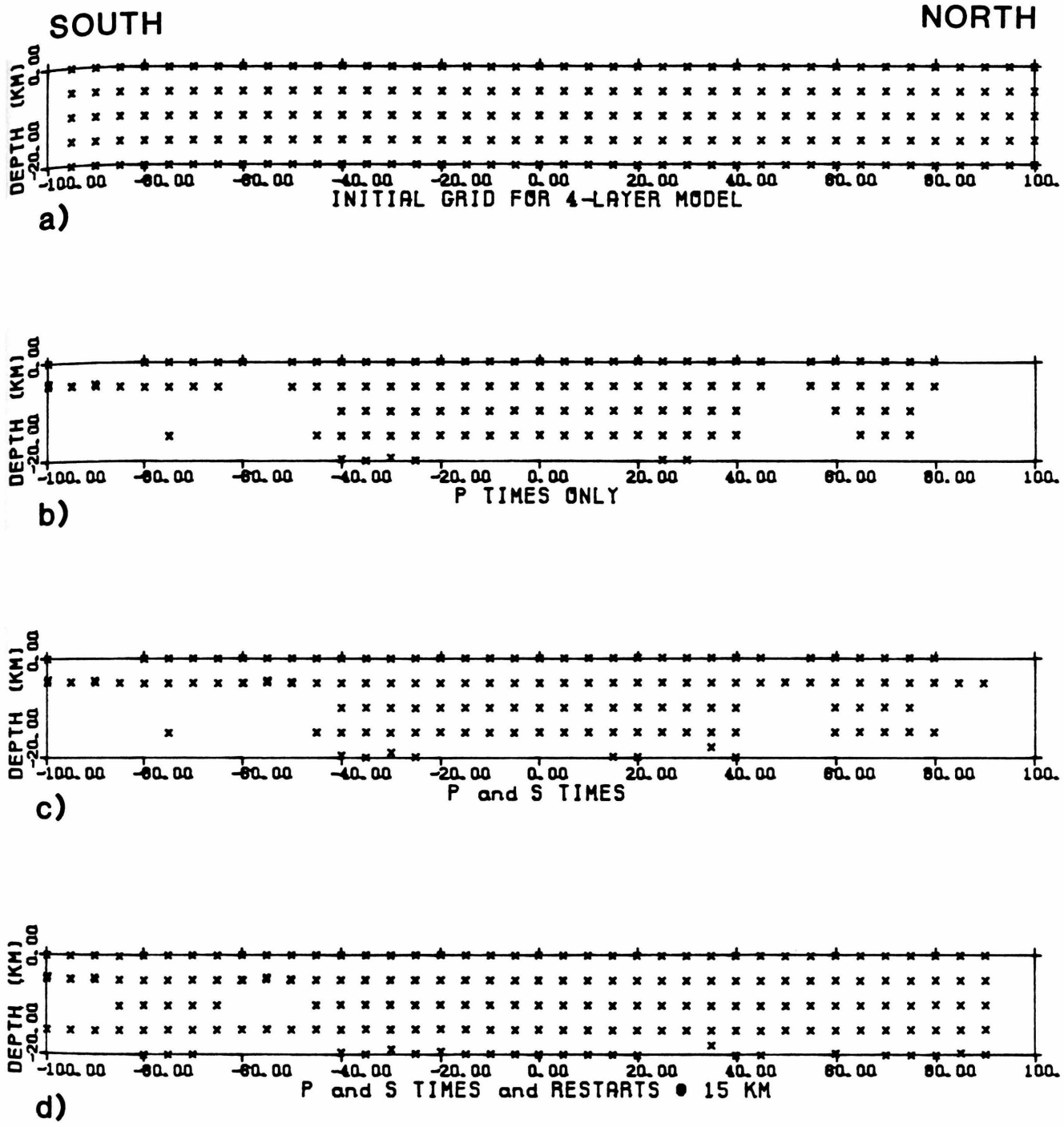

Figure 3-20. Cross-sections of synthetic A-quality earthquake locations done to test the effects of station distribution and location method.

events located within 1 km of their correct epicenters, but only 118 out of 205 located with quality-A (fig. 3-20b), due to incorrect depth. The missing events usually located at 5 km, the starting depth. In addition, at the south end, 3 events that should have been 10 km deep located at 5 km, but were erroneously rated as A. Our methods were discussed with some of the USGS personnel who locate and catalog these earthquakes on the CEDAR system and it was determined that some of the stations in San Bernardino Mountains area are particularly good for picking S-arrivals. S-times were thus generated for these selected stations, and the 205 artificial events were relocated. This improvement led to 133 events located as A-quality (fig. 3-20c), which filled in some of the holes. Again, a few events on the south end mislocated and were mistakenly classified as A-quality. When the Caltech catalog was finalized for 1978, a number of events got special attention. The CEDAR processors looked at the solutions and decided whether to start them at a new depth. This was simulated for the events that did not make quality-A on the first pass, by restarting them at 15 km depth. As seen in figure 3-20d, 191 out of 205 events now located well. There are still problems at the south end, probably due to the sparser station distribution there (see fig. 3-19). It is difficult to assess how many of the events in our A-catalog got this kind of special attention, but it was estimated that this is done to only about 2% of those in the whole catalog. It is apparent that more A-quality events could be obtained by relocating many B and C-quality events with a new starting depth.

There was also an attempt to test how sensitive the depths are to changes in velocity structure. Travel times were generated for 205 grid points from the standard 4-layer model used by Caltech for all of its locations, just as in the previous test. The events were relocated with two different half-space models. Both P- and S-times were used and all locations were started at 5 km depth. For figure 3-21b, a

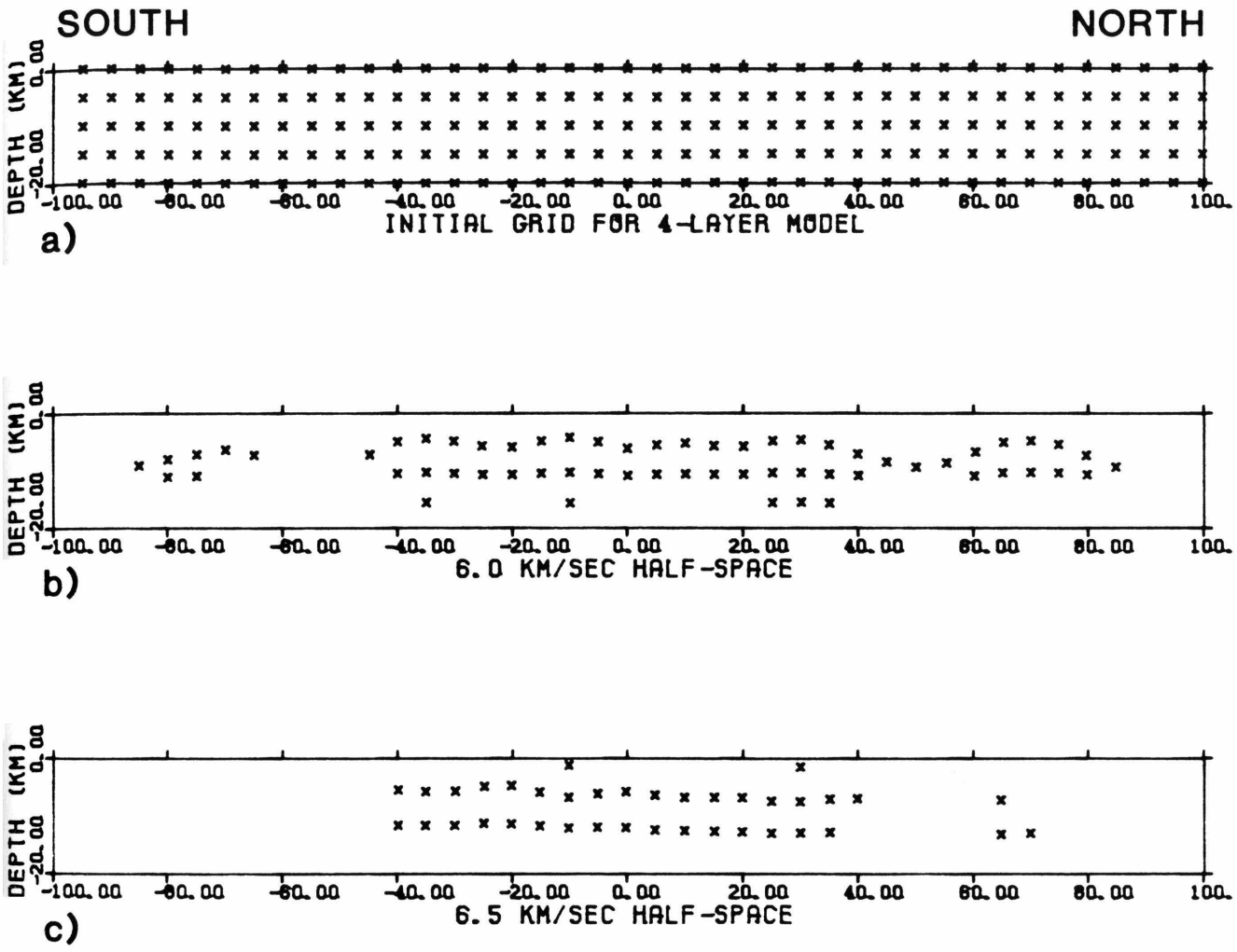

Figure 3-21. Cross-sections of synthetic A-quality earthquake locations done to test the effects of velocity model.

6-km/sec half-space was used. In this case, events at 0 km and below 10 km generally did not locate with quality-A. Events at 10 km locate reasonably well, while 5-km-depth events demonstrate a sway-back pattern with depths varying from 4 to 8 km (fig. 3-21b). Only 63 of 205 events located with quality-A, and generally only between -40 and +40 km on the cross-sections, which is probably an artifact of station density, as demonstrated by the previous test. For a 6.5-km/sec half-space (fig. 3-21c) only 38 out of 205 events located with quality-A, again with little success more than 40 km from the centerline. Depths, however, did not seem to be as badly mislocated.

There are two conclusions from the velocity-model test. First, this part of the numerical experiment indicates the difficulty of separating the effects of station distribution from the velocity model. Secondly, this experiment may be showing that the ability to locate events with quality-A is sensitive to the accuracy of the velocity model. Note, however, that the travel times used were generated from the theoretical southern California model (Table 3-1) and do not have the scatter inherent in real data. It is not certain that this second experiment adequately tests the effects of velocity structure, and there may be better ways to do this.

DISCUSSION

The numerical experiment demonstrates that there are problems in hypocentral locations, in that depths may not be reliably calculated in many parts of southern California. However, it seems to indicate that within 40 km of latitude 34° N, depth determination may be fairly accurate, due to the heavy concentration of stations along the Transverse Ranges themselves. Hence the data may be used to make reliable observations about the seismicity of the Transverse Ranges.

The seismicity of the Transverse Ranges exhibits basically two patterns, one corresponding to the sector west of Cajon Pass, and the other corresponding to the sector to the east. The seismicity in the western Transverse Ranges is primarily associated with the aftershock zones of moderate-sized earthquakes that have occurred since 1970. Usually the seismicity outlines north-dipping planar structures that may be interpreted as faults. The exceptions to this pattern are the 1979 Malibu aftershocks, the diffuse activity disseminated throughout the Los Angeles basin, and the cluster of minor seismicity on the San Andreas fault near Palmdale. The eastern Transverse Ranges are characterized by more intense seismicity, with the earthquakes pervasive from the surface down to the bottom of the seismic zone. The bottom of this seismic zone appears planar and dips south at 10° to 20°. Seismicity deepens abruptly south of the San Andreas fault. The only activity associated with an aftershock sequence is that of the Homestead Valley earthquakes of 1979.

In the Santa Barbara Channel, cross-section 3-10a intersects the aftershock zone of the 1978 Santa Barbara earthquake. This zone appears to exhibit a north-dipping fault which steepens at depth, which is at variance with the interpretations of Chapter 2. This appearance results from two events that occurred later and somewhat northeast of the aftershock zone. Also, note that these catalog events (fig. 3-9) plot 6 km south of the relocations given in Chapter 2 (cf. fig. 2-3). In addition, the catalog contains only about two dozen events of quality-A in this area, compared to 159 quality-A locations in Chapter 2. These differences point out the problems inherent in using catalog locations. They may be systematically biased, and one sees only a small subset of the data. The significance of the two deeper events is not clear, but it suggests that the results of Chapter 2 should be reevaluated by relocating all the more recent seismicity in the Santa Barbara Channel with the techniques employed in that chapter.

Structure beneath the San Bernardino Mountains

The most intriguing feature uncovered in this study is the pervasive seismicity under the San Bernardino Mountains and San Gorgonio Pass. The southward dip of the bottom of the seismic zone is clear on 3 cross-sections and suggestive on another 3, spanning over 100 km in the east-west direction. This structure suggests that the granitic rocks of the San Bernardino Mountains are behaving as a shattered brittle slab underlain by a more ductile layer. The ductile layer could be the same crystalline basement that underlies the mountains, softened by increasing temperature with depth. But the layer may also be of a material that is inherently more ductile, such as the Pelona schist, as indeed has been suggested by Yeats (1981). Let us consider the surface projection of this interface between seismic and aseismic crust. The interface would project 60 to 80 km north of latitude 34° N, at the location shown in figure 3-17. The line is inferred from the cross-sections and is necessarily only approximate.

Comparison to geology. The geologic history of the San Bernardino Mountains reveals no reason to expect a south-dipping structure under them. When it was part of the Mojave Desert, the north block of the mountains was eroded to a peneplain. In late Quaternary time the north block was elevated so that the old erosion surface is now a raised surface of low relief. The greatest uplift has been on the south and the erosional surface has been tilted north toward the Mojave Desert (Dibblee, 1975). In addition there are many range-bounding thrust faults on the north side of the range (Meisling, 1983), but no evidence for these can be seen in the cross-sections.

The geologic map of the area (Rogers, 1967) does not reveal Pelona schist cropping out at the line indicated in figure 3-17. However, the area north of the San Bernardino Mountains, in the Mojave Desert, is characterized by several large plutons exposed in the Rodman, Ord, and Granite Mountains, that are probably the northward

continuation of the basement rocks observed in the San Bernardino Mountains. These large granitic bodies end approximately along the line outlined in figure 3-17. North of this boundary, Miocene volcanics and smaller isolated plutons are prevalent. This observation supports the idea that the granitic slab of the San Bernardino Mountains pinches out on the north but does confirm that a different basement underlies it. It should be noted that on all of the cross-sections utilized, events become sparse where the seismic zone thins to 5 km, and there is no good evidence to project the planar feature above this depth. It is just as likely that it may flatten and persist at 5-km depth in the vicinity of Barstow.

Another possibility is that a 15-million-year-old detachment structure postulated by Leon Silver (pers. comm.) corresponds fairly closely to this suggested boundary (fig. 3-17). His interpretation is that this ancient detachment juxtaposes two differing granitic terranes, one atop the other. Thus there is no reason to expect a major change in mineralogy across this boundary. However, it is possible that a mylonitic or cataclastic zone is associated with this Tertiary thrust fault and may confine brittle behavior to the granitic "basement" above. Also, chemically, Pelona schist is not much different from the granites, and it is not clear that the granites will be any less ductile at depth.

San Gorgonio Pass and the San Andreas fault

Another noteworthy feature of the seismicity of the San Bernardino Mountains is the dramatic change in character at the south front of the mountains. The seismicity increases notably and deepens abruptly by 5 km, precisely at the north branch of the San Andreas fault. On figures 3-14d and 3-16a it is not immediately apparent if this change occurs as a continuation of the south-dipping ramp under the San Bernardino Mountains or occurs as a 5-km step in the bottom of the seismic zone. This critical

area is shown enlarged in figure 3-22, which includes data from 1977 to the present. In this figure it is clear that the increase in seismic activity and depth occurs abruptly, in less than 1 km, immediatedly under the surface trace of the north branch of the San Andreas fault (Mission Creek fault of Allen (1957)). The dip of the north boundary of the seismicity is at least 70° and may well be vertical, and the height of this step is at least 5 km and may be as much as 8 km. The zone of concentrated deep seismicity has a less sharp boundary on the south that corresponds roughly to the surface trace of the Banning fault (Allen, 1957). Seismicity is less intense south of this fault (see also fig. 3-15) and the depth of activity may decrease by 2 km. Seismicity still further decreases and becomes shallower to the south toward Mt. San Jacinto.

The complexity of the seismicity in this area correlates fairly well with the complex geology. Northwest of San Gorgonio Pass, the San Andreas fault splits into two branches that have both been active in late Quaternary time. The north branch of Jennings (1975) is actually composed of two aligned strands, the Mill Creek and Mission Creek faults, that are not quite continuous at the surface (Allen, 1957). Their juncture is complicated by the left-lateral Pinto Mountain fault, which trends northeast here. The north branch shows evidence of Quaternary but not Holocene movement (Dibblee, 1975). The south branch veers rather sharply to the south until it intersects the Banning fault at nearly right angles. East of this intersection, the Banning fault behaves as a shallowly dipping north-over-south thrust. To the east, the Banning fault gradually steepens, begins to exhibit right-lateral movement, and trends progressively more southeasterly until it rejoins the Mission Creek fault in the Coachella Valley. The present understanding of the geologic history is as follows: During Tertiary time the present-day Banning fault behaved as the transform boundary. Near the beginning of Quaternary time, the north branch of the San Andreas fault

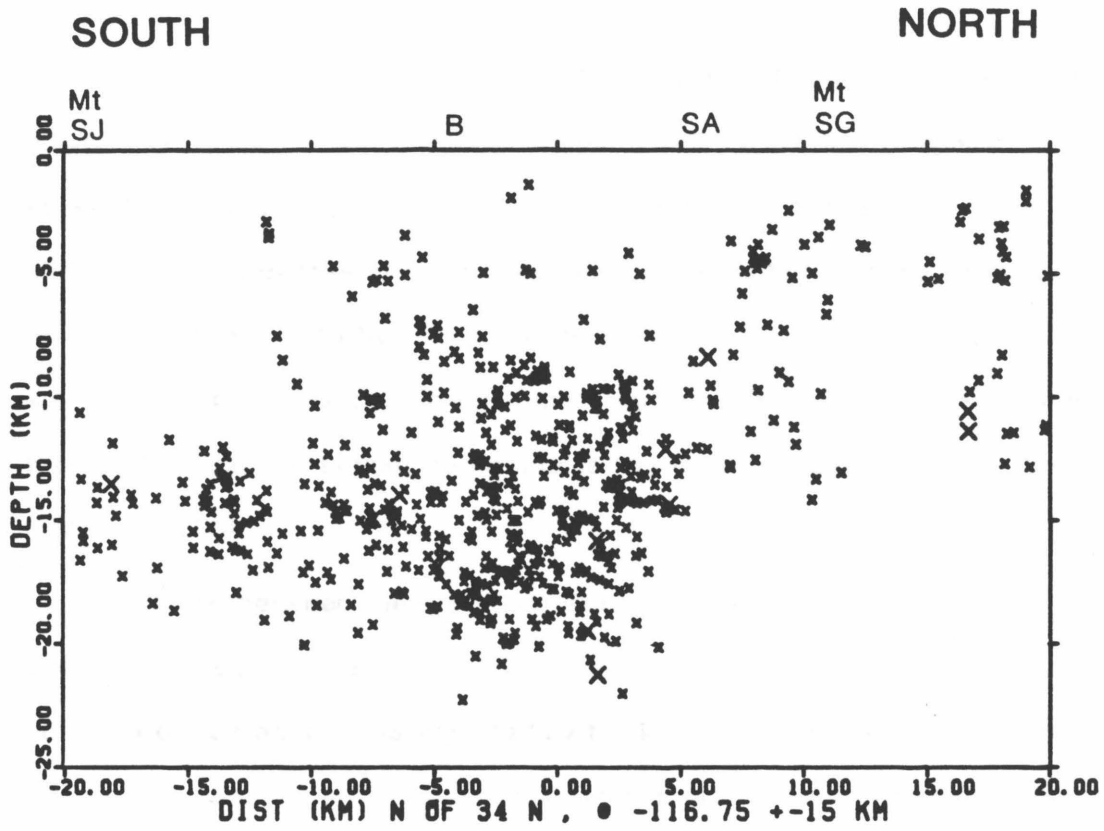

Figure 3-22. Large-scale cross-section of seismicity in San Gorgonio Pass, 1977 - August 1983. Same section as figure 3-16a, for longer time period. Mt SJ: Mt. San Jacinto; B: Banning Fault; SA: north branch of San Andreas fault; Mt SG: Mt. San Gorgonio.

took over displacement, while the Banning fault became inactive. In the late Quaternary, displacement shifted again to the south branch of the San Andreas fault and the reactivated east end of the Banning fault (Dibblee, 1975; Matti and Morton, 1982).

Although the presently active San Andreas fault and its predecessors have been primarily strike-slip faults, there has evidently been a vertical component of motion as well, as indicated by the mountainous topography. In San Gorgonio Pass, Tertiary sediments are in excess of 5358 feet thick. At the other extreme, basement rocks are exposed at the 11,502-foot summit of Mt. San Gorgonio, the highest peak in southern California. Hence, the structural relief is at least 5 km. Apparently most of the uplift of the San Bernardino Mountains has occurred during the late Quaternary (Dibblee, 1975).

The block between the north and south branches of the San Andreas fault is apparently caught in the middle of the bend of the fault. It is presently undergoing active brittle deformation as indicated by the intense seismicity. The mode of deformation is complex, as indicated by focal mechanisms. Green (1983) shows solutions that range from strike-slip through oblique to pure thrust mechanisms. All are consistent with north-south compression, but few have nodal planes parallel to the faults they are plotted near. The matter is complicated further by the work of Nicholson *et al.* (1983) who suggest left-lateral slip on northwest-trending planes.

The deeper seismicity may have one of two explanations. First, basement rocks on the two sides of the north branch of the San Andreas fault are very different. North of this fault, the granitic rocks are of Mojave Desert type, and to the south they bear affinity to the basement rocks of the San Gabriel Mountains (Dibblee, 1975). The two different types of basement have been juxtaposed by large lateral offset on the north branch of the San Andreas fault. Hence, the south block may be

mineralogically and structurally different enough so that the rocks behave brittlely to a greater depth. However, the earthquakes here occur at greater depth than anywhere else in southern California, including the San Gabriel Mountains. A second possibility is that a block of crust has been depressed south of the north branch. This is possibly supported by the 5+ km of structural relief seen here. Allen (1957) has suggested that the San Gorgonio Pass might have formed as a graben between reverse faults on either side of the pass, but pointed out the lack of surficial evidence for Holocene faulting on the south side of the pass. However, in figure 3-22, there is what appears to be a vertical seismicity zone at the x=-13 km mark, which is under the north flank of Mt. San Jacinto.

Eastern Transverse Ranges

The eastern edge of the Transverse Ranges is shown in the cross-section in figure 3-16d. It displays several vertical seismicity zones that correlate with east-trending left-lateral faults discussed by Powell (1981). These faults are, from north to south, the Pinto Mountain, Blue Cut, Porcupine Wash, Smoke Tree Wash, and Chiriaco faults. On the cross-section, the Blue Cut and Smoke Tree Wash faults show up most clearly (cf. fig. 3-15). In addition, there is an east-trending line of seismicity just north of the 34th parallel that does not correlate with any mapped structure of Powell (1981) nor Jennings (1975). Powell (1981) noted that these faults all showed evidence of Quaternary movement, were rather regular in spacing, and had the shared characteristic of displacement increasing towards the east. Powell (1981) stated:

> "The pattern and continuity of the left-lateral faults suggests that they have formed as a brittle mechanical response within a crystalline plate riding atop a substrate of less brittle material.... If such a brittle plate interpretation is correct, then it would seem reasonable to expect that hypocenters for earthquakes along the left-lateral faults within this plate

would occur no deeper than the base of the plate."

Powell (1981) also showed seismicity cross-sections to support this hypothesis. The more recent and higher quality locations used in my study tend to support his observation that most of the seismicity occurs above 12 km. In fact, most of the seismicity associated with the mapped faults (fig. 3-16d) is above 5 km. Powell (1981) further suggests that Pelona-type schist under the Chocolate Mountain thrust may project northward under the eastern Transverse Ranges.

CONCLUSIONS

From the numerical experiment there are three conclusions: 1) There are problems in locating events in certain parts of the network, but these problems probably are not critical for the dense station distribution along the Transverse Ranges. 2) Most of the quality-A events do have a precision of 2 km in their calculated depth. 3) It may be possible to get a clearer picture by relocating the many more B-quality and C-quality events with a better starting depth to improve them to quality-A.

There are two conclusions about the data: 1) In the western Transverse Ranges there appear to be a few north-dipping planar structures that extend down to 12 to 15 km depth, but there are several areas where events show no structure, but scatter down to 20 km depth. 2) In the eastern Transverse Ranges, especially under the San Bernardino Mountains, there does appear to be a bottom to the seismic zone. And this zone appears to shallow as you move north toward the Mojave Desert.

This study has not clearly answered the decollement question. The data may be supportive of the decollement idea in the area of the Transverse Ranges northeast of the San Andreas fault. In the western Transverse Ranges, however, the catalog locations show no clear evidence for sub-horizontal structures. The principal contribution of this chapter has been to add intriguing new evidence to the case and to

outline potential areas for more intensive study.

Chapter 4

Velocity Structure of southern California Continental Borderland as seen from Catalina Island, California

Introduction

At noon on November 8, 1981, 180,000 lbs. of ammonium nitrate was detonated in a single, undelayed quarry blast at the southeast end of Catalina Island. This location is south of Los Angeles, 45 km off the southern California coast (star, fig. 4-1). Portable seismographs were deployed on the island and the shot was timed on site by Chuck Koesterer of the USGS. This was a relatively large blast, registering 2.6 on the Richter scale, and it was well recorded on virtually all of the southern California stations shown on the map (fig. 4-1). The blast was timed on the CEDAR system, and the portable smoked paper records were read by Doug Given of the USGS. Hence the origin time and arrival times are well documented by Given and Koesterer (1983), who point out that blasts of this size occur in southern California only about once every 10 years, and this afforded a rare opportunity to study the seismic velocity structure of the Continental Borderland.

Setting

The blast occurred in the offshore province known as the southern California Continental Borderland. This area contrasts markedly with the nearly flat, 30 to 50-km-wide continental shelf that is typical of the rest of the California coast. The Continental Borderland is a 250-km-wide zone of bathyl deeps and elevated ridges that

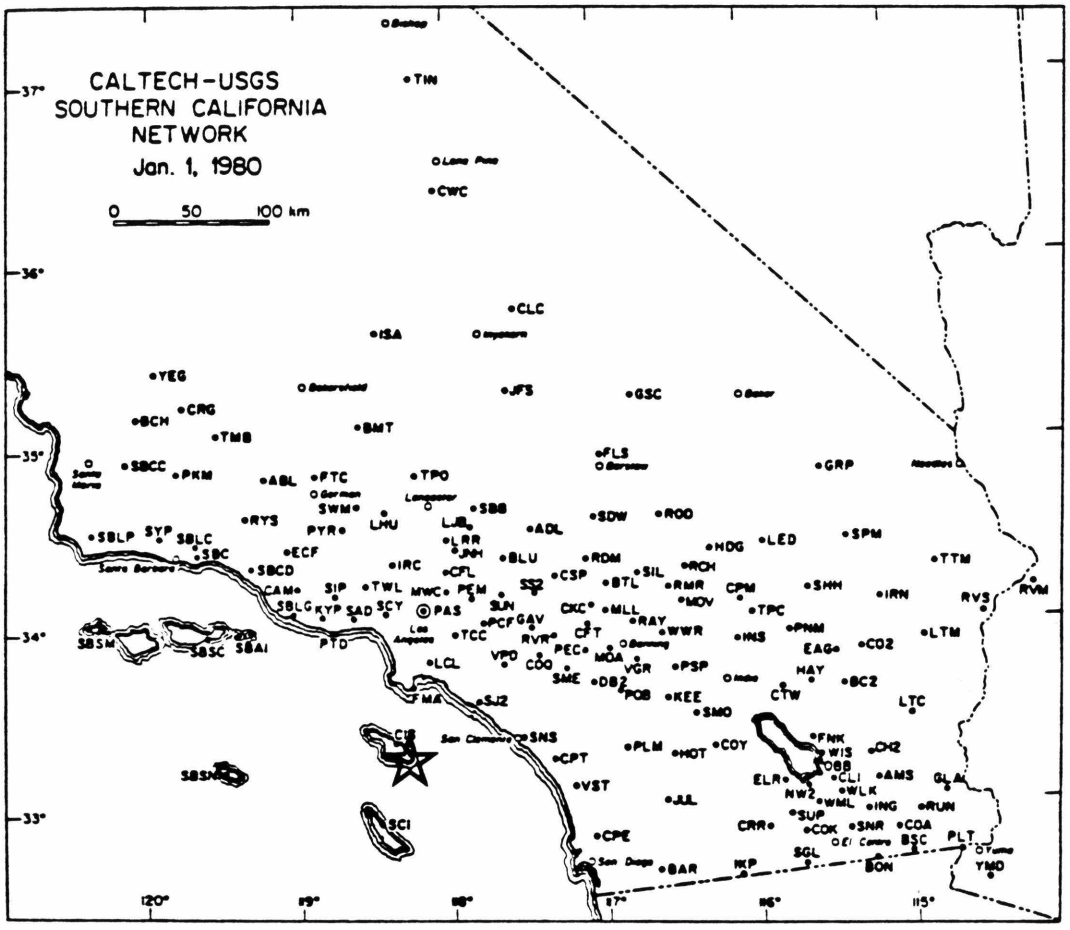

Figure 4-1. Map of seismographic stations recorded by the CEDAR system at the time of the Catalina Quarry blast. Location of blast indicated by star.

separate the southern California coast from the abyssal floor of the Pacific Ocean. The ridges breach the sea surface in places, forming islands, Catalina being one of these. The high bathymetric relief suggests structural complexity, and the relatively shallow water depths suggest a crustal thickness that is intermediate between the ocean (10-12 km) to the west and the continent (30-40 km) to the east.

Previous Work

The pioneering work in the offshore area has been by scientists at the Scripps Institute of Oceanography (SIO). They started refraction experiments in the borderlands in 1948, initially to test and develop equipment but later to study velocity structure. Navigation in the 40's and 50's left something to be desired. These were the days before LORAN and satellites, and many locations were "determined" by sun sights, dead reckoning, and soundings. It was not uncommon for the locations of the shooting ship *and* receiving ship to be off by miles. Most of this work remains unpublished except for meetings and SIO reports (Shor and Raitt, 1958a, 1958b). All of their work has been recently compiled and released by Shor *et al.* (1976). Despite the above-mentioned shortcomings, these studies provide a valuable framework in which to view more recent studies. Shor *et al.* (1976) have documented the rather sudden shoaling of the Moho seaward of the Patton Escarpment. They observed refractors of 8.2-km/sec velocity at 24-km depth under the Catalina Basin, at 14- to 17.6-km depth at the top of the escarpment and 9- to 10-km depth at the foot of the slope. Shor *et al.* (1976) defined the structure of several of the deep sedimentary basins, which contain 5 to 7 km of sediments. Shor and Raitt (1958a) noted that the depth to basement in many of the basins is the same as west of the Patton Escarpment. They observed "oceanic" velocities of 6.7 km/sec below 7 km and noted that the seaward thinning of the crust was at the expense of this lower

crustal layer. Most of their conclusions were from 5 widely spaced profiles across 300 km. Shor and Raitt (1958a) realized, of course, the limitations of their data and gave us an admonishment that still applies today.

> "The surface geology of the islands is varied, indicating similar variation beneath the submerged ridges and basins... for any set of seismic refraction data an infinity of interpretations is possible... The method is akin to that used by a field geologist trying to determine a structural map and section from a small number of outcrops."

More recently Crandall *et al.* (1983) have published a refraction study from an east-west traverse of the Santa Barbara Channel. While somewhat removed from the area of interest herein, this study defines structures that may occur in the southerly part of the borderlands as well. Crandall *et al.* (1983) observed 7 km of sedimentary fill in the channel that is underlain by 6.3-km/sec crust. This is in turn underlain by a 7.0-km/sec layer at 11.6-km depth and a 8.3-km/sec Moho at 22-km depth. Keller *et al.* (1983) ran a refraction line across the Santa Cruz Basin from San Nicolas Island north to Santa Cruz Island. Their interpretation is quite complicated, with many dipping layers and velocity gradients, but, in general, it shows 5 km of sediments underlain by crustal layers as in Crandall *et al.* (1983) and a Moho of 7.8 km/sec at 20-km depth. Hearn (in press) has used earthquake sources to invert for P_n velocities and crustal thickness for the whole of southern California. He determined a mean Moho velocity of 7.9 km/sec and a mean crustal thickness of 29 km, but found that velocities are faster and the Moho shallower offshore.

TECHNIQUE

Data

Most of the data were recorded on the Caltech Earthquake Detection and Recording (CEDAR) system and were timed by Doug Given (Given and Koesterer, 1983). This was supplemented by data from stations operated by the University of Southern California (USC) (Ken Piper, personal comm.). If we plot all the data on a reduced travel-time plot (fig. 4-2), it is obvious that there is much scatter. It should be emphasized that this scatter is not errors in the data. Most of the picks are accurate to better than 0.1 sec. Instead, this demonstrates the variability of southern California velocity structure, which is highly azimuthally dependent.

To alleviate this problem, data were selected for only 32 stations that were near shore or on islands (fig. 4-3). This ensures that the ray paths to these stations spend most of their transit in offshore crust of the Continental Borderland. These data resulted in 3 different velocity models corresponding to 3 areas within the offshore region (fig. 4-4), which are basically similar. They all consist of a 2.5- to 5.5-km-thick upper crust with a velocity of 5.2 to 5.5 km/sec. This is underlain by a 6.2- to 6.3-km/sec lower crust which shall be referred to as the P_g layer in this report. This layer is about 17-km thick. This is in turn underlain by a Moho of 7.8 km/sec (or more) at about 20-km depth. The three slightly different models result from looking at the data in different azimuths and ranges. The necessity for each model is clearly indicated by the data, and the evidence for each will be discussed in turn.

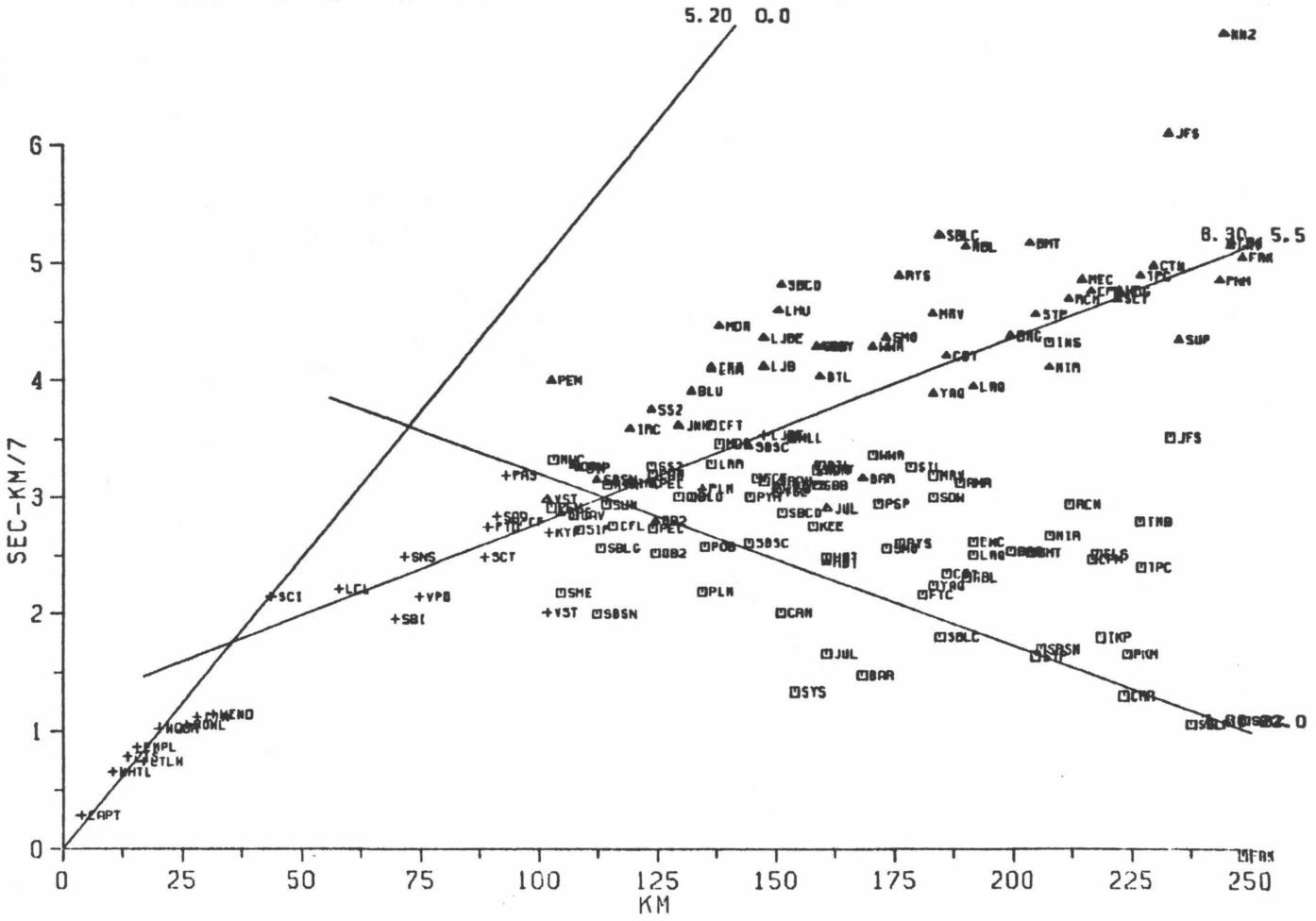

Figure 4-2. Reduced travel-time plot (reduced by 7 km/sec) showing travel-times to all Caltech-USGS stations. + P-arrivals; △ P_g-arrivals; □ P_n-arrivals.

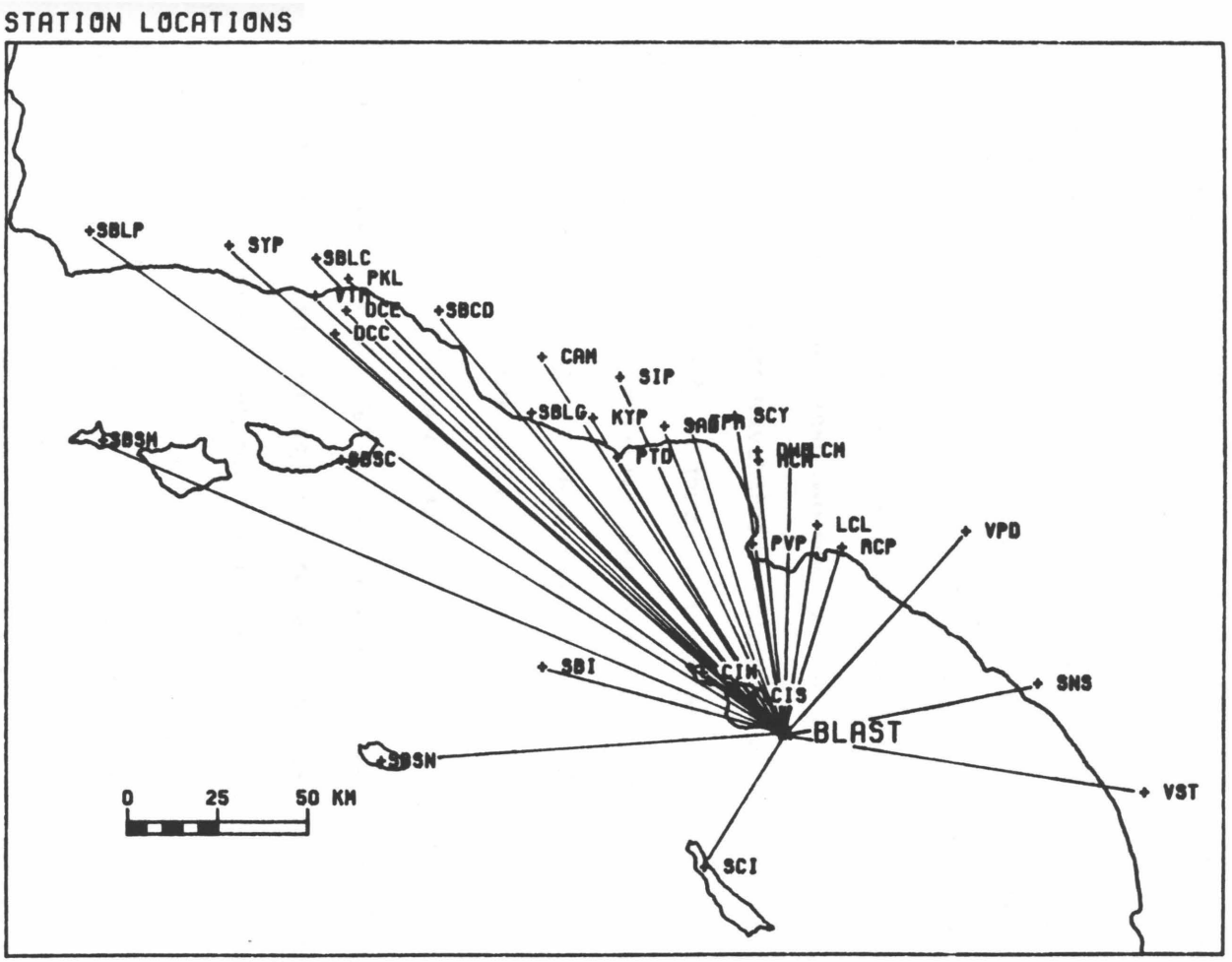

Figure 4-3. Location map of stations with Continental Borderland ray paths.

Method

Velocities and thicknesses were determined by the slope-intercept method. The data were initially plotted on ordinary travel-time plots. In this format, the data displayed 3 obvious branches. Slopes and cross-over distances were determined from this plot and used to calculate VM1 (fig. 4-4). The data and this model were re-plotted on a travel-time plot that was reduced by 7 km/sec. This method allows one to magnify the time scale and better assess the amount of scatter from the model. The reduced plot revealed some systematic deviations from VM1, which led to the derivation of the other two models. The slope-intercept method was deemed adequate because the travel-time plot displayed 3 clear linear branches (see fig. 4-5). The first (direct-P) and third (P_n) branches were remarkably well defined. More advanced inversion schemes were not considered appropriate, since the ultimate goal of this project was to provide a simple flat-layered model to use in an earthquake location program for Chapter 5 of this work.

At this point it became desirable to examine the original seismograms. This was problematic since although the CEDAR system does an excellent job of timing and archiving the seismic traces, software had never been developed to play them back. After considerable effort, the "code" was broken for the CEDAR seismograms and programs were written to plot out the traces individually or on record sections. After the breakthrough, the record sections were analyzed to confirm, and in some cases, better define the travel-time branches that had been observed previously. Coherent phases were recognized by their similar waveforms, and they could be seen to carry across the record section. Also phase breaks could be picked more accurately.

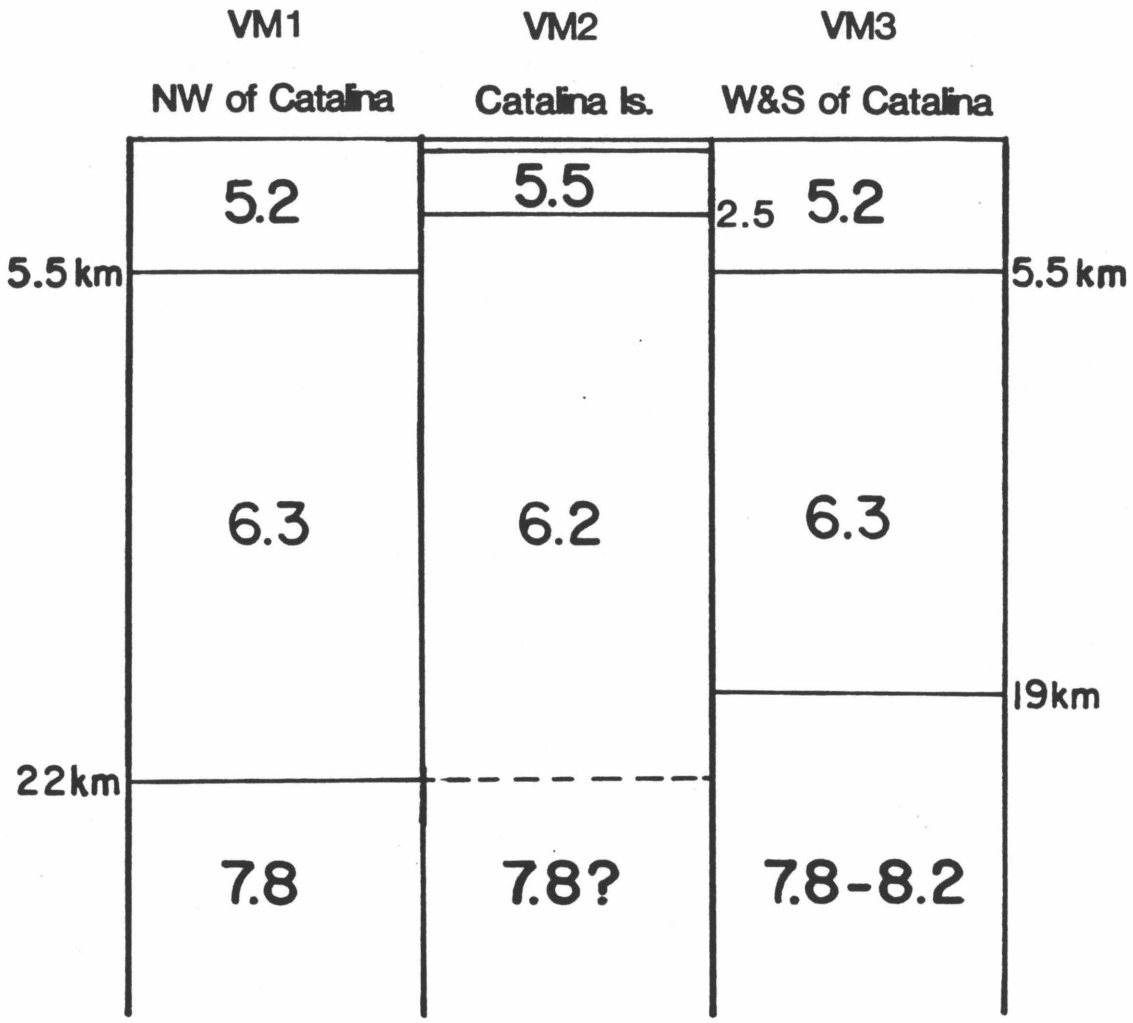

Figure 4-4. Crustal velocity models derived for different azimuths from blast. Velocities in km/sec.

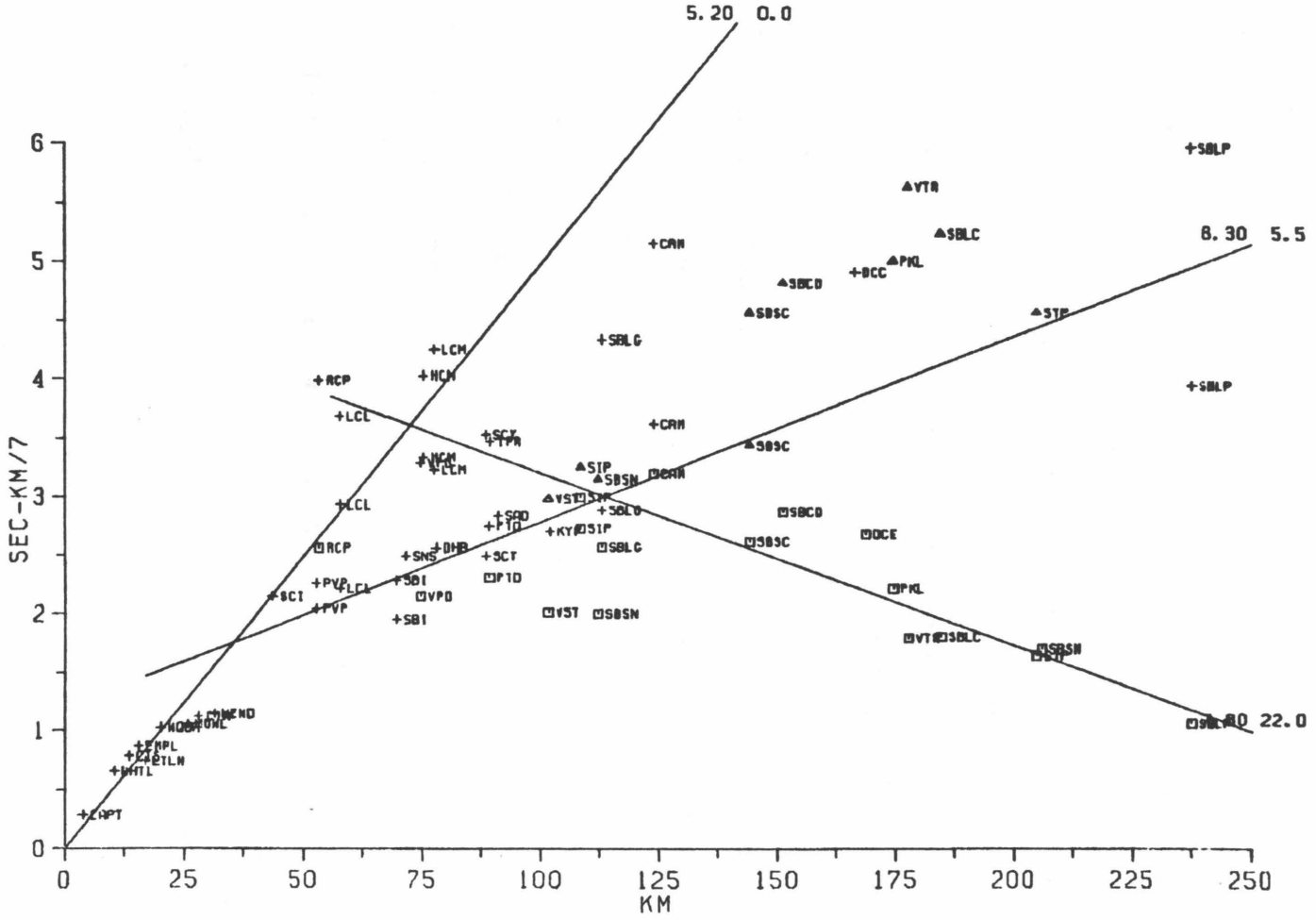

Figure 4-5. Reduced travel-time plot for stations with Continental Borderland ray paths. Lines indicate travel-times of refractions predicted by model VM1.

RESULTS

Northwest of Catalina -- VM1

Figure 4-5 shows how well velocity model 1 fits the selected data. The majority of the data falls along the three indicated branches, within 0.5 second of the calculated travel time. But, there are some noteworthy exceptions. 1) SBI (range, 70 km), PTD (89 km), and SBLG (113 km) each have two arrivals, with the second one coming in close to the time predicted for the first. The 3 early arrivals also have an apparent velocity of nearly 6.3 km/sec. 2) VST (101 km) and SBSN (112 km) exhibit $P_g - P_n$ intervals of nearly 1 second, 40 km before such a lag is predicted by the model. In fact, cross-over distance is not expected until 112 km. 3) Stations on Catalina Island show a very clear break-over to a higher velocity where none is predicted. And finally, 4) several stations beyond 150 km exhibit P_g arrivals that are over a second late. These deviations from the norm will be used to rationalize the other two velocity models (fig. 4-4).

All of the stations with P_n arrivals were on northwest to north azimuths as shown in figure 4-6. Note that the sections of the ray paths that were refracted along the top of the P_n layer are all located northwest of Catalina. Hence, all the evidence for a 7.8-km/sec Moho at 22-km depth comes from this area, i.e., the Santa Monica basin and the east edge of the Santa Cruz-Catalina ridge. The P_g paths cover a much wider range of azimuth, nearly 180° from west through north to east (fig. 4-7). If a similar plot was shown for the direct-P paths, it would show rays going due north to Los Angeles basin stations, and due south to SCI. These plots show that we are not getting a true velocity profile. Station azimuth is dependent on station distance due to the coastal geography. However, the area of maximum overlap is north-northwest of Catalina, and VM1 is probably most appropriate in this

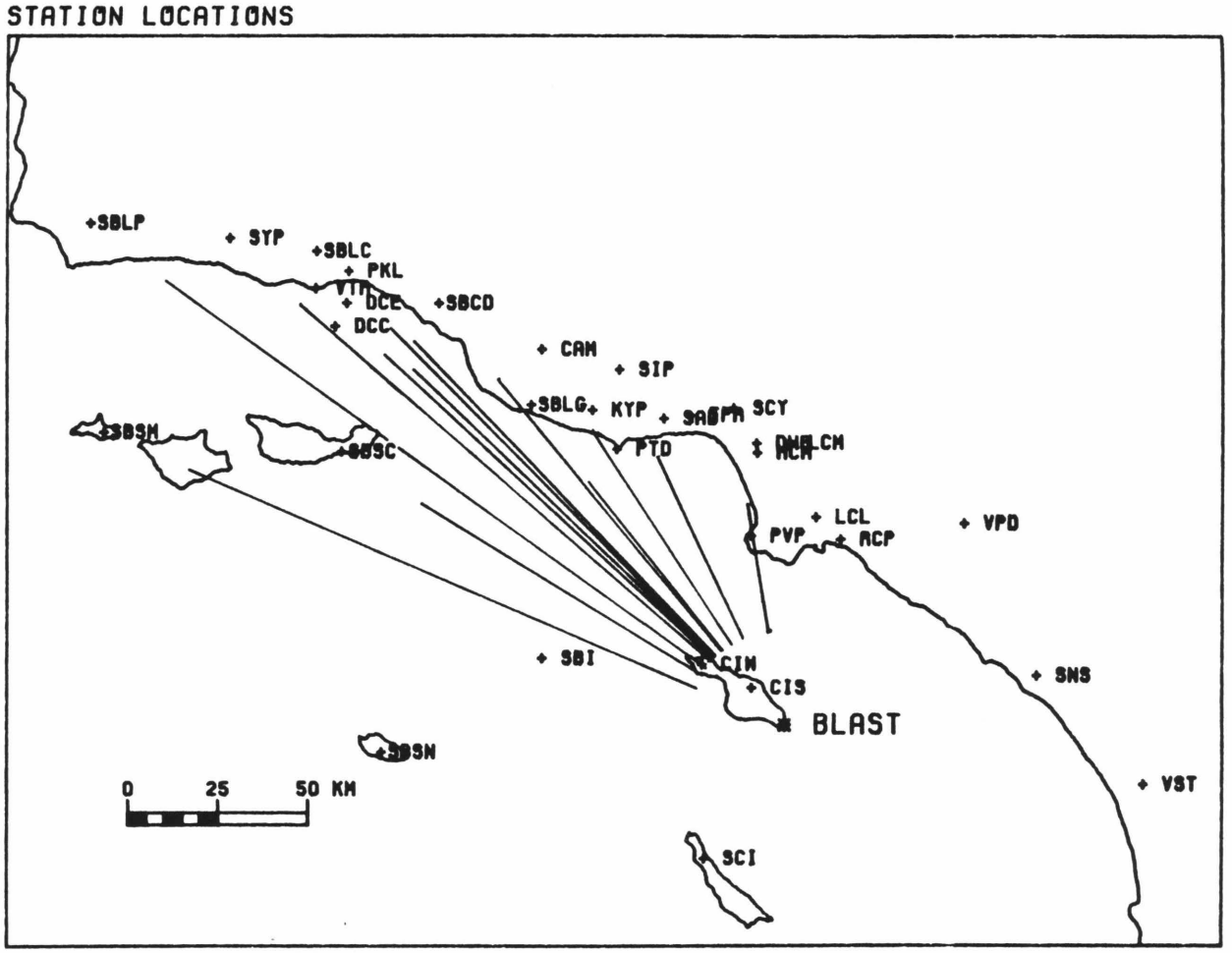

Figure 4-6. Ray paths along top of P_n refractor of VM1.

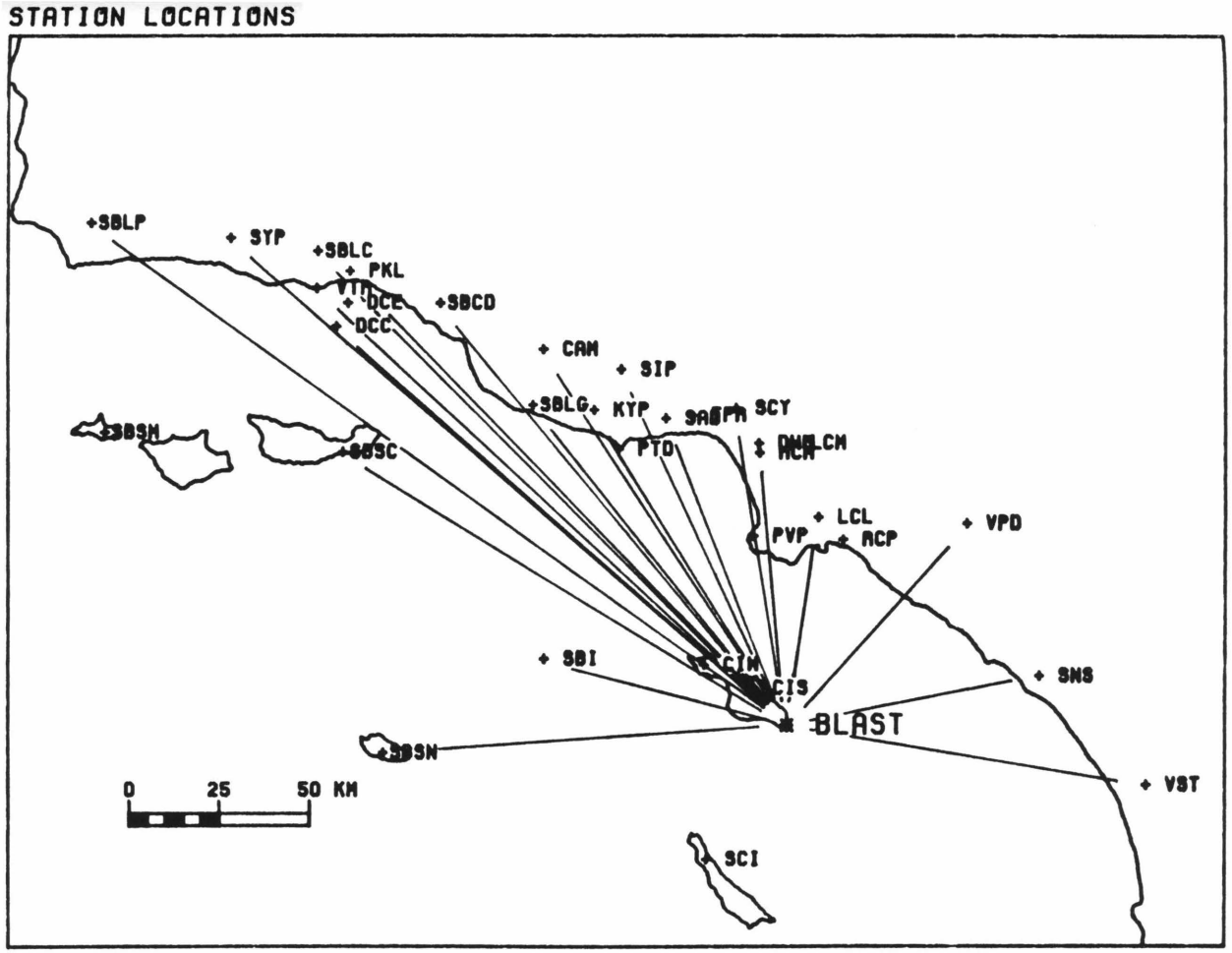

Figure 4-7. Ray paths along top of P_g refractor of VM1.

region.

Refraction vs. Reflection

In an attempt to understand the late P_g arrivals beyond 150 km, a synthetic seismogram was generated from VM1 for one of these stations: SBLC (fig. 4-8). As would be expected, it shows emergent P_n and P_g refractions followed by an impulsive Moho reflection: $P_m P$. The reflection's amplitude was larger than expected, and it appears probable that the CEDAR timers (human) were picking the relatively larger reflection as P_g. With this in mind, reflection travel-time curves were also calculated for VM1 (fig. 4-9). As shown, the $P_m P$ curve comes much closer to fitting the late arrivals beyond 150 km, and may also explain why 3 arrivals were observed at some stations (e.g. CAM and SBSC). The arrivals are still generally about half a second late. Note that most of these stations are in the Santa Barbara region and the upgoing leg of the reflection would have to cross the Santa Barbara Channel at a shallower depth than the Moho refraction. Thus, these rays may also be slowed by the low-velocity sediments that fill the Santa Barbara Channel to a depth of 7 km (Keller, *et al.*, 1983; Crandall, *et al.*, 1983).

Catalina Model -- VM2

The stations on Catalina (0-35 km range) exhibit a very clear break-over to a higher velocity at about 20 km. To fit these data, I used a higher velocity upper crust (5.5 km/sec) and a slightly slower (6.2 km/sec) P_g layer that is also 3 km shallower. The 5.5-km/sec layer has a non-zero intercept, and this was accommodated by a 300-m-thick 2.5-km/sec layer. The 2.5-km/sec velocity was observed in the quarry by Given and Koesterer (1983). This velocity model is VM2 on figure 4-4. The fit to the data is shown in figure 4-10. Although VM2 fits the Catalina

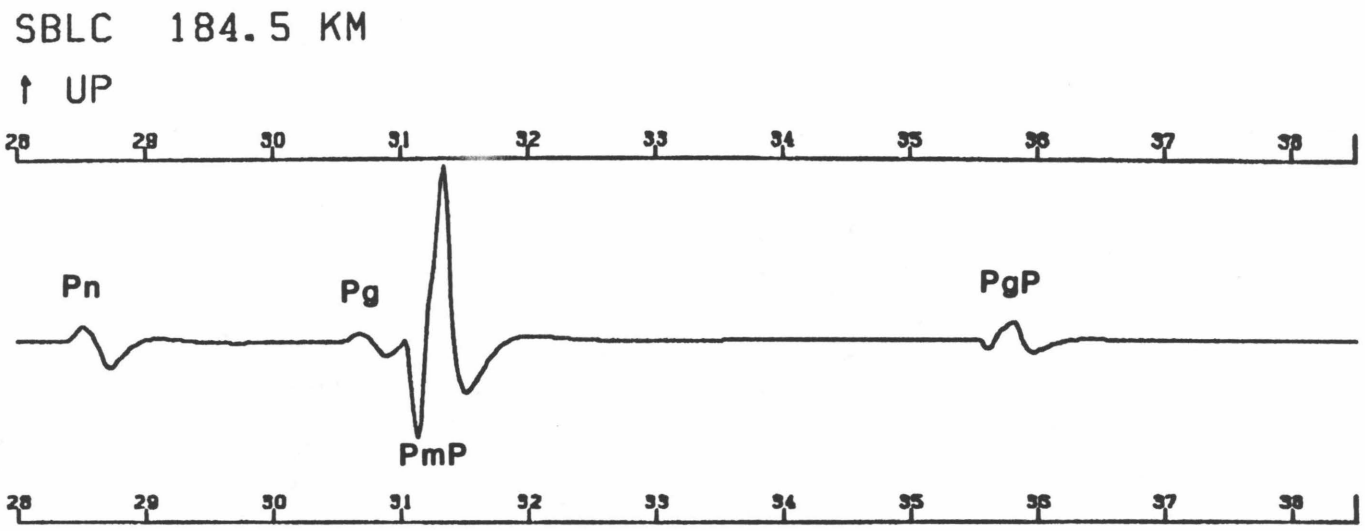

Figure 4-8. Synthetic seismogram for station SBLC, generated from model VM1.

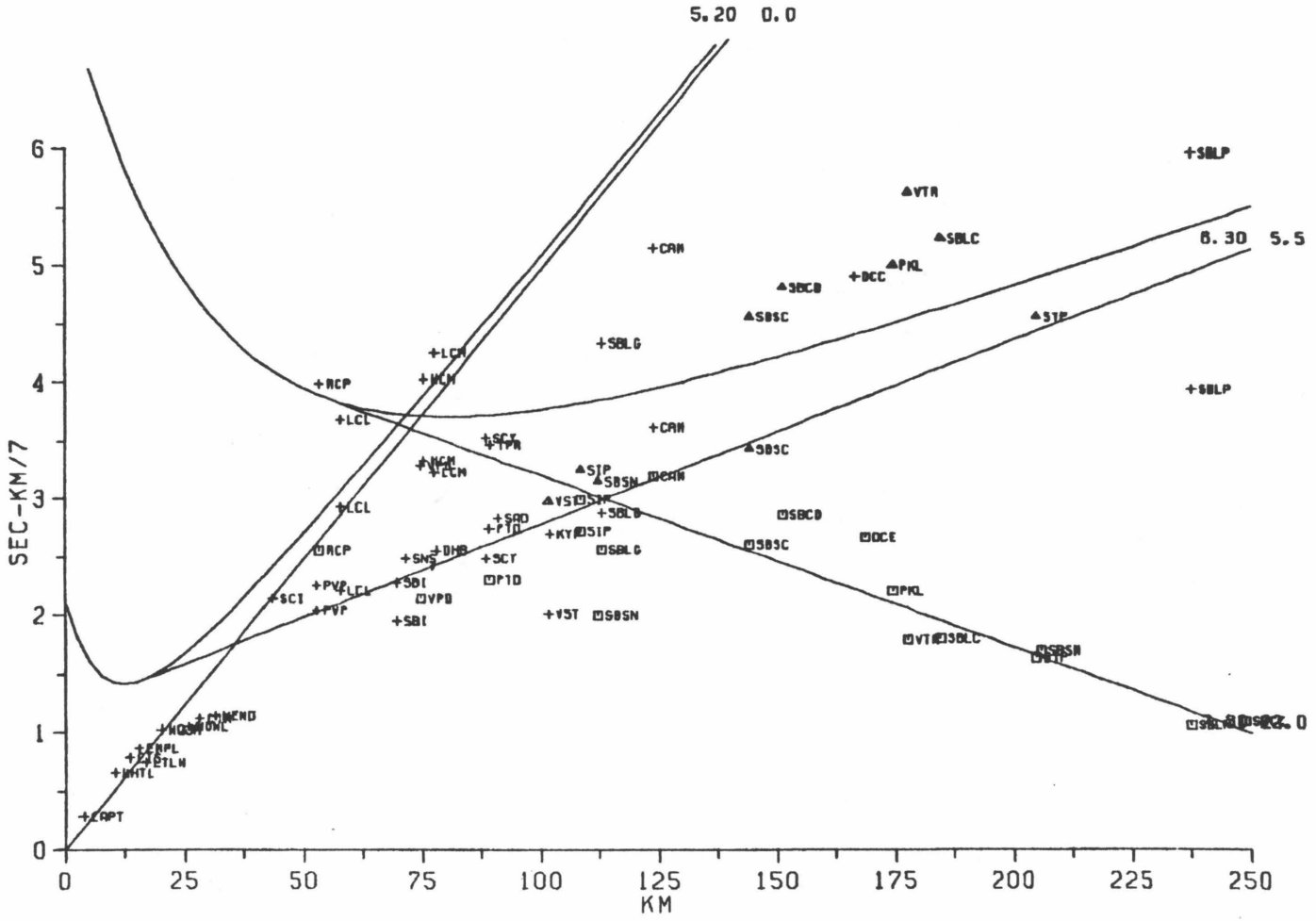

Figure 4-9. Reduced travel-time plot showing refractions (straight lines) and reflections (curves) predicted by VM1.

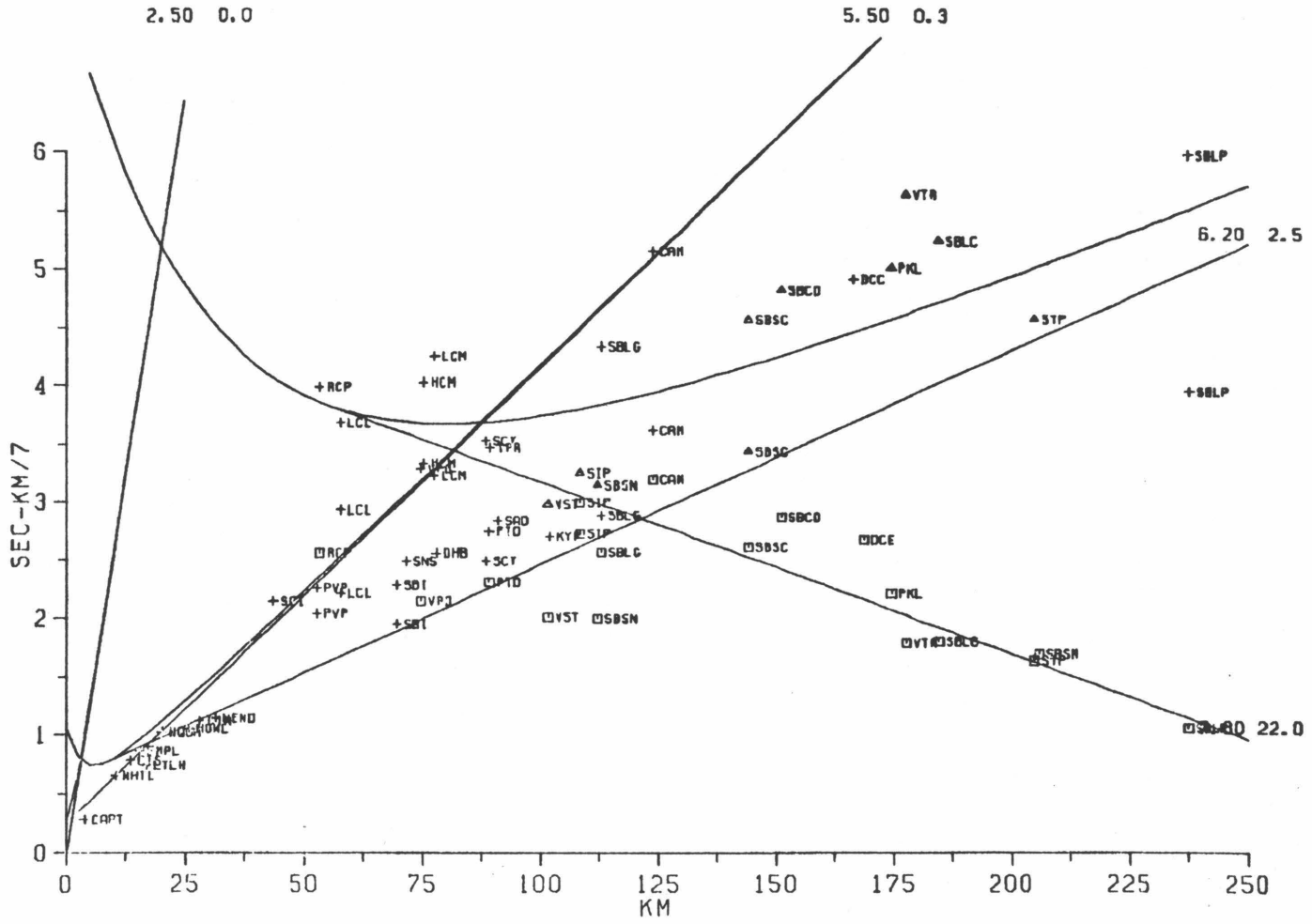

Figure 4-10. Reduced travel-time plot showing refractions (straight lines) and reflections (curves) predicted by VM2.

stations better, it does so at the expense of stations in the intermediate range (50-120 km). Figure 4-11 shows the direct-P and P_g ray paths on Catalina. The data from these 9 stations sample the whole island and strongly constrain its structure.

An interesting side effect of this model is that it better explains the first arrivals seen at SBI, PTD, and SBLG. Note on figure 4-7 that the direct path to SBI grazes the south side of Catalina. It is possible that that energy may be laterally refracted along Catalina and is arriving before waves that take the direct route. This makes some sense if one looks at the seismogram for SBI. The first arrival is small and emergent; the second arrival is large and impulsive. The SBLG seismogram also exhibits this characteristic, but it is not as pronounced. The PTD record is noisy and this observation is uncertain. In short, seismic waves refracting into the shallower P_g layer on Catalina may get a head start on waves taking a more "oceanic" path and this may cause early arrivals at these three stations.

Digital Record Section

Twenty-two of the thirty-two stations were recorded digitally by the CEDAR system and I have constructed a record section (figure 4-12). Note that I have been selective in plotting traces since some would plot on top of others. However, traces neglected in figure 4-12 are shown on later figures. The record section shows that only the closest two stations (on Catalina) were clipped, and there was good signal out to almost 240 km. The phases predicted by VM1 show up reasonably clearly, especially the high amplitude Moho reflections in the range 70 to 120 km, which is at the distance for critical angle and beyond. The most critical area for constraining the model is in the range 40 to 120 km, and this is shown in blowups (figs. 4-13 and 4-14). On fig. 4-13, the P_g phase is seen clearly at SBI, SNS, and VPD, coming in within a few tenths of a second of the calculated time. Note the small emergent arrival at

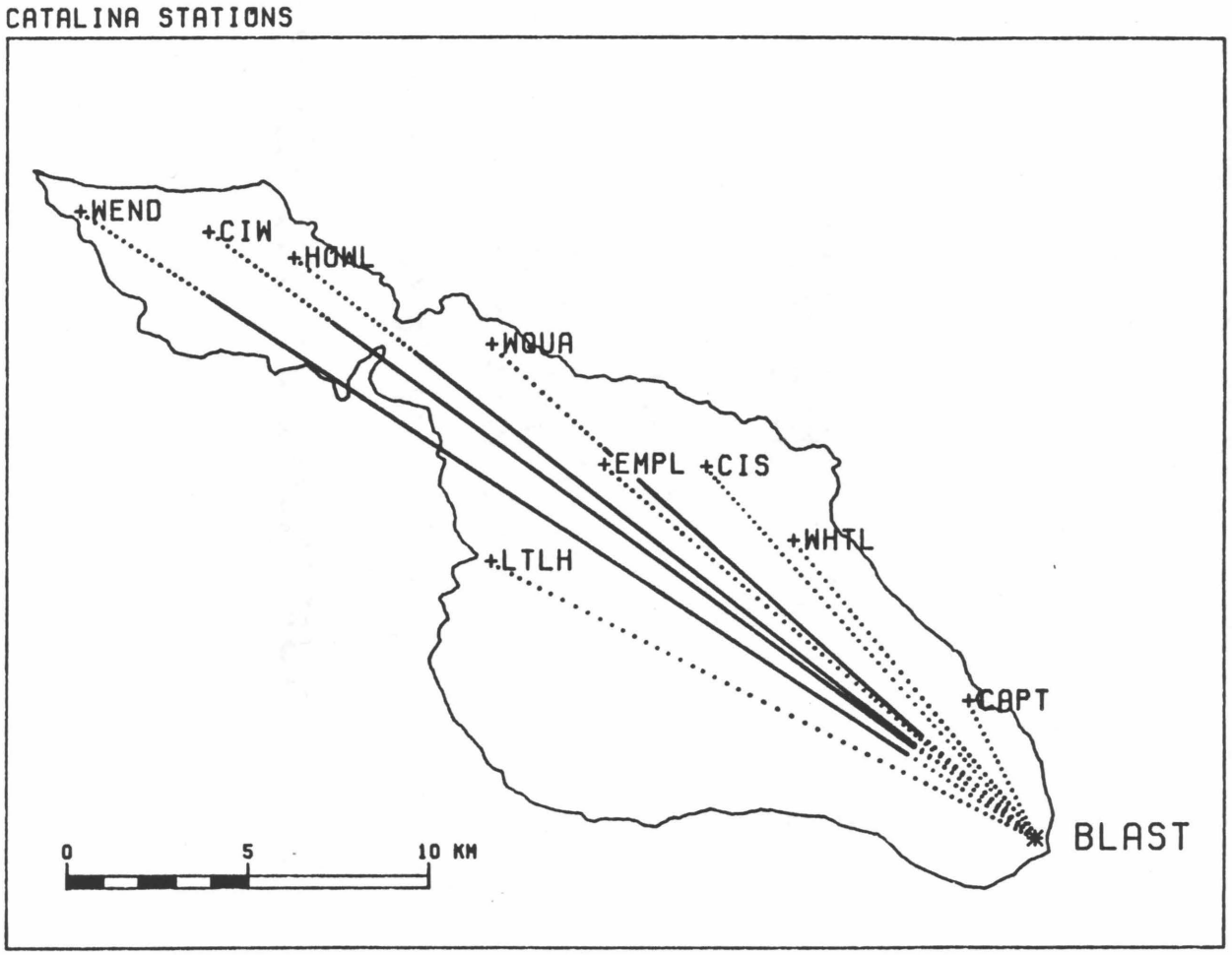

Figure 4-11. Map of Catalina Island showing ray paths to permanent and portable stations, for direct-P (dotted) and P_g.

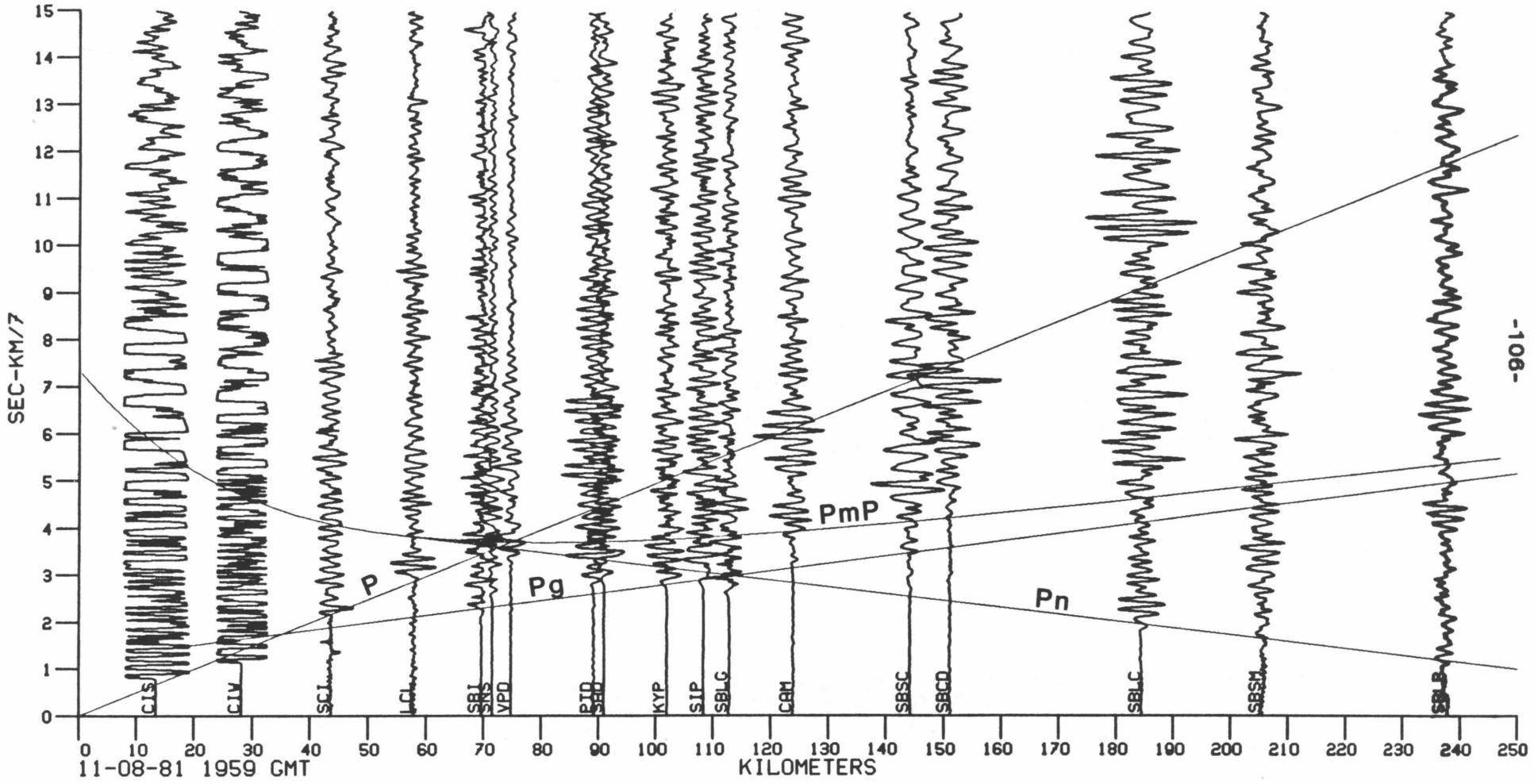

Figure 4-12. Record section (reduced by 7 km/sec) for stations recorded digitally by CEDAR. Lines indicate direct-P, P_g refraction, P_n refraction, and P_mP reflection predicted by VM1.

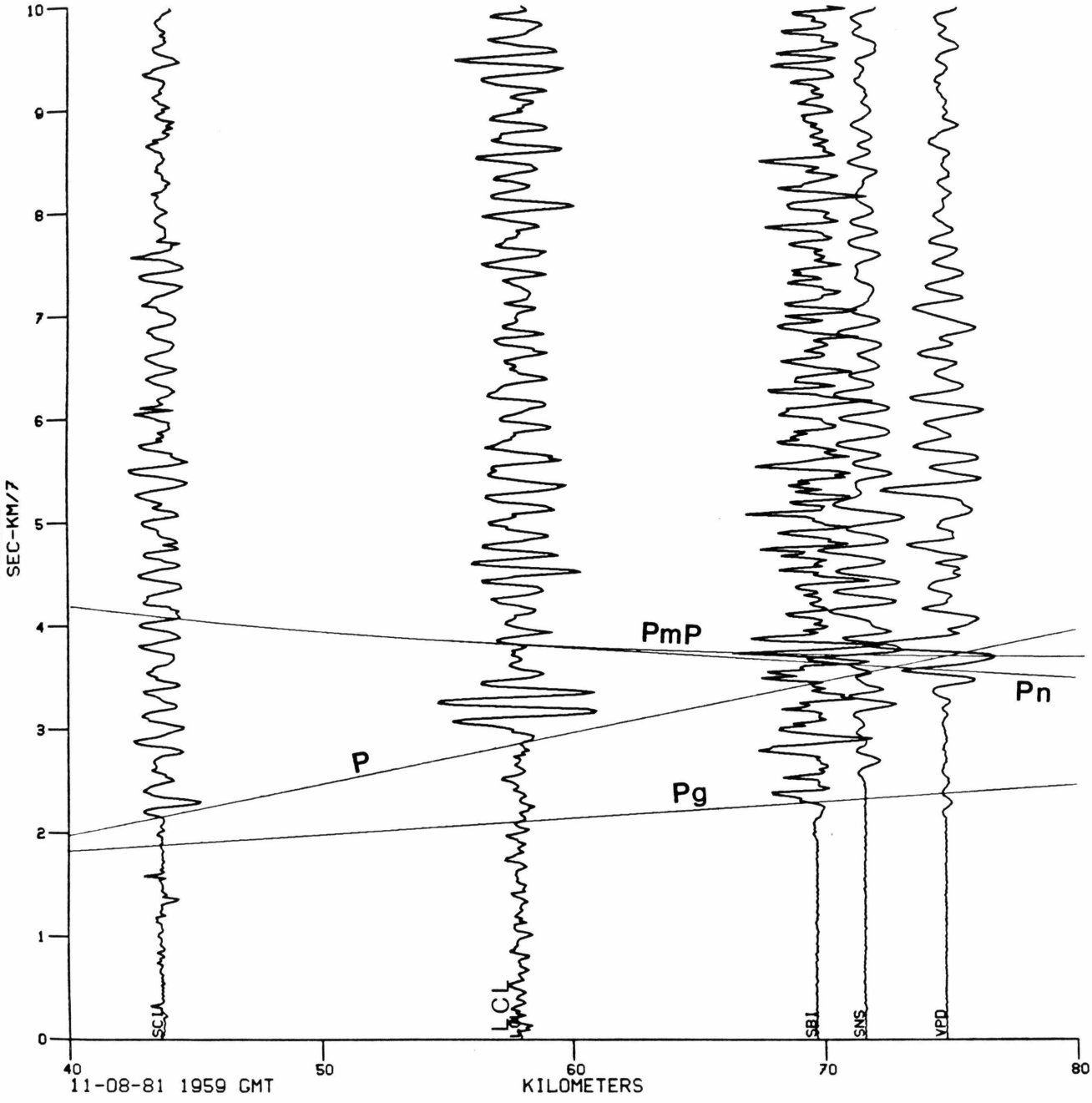

Figure 4-13. Record section for the range 40-80 km from the blast. Lines indicate predicted travel-time curves for VM1.

SBI that precedes the larger second arrival. The P_mP reflection is seen weakly at LCL and strongly at SBI, SNS, and VPD. On figure 4-14, the P_mP is also clear, and it is noticeably early at SBSN. The P_n can be seen interfering at SAD, KYP, and SIP as it starts to "catch up" to the P_g. Noting that PTD has reversed polarity, the emergent form of the P_g carries nicely across fig. 4-14. This is even true at SBSN, in spite of the arrival of a preceding phase. The coherency of the P_g argues that the upper part of VM1 is appropriate for SBSN, and the early arrival of energy is due to something below the top of the P_g layer.

Model for Stations South and West--VM3

I interpret the arrival as an early P_n which can be due to either a shallower or faster Moho, or both. Two possible interpretations are 7.8 km/sec at 19 km, or 8.2 km/sec at 22 km depth. The fact that the Moho reflection also comes in early favors the shallower Moho hypothesis. This choice is illustrated in figure 4-15. This model, called VM3, appears to explain the first three arrivals at SBSN reasonably well. Note that this model also seems to explain VST, which was also plagued by an early P_n arrival. Note, however, that VST is in the opposite direction from SBSN (see fig. 4-7). Later in the record section (fig. 4-15) two additional curves are drawn for the double and triple Moho reflections P_mP_2 and P_mP_3. And it appears that these are indeed seen on the record from SBSN. If so, this would also favor the Moho depth averaging 19 km along the route to SBSN.

To test the multiple reflection idea, VM3 was used to generate a synthetic seismogram for SBSN which was compared to the real record (fig. 4-16). Although the observed seismogram has more character than the synthetic, the timing and relative amplitude of the first 5 phases agree reasonably well. However, the amplitude predicted for P_mP_3 is diminutive. This is apparently because VM3 predicts that

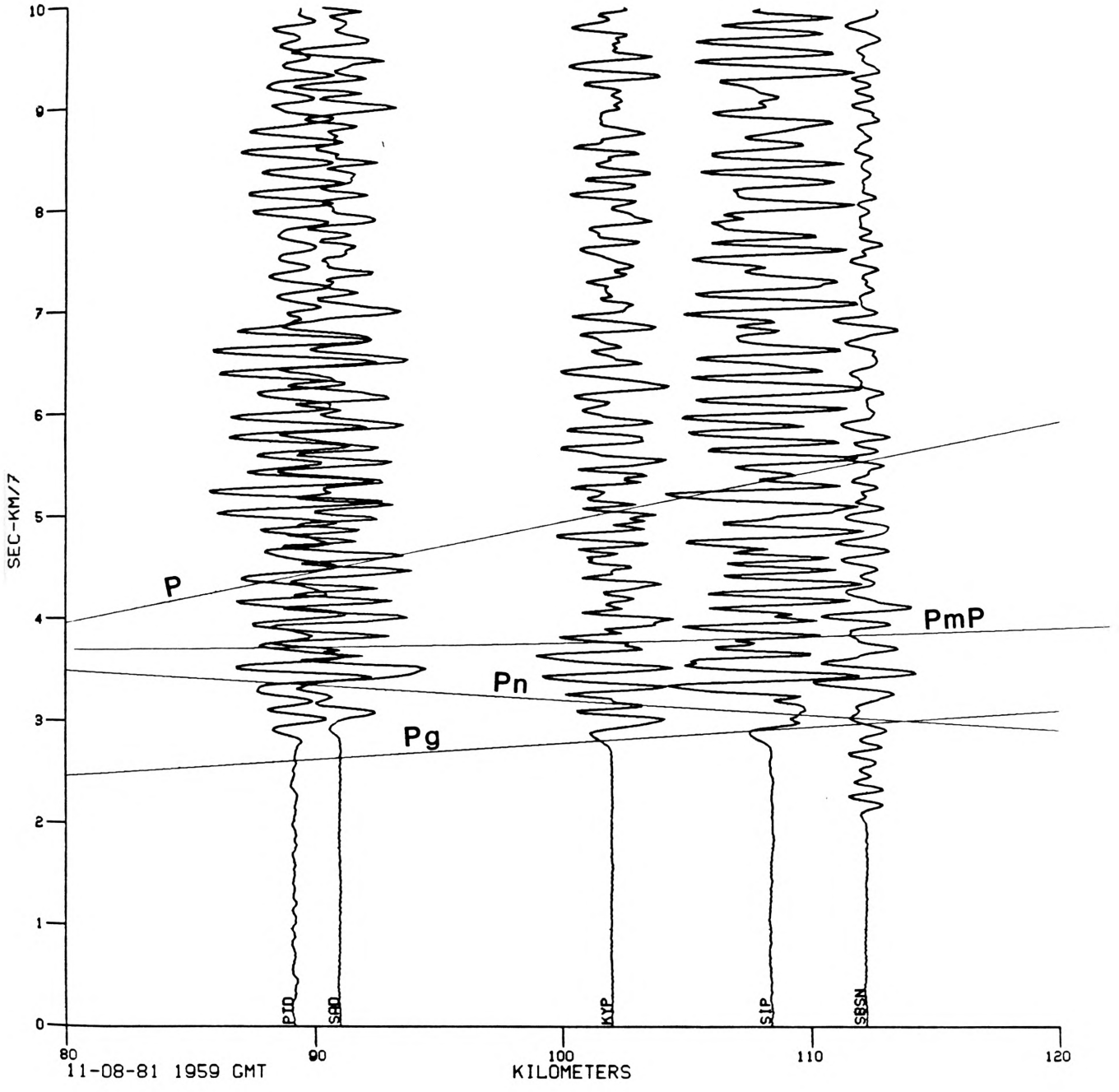

Figure 4-14. Record section for the range 80-120 km from the blast. Lines indicate predicted travel-time curves for VM1.

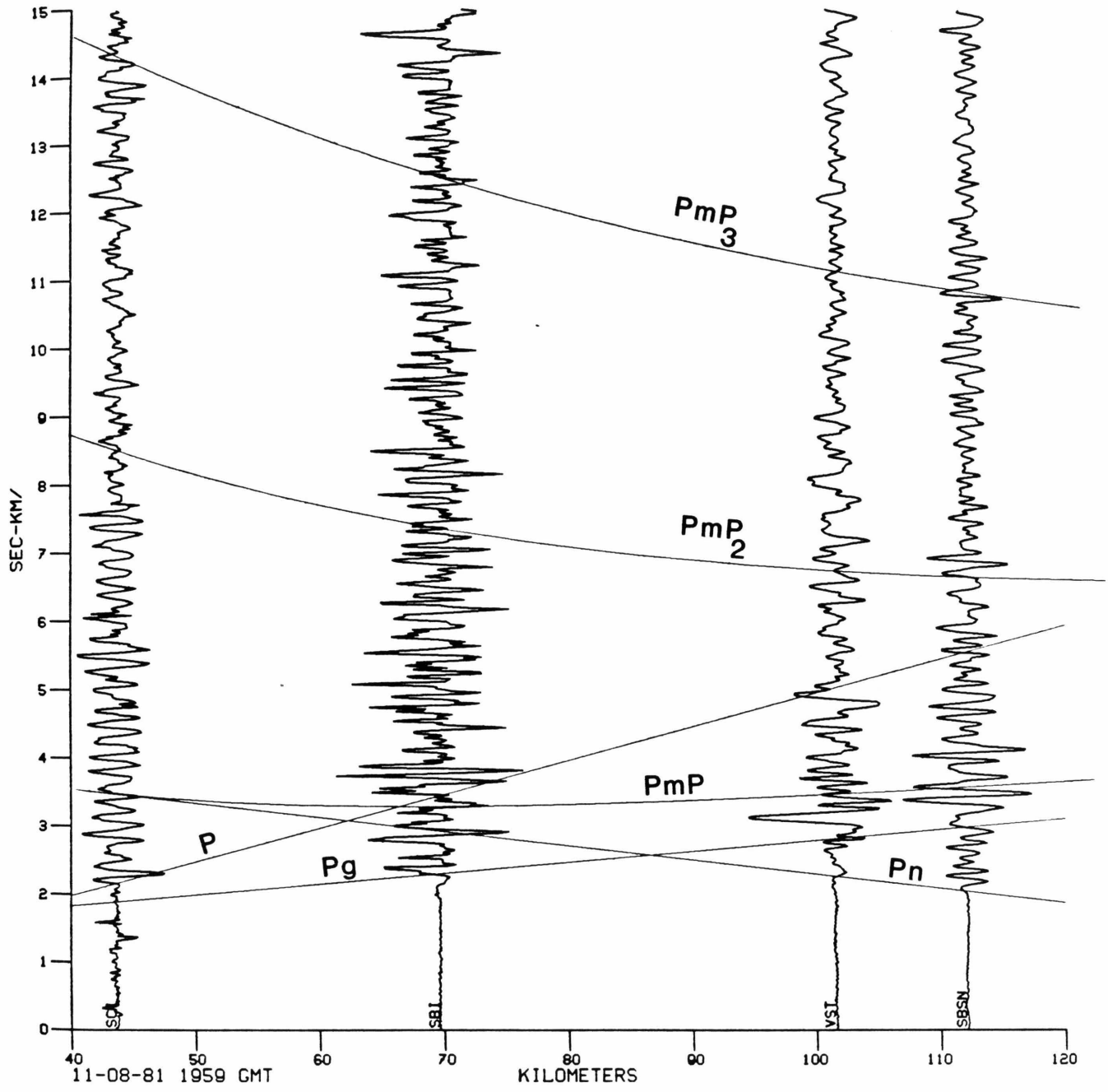

Figure 4-15. Record section for the range 40-120 km from the blast. Lines indicate predicted travel-time curves for VM3. Later curves are for $P_m P_2$ and $P_m P_3$.

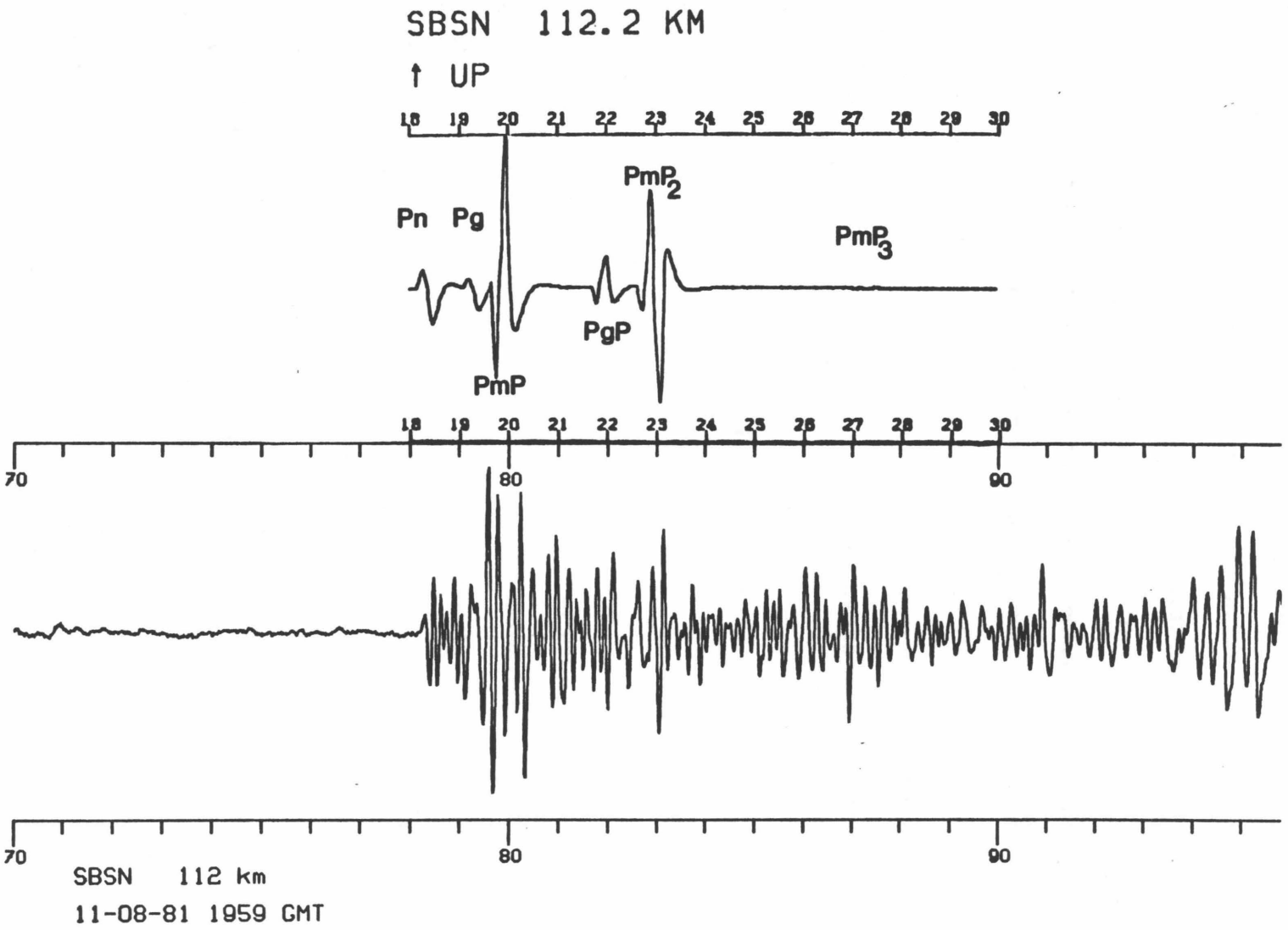

Figure 4-16. Synthetic seismogram (upper trace) generated from VM3 compared to digital record (lower trace) from SBSN.

critical reflection from the Moho occurs beyond 50 km (see fig. 4-15). Since the first pair of legs for P_mP and P_mP_2 are 112 and 56 km, respectively, they are super-critical, resulting in total reflection. The first leg of P_mP_3 would be 37 km, which is sub-critical with a reflection coefficient of 0.3. For three bounces, $(0.3)^3$ is .027. Thus, the waveform seen on the record is either the coincident arrival of an unknown phase, or there is a structural complication that allows a high amplitude P_mP_3. However, in looking at the record for SBSN (fig. 4-16), the similarity of the three waveforms, their equal spacing, and the apparent linear decay from one to the next at least suggests that they were produced by the same mechanism.

DISCUSSION

Structural Implications of VM1

The simplest interpretation of the data is that the Santa Monica Basin and the Santa Cruz-Catalina Ridge are underlain by the flat-layered structure indicated by VM1 (fig. 4-4). And this is all the interpretation that was necessary to use in Chapter 5 to locate earthquakes in this region. However, this interpretation alone would be incredibly naive, considering the structural complexity of the region. The ray paths used in this model (fig. 4-7 and 4-8) cross the deep sedimentary Santa Monica and Santa Barbara basins, the elevated bedrock of the Santa Cruz-Catalina Ridge, two strike-slip faults (one left, one right), and the North Channel Island platform, as well as the major structural boundary between the Transverse Ranges and Peninsular Ranges. In addition, the refraction "profile" is unreversed. The variation from the norm is probably greatest in the mid to lower crust, as indicated by the scatter about the P_g branch (fig. 4-9). The scatter about the P_n branch is rather small, which suggests that this interface is at least planar. However, since the

profile is unreversed, 7.8 km/sec should only be taken as an apparent velocity for the Moho. Shor and Raitt (1958a) observed Moho velocities of 8.2 km /sec. If we use this number for a calculation assuming a dipping interface, it would imply a northwest dip of 3.6°, and 22 km only represents the depth of the point at which critical refraction begins.

VM1 vs. VM2

The feature of VM2 that the P_g layer is 3 km shallower than in VM1 is intriguing and suggestive. One possibility is that Catalina has been uplifted as a block as much as 3 km. Catalina has plentiful evidence of uplift. The island is geomorphically a plateau, with steep sides and a gently rolling upper surface. Marine terraces occur at 300 m above sea level (Smith, 1900), and the total relief from the top of the island to the foot of the Catalina Escarpment is 1200 m. Pliocene beds exposed on the island today were probably deposited at 2,000 m depth (Howell and Vedder, 1981).

It is possible that the P_g layer dips to the northwest (as was suggested above for the P_n layer). The difference between 6.3 and 6.2 km/sec is within the error limits of these data, but the slightly lower P_g velocity might also be a reflection of northwest dip on the interface. The island of Catalina might thus be the high end of a much larger block that has been tilted. The bedrock of the island is predominantly Catalina Schist, which is genetically and mineralogically equivalent to the Franciscan formation (Platt, 1976). Stewart and Peselnick (1978) have reported seismic velocities of 5.2 to 6.4 km/sec from laboratory testing on the Franciscan. The crustal velocities observed in VM2 are within these limits.

VM1 vs. VM3

Admittedly, VM3 was derived on the basis of one seismogram from SBSN. Coincidentally or not, it also appears to satisfy the early P_n arrival at VST, which is in the opposite azimuth. This suggests the possibility that the Moho depth may have an average depth of 19 km on a line from VST to SBSN, which passes just south of Catalina. This is 3 km shallower than in VM1. This might also suggest that Catalina is block-faulted or tilted up relative to points northwest. Since the ray path to SBSN is better constrained, due to the multiple reflections, a more rigorous conclusion would be that the Moho shallows in the seaward direction. This makes sense isostatically, as we approach the 10- to 12-km-thick oceanic crust beyond the Patton Escarpment, and is also suggested by observations of Shor and Raitt (1958a).

Comparison with Previous Work

Press (1956) was the first to suggest that the Continental Borderland crust may be 50% thinner than onshore. On the basis of Rayleigh wave phase velocities he estimated it to be 15-20 km thick. Hearn (in press) carried out a P_n inversion for all of southern California and noted that P_n arrivals were early at the offshore stations. Assuming an average crustal velocity of 6.3 km/sec, he maps the Moho at 26 km depth in the vicinity of Catalina, with it shallowing seaward. The differences between his time terms would imply that the Moho is 3 km shallower at San Nicolas than it is at Catalina. However, he estimates Moho velocities to be 8.0 to 8.2 km/sec in the offshore region. Hearn's work differs from my own in that he defines a deeper and faster Moho, but we are both observing travel times, which trade off depth with velocity. Keller (1983) used ten earthquakes and two blasts to determine P_n velocities in the western Transverse Ranges. His data included the Catalina blast as well as a 4.1 M_L earthquake between Catalina and the mainland. All of his

travel-time plots show 7.8 km/sec for P_n.

Several models for southern California in general, and the Continental Borderland in particular, have been derived from refraction studies, and these are summarized in fig. 4-17. In general, the upper part of the various models agrees well with the interpretations in this study (fig. 4-4). There is, however, one disturbing point. All of the other studies indicate a deep crustal layer with higher velocities (6.7 to 7.0 km/sec). This layer was not observed in the data from the Catalina blast. This is somewhat surprising, since one would expect rock densities and crustal properties to vary with depth, and one would not expect the P_g layer to extend to the Moho.

A lower-crust layer may indeed exist, but it may be deep enough that it is never observed as a first arrival and is masked by the upper layers, especially for surface-focus events. There is evidence for this layer however in earthquake data (Keller, oral comm; Stierman and Ellsworth, 1976). The record section (fig. 4-12) was carefully examined to look for travel-time branches with slopes and intercepts suggested by the above models. Although most seismograms exhibit amplitude changes and interference patterns suggestive of later arrivals, in general they are not coherent across the record section. Two possible phases were noticed, and they are illustrated in figure 4-18. The later one has the equation: $x/7 + 4.72$. This is quite late, and the intercept time would imply that a 7-km/sec layer lies at 29.4-km depth. The earlier one is $x/6.7 + 3.18$. This would imply a 6.7-km/sec layer at 22.6-km depth. These depths are considerably greater than in any of the other published offshore models. Also, the P_n refraction has the equation: $x/7.8 + 4.67$. When the calculations are done for the intercept contribution between the 6.7 (or the 7.0) and 7.8 layers, negative thicknesses are calculated for these lower crustal layers. The physical significance of this is unknown, but it might be that the identification of these "phases" is incorrect. Lower crustal layers with the "correct" depth, as

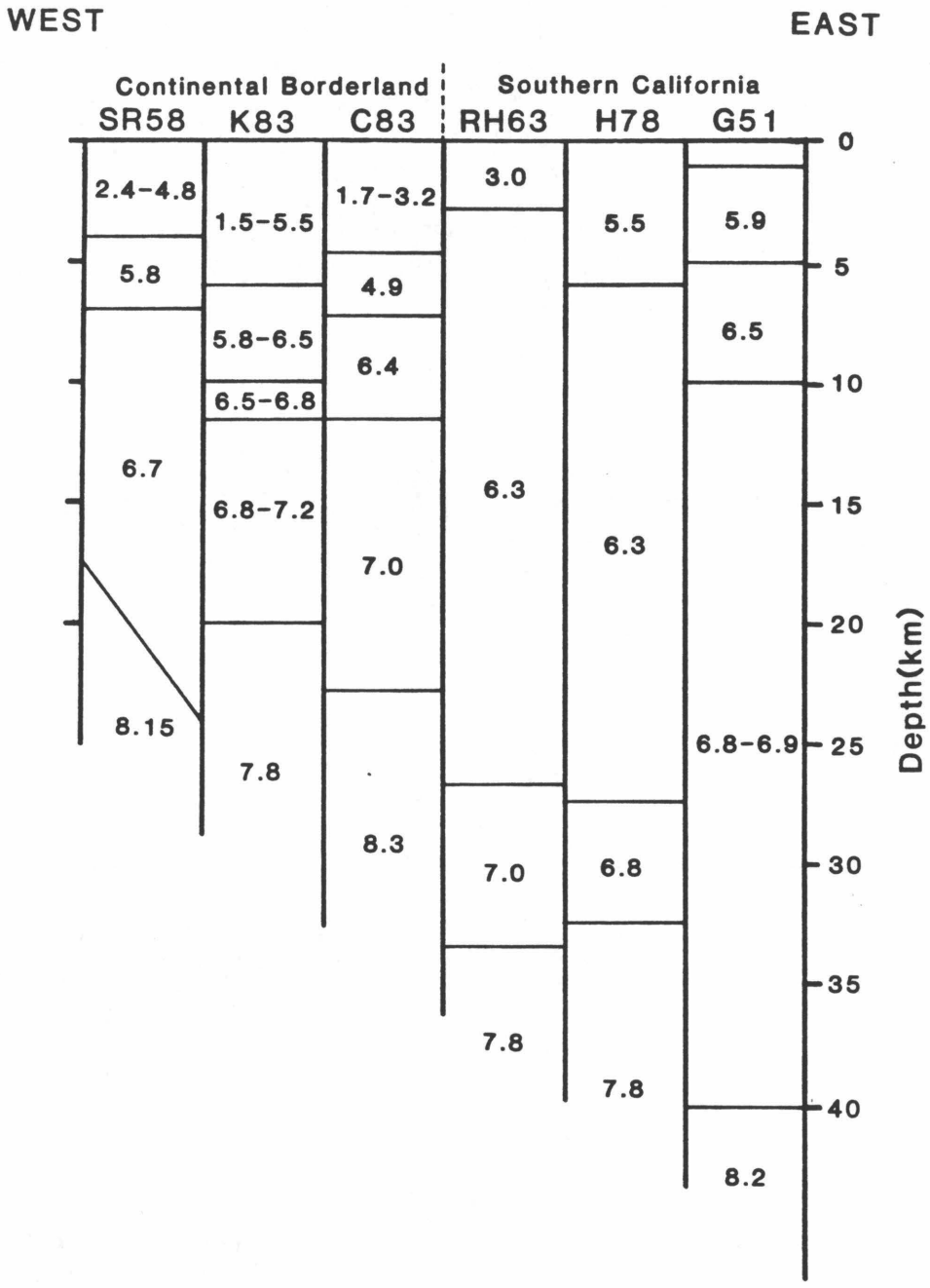

Figure 4-17. Previous velocity models arranged (roughly) west to east. Velocities in km/sec.

SR58: Shor and Raitt (1958a), figure 2, Continental Borderland.

K83: Keller *et al.* (1983), figure 3, Santa Cruz Basin.

C83: Crandall *et al.* (1983), table IIb, eastern Santa Barbara Channel.

RH63: Roller and Healy (1963), east of Santa Monica Bay, model II.

H78: Hadley (1978), figure 2.3a, southern California (Mojave).

G51: Gutenberg (1951), table 1, southern California.

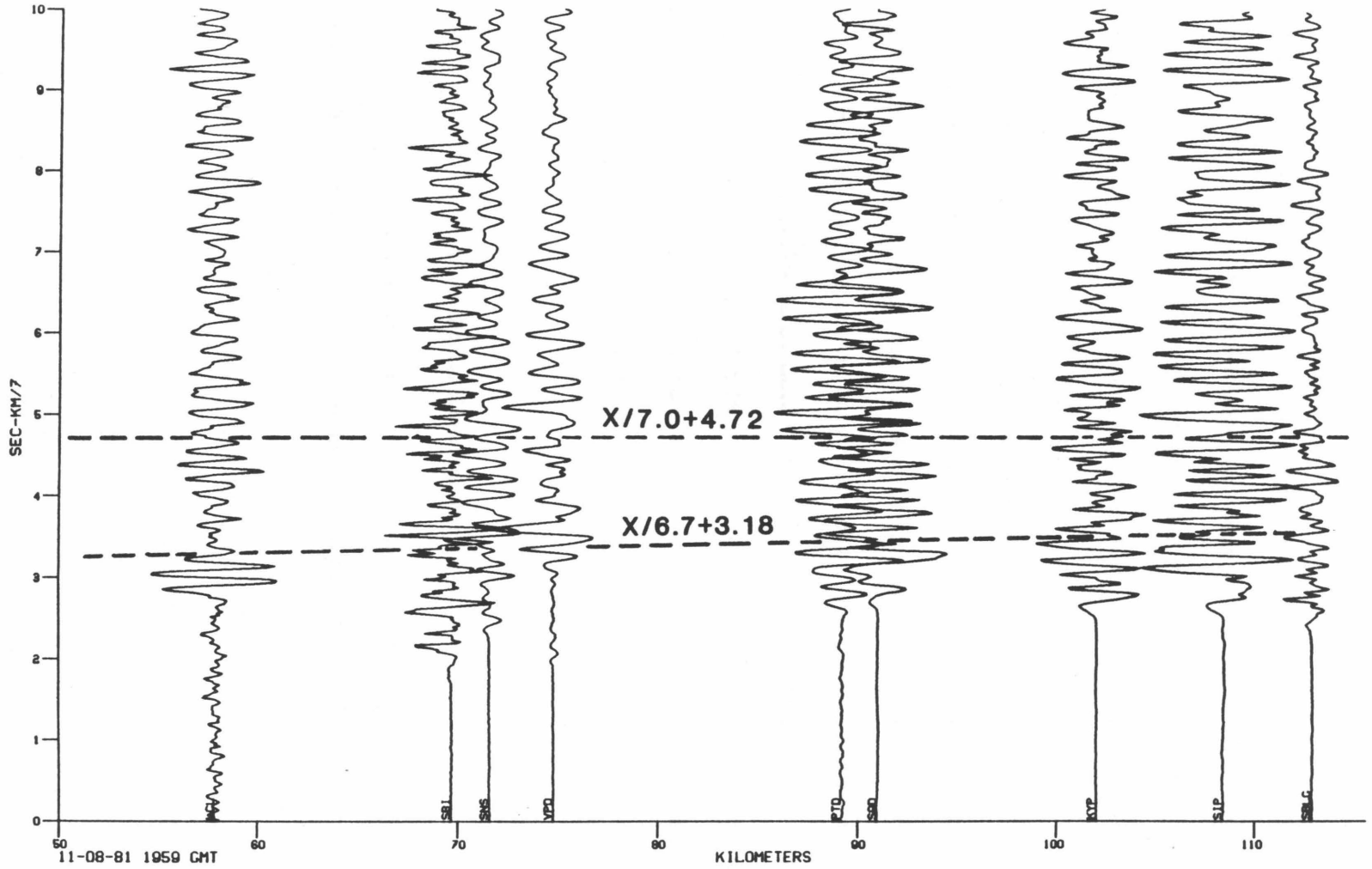

Figure 4-18. Record section for the range 50-115 km from the blast. Lines indicate possible phases with velocities characteristic of the lower crust.

indicated by previous workers, should have t-intercepts in the range 1.5 to 2.5 seconds. On figure 4-18, there does not appear to be any other phase that is 1 second ahead of the suspected 6.7 branch, but it also apparent that it would be difficult to pick one out from the readily apparent P_n, P_g, and P_mP phases. In short, the unknown "phases" come in too late to be simple crustal refractions, and if they are real, they are delayed by some mechanism. One possibility is that the flat-layer assumption may be invalid. Dipping layers would skew the t-intercepts and lead to miscalculation of refraction depths. Another possible delaying mechanism is a low-velocity zone in the lower crust. Such a structure has been previously suggested for onshore southern California by Gutenberg (1951) and Hadley (1978). Of course it is still possible that there is not a lower crustal refractor northwest of Catalina, or it might be transitional and not produce a clear refraction. But, the most likely interpretation is that there is indeed a lower-crustal layer and it is simply not discernable in the data.

Gravity Measurements in the Continental Borderland

Another geophysical measurement that reveals crustal structure is gravity. This method differs from velocity studies in that gravity observations are much more sensitive to density changes, but it has the disadvantage that it is very sensitive to shallow structures which may mask deeper, more significant anomalies. Gravity maps of the region (Oliver, 1980; Beyer, 1982) show that the gravity contours have a northwest-southeast grain, reflecting regional structure.

Beyer (1980) notes a regional gravity decrease towards the northeast of 0.55 mgal/km. He attributes this to crustal thickening in this direction. His Bouguer gravity map shows a high correlation with topography, i.e., highs on ridges and islands, lows over the sediment-filled basins. The largest gravity high is +90 mgal on the ridge

extending northwest from San Clemente Island. Another notable high (+70 mgal) is centered on Santa Cruz Island, the south flank of this gravity high turns southeast and parallels the Santa Cruz-Catalina Ridge to another high of +50 mgal centered on Catalina. A third high of +60 mgal is associated with San Nicolas Island. It is noteworthy that the island stations exhibit early P_n arrivals, as shown by this study and by Hearn (in press). The deepest lows are in the Ventura Basin (-80 mgal) and the Santa Monica Basin (-50 mgal), probably reflecting the great thickness of low-velocity sediments. At the Patton Escarpment, gravity increases steeply from 80 to 220 mgal. Harrison *et al.* (1966) attribute this feature to rapid crustal thinning from 22 km in the continental Borderland to 11 km under the ocean. They state that here the dip of the Moho appears to exceed 45° under the Continental slope and may well be vertical.

SUMMARY

A 90-ton explosion on Catalina Island was used to study the velocity structure of the southern California Continental Borderland. This blast generated coherent refractions and reflections that can be interpreted with a simple well-constrained model. The basic model is a 5.5-km-thick upper crust (5.2 km/sec) underlain by a 6.3-km/sec P_g layer, with a Moho of 7.8 km/sec at 22-km depth. The model was sightly different for Catalina Island, with the P_g layer located at 2.5 km-depth. In conjunction with geological data, this suggests possible uplift of 3 km for Catalina. The seismogram from San Nicolas Island exhibited an early P_n and single, double, and possibly triple Moho reflections. These strongly constrain the crust to average 19 km thickness along a path towards San Nicolas. In general, these observations agree well with previous studies, with one notable exception. Most of the previous workers reported lower crustal velocities of 6.7-7.0 km/sec which were not observed in this

study. Phases with these velocities were possibly observed, but they occur too late to be simple critical refractions. Structural complications or a low-velocity zone may explain their absence at the expected time. The simplified flat-layer model will be used to locate earthquakes in Chapter 5.

Chapter 5

THE SANTA BARBARA ISLAND, CALIFORNIA EARTHQUAKES OF SEPTEMBER - OCTOBER 1981

Introduction

On September 4, 1981, a moderate earthquake that occurred at 15:50:50.3 GMT (8:51 A.M. PDT) was felt throughout coastal southern California. It registered 5.3 on the Richter scale, but it was located 50 km offshore from the southern California coast so that it did no real damage. Its epicenter is indicated by the star on figure 5-1. The closest point of land is tiny Santa Barbara Island, which is 1 km by 2 km and was uninhabited except for a solitary U.S. Park Service Ranger, who was the only person strongly shaken by the temblor (Ken Giles, pers. comm., his account is included in the Appendix). The earthquake and its many aftershocks were well recorded by the many seismographic stations in southern California. At that time, the Geophysical Laboratory of the University of Southern California (USC) was operating 22 stations in the area, including the 2 closest (SBI & CIW). In addition, the 160 stations of the Caltech-USGS southern California network were being recorded by the Caltech Earthquake Detection and Recording (CEDAR) system. Hence, by the joint efforts of Caltech and USC, this seismic activity had good azimuthal coverage. A preliminary report has been given by Corbett and Piper (1981). Subsequent studies have led to a better understanding of offshore velocity structure, and hence improved locations for this earthquake and its aftershocks. The new improved locations and their interpretation are the basis of this chapter.

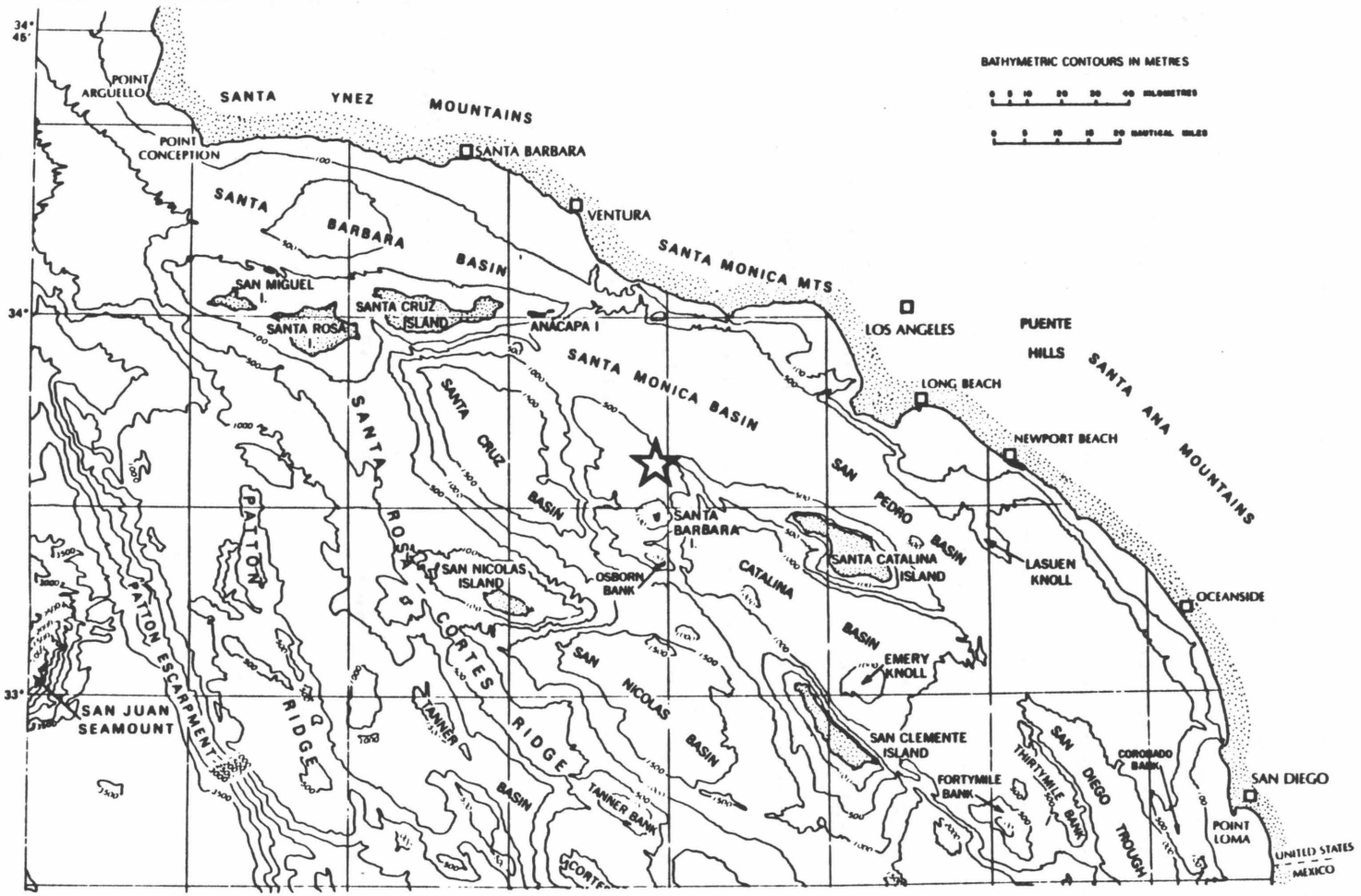

Figure 5-1. Physiography of the southern California Continental Borderland. Bathymetic contours at 500 m interval. Mainshock epicenter indicated by star. Modified from Vedder *et al.* (1974).

Geological Setting

This earthquake occurred in a physiographic province known as the southern California Continental Borderland. The Continental Borderland extends from Point Conception on the north to Bahia Sebastian Vizcaino on the south, and from the southern California coastline on the east to the Patton escarpment on the west. At the Patton escarpment, the ocean floor drops precipitously to the 4,000-m depth of the Pacific abyssal plain. The Continental Borderland is different from most of the continental margin along the California coast in that it is a 250-km-wide offshore area of deep sedimentary basins and intervening bedrock ridges, with local relief exceeding 2,000 m in places. (See figure 5-1.) At their highest points, the ridges protrude above the sea surface to form the 8 Channel Islands. Many of the submarine ridges are nearly flat-topped, having been beveled by erosion when they were exposed during the low-sea stands of the Pleistocene (Junger, 1976). The earthquake occurred along one of these: the Santa Cruz-Catalina ridge, at the location indicated by the star in figure 5-1.

Regional Geology

The Continental Borderland is considered to be part of two of the geomorphic provinces of southern California (Vedder, 1976). The northern end is characterized by the east-trending faults and structures typical of the Transverse Range province. The southern portion is characterized by the northwest-trending structures of the Peninsular Ranges Province. The two provinces are separated by the Dume-Santa Cruz Island fault trend which runs along the Malibu coast and the south side of the northern Channel Islands. The 1981 earthquake activity occurred in the southerly Peninsular Ranges province, 30 km south of the boundary with the Transverse Range province. The generalized geology of the region is depicted in figure 5-2. The main

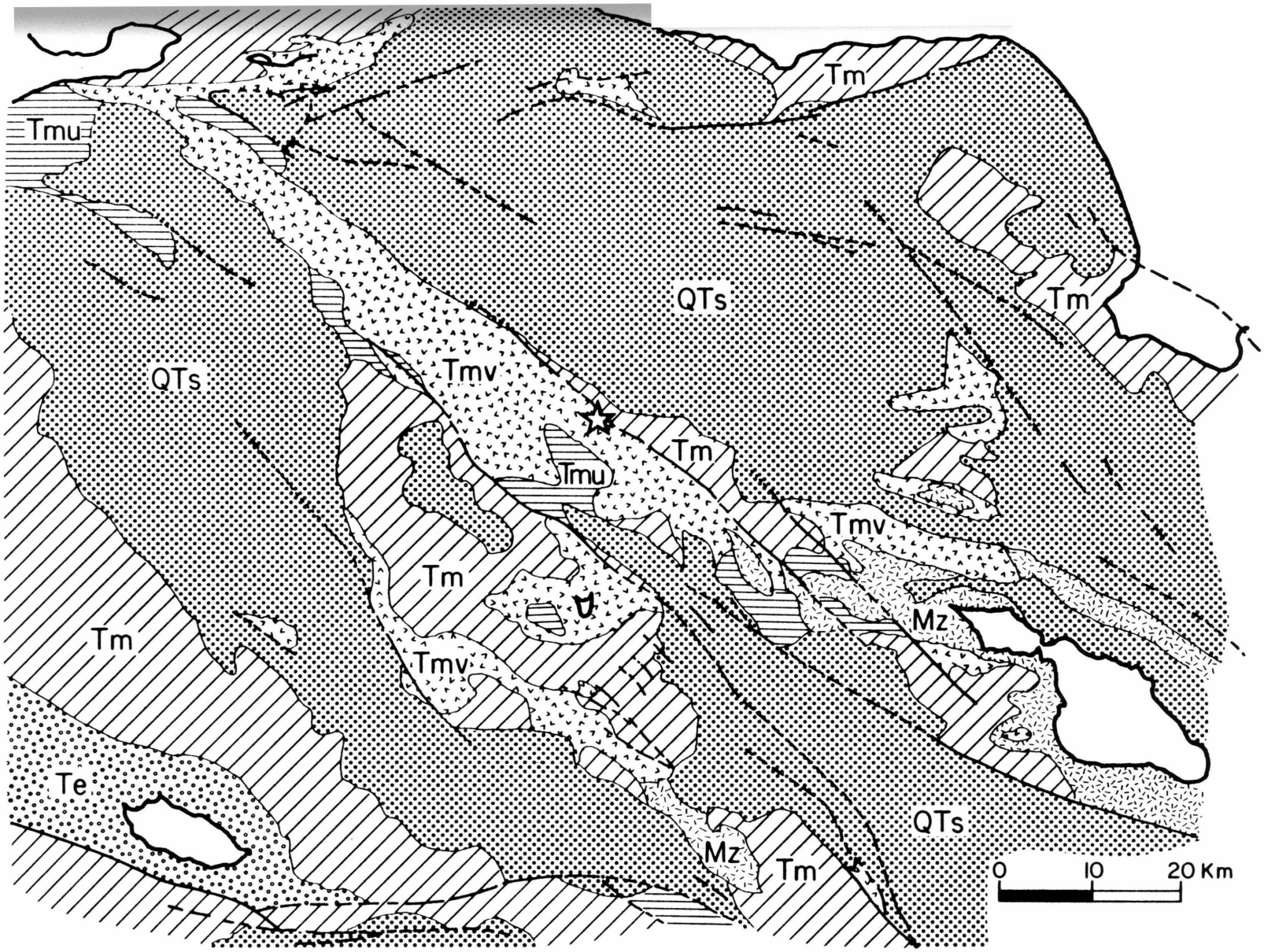

Figure 5-2. Generalized geologic map of the region surrounding the mainshock (star). QTs is Quaternary-Pliocene sediments. Tm is Miocene sediments. Tmv is Miocene volcanics. Tmu is Miocene, undifferentiated. Te is Eocene sediments. Mz is early Tertiary and Mesozoic basement (mostly Catalina Schist). After Vedder *et al.* (1974) and Blake, *et al.* (1978).

feature is the northwest-trending exposure of Miocene volcanics that makes up the Santa Cruz-Catalina ridge, which lies between the Santa Monica basin on the east and the Santa Cruz basin to the west. These basins are both floored with Pliocene and Quaternary marine sediments. The Santa Cruz-Catalina ridge is cut and, in places, delimited by several major bedrock faults. In particular, a prominent bedrock fault between the volcanics and Miocene sediments bounds the east side of the Santa Cruz-Catalina ridge in the vicinity of the September 4, 1981, mainshock epicenter.

The basin-and-ridge topography of the Continental Borderland is indeed curious, and many theories abound as to its origin. The northwest-grain that controls the edges of the ridges and basins is believed to be fault controlled, as first suggested by Shepard and Emery (1941) in their pioneering work on the offshore area. Most authors believe that the basin-ridge structure has been formed since the early Miocene. The basic hypotheses are that the Continental Borderland has been formed by rifting (Yeats, 1968a, 1976), by strike-slip faulting (Howell, *et al.*, 1974; Crouch, 1979), by folding (Junger, 1976), or as pull-apart basins (Crowell, 1974). All of these models are now complicated by recent paleomagnetic work that indicates that several of the Channel Islands have also been rotated 90° in the clockwise direction since the Miocene (Luyendyk *et al.* 1980; Kamerling and Luyendyk, 1981). Whatever the original mechanism, most of the above workers seem to agree that the original Miocene structures have subsequently been taken over by the right-shear system associated with the San Andreas fault system, and the southern California borderland is now behaving under convergent wrench tectonics similar to that seen on the Newport-Inglewood fault (Harding, 1973; Yeats, 1973).

It is not clear that present-day seismicity can determine which of the above models is correct. However, the data of this chapter indicate clearly what the

present-day tectonic process is, at least on one of the northwest-trending structures. And it is presumed that this process has been going on for some geological length of time. Knowledge of past tectonics gives insight into the present process, because it constrains where the crustal pieces could have come from. Likewise, present activity places neo-tectonic constraints on all models of the geologic evolution of the southern California Continental Borderland.

Previous Seismicity

In contrast to the plentiful literature on the Tertiary geological history of the southern California Continental Borderland, there is a dearth of seismological studies on the area. The reasons for this appears to be two-fold. First, there are not many seismographic stations offshore, since they are necessarily limited to islands; and these have only become numerous within the last few years. And secondly, no large earthquakes have occurred offshore since instrumental recording began in the 1930's.

The first study of offshore seismicity was done by USC oceanographers who were looking for some relation to offshore geology (Clements and Emery, 1947). These workers noted that there was a correlation between epicenters and the location of offshore escarpments. Of particular interest, they noted epicenters along the San Clemente escarpment and the Santa Cruz-Catalina ridge. The only study since that time has been by Legg (1980). He also noted weak correlations with the San Clemente fault trend. Even the more recent data that Legg (1980) studied were still subject to poor locations offshore, as well as the scarcity of detectable events (compared to onshore southern California).

The seismic history dates back to 1812 when two large earthquakes rocked the missions along the southern California coast. The earthquake of December 8

destroyed the mission at San Juan Capistrano. Isoseismal studies place its epicenter near the coast in the vicinity of Santa Ana with a magnitude of 6.9 (Toppozada *et al.*, 1981). On December 21, 1812, another earthquake did extensive damage to the missions at Santa Barbara, La Purisima, and Ventura. Toppozada *et al.* (1981) estimate a magnitude of 7.1 and place its epicenter in the Santa Barbara Channel. Although both events are poorly located, it is unlikely that either was near the epicenter of the 1981 earthquake. On December 9, 1861 an earthquake of unknown size and location was felt on Catalina (Townley and Allen, 1939). Since that time, the only documentation of offshore events has been by the Caltech Seismological Laboratory (Gutenberg *et al.*, 1932; Gutenberg, 1941; Wood, 1947; Hileman *et al.*, 1973). The 6.3 M_L Long Beach earthquake of March 10, 1933 was evidently on the Newport-Inglewood fault with an epicenter located just barely offshore (Hileman *et al.*, 1973). The largest known shock in the southern offshore province is a 5.9 M_L event that occurred on the southeast tip of San Clemente Island on Dec. 25, 1951 (Richter, 1958, p. 535). This earthquake had the curious characteristic of not having a single known aftershock. In addition, this event had compressional first motions at all of Caltech stations which would be unexpected for a right-lateral event on a northwest-trending fault (Allen *et al.*, 1960). Its epicenter was at the southern tip of a restricted U.S. Navy base, which has led some to speculate that its origin was other than natural. Legg (1980) attempts to dispel this notion by observing that many borderland earthquakes exhibit disparately few aftershocks and noting that a number of "reverse mechanism" earthquakes have occurred in this same region. In any case, very few events larger than magnitude 5 have been observed in the Peninsular Ranges province of the Continental Borderland, and the 1981 event is the second largest instrumentally recorded event in this province.

The Caltech catalog was searched for all quality A, B, or C events reported in the vicinity of the Santa Cruz-Catalina ridge prior to the 1981 activity and the results are shown in figure 5-3. Figure 5-3a shows scattered activity occurring throughout the area between 1932 and 1966. The scatter pattern is probably due largely to poor locations during this time period. Locations were hampered by the fact that the station on San Nicolas Island was not installed until 1958, and the Catalina station, not until 1971. The plotted epicenters could be in error by as much as 15 km. The largest event during this time period was a magnitude 5.0 event in the vicinity of San Nicolas Island on November 18, 1947. It apparently had only one detectable aftershock. In addition, two magnitude 4 events occurred in the general vicinity of the Santa Cruz-Catalina ridge, one in 1952, and the other in 1956.

Figure 5-3b shows all the activity occurring during the 10-year period, 1967-1976, with the location of the future 1981 mainshock superimposed. The most noteworthy activity occurred southwest of Santa Barbara Island in 1969. It commenced on October 24, with a 5.1 M_L mainshock and was followed by numerous aftershocks, including two of magnitude 4.7 and 4.8. The 1969 activity is probably more tightly clustered than the poor-quality locations indicate, and a relocation study of them would probably produce interesting results. Although the accuracy of epicenters is probably no better than 10 or 15 km, it is nevertheless clear that they occurred well to the south of the 1981 activity and were probably located along another fault southwest of Santa Barbara Island. Legg (1980) did a focal mechanism of the mainshock and indicates that it is consistent with right-lateral slip on a northwest-trending fault. Note that there is very little seismicity near the locus of the 1981 mainshock--only three small events within 20 km during this 10 year period.

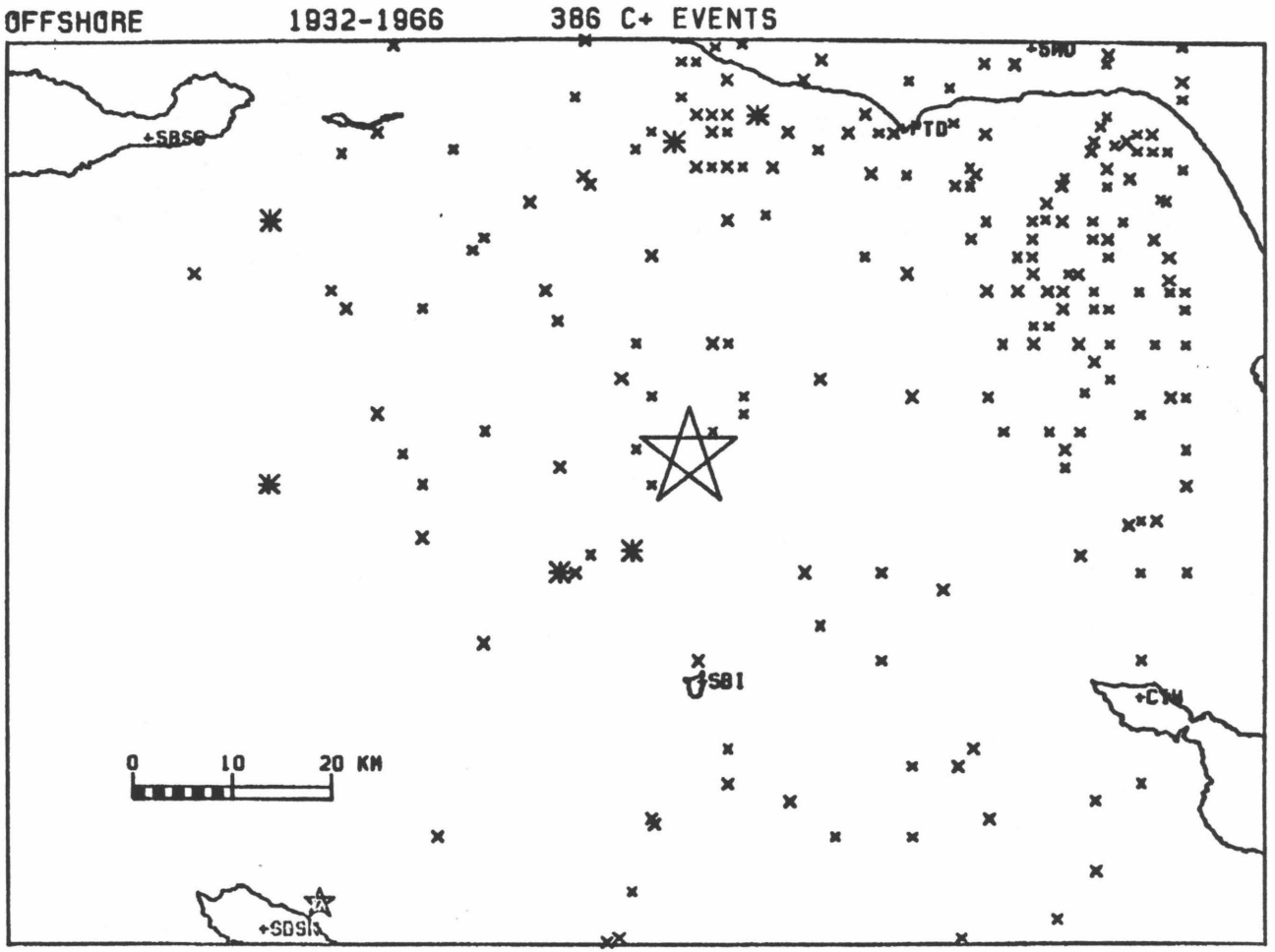

Figure 5-3a. Regional seismicity, 1932-1966. Quality A,B,C locations from Caltech catalog. x : magnitude 0-3; X : magnitude 3-4; ✱ : magnitude 4-5; ☆ : magnitude 5-6; large ☆ : epicenter of 1981 mainshock.

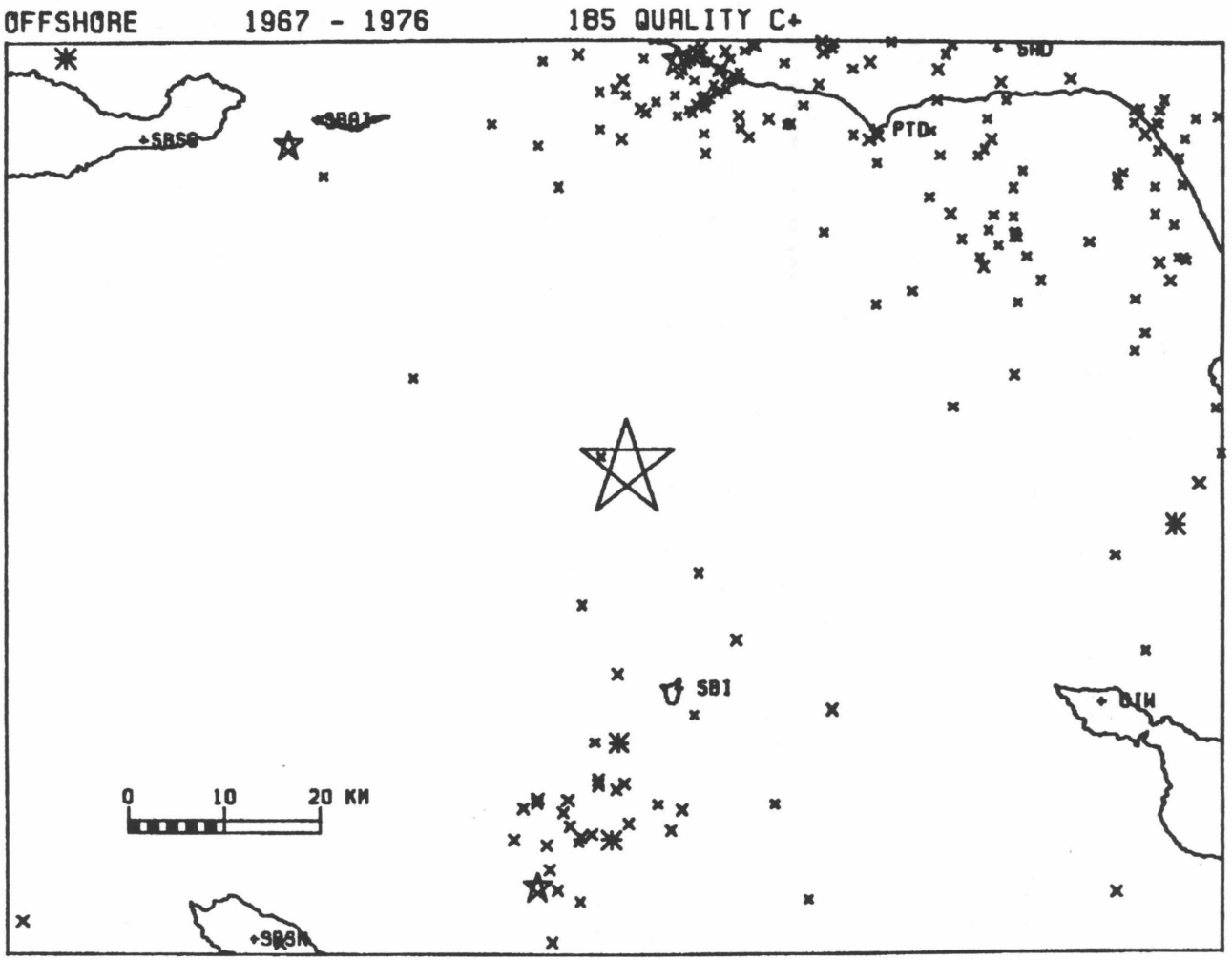

Figure 5-3b. Regional seismicity 1967-1976.

In 1977, the Caltech CEDAR system came on line with better timing, better station coverage, and presumably better locations than at any time in the past. It is believed that since 1977, location accuracy is better than 5 km, and the main source of error has now become systematic bias due to uncertainties in the velocity structure. Figure 5-3c shows the activity from 1977 up to the day before the 1981 earthquake. The main activity during this four-year interval is the 5.0 M_L New Year's Day, 1979, earthquake that occurred just south of the Malibu coast. It was accompanied by numerous aftershocks, indicated by the heavy concentration in the northeast corner of the map. Notice that during that time period, no activity occurred within a 20 km radius of the impending mainshock. Figure 5-3d combines the activity from 1967 to 1981. This figure gives the appearance that the 1981 mainshock occurred in the center of a quiet zone that was ringed by an aureole of seismicity. This bears some resemblance to the doughnut pattern described by Mogi (1969) as a precursor to earthquakes.

1981 Seismicity

The Data

The data to study this new activity came from several sources, at Caltech and USC. The current Caltech-USGS Seismic Processing (CUSP) system produces index tapes known as Q-tapes. These were searched for phase data for all events occurring within the box delimited by the edges of figure 5-3 between February 1981 and December 1982. When seismic activity commenced on September 4, the stations, SBI and CIW were being recorded on analog magnetic tape, and SBI was also being recorded on paper at USC, but neither station was being recorded at Caltech. Phone lines were exchanged with USC and the two stations began recording on the CEDAR

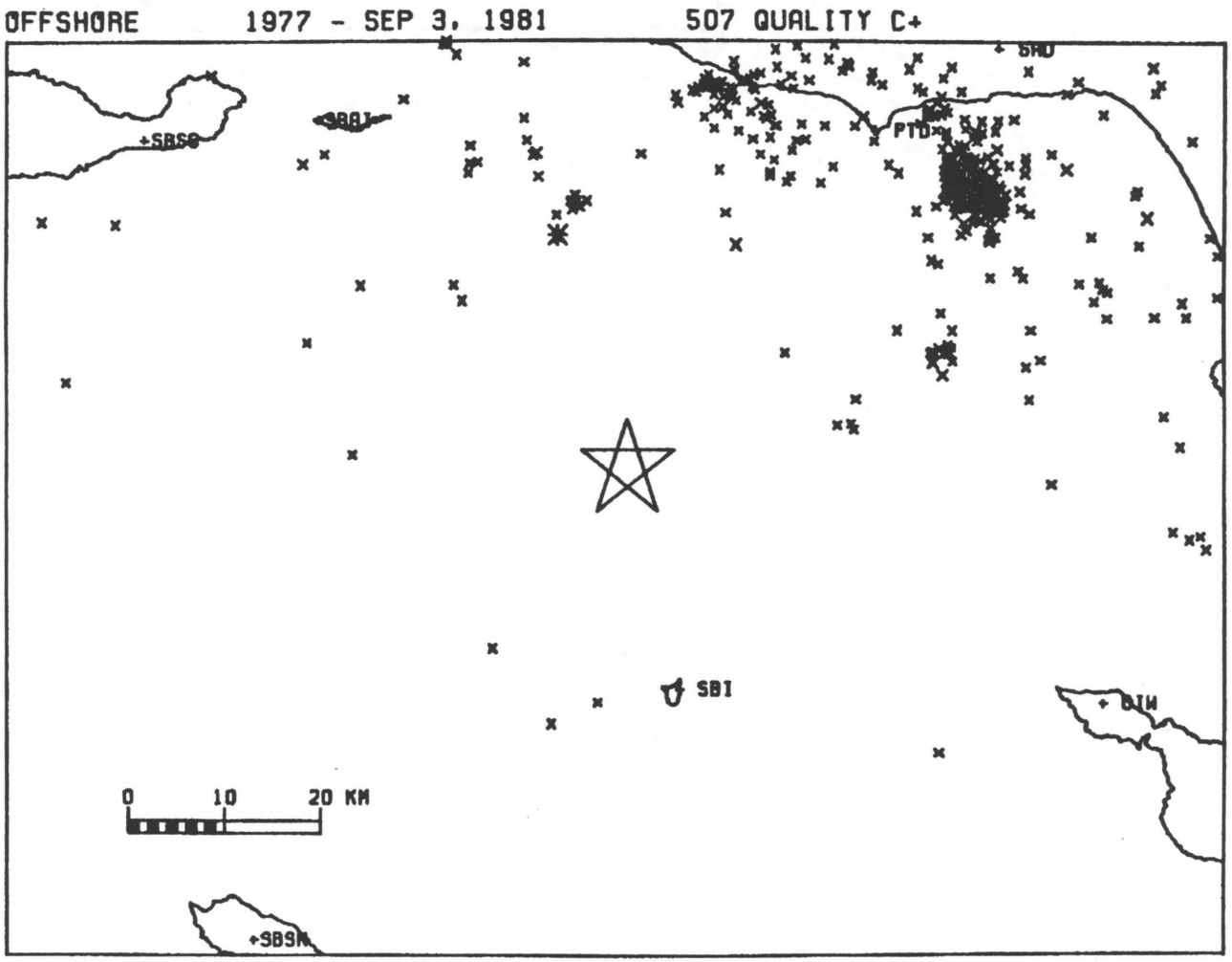

Figure 5-3c. Regional seismicity 1977-Sept. 3, 1981.

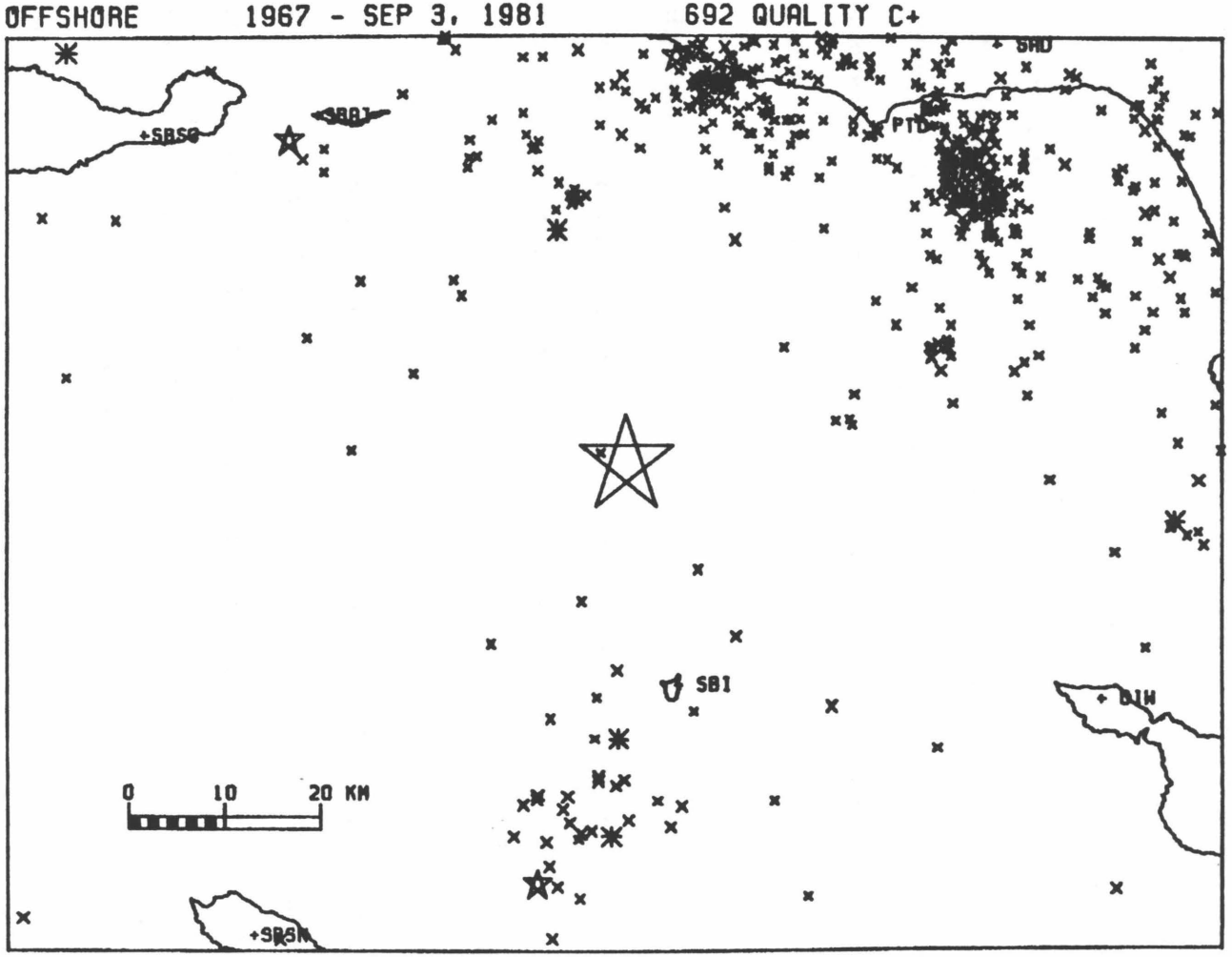

Figure 5-3d. Regional seismicity 1967-Sept. 3, 1981.

system by September 11. All data on the CEDAR system is routinely read to an accuracy of .02 sec. In all, 858 events triggered and were located by the CEDAR system in this offshore region. These data were supplemented by the following data from USC for the period from Sept. 4 to Sept. 11. The USC network stations were read by Ken Piper for all events above magnitude 2.5, to an accuracy of .02 sec. The USC network analog tape was saved for only the first 24 hours of activity. This was subsequently played back, and all of the events that had triggered the CEDAR system were read at SBI, to an accuracy of .02 sec by Ken Piper. The only records for smaller events from Sept. 5 to Sept. 11 were the paper drum recordings for SBI, and these were read by myself, to an accuracy of only 0.1 sec.

Velocity Model

The earthquakes were initially located with the Santa Barbara Channel velocity model used by Corbett and Johnson (1982). It was used on the weak criteria that: 1) it produced lower residuals than the standard Caltech southern California model; and 2) it might correspond more to offshore crust than onshore crust. The results of this study have been presented previously by Corbett and Piper (1981). At that time it was suspected that this model had introduced a bias, because all the epicenters plotted systematically west of the submarine escarpment between the Santa Monica basin and the Santa Cruz-Catalina ridge.

A most fortunate opportunity to calibrate the network for velocity structure occurred on November 8, 1981 when a large quarry blast was detonated on the south end of Catalina Island. It was timed in the field by USGS personnel (Given and Koesterer, 1983), as well as recorded by portable seismographs deployed on Catalina. All of the seismographic stations of interest for this earthquake were at this time now being recorded on the CEDAR system, and hence the explosion was well recorded.

The velocity structure derived from the blast has been presented by Corbett (1983) (also Chapter 4, this volume). The VM1 model of Corbett (1983) is most appropriate for the area northwest of Catalina, and it was selected to relocate the earthquake activity (Table 5-1).

Table 5-1. Velocity Model

P-velocity (km/sec)	Depth (km)
5.2	0.0
6.3	5.5
7.8	22.0

Location Procedures

All locations were determined with the computer program QED1 written by Johnson (1979). Selecting the proper location procedure is difficult, and it depends critically on what assumptions one makes about velocity structures, stations delays, and the quality of picks. Several different location procedures were tested on the first 24 hours of activity to see what kind of biases they could produce. These tests are discussed in detail in Chapter 6, and only the final results are summarized here. First, the Catalina quarry blast was used as a calibration event. Its location was fixed at that given by Given and Koesterer (1983) and station residuals (P-delays) were calculated. These delays are summarized in column 2 of Table 5-2.

Table 5-2. Station Delays			
	Catalina Blast	Master Event	
Station	2000 8 Nov 1981	1008 21 Sep 1981	
	P-delay	P-delay	S-delay
CAM	0.35	0.32	-
CIS	0.13	0.05	0.50
CIW	-0.26	-0.05	0.32
ECF	0.63	0.96	-
IRC	0.20	0.82	-
KYP	-0.10	-0.12	-0.38
MWC	0.49	0.91	-
PAS	0.51	0.37	-
PTD	0.14	0.02	0.11
SBI	-0.01*	-0.06	0.50
SBLC	-0.15	0.47	0.80
SBLG	-0.43	-0.40	-
SBSC	0.06	-0.77	-0.64
SBSN	-0.96	-0.96	-1.31
SCI	0.27	-	-
SCY	-	0.35	-
SIP	-0.19	-0.06	-0.15
SYP	-0.01	0.58	0.74
VPD	-0.23	0.41	-
VST	-0.79	-0.26	-
* second arrival (see Chapter 4)			

After testing, it was decided that the best results for locating regional seismicity would be achieved by locating the earthquakes with these P-delays and a freed starting location. This step is referred to as Phase I and the results are shown in figure 5-4. Subsequently it was desirable to relocate the activity in just the aftershock zone (box in figure 5-4) with a master event chosen from the aftershocks. An aftershock is probably more appropriate than the quarry blast because it is located closer to all the seismicity, and it has occurred at some depth. An aftershock also has the advantage that one can use S-delays, which improve the location of small events and constrain depth. It was decided to pick an event that occurred after September 11, so that SBI and CIW would both be recording on the CEDAR system.

The aftershock at 1008 on September 21 was chosen because it showed the largest number of clear P- and S- readings at all the key stations. Its location was

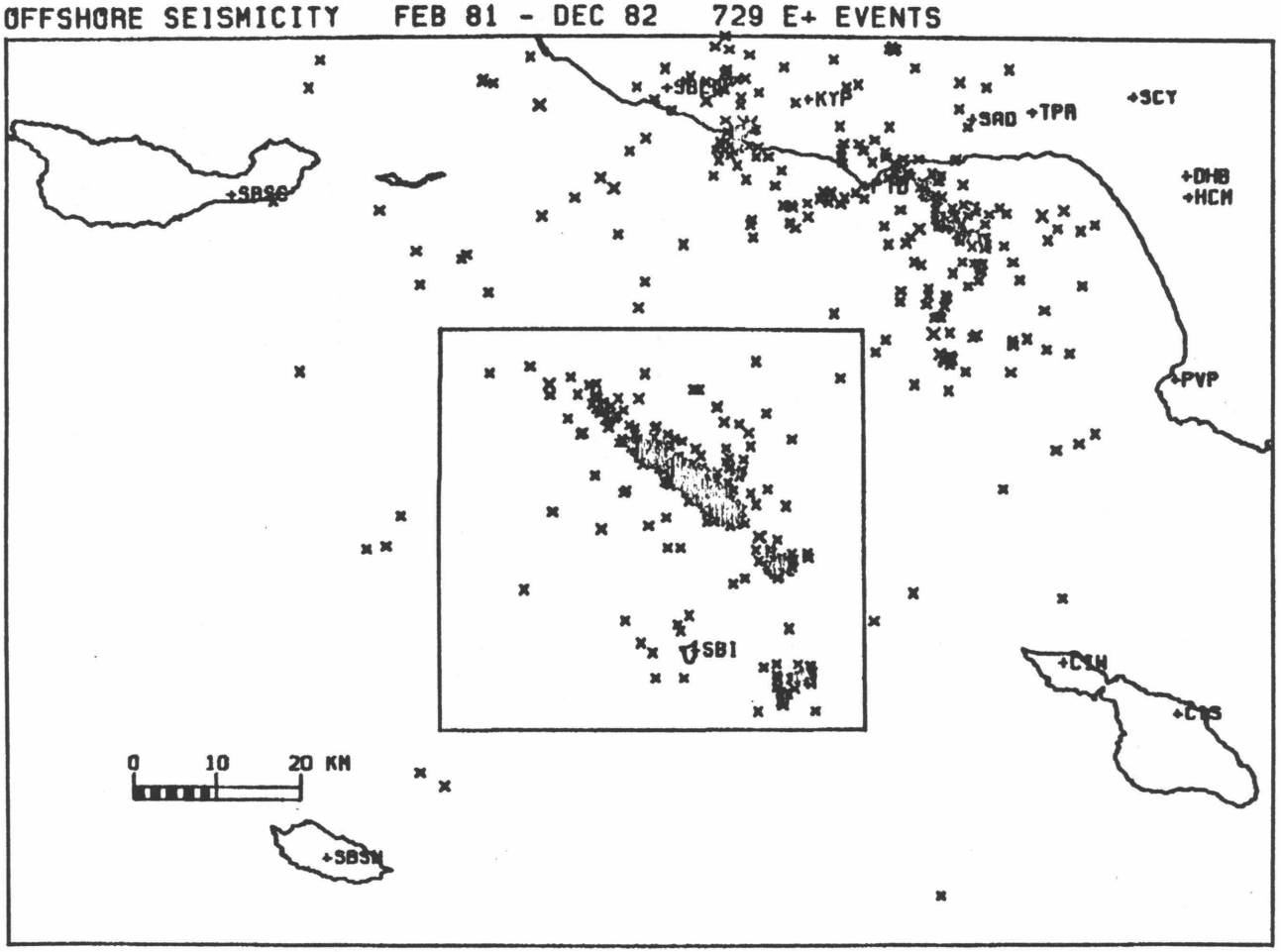

Figure 5-4. Phase I locations, Feb 81 - Dec 82, all events. Square denotes area used for Phase II locations. Symbols as in figure 5-3.

started at several different depths to test how well depth is constrained by the data. When started at 5 km, the solution did not iterate in depth, indicating insufficient depth control to locate very shallow earthquakes. When started at 10, 15, or 20 km, the solution consistently iterated to 10.65-km depth. This was taken as the master event's depth. The delays for this event are indicated in the last two columns of Table 5-2. All of the earthquakes were then relocated with these delays and with master event hypocenter as the starting location (Phase II).

EARTHQUAKE LOCATIONS: PHASE I

Figure 5-4 shows the 729 events located in phase I. Roughly half of these are quality C or better, and these are plotted in figure 5-5. As can be seen, most of the east-west spread in the aftershock locations in figure 5-4 is probably due to poor locations. These Phase I locations are considered to be significantly better than Caltech-USGS catalog locations, and they are listed in Table I of the Appendix.

Foreshocks?

Figure 5-6 shows the distribution of precursory seismicity relative to the aftershock zone. One event occurred on June 24 (2.7M_L), 5 km west of Santa Barbara Island, in the vicinity of the 1969 activity (figure 5-3b). It is well off the aftershock trend and over 20 km south of the impending mainshock, although still closer than some of the aftershocks. Commencing July 29, (36 days before the mainshock), a series of events began to occur 35 km northeast of the aftershock zone (figure 5-6b). This is as close as any activity occurred during the preceding 4 years (figure 5-3c). The events located under the floor of Santa Monica Bay, in the vicinity of the San Pedro basin fault zone. Although the precursory seismicity is intriguing, it clearly does not occur on the aftershock trend of September 1981. Hence these

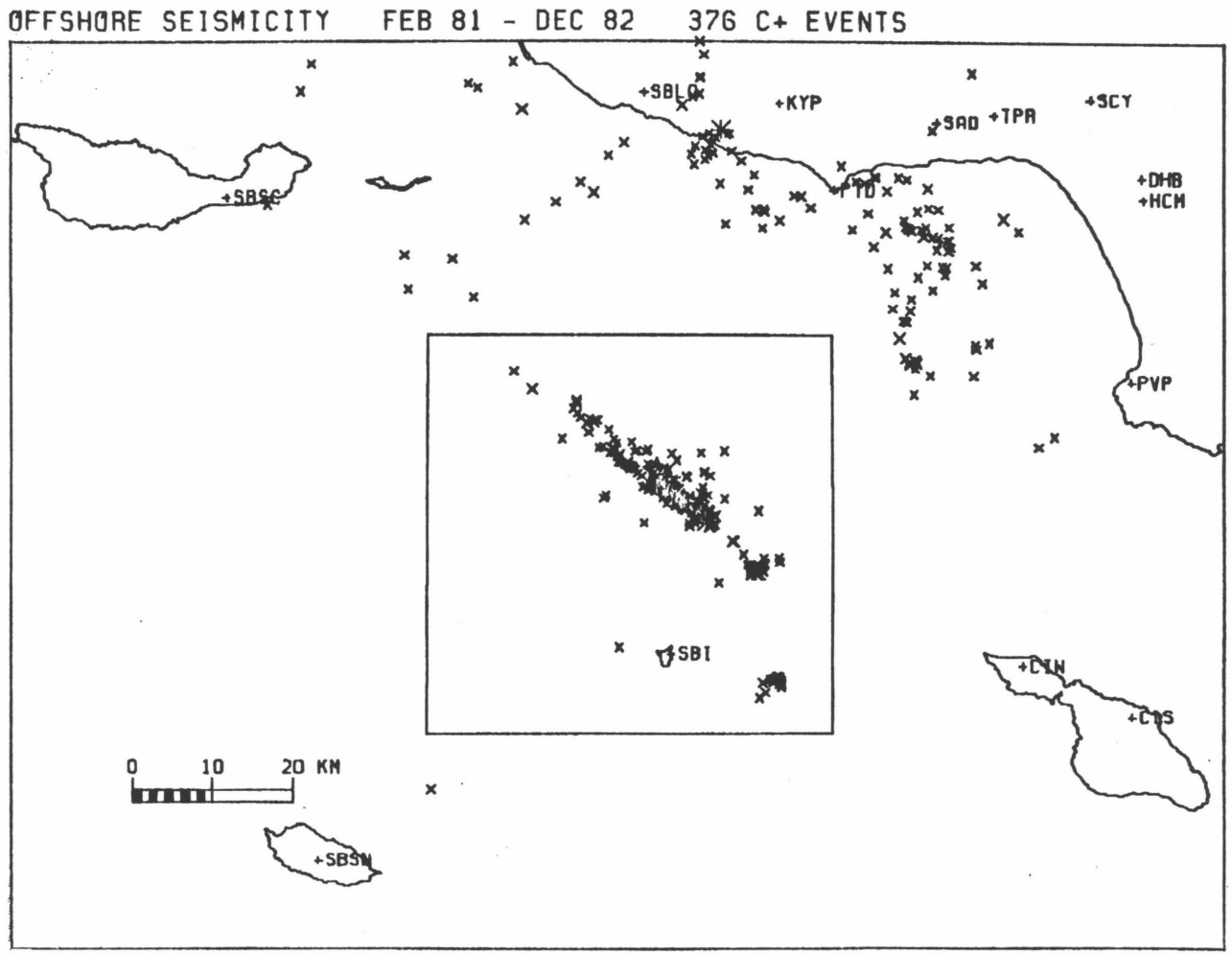

Figure 5-5. Phase I locations, Feb 81 - Dec 82, quality A, B, C. Symbols as in figure 5-3.

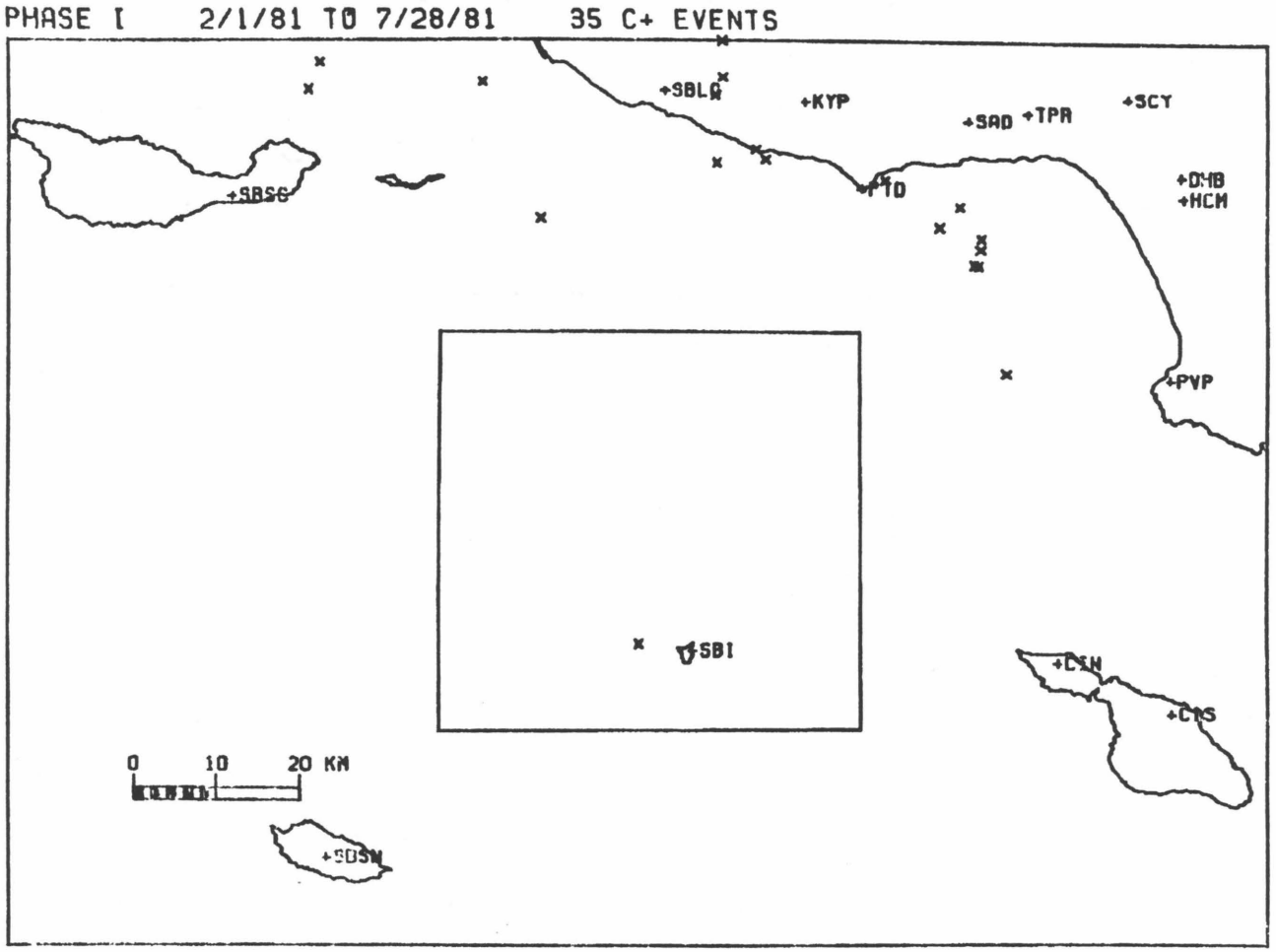

Figure 5-6a. Previous seismicity: Feb 1-July 28, 1981. Phase I locations, quality A, B, C. Symbols as in figure 5-3.

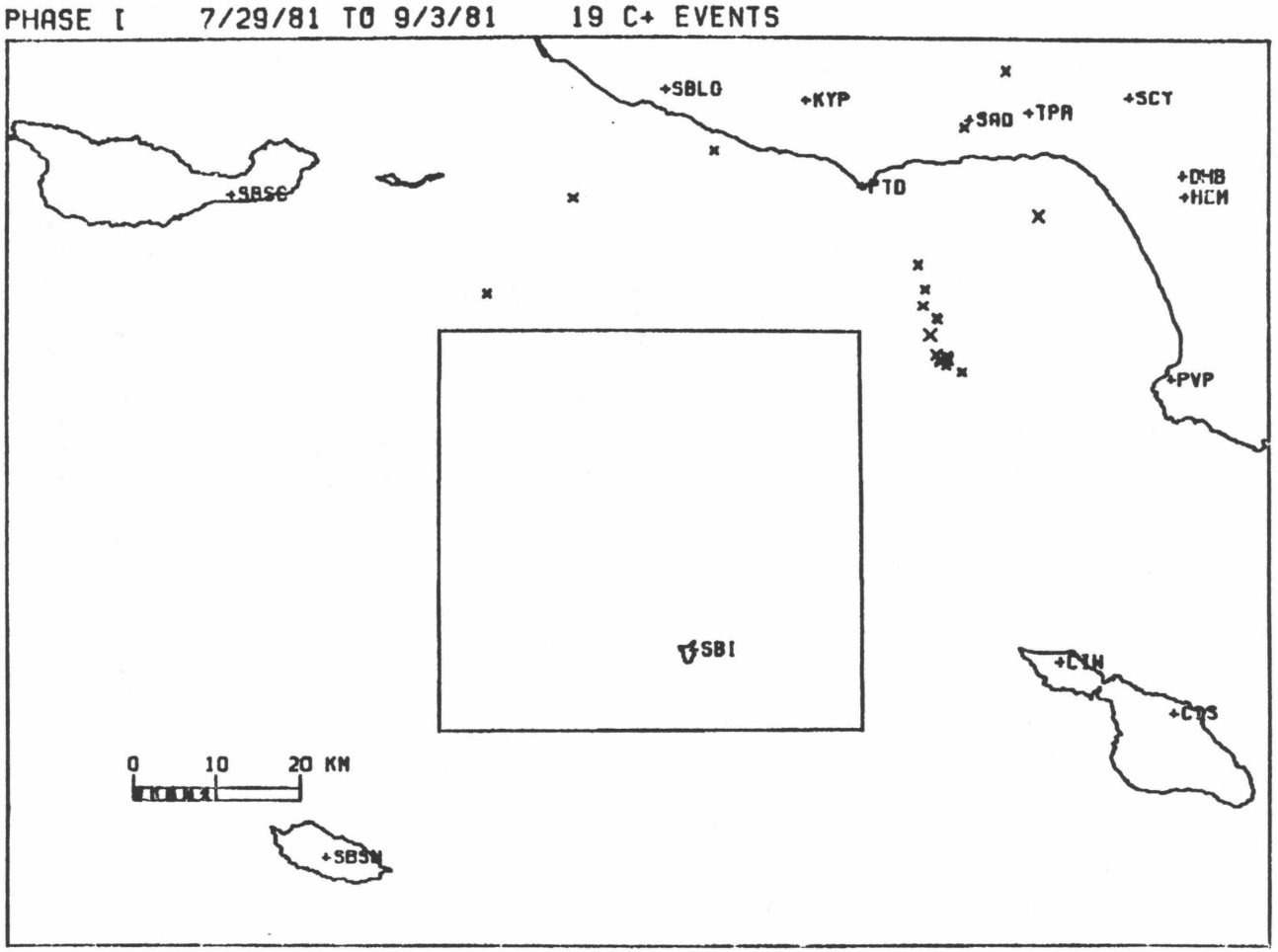

Figure 5-6b. Previous seismicity: July 29 - Sept. 3, 1981. Phase I locations, quality A, B, C. Symbols as in figure 5-3.

earthquakes cannot be termed "foreshocks" *sensu strictu*.

EARTHQUAKE LOCATIONS: PHASE II

The Phase I locations were winnowed by selecting all earthquakes within the box in figure 5-4. This left 458 events, which were relocated in Phase II with the master event. The results are plotted in figure 5-7a and the location parameters are listed in Table II of the Appendix. The main aftershock zone is 25 km long, 5 km wide, and trends N50°W. The mainshock is nearly centrally located. Two additional clusters of aftershocks occurred 18 and 30 km southeast of the mainshock epicenter. Figures 5-7b and 5-7c show progressively higher qualities of event locations. They seem to indicate that the east-west spread of the aftershock zone is probably due primarily to mislocations and not structures. Another way of filtering for quality is shown in figure 5-7d, which depicts all events larger than magnitude 3. These large events are presumably clearly recorded at a large number of stations and there is little doubt as to P-arrival times. Almost all of these larger events occurred within .5 km (the location precision) of a line trending N 50° W. This strongly favors a straight, nearly vertical fault as the causative structure.

Mainshock

The calculated location of the mainshock is 33° 40.92' N and 119° 3.60' W. The corresponding origin time is $15^h 50^m 50.68^s$ GMT. The depth was calculated at 11.48 km. It should be remembered that this depth is relative to the master event (10.65 km depth) and may be in error as much as 5 km. This location puts the mainshock in a spot strongly suggestive of fault topography. This is on the Santa Cruz-Catalina ridge escarpment at the head of a 500-ft. deep canyon leading down into a closed depression (figure 5-7d). This general area has been previously referred to as a rift valley

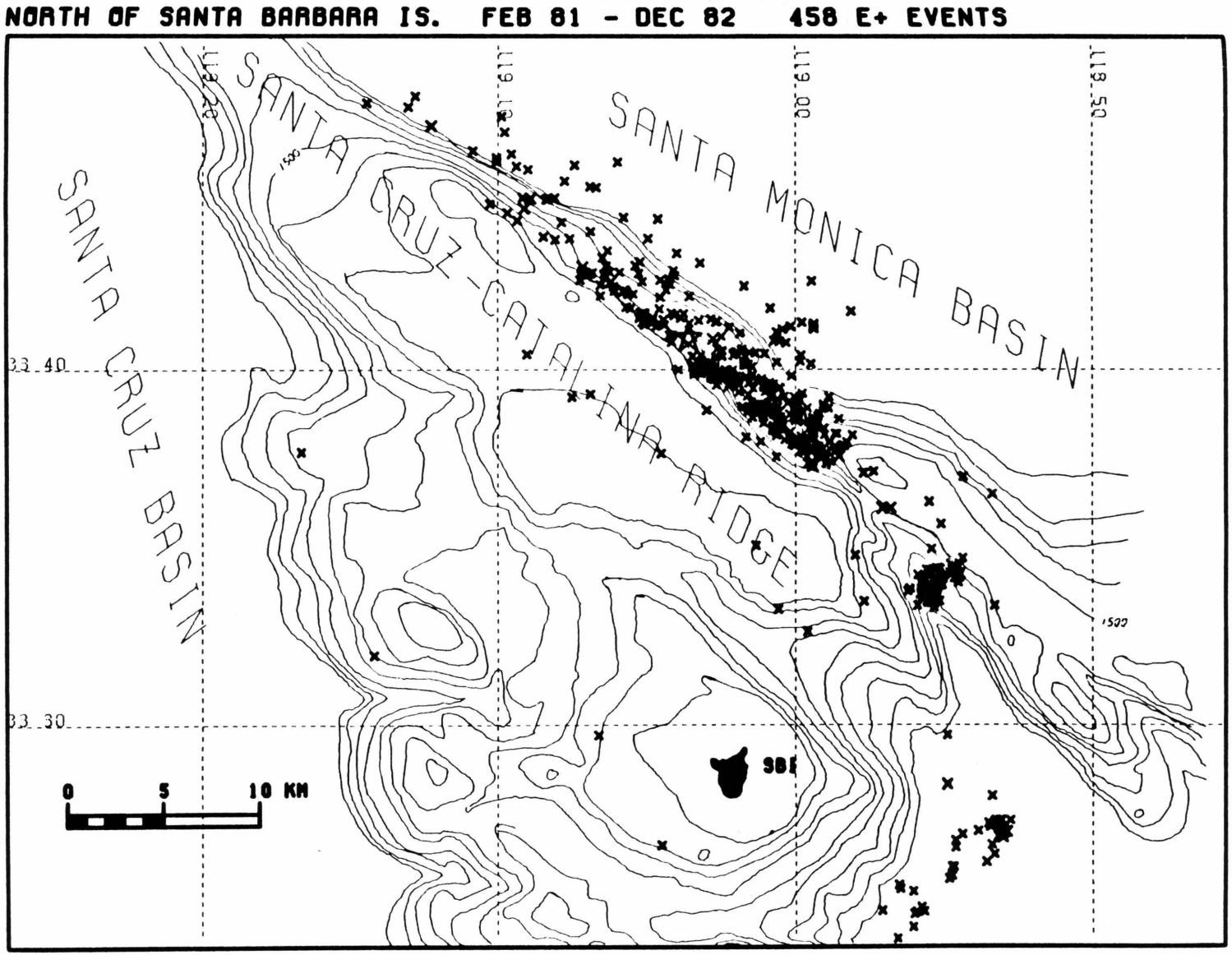

Figure 5-7a. Mainshock and aftershocks. Phase II locations, all events. Light lines show submarine topography, contour interval 300 ft. Symbols as in figure 5-3.

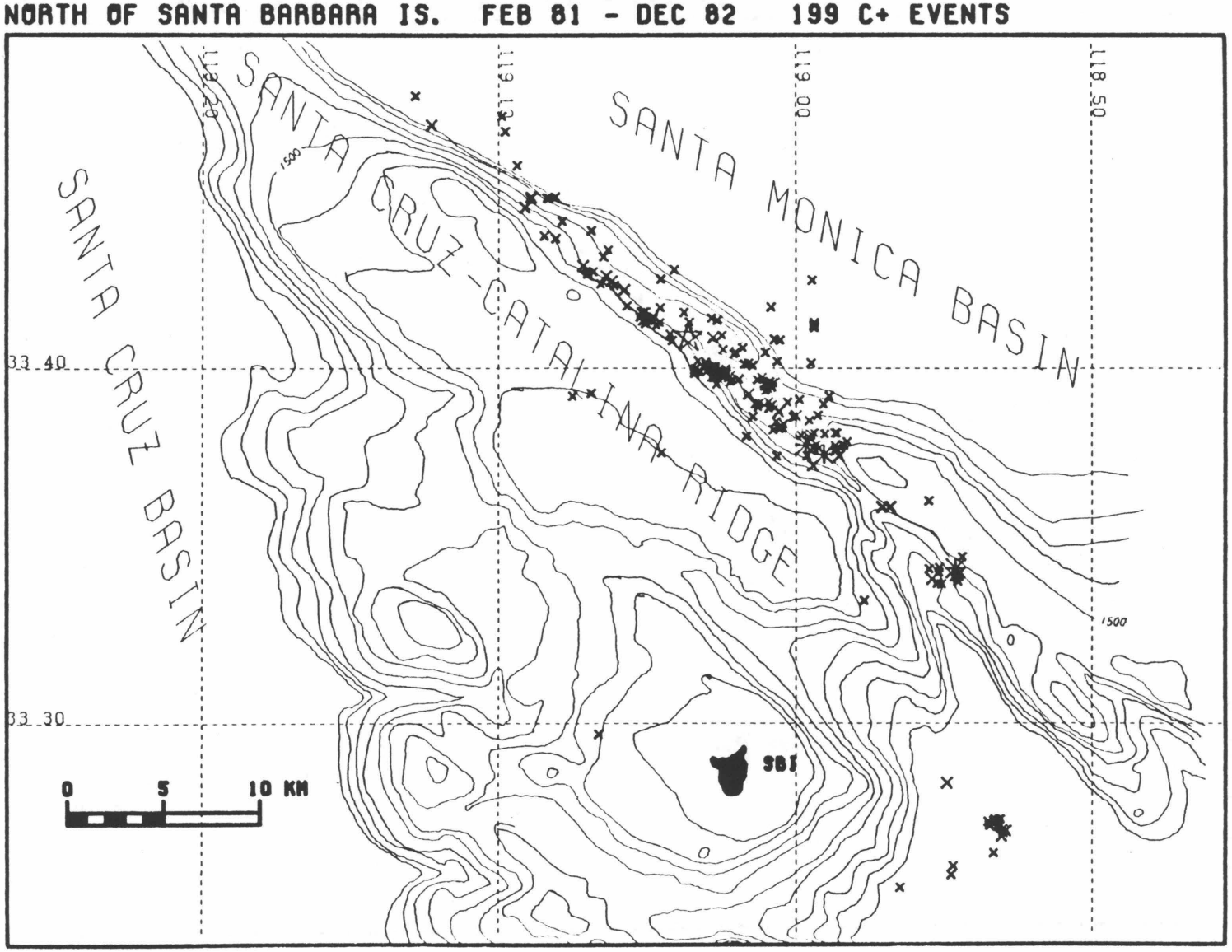

Figure 5-7b. Mainshock and aftershocks. Phase II locations, quality A, B, C. Light lines show submarine topography, contour interval 300 ft. Symbols as in figure 5-3.

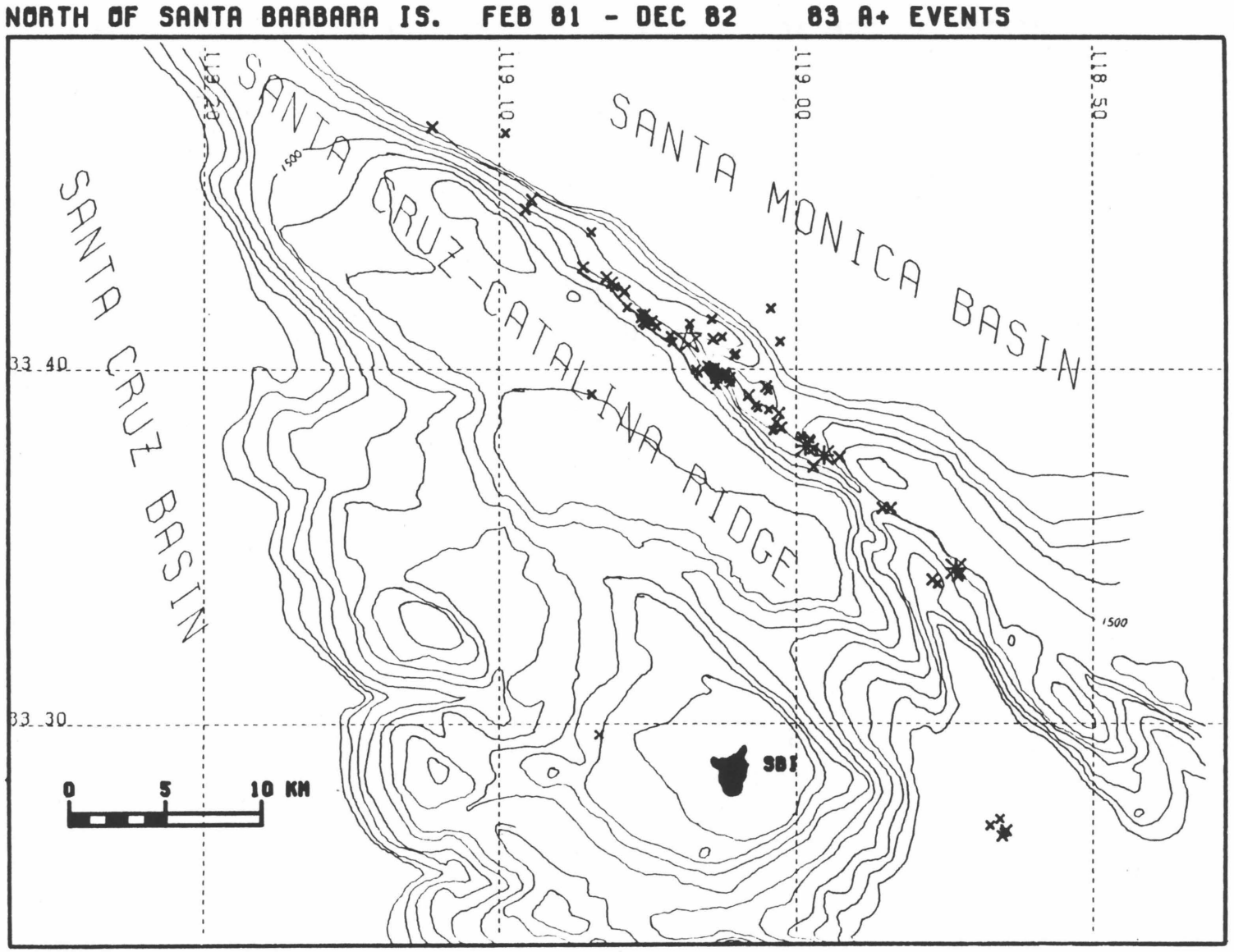

Figure 5-7c. Mainshock and aftershocks. Phase II locations, quality A only. Light lines show submarine topography, contour interval 300 ft. Symbols as in figure 5-3.

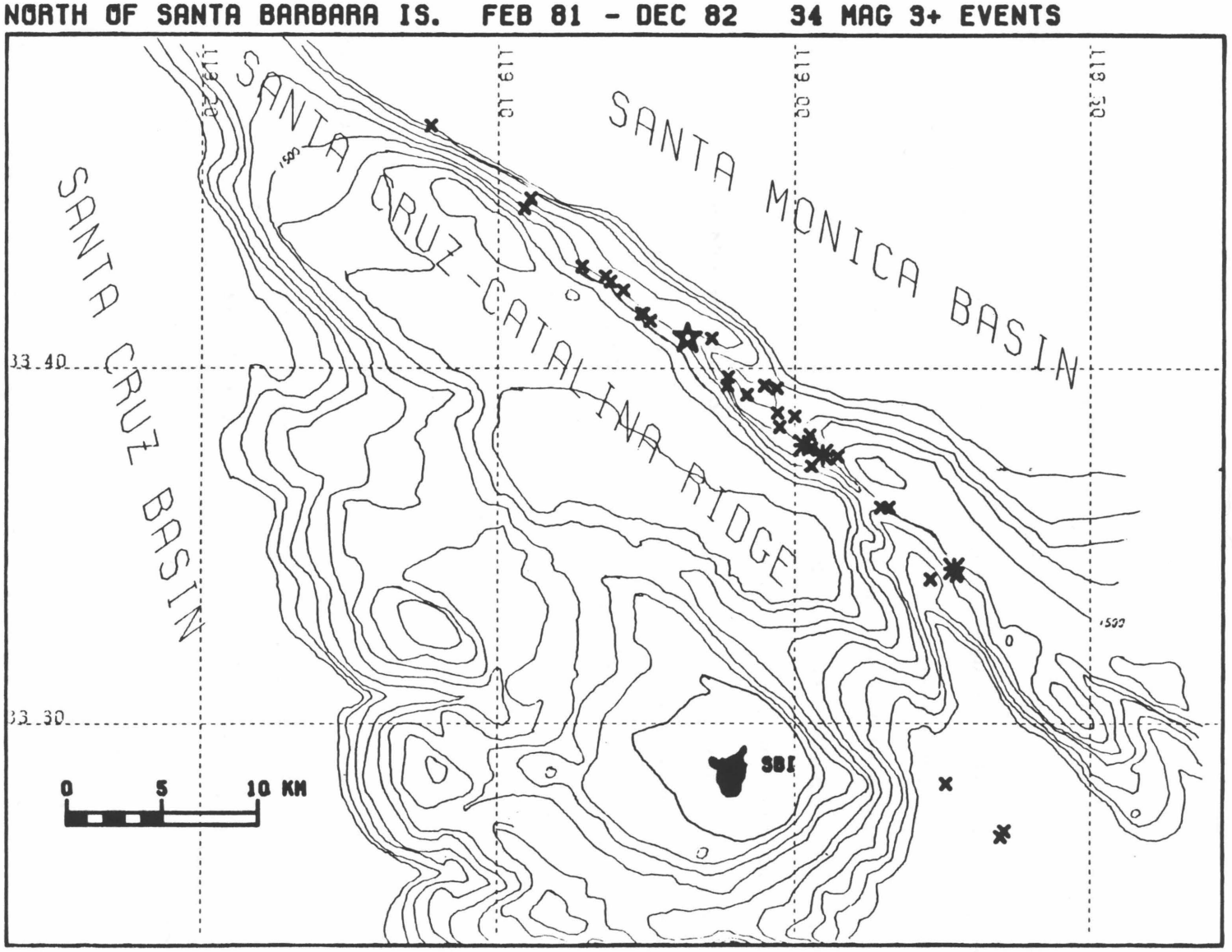

Figure 5-7d. Mainshock and aftershocks. Phase II locations, all events larger than magnitude 3. Light lines show submarine topography, contour interval 300 ft. Symbols as in figure 5-3.

by Shepard and Emery (1941).

Aftershocks

The aftershocks line up along the submarine escarpment as well as along a mapped bedrock fault shown in figure 5-2. The main aftershock zone is about 25 km long, stretching equal distances on both sides of the mainshock. The heaviest aftershock concentration is on the reach southeast of the mainshock (figures 5-7a and 5-7b). A cluster of aftershocks occurred 18 km southeast of the mainshock (including a magnitude 4.0 event), and they appear to be on the continuation of this same fault trend. Another aftershock cluster occurred 30 km south-southeast of the mainshock. This appears to be on another fault trend to the southwest that is delineated by the northwest-trending escarpment along the northeast side of Santa Barbara Island (fig. 5-7), and is also apparent in the bedrock geology (fig. 5-2). The temporal development of the aftershocks will be discussed in detail in a later section.

FOCAL MECHANISMS

Mainshock

The mainshock was well recorded throughout southern California, and clear, impulsive (0 weight) first motions were obtained for 74 stations. They are plotted in figure 5-8a, along with the derived focal mechanism. Azimuthal control was good, with a sweep of over 180°. The dips of the planes are not as well controlled. Note on figure 5-8a that there is poor control to the south and west. The stations plotted there are northeast stations whose upgoing rays are projected onto the lower hemisphere. Nevertheless, the interpretation is clear. The mechanism must be very nearly vertical-strike slip, with northwest and northeast-trending nodal planes. Two

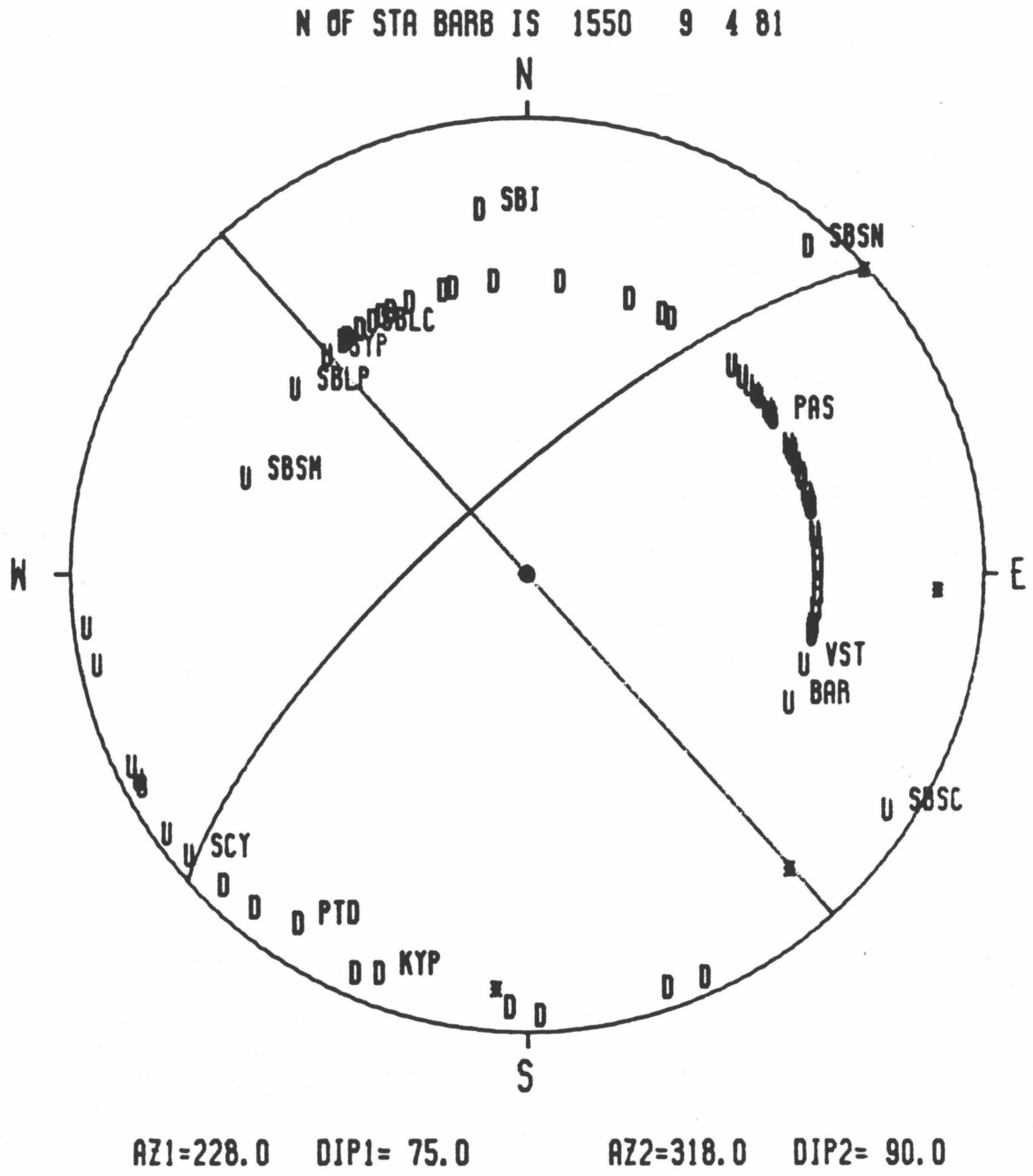

Figure 5-8a. Focal mechanism of mainshock. Equal-area, lower hemisphere projection. U=up, D=down direction of first motion. Names of key stations are designated.

nodal points where compressions flip to dilatations are well controlled, one to the northwest and the other to the northeast. The angle between these points is nearly 90°, although station azimuths constrain it to be (barely) significantly less, between 82° and 87°. This requires there to be a slightly less than vertical dip on the nodal planes. The preferred interpretation is that it is the northeast-striking plane that is non-vertical, dipping northwest at about 75°. The dip on this plane could be as little as 70°, but could not be less. Admittedly, this much precision is pushing the limits of how well we can calculate take-off angles, and does not allow for possible lateral refractions. And a slightly different velocity model such as used earlier (Corbett and Piper, 1981) would give less constraint on dips. Nonetheless, if correctly plotted, the azimuthal distribution of first motions requires at least one plane to be non-vertical. The northwest plane strikes N 42° W; reasonably close to the aftershock zone and the mapped fault. This compares favorably with the routine moment tensor solution published in the PDE: strike 314°, dip 72°, slip -174° (NEIS, 1981).

Aftershocks

Several aftershocks were also well recorded with many impulsive first arrivals, but the number of good first motions decays rapidly with magnitude. The three largest aftershocks were of magnitudes 4.6, 4.6 and 4.0; and their focal mechanisms are presented here. Figure 5-8b depicts the first motions for the first magnitude 4.6 aftershock on October 23. As can be seen, it is also well-constrained azimuthally, less so in dip. The inter-nodal gap is 78° to 93° and the most straightforward interpretation is vertical strike-slip. The northwest-trending plane corresponds to right-lateral motion, and it strikes N 48° W.

The second magnitude 4.6 aftershock occurred 2 hours after the first, and its corresponding first-motion plot is figure 5-8c. It was located at the same epicenter

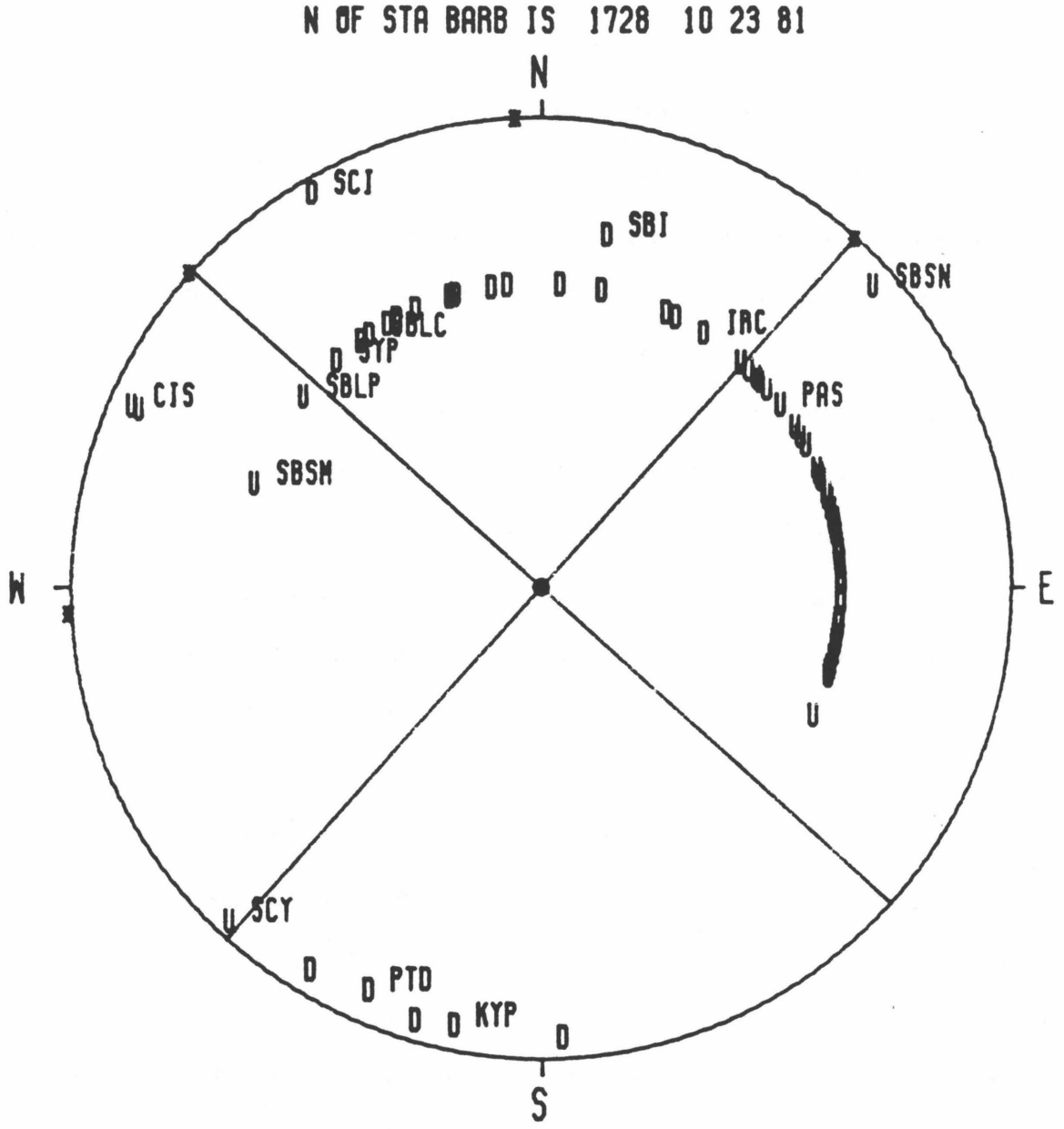

Figure 5-8b. Focal mechanism of 1st 4.6 M_L aftershock.

as the previous one, and all first motions were identical: there were fewer clear arrivals, and the inter-nodal gap is slightly less constrained: 67° to 93°. The simplest interpretation is again vertical strike slip with the northwest-trending plane striking N 50° W. However, the data do allow a non-vertical dip on either plane.

The magnitude 4.0 aftershock occurred 9 months after and 18 km southeast of the mainshock. First motions are plotted in figure 5-8d. Note that station SBI has switched polarity as the result of the different location, Santa Barbara Island is now in the west quadrant of this mechanism. The nodal planes are noticeably less well-constrained than in the previous example. The inter-nodal gap is 70° to 116°, and the mean interpretation is vertical strike-slip with a N 45° W right-slip nodal plane.

In summary, focal mechanisms for the mainshock and 3 largest aftershocks support vertical strike slip, with the strike of the right-lateral plane varying between N 42° W and N 50° W. But some oblique motion is suggested.

TEMPORAL DEVELOPMENT OF AFTERSHOCK ZONE

A study was done of the growth of the aftershock zone with time, using only the locations of quality C or better (ERH < 5 km) (figure 5-7b). These are shown in a series of time slices as figure 5-9. During the first three hours of activity (figure 5-9a), all of the aftershocks, save one, were along a stretch of 8 km southeast from the mainshock, strongly suggesting unilateral rupture in this direction. In fact, during the first hour of activity, this stretch was only 6 km long, raising the possibility that the initial rupture was less than 6 km in length. The first decipherable aftershock (3.6 M_L), 7 minutes after the mainshock, was 4.3 km southeast, and this might be interpreted as a minimum rupture length. The single aftershock 9 km to the northwest of the mainshock is a bit of an enigma, but it suggests that bilateral rupture cannot be ruled out. It occurred 28 minutes after the mainshock.

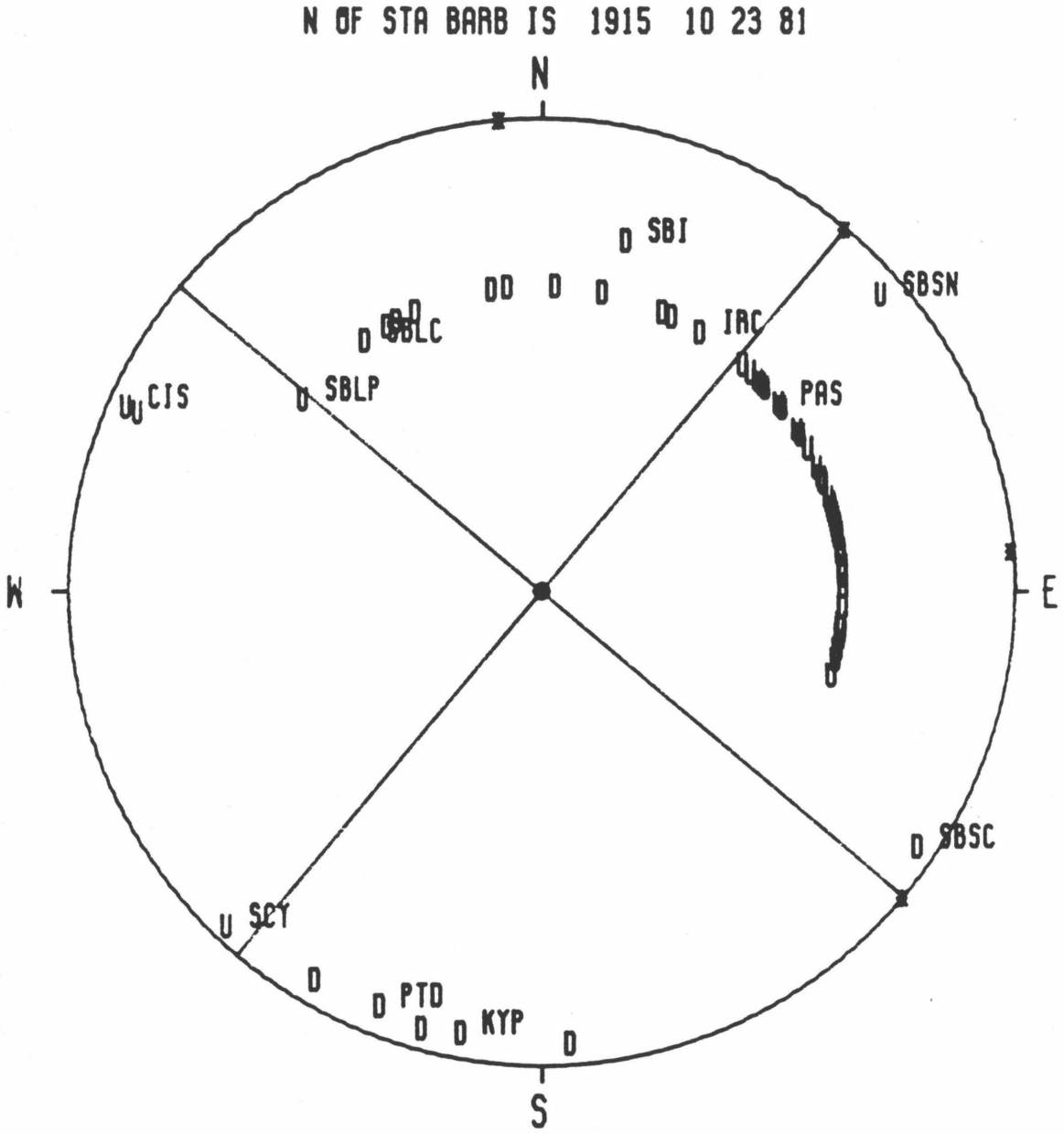

Figure 5-8c. Focal mechanism of 2nd 4.6 M_L aftershock.

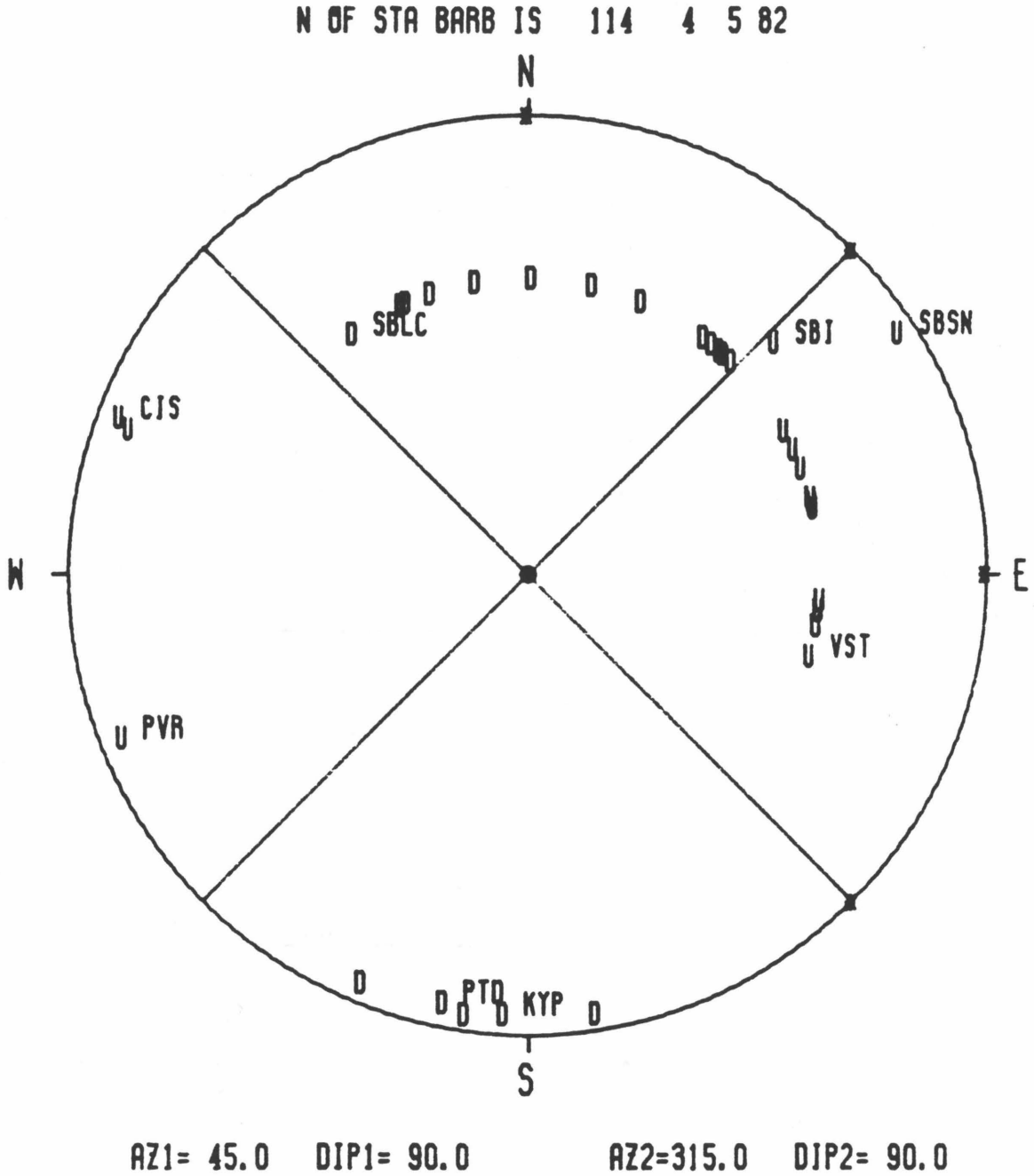

Figure 5-8d. Focal mechanism of 4.0 M_L aftershock.

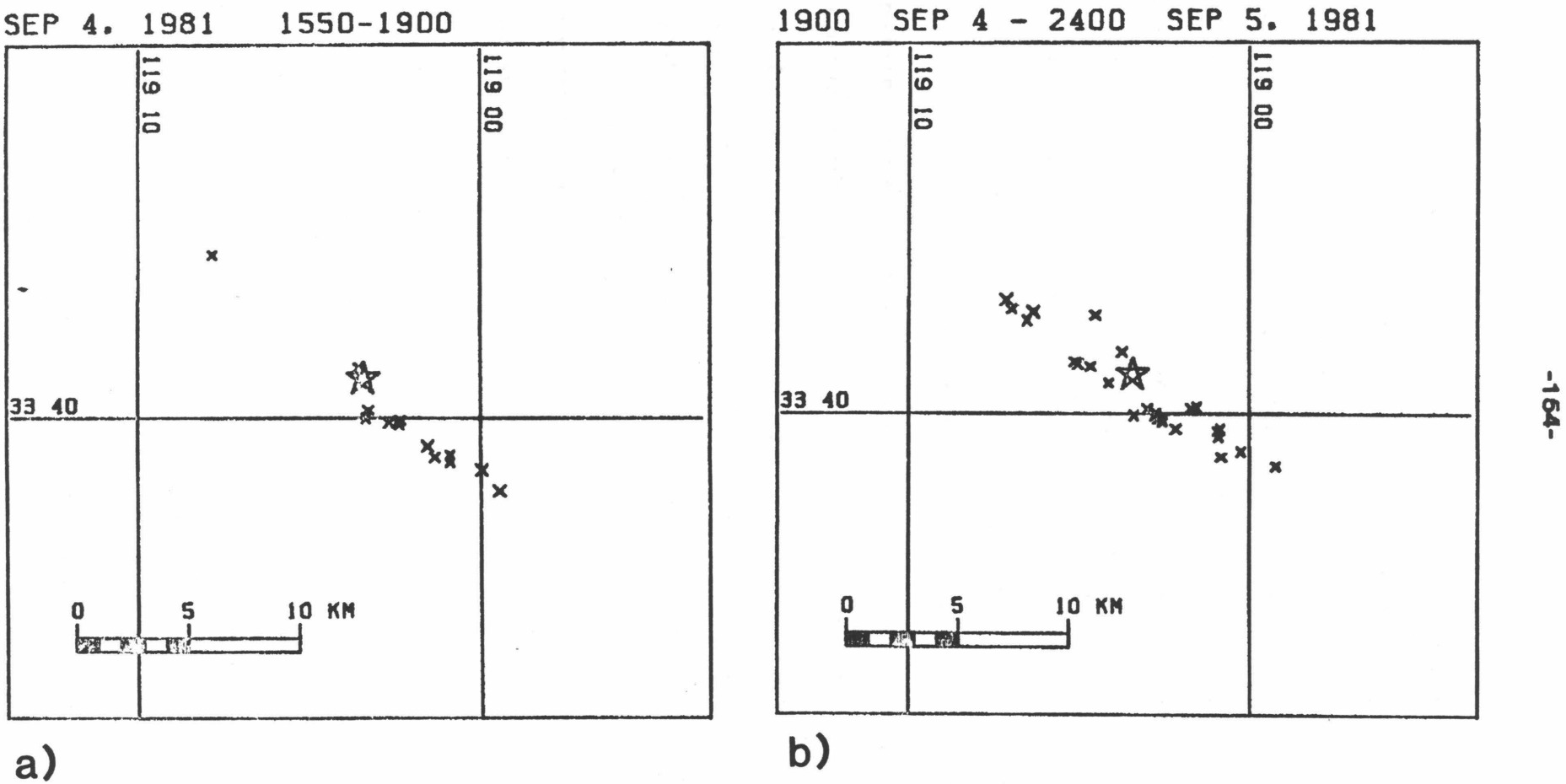

Figure 5-9. Distribution of aftershocks for dates and times indicated (GMT). Mainshock shown for reference.

During the following 29 hours (fig. 5-9b), the aftershock zone clearly grew 7 km northwest from the mainshock, but remained 8 km long to the southeast. During the succeeding 9 days (fig. 5-9c), the aftershocks extended to 11 km northwest and 10 km southeast. For the month following (fig. 5-9d), a few events occurred as far as 18 km northwest, and several events up to 14 km southeast. Also during this time, "wings" of aftershocks began to appear 7 km northeast and 7 km southwest of the main one. Commencing October 23, new activity began 9 km southwest of the mainshock, with the two largest aftershocks, both 4.6 M_L, two hours apart. Their epicenter continued to mark a hot spot for the next 3 weeks (fig. 5-9e). For the following 7 weeks, up to the end of the year (fig. 5-9f), most of the activity continued in the 10 km northwest of the mainshock. During the first 3 months of 1982 (fig. 5-9g), diffuse activity continued along the zone from 17 km northwest to 15 km southeast. On April 15, 1983, the third largest aftershock (4.0 M_L) occurred at a point 18 km southeast of the mainshock (fig. 5-9h). It was succeeded during April and early May with a cluster of aftershocks at the same epicenter. The rest of the year was characterized by diffuse activity, mostly within 7 km of the mainshock. In summary, the aftershock zone showed a clear temporal growth from a 6-km length at the end of one hour, to 15 km for one day, to 21 km after 10 days, to 35 km after several months.

AFTERSHOCK DEPTHS

Calculating depths for these earthquakes is difficult for this station geometry. The closest station to the activity is SBI, which is 15 to 25 km from most epicenters. The assumed depth for most of the earthquakes (from the master event) is about 10 km. The calculated takeoff angles from the hypocenter to SBI range around 110°, which corresponds to a dt/dz of .06 sec/km. In other words, depth resolution is

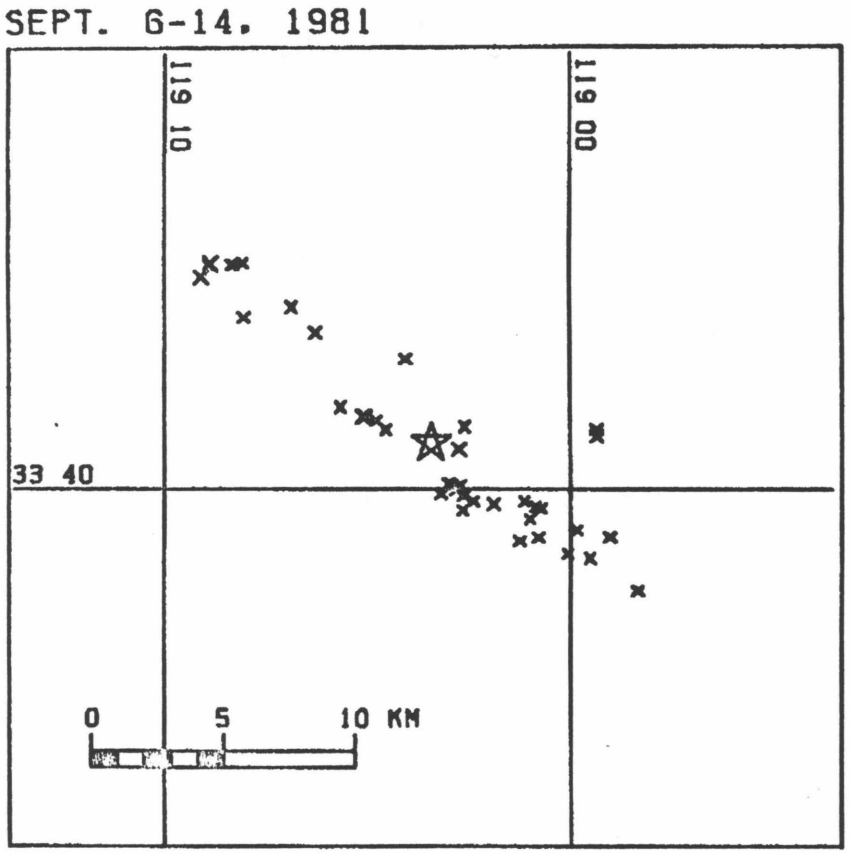

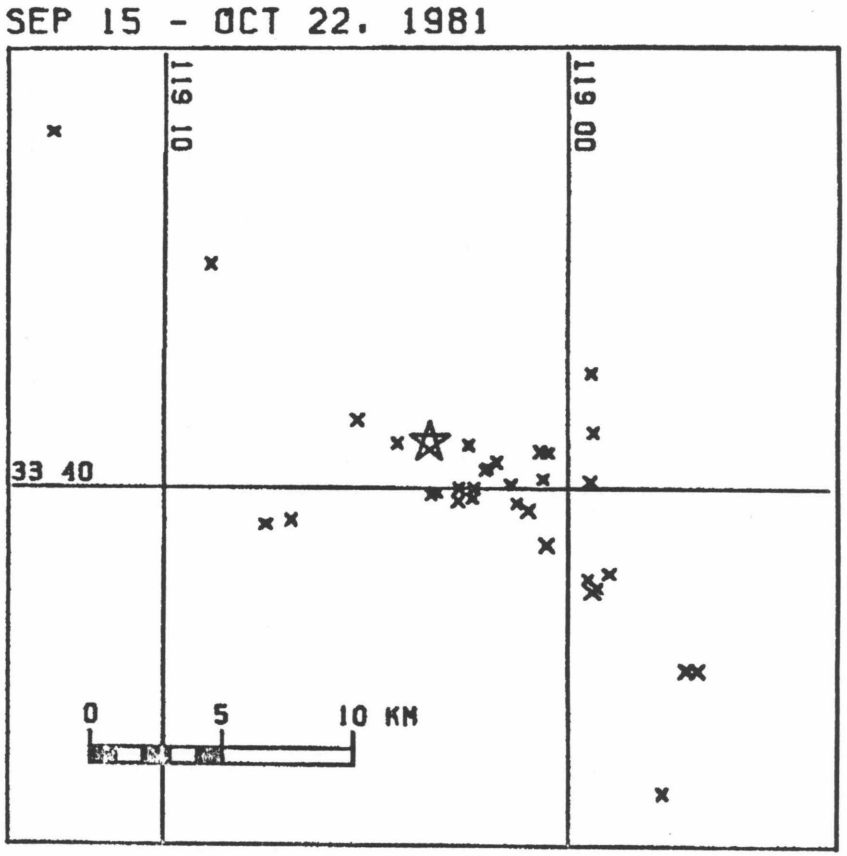

Figure 5-9. Distribution of aftershocks for dates and times indicated (GMT). Mainshock shown for reference.

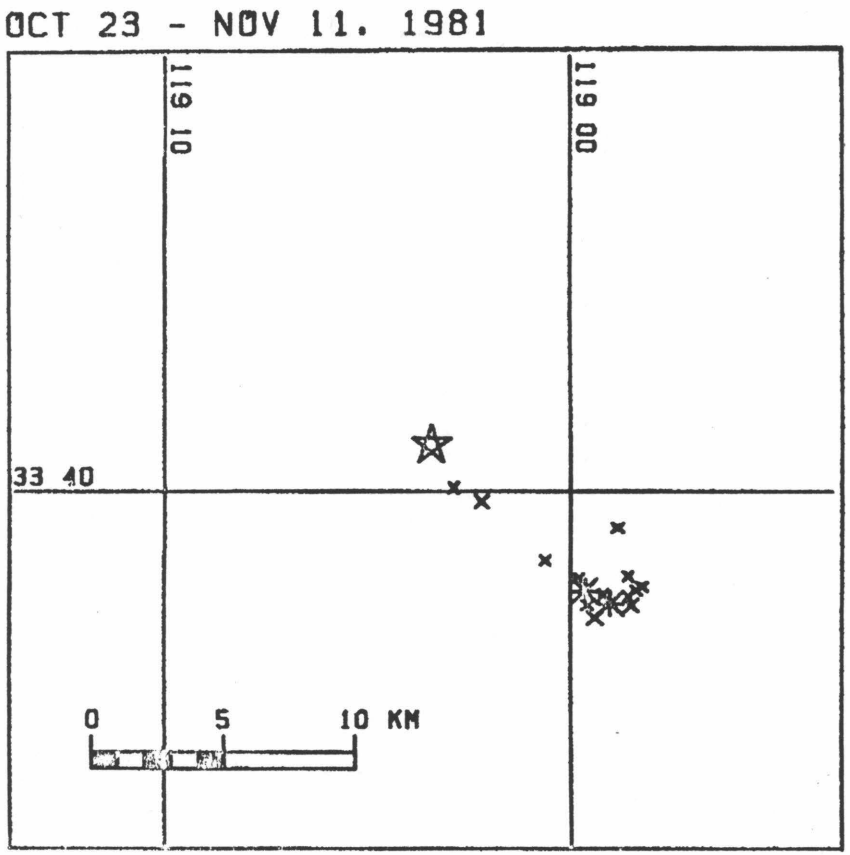

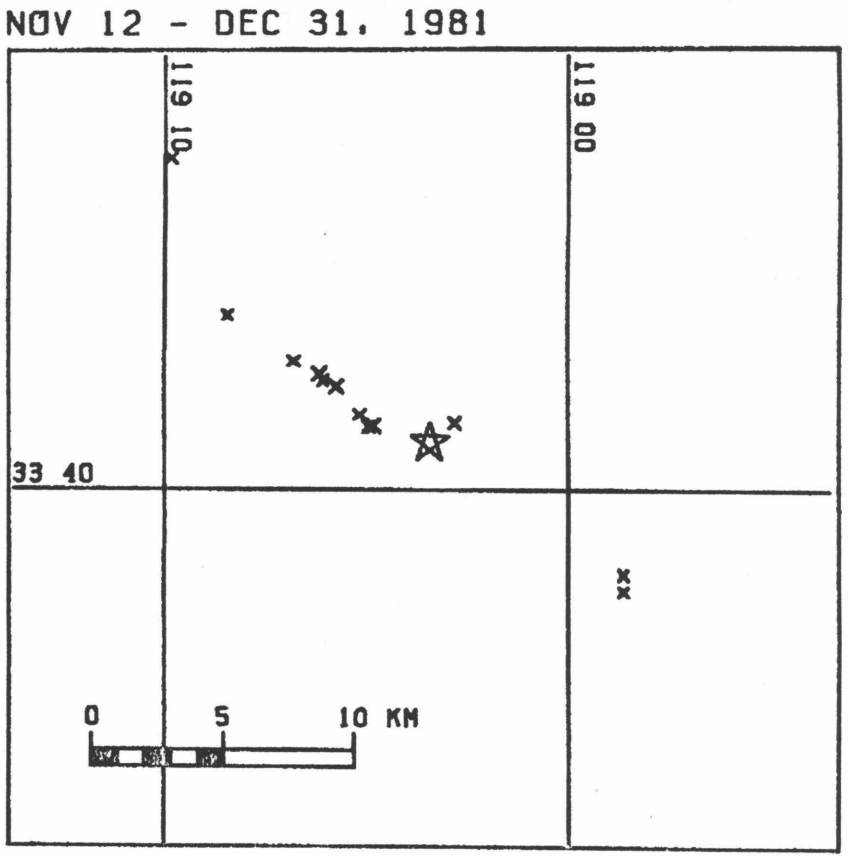

Figure 5-9. Distribution of aftershocks for dates and times indicated (GMT). Mainshock shown for reference.

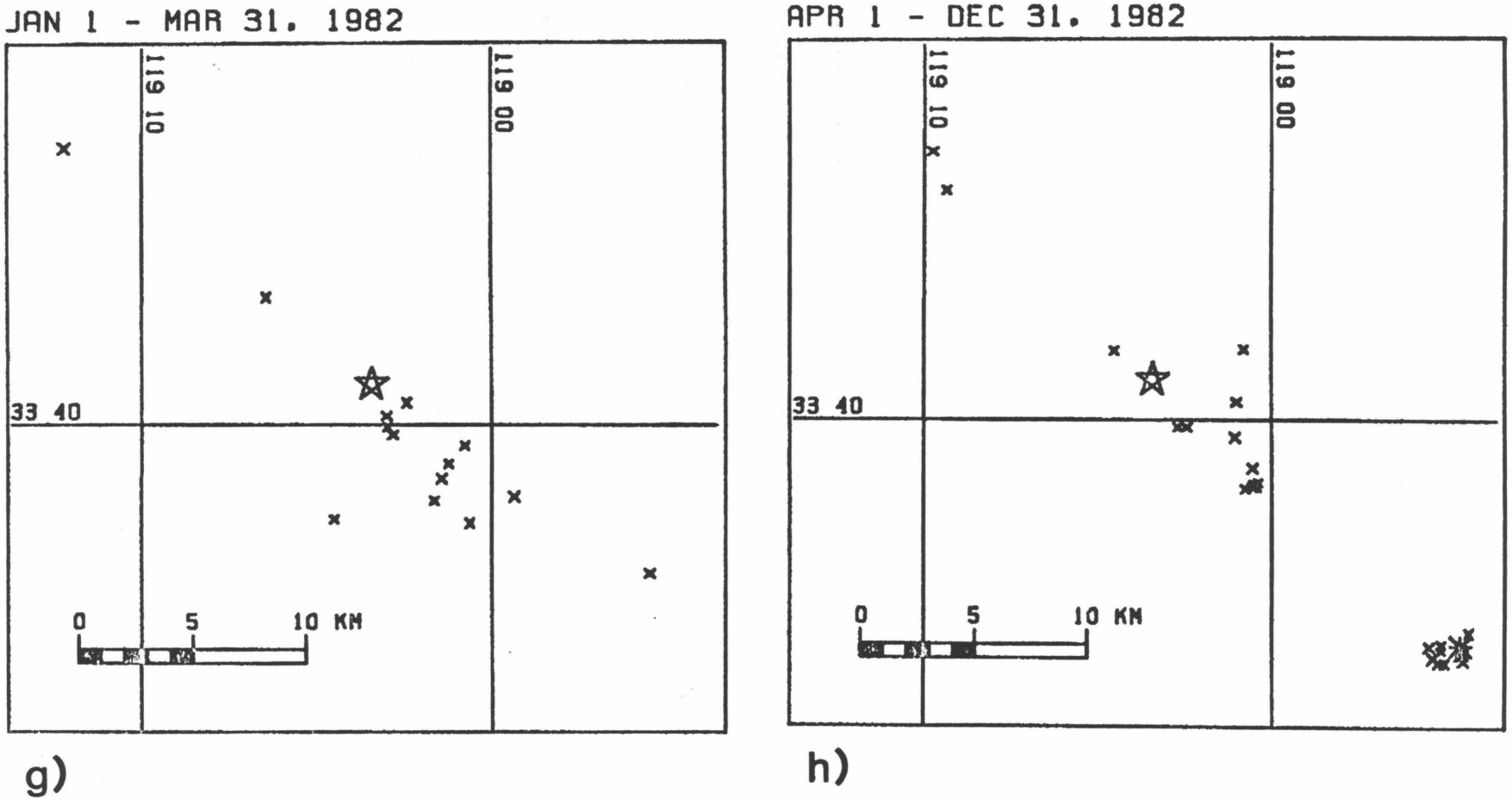

Figure 5-9. Distribution of aftershocks for dates and times indicated (GMT). Mainshock shown for reference.

rather small. An uncertainity of .10 sec in arrival at SBI would correspond to an uncertainty of 1.7 km in depth at the hypocenter. Nonetheless, the computer program used, QED1 (Johnson, 1979), calculates that 83 events (including the mainshock) have A-quality locations. This is defined as ERH < 1 km and ERZ < 2 km. And evidently most of these earthquakes have depth control that is probably not much better than ±2 km. In this light, the following remarks on the depth distribution of aftershocks should be taken with some caution. And note that all depths are relative to a starting depth of 10.65 km. Absolute errors may be ±5 km.

The 83 A-quality events are shown in cross-section in figure 5-10. Both sections are centered on the mainshock, and events within 15 km of the specified plane are projected onto that plane. The cross-section transverse to the aftershock zone (fig. 5-10a) is the view from Catalina looking northwest. It shows a planar structure that is either vertical or dipping steeply southwestward. A few events scatter off to the northeast, on the Santa Monica Bay side of the aftershock zone. The locations are significantly distant so that they probably do indicate subsiduary faulting off of the main fault trend, but they do not delineate a particular structure.

The longitudinal cross-section (fig. 5-10b) shows the view from Santa Monica Beach looking seaward. It gives the appearance of discrete patches of activity on the fault plane. On the southeast side of the mainshock is a heavy concentration of small aftershocks that outline a zone 3 km long and 4 km deep, which I will call zone 1. Southeast of this zone, all of the aftershocks are at the mainshock depth or up to 3 km shallower. This extends 15 km southeast and shall be called zone 2. The third zone is northwest of the mainshock. All of the aftershocks here are at or below the mainshock depth. Zone 3 is 17 km long by 4 km deep.

The earlier discussion of the temporal distribution of aftershocks raised the possibility that the initial rupture plane may have been less than 6 km long. One possible

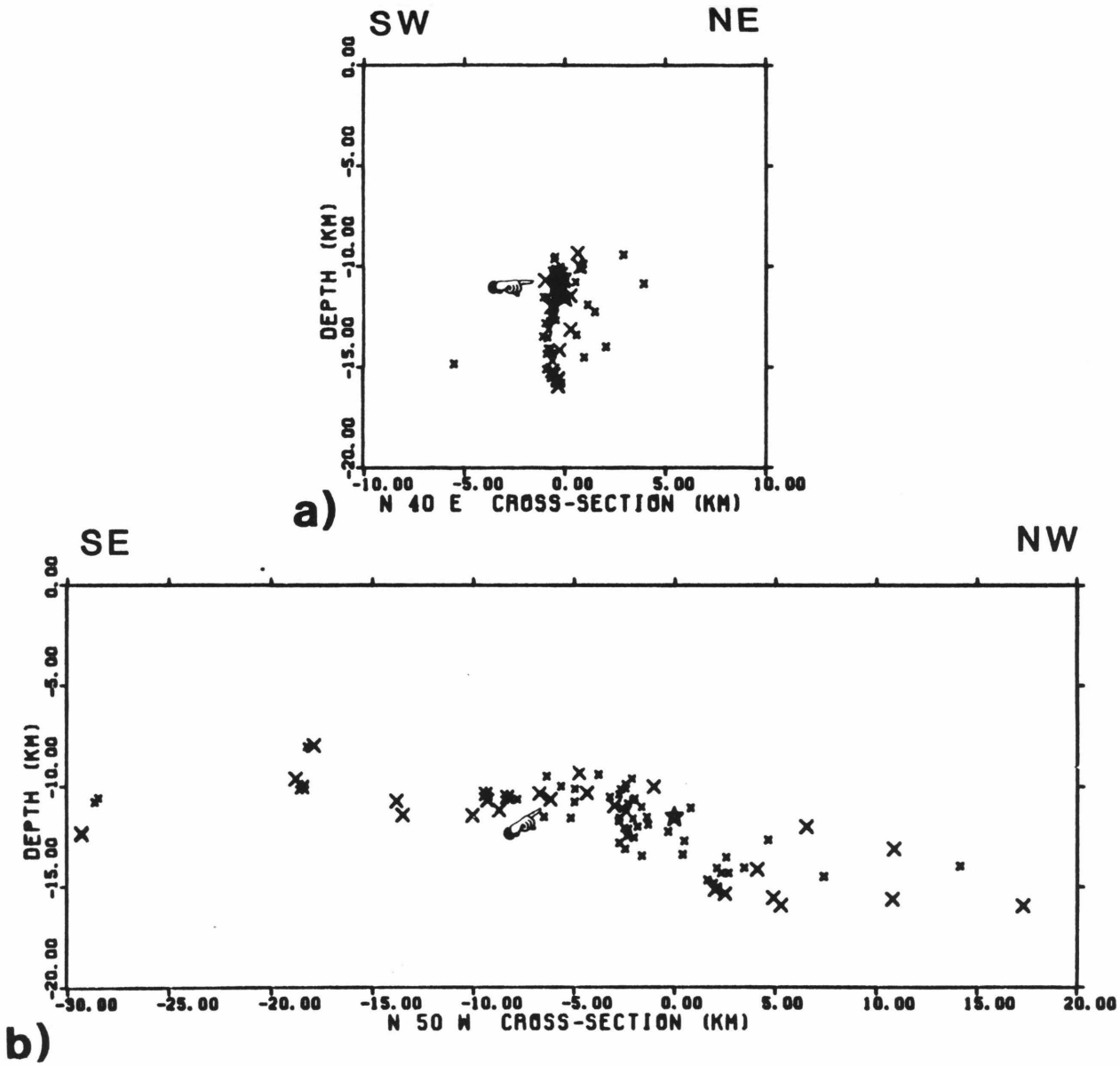

Figure 5-10. Depth of aftershocks. Phase II locations, quality A only. a) southwest-northeast cross-section; b) southeast-northewst cross-section. Master event indicated digitally.

interpretation of the depth distribution is that zone 1 represents the area of the initial rupture plane, with an area of only 12 km^2. Then, the aftershock zone grew during the succeeding days and weeks by progressive rupture to the southeast along zone 2 and to the northwest along zone 3. There are no clear reasons why aftershocks should occur above the mainshock in zone 2 and below the mainshock in zone 3, but this might indicate the presence of asperities. It is interesting to compare these same events on figure 5-7c and note how surface topography along the Santa Cruz-Catalina ridge changes at the mainshock location.

The above interpretation may be reaching beyond the depth precision, and there may be other explanations for the observed pattern. Another way to look at fig. 5-10b is that depths are getting systematically greater to the northwest. This could be due to variations in velocity structure. It was noted in chapter 4 that the top of the P_g layer may be dipping to the northwest. Also, as one moves northwest, depth control from SBI gets progressively worse. Another factor to be considered is that locations often cluster around the master event because its hypocenter was used as the starting location. This does not appear to be a severe problem in figure 5-10b. The master event is 6 km southeast, while the clustered events are 0 - 3 km southeast of the mainshock. However, clustering above and below the starting depth might be occurring, even if it isn't happening close to the epicenter. Hence patterns seen in figure 5-10 may only be reflections of lateral velocity variations and artifacts of the location problem.

DISCUSSION

Tectonic Implications

A number of studies have been carried out that bear on the question of whether or not an active fault is present along the northeast escarpment of the Santa Cruz-Catalina ridge. A look at the detailed bathymetry (fig. 5-7) suggests several faults along the steep banks and narrow canyons in the offshore region northwest of Catalina. Emery (1960) drew in several faults strictly on the basis of topography (fig. 5-11). His map suggests a complicated pattern of bifurcating and anastomosing structures with northwest and west-northwest trends. More recent work by Vedder *et al.*(1974) (fig. 5-2) shows a pattern of northwest-trending *en echelon* faults that are not necessarily connected. Of particular interest is a mapped bedrock fault between Miocene volcanics and sediments that parallels the aftershock trend and passes 1 km northeast of the mainshock epicenter. If this is the causative fault, this small discrepancy may be accounted for by the suggestion of a steep southwest dip on the aftershock zone, but this is certainly within the accuracy of the epicentral locations. In addition, Vedder *et al.* (1974) show this fault as dying out 15 km northwest of the mainshock, which is at about the same point as the aftershocks end. They continue the fault 40 km to the southeast where it disappears under the margin of the Catalina basin.

This fault was also picked out by Ziony *et al.* (1974) as an "offshore topographic lineament that may represent possible fault or fault zone". Their work was no more detailed than that of Emery (1960). Much more detailed work has been done by Junger and Wagner (1977) who ran several seismic reflection lines across the Santa Cruz-Catalina ridge. Of particular interest is profile C-C', which they made directly across the epicentral region (fig. 5-12). On their map they show the fault as cutting

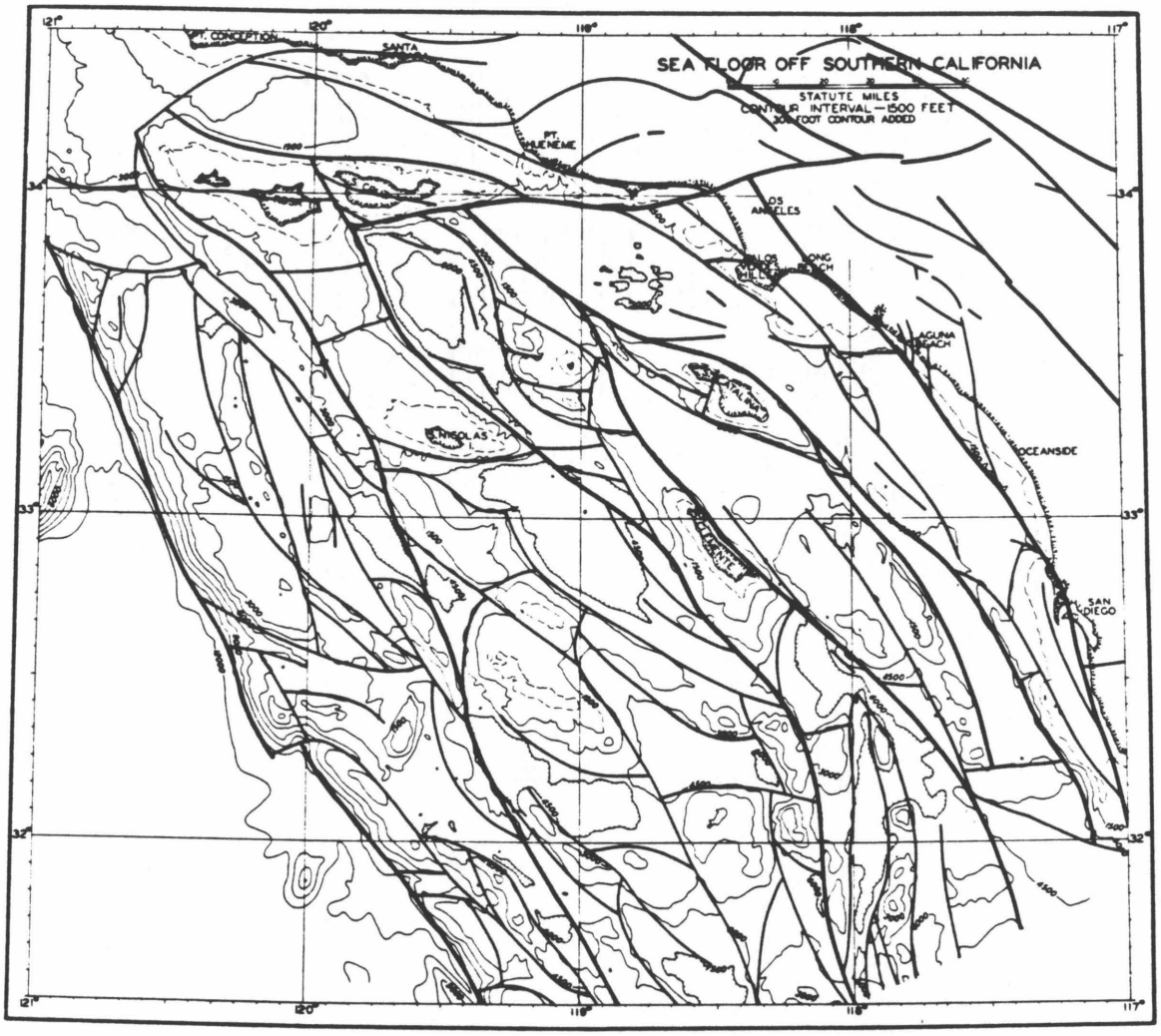

Figure 5-11. Fault map based chiefly on sea floor topography. Wide lines indicate long primary faults; narrow lines show shorter secondary faults, some of which may prove to be limbs of folds. Note that many of the secondary faults have a more westerly trend than the primary faults. (Emery, 1960).

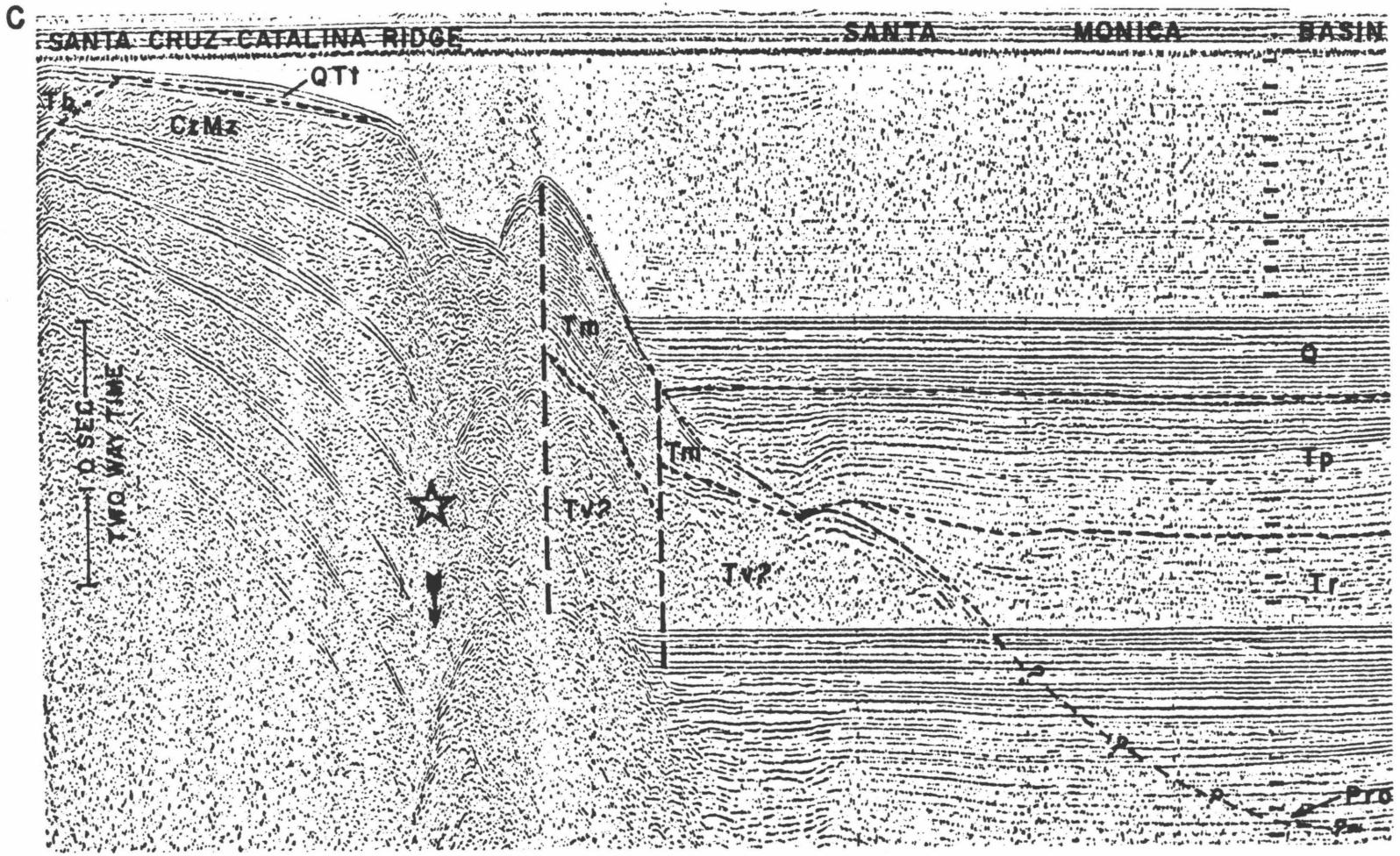

Figure 5-12. Seismic reflection profile of epicentral region. Mainshock location indicated by star, actual depth is much greater than shown. Modified from Junger and Wagner (1977).

Pleistocene rocks (cutting the sea-floor in places) with sediments downthrown to the northeast against volcanic rocks. In the accompanying text they state that the age of the fault is "indeterminate". Their next cross-section to the northwest, profile B-B' shows the fault as truncated by the Pliocene Pico formation. However, the wave-cut truncation at the north end of the Santa Cruz-Catalina ridge and the terrace deposits along the ridge have subsided, locally as much as 600-650 m. Junger and Wagner (1977) estimate the age of subsidence to be early late Pliocene (~ 3 million years ago), but feel that it was accomplished by steepening of the north flanks, i.e., folding, not faulting.

In short, it appears that the 1981 activity is associated with a major bedrock fault, but it is not clear that it would have been identified as active on the basis of the geological evidence alone.

Fault Mechanics

If this structure is an active fault that has been operating for a geological length of time, the relevant question is, what is the extent of displacement to the northwest and southeast. Emery (1960) connected it to the south with the San Clemente fault. This is a major active structure along the 2300-m-high San Clemente escarpment, flanking the northeast side of San Clemente Island (Jennings, 1975; Ridlon, 1972; Lonsdale, 1979; Legg, 1980). However, this fault appears to truly die out at its northern end, under the Catalina basin where it is covered by surficial sediments (Ford and Normark, 1980). And there is no evidence that the Santa Cruz-Catalina fault continues to the south beyond the Catalina escarpment (Vedder, *et al.*, (1974). On the north, Vedder *et al.* (1974) terminate the fault 15 km northwest of the epicenter, but Blake *et al.* (1978) project it along the bedrock contact between the elevated Miocene volcanics of Santa Cruz-Catalina ridge and the Plio-Pleistocene

sediments of the Santa Monica basin--all the way to the intersection with the east-west Santa Cruz Island-Dume fault trend. The Santa Cruz Island-Dume fault is apparently geologically active with well-documented left-lateral slip (Patterson, 1978; Junger and Wagner, 1977; Jennings, 1975). This poses a significant structural problem. If the Santa Cruz-Catalina fault is undergoing right-lateral shear, why hasn't it offset the Santa Cruz Island-Dume fault? It may be that the Santa Cruz Island-Dume fault is geologically younger. But if this is the case, where is the left-offset north end of the Santa Cruz-Catalina fault? There are no mapped northwest-trending right-lateral faults north of this boundary. It appears that the northwest-trending Peninsular Ranges structures end abruptly at this boundary, while the Transverse Ranges structural trends begin, just as suddenly.

This structural problem is not unique to the Santa Cruz-Catalina fault. An analogous situation occurs 90 km to the east in the Los Angeles basin with the Newport-Inglewood fault. This fault is presently active and has well-documented evidence for right-lateral slip (Harding, 1973; Barrows, 1974). Yet at its northern terminus, it abuts against the Santa Monica fault, without any measurable offset (Barrows, 1974; Hill *et al.*, 1979). The Newport-Inglewood fault clearly does not continue into the well-exposed rocks of the Santa Monica Mountains. Barrows (1974) speculates that the Newport-Inglewood fault veers to the west at its northern extremity and is overridden by thrust faults that are branches of the Santa Monica fault.

The best geological data on the structure at the intersection of the Santa Cruz Island-Dume fault and the Santa Cruz-Catalina fault come from Junger (1979) (fig. 5-13). He shows the wedge between the two faults as being occupied by lesser faults of intervening azimuths. All of these faults are down-faulted towards the inside of the wedge, forming a graben within a graben. This gives the appearance that this area is undergoing extension. This suggests that the Santa Monica basin is

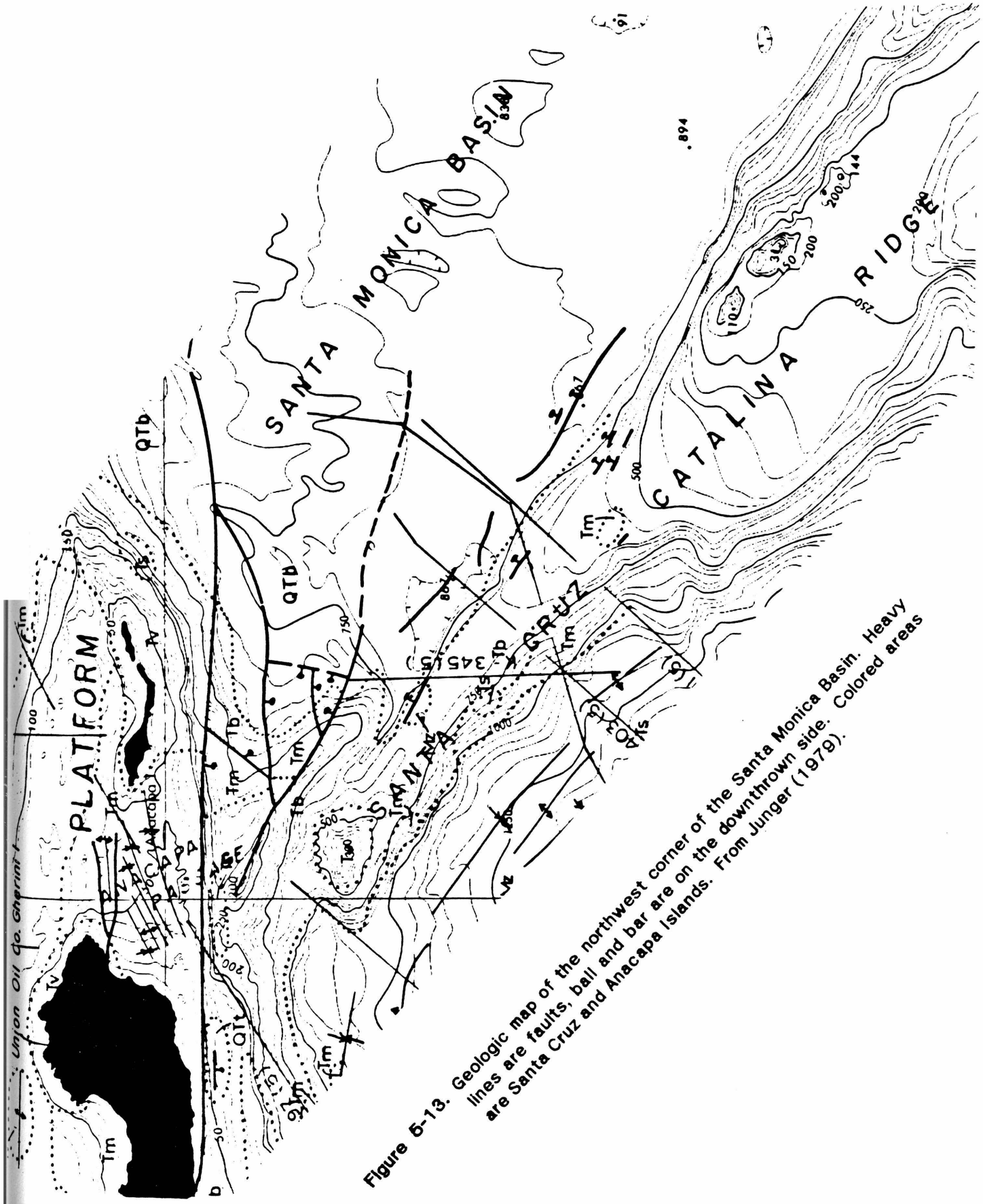

Figure 5-13. Geologic map of the northwest corner of the Santa Monica Basin. Heavy lines are faults, ball and bar are on the downthrown side. Colored areas are Santa Cruz and Anacapa Islands. From Junger (1979).

being pulled southeastward relative to Santa Cruz Island, and the tip of the fault wedge is subsiding as it loses lateral support. This is much like what happens at the tip of a slice of hot apple pie as it is served.

This model has certain geological implications that can be tested. One implication is that the rate of left-lateral offset on the Santa Cruz Island-Dume fault increases east of its intersection with the Santa Cruz-Catalina fault. Another is that the southwest side of the Santa Cruz-Catalina fault may be fixed relative to the south side of Santa Cruz Island (south of the Santa Cruz Island fault). Thus motion relative to the Transverse Ranges may be occurring only on the northeast side of the Santa Cruz-Catalina fault. This is not necessarily required. Junger and Wagner's (1977) observation that the northwest end of the Santa Cruz-Catalina ridge may be down-faulted 600m may indicate that it too is being pulled away from Santa Cruz Island, but at a lesser rate than Santa Monica basin. This might be structurally necessary to accommodate the next right-lateral fault to the west.

Another implication of this model is that down-to-the-east movements on the Santa Cruz-Catalina fault may be shallowly rooted, and the major deformation at depth could be pure strike-slip. This brings up the question of what caused the 800-m-high escarpment facing Santa Monica basin. One suggestion might be that displacement is purely strike slip and the escarpment might have been caused by pulling away the high ground around Catalina to the southeast. This would require over 60 km of offset. This seems unrealistically high, especially with regard to the hole it would create in the crust. Junger and Wagner (1977) indicate that the Santa Monica basin has been down-warped "only" 3,000 m since the late Miocene, and this greatest down-warping also occurs in the northwest corner of the basin. In fact, Junger (1975, 1976) feels quite strongly that the Continental Borderland basins were formed primarily by folding, and in particular, he maps the Santa Cruz-Catalina

ridge as an anticline (Junger, 1976).

Another possibility is that the Santa Cruz-Catalina fault is a right-lateral fault with a vertical component. The 1981 mainshock focal mechanism does allow a vertical component of motion. The interpretation shown in fig. 5-8a gives 75° of northwest dip to the auxiliary plane. This corresponds to 15° of oblique, down-to-the-northeast slip. The calculated ratio of vertical to horizontal slip would be about 25%. At this rate, an 800-m-high escarpment could be produced with 3.2 km of right-lateral slip. This seems to be a reasonable amount of slip that would not produce too big a hole in the northwest end of the Santa Monica basin.

There is also the question of what happens to the southeast end of the Santa Cruz-Catalina fault. Vedder *et al.*(1974) carry the fault to the edge of the Catalina basin and end it there. However, 12 km farther southeast on the same trend, the Catalina escarpment abruptly begins. This is a 1200-m-high slope, striking N 75° W that separates Catalina Island (highest elevation 700 m) from the Catalina basin (deepest depth 1400 m). Junger (1976) has interpreted this escarpment as a thrust fault, with Catalina being shoved southward over the adjacent basin. Note that this structure strikes 25° more westerly than the Santa Cruz-Catalina fault, which means that right-shear movement from the northwest would have to be taken up with a thrust component on the Catalina escarpment. The connection at this end of the fault is, however, purely conjectural. There is no geologic, seismic, or seismological evidence linking these two faults. These two faults are merely consistent in terms of the local tectonic pattern.

The overall tectonic picture may be as follows. The Santa Monica basin block appears to have pulled southeast, away from Santa Cruz Island. As a result of this, at the northwest end of the basin, extension and downwarping are occurring. At the southeast end, compression and uplift is occurring. Catalina surely shows signs of

uplift. The island has plentiful uplifted marine terraces (Smith, 1900). Early Pliocene beds now exposed were probably deposited at depths greater than 2,000 m (Howell and Vedder, 1981). And the Catalina Schist basement rocks are believed to have been emplaced originally in a subduction zone at 30-40 km depth (Platt, 1976).

This simple tectonic model is undoubtably an oversimplification. The only supporting evidence is for right-lateral motion at one side, along a length as short as 30 km. It may well be that this is the only place along the fault where measurable offset is going on, with displacement dying out at the ends.

Relation to other models

There are five different proposed models to explain the formation of the southern California Continental Borderland. They all agree in that deformation started at some time in the Miocene. They seem to disagree as to whether the deformation is ongoing; deformation may have ended in the Pliocene with present topography maintained because of the relatively slow rate of submarine erosion. They all appear to agree in that, whatever the original mechanism, the formative structures have been taken over by the current San Andreas right-shear tectonics. Modern-day seismicity certainly cannot delineate what has been happening ever since Miocene time, but the data presented here may put limitations on how well the west side of Santa Monica basin fits the various models.

Yeats (1968a, 1976; Yeats *et al.*, 1974) and Cole (1975) have suggested that the Continental Borderland has been formed by east-west rifting. Shepard and Emery (1941) also felt that the area was formed by extension and even referred to the area as "Basin and Range." This model would seemingly imply normal faulting on the boundaries between ridges in basins. Along the Santa Cruz-Catalina fault, Monterey formation is downfaulted against older (?) Miocene volcanics (Junger and Wagner,

1977; Vedder *et al.*, 1974). However, the focal mechanisms of the 1981 earthquakes (fig. 5-8) and the transverse cross-section (fig. 5-10a) appear to indicate that this fault is vertical or dipping steeply *away* from the basin.

Crowell (1974) thought that the Continental Borderland might have been formed as a series of pull-apart basins. He envisioned right-stepping right-lateral faults with the zones between being pulled apart by the transfer of strain between the two faults. This might well describe what is happening to the Catalina basin, which has the San Clemente fault on the southwest margin and the Santa Cruz-Catalina fault at its northeast corner. This model is, however, a bit difficult to apply to the Santa Monica basin. The basin evidently is bounded on the southwest by a right-lateral fault. However, there is no right-lateral fault to the northeast, due to the intersection of the basin with the Transverse Range province. However, left-lateral displacement on the east-trending Dume fault would have the same effect in pulling apart the Santa Monica basin.

Howell *et al.* (1974) and Crouch (1979) used palinspastic reconstructions to argue that the outer Continental Borderland has been offset 120-160 km to the northwest since the early Miocene. To explain this they proposed the East Santa Cruz Basin fault system, which they envisioned to be a broad zone of northwest-trending right-lateral faults. The Santa Cruz-Catalina fault might be part of this system. However, it probably has not taken up all of the 160 km of displacement.

Junger (1975, 1976; and Wagner, 1977) felt strongly that the ridges and basins were formed primarily by folding, and faulting was only a secondary feature. His tectonic map shows the Santa Cruz-Catalina ridge as an anticline between the down-warped Santa Monica basin and Santa Cruz basin (Junger, 1976). Structure contour maps (Junger and Wagner, 1977) show the top of the Miocene to be downwarped as much as 3000 m in Santa Monica basin. And reflection profiles (fig.

5-12) do show anticlinal structures on the Santa Cruz-Catalina ridge. Junger (1976) conjectured that the Continental Borderland is underlain by several deep-seated convergent wrench faults, and the upper crust is folding in response to their displacement. The data in this chapter demonstrate strike-slip at 10 km depth, but evidently on a fault that does reach the surface. This does not refute Junger's (1976) model, but it raises the possibility that fault displacement may contribute to the deformation as much as folding.

The Junger (1976) model is in analogy to the wrench fault tectonics of the Newport-Inglewood fault (Harding, 1973; Wilcox *et al.*, 1973) which is on land in the Los Angeles basin. Harding (1973) used clay models to show that the discontinuous faults and aligned folds of the Newport-Inglewood structure are the expected result of plastic deformation in soft sediments due to parallel shear along an underlying wrench fault. Although maps such as Vedder *et al.* (1974) show the Santa Cruz-Catalina fault as continuous, it must be remembered that it was "mapped" from ship tracks that crossed it at widely-spaced points. It is just as possible that it too is made up of discontinuous segments at the surface. In addition, Pilger (1976) mapped the Santa Cruz-Catalina ridge by reflection profiling and shows many folds, parallel and oblique to the ridge trend, as well as a prominent anticlinal structure along the northeast flank of the Santa Cruz-Catalina ridge. Pilger (1976) concludes that this structure is consistent with oblique convergent right-lateral shear. However, he also concludes that most of the deformation was pre-late Miocene and that plate motion is no longer being transformed across the Continental Borderland to the San Andreas fault, but is now being absorbed by underthrusting at the Transverse Ranges.

Since we are considering an analogy with the Newport-Inglewood fault, it is relevant to consider its juncture with the Transverse Ranges. Like the fault offshore,

the inland fault apparently does not offset the range front fault, despite the fact that it has documented right-lateral slip of 200 to 800 m in fold axes and other structural elements observed in oil fields (Harding, 1973). The Newport-Inglewood fault is evidently the southwestern structural boundary of the Los Angeles basin. The Los Angeles basin is quite deep: basement rocks are 10 km deep and the top of the Miocene is at 6-km depth (Yerkes, *et al.*, 1965). This deepest part is in the northwestern wedge of the basin, similar to Santa Monica basin. At the junction between the Newport-Inglewood fault and the Santa Monica fault, Hill *et al.* (1979) show subsidence of the northeast side of the Newport-Inglewood fault occurring between 1955 and 1977. The tectonic significance of this is questionable since the area is pumped by the Beverly Hills Water Department and is located over the Beverly Hills (East) oil field. However, Hill *et al.* (1979) conclude that the subsidence is partly due to fluid withdrawal and is partly due to tectonic movements. In summary, there is some evidence for subsidence of the wedge between the Santa Monica fault and the Newport-Inglewood fault. Thus, this area too may be in extension due to the Los Angeles basin being pulled away from the Transverse Ranges, as was suggested for the Santa Monica basin.

Subsidence between diverging faults in the Continental Borderland has also been discussed by Nardin (1981). He referred to these as "tipped fault wedges" by analogy with the model of Crowell (1974). Nardin (1981) documented a graben structure between the faults along the San Pedro escarpment and the San Pedro Basin fault zone.

Finally, there is the work by Kamerling and Luyendyk (1979, 1981) presenting paleomagnetic evidence that parts of the Transverse Ranges and several of the offshore islands have been rotated as much as 90° in the clockwise direction since the early Miocene. In particular, Santa Cruz, Anacapa, and Catalina islands have

been rotated, and Santa Barbara and San Clemente islands have not been. In an attempt to explain these data, Luyendyk *et al.* (1980) have proposed a model in which the Transverse Ranges have been rotated clockwise as a whole. To accommodate this rotation, the blocks of the Peninsular Ranges to the south, slipped right-laterally relative to each other. A series of triangular gaps would be created between the northern tips of the Peninsular Ranges blocks and the Transverse Ranges blocks. These gaps could be interpreted as the loci of the many deep sedimentary basins formed during the Miocene. This model could explain the creation of the Santa Monica basin, which I suggested was formed by pulling away from the Transverse Ranges. However, the apparent 90° rotation of Catalina complicates the model at this point. Rotating the Catalina block would cause the Santa Monica basin to open as a rhomboid instead of a triangle (Luyendyk *et al.*, 1980). Inasmuch as they feel that most of the rotation occurred by the end of the Miocene time, the present day activity may only represent a continuation of post-Miocene activity. The shape of Santa Monica basin could be fit equally well by a rhomboid or a triangle. But if Miocene-type deformation is continuing still today (at a lower rate), the Luyendyk *et al.* (1980) model raises the possibility that Catalina could be pivoting around its west end, as Santa Monica basin pushes southward.

In summary, several different models have been suggested for the formation of the basins and ridges of the Continental Borderland. Although the geological evidence makes it clear that the bulk of the deformation occurred in Mio-Pliocene time, it is possible that some of the formative processes have continued into the present. Yeats (1968a, 1976) rifting model cannot be operating presently. Strike-slip as proposed by Howell *et al.* (1974) or wrench tectonics with folding (Junger, 1976) could be carrying on into the present day. Also, some elements of Crowell's (1974) pull-apart-basin concept could be operating today. In short, the present-day tectonics

could be a combination of these three models. Kamerling and Luyendyk's (1979, 1981) data require reconsideration of some aspects of all of the above models, but one element of Luyendyk *et al.*'s (1980) model could well explain the basin formation. However, any neo-tectonics model must consider that right-lateral faulting is now occurring along the Santa Cruz-Catalina fault. It is suggested that previous geologic evidence and the seismological data presented in this chapter favor the Luyendyk *et al.* (1980) model insofar as it applies to the formation of Santa Monica basin and Santa Cruz-Catalina ridge.

Seismological Implications

The tectonic model suggested above also has a seismological implication that can be tested. That is, it would imply that active normal faulting is taking place at the northwest wedge of the Santa Monica basin block. Although this has not yet been seen, there are some 1981 aftershocks in this region (see fig. 5-5) that may bear investigation. Further east, there may be an analogous tectonic environment where the northwest-trending Whittier fault abuts against the Santa Monica-Hollywood fault. Real (in press) indicates that earthquakes with normal mechanisms are occurring there.

Magnitude and Moment. The 1981 earthquake exhibits a discrepancy between long-period and short-period magnitudes. For comparison, other calculated magnitudes are 5.6 M_L (Berkeley), 5.4 m_b, and 5.9 M_S from the PDE (NEIS, 1981). The PDE also lists a moment of 7.0×10^{24} dyne-cm for the 1981 earthquake. This corresponds to an M_W of 5.9 (Kanamori, 1978), which is in agreement with the M_S observation. This moment was used with the formulas of Kanamori and Anderson (1975) and the time-dependent assumptions of fault dimensions to calculate stress drops ($\Delta\sigma$) and average displacement (D) in Table 5-3.

Table 5-3. Range of fault parameters.					
time	W	L	A	D	$\Delta\sigma$
7 min	4 km	3 km	12 km^2	194 cm	93 bars
1 hr	4	6	24	97	46
3 hr	4	8	32	73	35
24 hr	5	15	75	31	12

If we use the aftershock zone for the later times (3-24 hrs) as the size of the fault rupture, the implied average stress drops and average displacement are typical for shallow earthquakes. However, the small size of the initial aftershock zone may suggest that the rupture plane was much smaller with the corresponding high stress drops and displacements.

Let us consider the possible Mogi doughnut, the lack of precursory activity on the fault plane, and the M_s *vs.* M_L discrepancy in terms of an asperity model (Kanamori, 1981). There were clearly no events detected in the 1981 aftershock zone during the 4 years preceding the mainshock (fig. 5-3c) and only 4 or 5 detectable events during the 14 years preceding it (fig. 5-3d). Meanwhile, seismicity was evidently frequent on surrounding faults. If we interpret the 1981 mainshock as occurring at an asperity on a much longer fault, the model of Kanamori (1981) would infer that the surrounding fault plane was much weaker than the asperity itself. It had either mostly slipped before 1967 or it was slipping aseismically during the 14 years prior to 1981. Finally, the concentration of stress broke through the asperity with the 5.3 M_L earthquake. Exactly what happened at rupture depends on whether one interprets the calculated seismic moment (NEIS, 1981) to have been released: 1) on a small fault plane, as indicated by the 5.3 M_L; or 2) on a larger fault plane as suggested by the 5.9 M_S. In case 1, it is presumed that a $\sim$ 20 km^2 asperity ruptured with the implied high stress drop and large displacement (Table 5-3). The aftershock zone then would have spread quickly due to the relatively low strength of the rest of the fault plane. In case 2, it would appear that failure of the asperity would have

allowed 75 km^2 to rupture bilaterally with the early aftershock concentration due to the inherent roughness of the former asperity. Which is the correct case depends on whether the discrepancy between M_L and M_S is a valid measurement of energy release at different frequencies, or is a reflection of the uncertainity in magnitude determinations. These observations raise the possibility that other earthquakes may exhibit this pattern if scrutinized in as much detail. If so, many earthquakes may have primary rupture planes much smaller than indicated by the ultimate aftershock zone. This could mean that previous calculations of stress drop may be inaccurate in some cases.

Magnitude and Fault Area. If one believes the depth control on the 1981 earthquakes (fig. 5-10), the fault rupture plane may have been initially small, perhaps only 12 km^2. This has been observed for other earthquakes by Corbett and Johnson (1982) and Ebel (1980). The question arises: Is this an appropriate size fault plane for a magnitude 5.3 earthquake? There are several theoretical and empirical equations available in the literature that relate magnitude to fault length (L) or fault area (A). All of these relationships are based primarily on M_S for earthquakes larger than magnitude 5.5, and the appropriateness of downward extrapolation may be questioned. However, three of these equations were tested with consistent results. Kanamori and Anderson (1975) derived: $\log A = M_S - 4.0$, theoretically, assuming a stress drop of 30 bars. This would imply that a 5.3 M_S earthquake would have a rupture area of 20 km^2. Slemmons and Chung (1982) regress surface rupture length on magnitude for data from strike-slip faults with the result: $\log L = 0.752\ M_S - 3.459$. This yields L = 3.4 km for 5.3 M_S. Probably the most appropriate relation is that of Wyss (1979) who uses data from the M_W, M_S, and M_L magnitude scales. He calculates the median line through the data as $M = \log A + 4.15$, but cautions that it is derived only for $M > 5.6$. However, if we assume fault dimensions from the

aftershock pattern and test the two extremes with Wyss's (1979) equation, 12 km^2 corresponds to 5.2 M and 75 km^2 corresponds to 6.0 M. So, evidently the observations of initial fault rupture area made in this chapter are consistent with the relationships derived for larger earthquakes.

This study is evidently only the third seismological report on the Continental Borderland. Clements and Emery (1947) recognized the correlation between epicenters and topography, despite poor locations. Legg (1980) makes it clear that right-lateral mechanisms have occurred throughout the Continental Borderland, in particular along the San Clemente Island trend. The main contribution of this chapter is to document the strike-slip nature of tectonics along the boundary between Santa Monica basin and Santa Cruz-Catalina ridge, and to attempt to fit the movement into the larger tectonic picture.

CONCLUSIONS

Systematic location biases of earthquake locations due to velocity structure in the Continental Borderland have been identified and corrected for. The improved locations and focal mechanisms indicate that the September 4, 1981 Santa Barbara Island earthquake was probably caused by right-lateral strike slip along a bedrock fault located along the northeast escarpment of the Santa Cruz-Catalina ridge. Aftershock distributions indicate: 1) the first rupture may have been unilateral to the southeast; and 2) the fault plane grew progressively with time. The length of the aftershock zone grew from 6 to 36 km, and the initial rupture area may have been as small as 12-30 km^2. These earthquakes and previous geological studies suggest the following model for the neo-tectonics. Santa Monica basin may be sliding southeast relative to the Transverse Ranges. This is resulting in extension at the northwest corner of the basin and compression at the southeast end, with Catalina overriding

the Catalina escarpment. This model is in partial agreement with previous models of the tectonic development of the southern California Continental Borderland.

Chapter 6

Earthquake Location Methods -- Some Conclusions

Introduction

The basic tool used in all of the previous chapters was an earthquake-location program, and thus it is appropriate to consider how this tool works, what its limitations are and how it was used in these studies. The most basic data used in seismology are the arrival times of seismic phases, and thus the oldest problem has been to invert these arrival times to learn the origin of the causative earthquake. As in all sciences, the first seismological studies were empirical, and consisted of observations of arrival times from an earthquake with a "known" source. These observations quickly led to travel-time plots that showed the coherent relationship between times and distances. The observed relationships led to theory and to the understanding of the physical mechanisms of wave propagation in the earth. Understanding led to more careful and more precise recognition and timing of phases, and this led to further refinement of velocity models. Hence the history of seismology has been circular, with improved travel-time observations being used to calibrate better our model of the earth at each cycle. A limiting factor has always been the accuracy to which arrival times could be measured. In modern-times, the advent of digital seismology has greatly reduced that limitation. In addition, modern day experiments with controlled sources (i.e. explosions) eliminate the location ambiguity.

Earthquake Location Methods

In the early days of seismology, many schemes were tried to deduce earthquake location. Most were graphical methods, which involved swinging arcs and dropping perpendiculars, on the basis of S-P times and other phase differences. These inevitably required many approximations of earth geometry and of the velocity model. One of the oldest methods of inverting travel times for hypocenter is that of Geiger (1912), popularly known as the "least squares method." Due to the great number of tedious calculations required, it was not very popular in the first half of this century. With the advent of the digital computer in the 1960's, however, it became immediately practical and was quickly rediscovered (Pavlis, 1982). Virtually all modern location programs use this method in one form or another.

Geiger's Method

For an observed arrival time (T_i) at a station (x_i,.y_i, z_i), a trial hypocenter is assumed (x_0, y_0, z_0), with a trial origin time (t_0).

This allows one to calculate a predicted arrival time,

$$t_i = t_i\,(x_0, y_0, z_0, t_0, x_i, y_i, z_i),$$

which is usually a non-linear function of the velocity structure.

The residual is defined as the difference $\quad r_i = T_i - t_i.$

If the hypocenter were adjusted by the amount: Δx, Δy, Δz, Δt, we would get a new residual

$$r'_i = T_i - t'_i(x_0 + \Delta x, y_0 + \Delta y, z_0 + \Delta z, t_0 + \Delta t, x_i, y_i, z_i).$$

This is linearized by the approximation

$$t'_i = t_i + \frac{\partial t_i}{\partial x_0}\Delta x + \frac{\partial t_i}{\partial y_0}\Delta y + \frac{\partial t_i}{\partial z_0}\Delta z + \frac{\partial t_i}{\partial t_0}\Delta t \ .$$

$$\text{So,} \quad r'_i = r_i - \left(\frac{\partial t_i}{\partial x_0}\Delta x + \frac{\partial t_i}{\partial y_0}\Delta y + \frac{\partial t_i}{\partial z_0}\Delta z + \frac{\partial t_i}{\partial t_0}\Delta t\right) \ .$$

The object then is to minimize $\sum_1^N (r'_i)^2$ for all N stations. This is achieved by partial differentiation with respect to all 4 parameters which results in 4 equations known as the normal equations

$$\begin{bmatrix} S_{xx} & S_{xy} & S_{xz} & S_{xt} \\ S_{yx} & S_{yy} & S_{yz} & S_{yt} \\ S_{zx} & S_{zy} & S_{zz} & S_{zt} \\ S_{tx} & S_{ty} & S_{tz} & S_{tt} \end{bmatrix} \begin{bmatrix} \Delta x \\ \Delta y \\ \Delta z \\ \Delta t \end{bmatrix} = \begin{bmatrix} R_x \\ R_y \\ R_z \\ R_t \end{bmatrix},$$

where $S_{xy} = \sum_1^N \frac{\partial t_i}{\partial x_0}\frac{\partial t_i}{\partial y_0}$, etc., and $R_x = \sum_1^N \frac{\partial t_i}{\partial x_0} r_i$, etc.

This is solved by the methods of linear algebra for Δx, Δy, Δz, and Δt, and the hypocenter is adjusted by these amounts. The process is re-iterated until some convergence criteria are reached. This method is straightforward mathematically, but it is based on some assumptions that may not always be valid. These flaws in the method are discussed in detail by Pavlis (1982) and are summarized here. Some of the problems with the method are:

1) Not all of the data may be of equal quality.

2) Inversion will frequently fail because the matrix is singular.

3) The method assumes that the velocity model is perfect, and the only source of error is statistical error in measuring arrival times.

Attempts at improvement

Data weighting. The data are in fact of variable quality because of factors that may vary from station to station. These factor include: signal-to-noise ratio, whether the onset is impulsive or emergent, size of the event, magnification of seismometer, method of timing, distance from source, etc. The usual method for dealing with these problems is to weight the data. Common weighting schemes are quality weighting, distance weighting, and residual weighting.

Quality weighting is usually based on the opinion of the timer. A common system is that used in HYPO71 (Lee and Lahr, 1975), where the arrival is rated 0 for full weight; 1: three-quarters weight, 2: half weight; 3: quarter weight; and 4 for zero weight. This method is subjective, and it is not clear that it is a reasonable method because it produces a rigorous number that controls the inversion. A better method would be one that mathematically considers the accuracy of the measurements. One such method, used at the University of Washington (Pavlis, 1982), weights the data according to $\frac{1}{\sigma_i}$, where σ_i is the estimated error in arrival time. An identical system is that used by the USGS (Caltech) to weight the data according to how precisely the timer observes a particular arrival, according to the standards in Table 6-1.

Table 6-1. Phase Pick Error Bars	
Weight	Error
0	±0.02 sec
1	±0.05
2	±0.10
3	±0.30
4	∞

The location program can then calculate the actual variance of the data and use this in the inversion.

Distance weighting is employed because of the observation that travel-time errors increase linearly with distance (Ergas and Jackson, 1981), for three reasons: 1) the scattering of wave energy (Aki, 1973); 2) decay in phase amplitudes; and 3) uncertainity in the velocity model (Pavlis, 1982). Distance weighting is usually handled by a simple distance cutoff, or a ramp function that linearly down-weights data with distance.

Residual weighting is based on the assumption that large residuals are the results of gross errors in picking arrival time. Consequently large residuals are down-weighted, usually by Jeffreys' weighting method, as in HYPO71 (Lee and Lahr, 1975) or QED1 (Johnson, 1979). This method is the one that is most prone to misuse by blind computing and is known colloquially as the "residual eater."

The problem with using three weighting functions is the potential for feedback between them. An extreme example is as follows: A subjective timer may give a P-arrival a low quality-weight because of its low amplitude. This may, however, be the result of being from a distant station, so the distance-weighting subroutine rates it even lower. Consequently, the datum from this station does not have much influence on the inversion, and a high residual may result. And the residual weighting algorithm thus weights the station even lower. So, important data often get ignored because of the vagaries of the weighting routines. On the other extreme, the weighting

algorithms have a disconcerting tendency to zero-weight the data from the closest stations. This apparently results because they have the most influence on the solution, and discarding them can lower the rms. In other words, the more numerous distant stations "outvote" the nearby stations. This feedback is a real problem, and is the result of using too many weighting functions at once. Most typical location programs use all three types of weighting, including HYPO71, QED1, and HYPOINVERSE (Klein, 1978). My experience has taught me that data weighting in all of these programs is dangerous, and weighting must be done very carefully. If the programs are not used systematically, they do not produce repeatable locations.

I propose that only a single weighting method be used, and it should be a method that reflects the accuracy of the arrival times, as in Table 6-1. This observation simultaneously reflects the effects of the earthquake magnitude, noise on the record, and amplitude decay with distance. Whether or not to use a distance weighting factor depends on whether one has proper station corrections. If station corrections are used that are accurate for the particular area under study, the effect of velocity-model uncertainty with distance and azimuth is eliminated. If distance weighting is used, it should probably be an all-or-nothing distance cutoff, so that a systematic choice of stations is made. Residual weighting may be useful for identifying bad picks, but once the bad data are identified, they should not be used, and there is thus no need for residual weighting.

Inversion Method. Another major problem with Geiger's (1912) method is that it may be numerically impossible to solve the linear equations because the matrix is singular. This is usually caused by the hypocenter being poorly constrained by the data (e.g. the location is shallow or outside the network). This may also be caused by a poor starting location, resulting in high residuals with the first iteration. Most location programs solve the latter problem by starting the location at the first arrival

station (e.g. HYPO71, QED1). A more clever method is that of Anderson (1981), which uses the arrival order at stations to estimate location. I suggest an alternate method of selecting a first approximation starting location: One might use the first four clear arrivals (which are usually the four closest stations) to solve the travel-time equations for the four unknowns, which are linear if one assumes an average velocity.

HYPO71 attempts to solve the inversion stability problem by using a step-wise multiple regression. Since r_i is a function of Δx, Δy, Δz, and Δt, a statistical analysis is performed to determine which independent variables are the most significant, and the normal equations are set up for only those variables (Lee and Lahr, 1975). One problem with this method is that often only one variable at a time will invert, so epicenters have a tendency to "walk" along latitude and longitude lines during iteration. This leads to a grid pattern and/or misleading line-ups of epicenters on location plots.

All of the locations in this dissertation were done with QED1 (Johnson, 1979). It uses the superior approach of the generalized inverse, after Wiggins (1972). While HYPO71 is restricted to the coordinate system of latitude, longitude, and depth, the generalized inverse approach transforms the coordinate system to one dictated by the "data space". A set of normal equations that is well-conditioned in the new coordinate system is inverted, and the results are transformed back. Consequently, all four parameters are varied simultaneously, instead of in a step-wise fashion. The generalized inverse is also used by HYPOINVERSE (Klein, 1978).

Station Corrections. The third major problem with Geiger's method is the implicit assumption that travel-time curves are perfect, and the only source of error is in measuring arrival times. In fact, systematic velocity variations are common and are usually caused by geologic structure. And it is in fact these systematic velocity variations that have taken the most consideration in the work of this thesis. This is

mainly because of the recent advances in methods of timing. Computer-based digital systems now routinely time arrivals to a few hundredths of a second. Thus our ability to measure short-wavelength velocity changes now greatly exceeds our understanding of the velocity structure. The usual way of dealing with this problem is to introduce station corrections (also called station delays) which are added to the time calculated from the velocity model. Common examples are large positive delays for stations in deep sedimentary basins and negative delays for stations on high-velocity bedrock. All station delays are valid only for the velocity model for which they were derived.

There are many ways of deriving station delays. The best would be to set off an explosion at the hypocenter of interest. Since this is never practical, the second best solution is a well-timed source at the surface. Explosions comparable in size to earthquakes are rare, and expensive to produce. Consequently, many methods employ the earthquake data themselves to determine station delays. This is difficult to do correctly, and care must be taken to ensure that the model used is truly independent of the data it is processing.

One popular method is to average station delays for a large number of events. For example, HYPO71 outputs a new station list with new delays which are calculated as a weighted sum of residuals, and their weights assigned by the location program. This process is frankly referred to as "generating delays". It is standard practice to relocate the same data with the new delays and repeat the process in order to reduce rms values for all the earthquakes. This procedure is questionable because the nature of location programs is to reduce residuals. Hence, the process produces station delays that minimize residuals, but it does not discover the systematic velocity variations.

Relative Location Methods

Relative location methods differ from absolute methods in that they attempt to locate earthquakes relative to other earthquakes or explosions. Relative locations may be less accurate than absolute locations, but they are more precise. A group of earthquakes may be located well relative to each other, but as a group they may be systematically mislocated in the absolute sense. Thus accuracy may be sacrificed in favor of better resolution of structure. According to Pavlis (1982), the two most commonly used methods of relative location are the Master Event Technique and Joint Hypocenter Determination (JHD).

Master Event Location

The master-event method is to simply make residuals equivalent to station corrections. It is a rather obvious thing to do and it would be difficult to attribute its invention to a particular individual. One of the earliest applications was by Gutenberg and Richter (1937) who used travel-times differences between stations to determine relative positions of teleseismic epicenters. They plotted travel-time differences vs. azimuth on "sine plots", and noted that the amplitude of the sinusoid corresponds to distance between shocks, while the phase determined the direction of offset. Gutenberg (1943) used travel-time difference and the sine plots to determine relative locations of local shocks in southern California. Also, he improved these locations as a group using the corrected times for all the events involved, which was an early version of JHD. Richter *et al.* (1958) located the Desert Hot Springs earthquakes by the method of time differences with respect to "key shocks". A rather similar method called arrival time "differencing" had been used by Gardner (1964). He studied pairs of events and attempted to write a computer program to invert their arrival-time differences for the displacement vector between the two events. He

quickly discovered his problem was equivalent to an earthquake location inversion. Evernden (1969, p. 3840) used the "master-event" method to relocate nuclear explosions and teleseisms, and described it as follows:

> "The master event approach is to use the data from large events to evaluate the effect of earth inhomogeneities on P travel times (i.e. determine station residuals), and to then adjust the observed travel times for small events to create for computational purposes, a fictional homogeneous earth to which our travel-time curves apply in detail. The residuals are of course computed against a specific travel-time curve and are only valid with that curve..... The procedure is to select and locate master earthquakes, to compute their station-time anomalies or residuals for all stations used, and then to apply these residuals to observed travel times for small events.

In recent times, the improvement in station coverage and timing accuracy has turned the master-event method into a powerful tool for locating local events. Johnson and Hadley (1976) used the master-event technique to locate earthquakes precisely in the Imperial Valley. They noted that using travel-time residuals as station delays is "precisely equivalent to fitting a relative location vector to arrival-time differences between an event and a master event". Johnson and Hadley (1976) determined *a priori* delays from station site geology and carefully located a master event with their model. They then located a second master relative to the first and all the hypocenters in their study were located relative to the closer master. They achieved very small residuals and estimated location errors of 100 to 300 meters. Johnson and Hadley (1976) tested their method by adding a "mislocation vector" to the master-event hypocenter and recalculated the relative locations with re-derived delays. They found the pattern of seismicity to be unchanged, but each event was translated by an amount comparable to the original mislocation vector. Johnson (1979) carried this method even further by establishing a "network" of master events with which he was able to resolve intricate details of the seismicity of the Imperial Valley.

The principal advantage of the master-event method is its simplicity. However, according to Pavlis (1982), it has two major disadvantages: 1) it requires the master event to be recorded at every station used; 2) the station corrections have large uncertainty because each is based on only a single data point per station. I think that I have surmounted these difficulties in my studies by using a calibrated master event (CME), which will be discussed later in this section.

Joint Hypocenter Determination (JHD)

Pavlis (1982) argues that JHD is the "best" method of relative location. It works as follows: The data from a suite of earthquakes in the same area are inverted simultaneously for hypocenters and station corrections. If there are m events recorded at n stations, there will be $4m + n$ parameters derived from $m \times n$ data points. For the problem to be overdetermined, one needs $n > \frac{4m}{m-1}$ stations or $m > \frac{n}{n-4}$ events. Obviously, to be rigorously overdetermined requires considerable data. The problem is solved in a manner similar to Geiger's (1912) method, but now there are $4m + n$ normal equations. The method was largely developed by Douglas (1967) and Dewey (1971). This method has a fundamental ambiguity that it shares with the master-event method. The average value of station correction is arbitrary and can be compensated for by a constant offset in the origin time of all the events. JHD requires that for the matrix to be non-singular, the average station delay, or at least one station delay, must be set to zero. The matrix also becomes singular as the hypocenters approach a single point. Thus inversion may fail for tightly clustered activity. The problem is usually dealt with by holding a "master event" as fixed. The principal advantage of JHD is that it is statistically more rigorous than the simple master-event method. The principal disadvantage of the

JHD method is that the system of equations grows rapidly as data are added, so that the inversion becomes a major computing job. It has been used effectively for teleseismic studies of large regions (e.g. Dewey, 1972), and it appears to improve greatly results in parts of the world where velocity structure is poorly known. However, its disadvantages and the rather arbitrary selection of the master event reduce its superiority over the simple master-event method for local earthquake locations.

Calibrated Master Event (CME)

The difference in the master-event technique, as defined by Evernden (1969), and the CME method is that the former method uses a presumably well located large event to relocate associated smaller events, while the CME method uses a well-calibrated smaller event to locate events of its size and smaller. In the first case, one may simply assume that a master event is located "well enough" and then locate associated seismicity relative to it. This was done by Yelin and Crosson (1982), who relocated aftershocks using the mainshock as the master event. This improved the aftershock locations sufficiently that they were able to identify one of the nodal planes of the mainshock focal mechanism as the probable fault plane. They may have mislocated the position of the fault, but they had no hope of identifying a surface fault since the earthquake occurred in a region with deep glacial overburden.

In my own work, I have preferred to locate the master event first with the best possible absolute location. This has allowed me to correlate seismicity with particular geologic structures as well as to study the structures in detail. The calibrated master event overcomes some of the problems normally associated with master events. Normally a CME is calibrated with a well-timed explosion. If this is not possible, it may be possible to calibrate with earthquake data, but only if the earthquake-location data are kept independent of the station-correction data. And in some

cases it has been possible to use a combination of earthquake data and explosion data.

Examples of Calibrated Master Events

Borrego Mountain--1968

On April 9, 1968, a magnitude 6.4 earthquake struck the southern California desert in the Borrego Mountain region (Sharp, 1972). By April 12, a dense array of portable stations had been installed by the USGS and began recording high-precision data (Hamilton, 1972). Hamilton (1970) calibrated the network with a series of explosions and carried out a time-term analysis to derive a well-controlled velocity model and station delays. This model was used to locate accurately the Borrego Mountain aftershocks after April 12 (Hamilton, 1972). I relocated the seismicity from 1960 to April 9, 1968, including the mainshock and its foreshock. Prior to 1968, seismicity was recorded by the 14 stations of the Caltech regional network. In 1968, these same stations also recorded some of the larger aftershocks that had been well located by Hamilton (1972). The 22 largest aftershocks during this time period were selected, and the locations calculated by Hamilton (1972) were compared to the locations calculated with the data from the 14 Caltech stations (Fig. 6-1a). It is obvious that there is a systematic difference between locations. The Caltech locations usually locate 3 to 5 km west of Hamilton's (1972) locations. This is probably the result of crustal velocities decreasing towards the Imperial Valley, and the azimuthal bias of the Caltech stations (12 of the 14 being northwest of Borrego Mountain).

Since Hamilton's (1972) locations were the most accurate available, they were used to calibrate the Caltech stations. The 22 aftershocks were fixed at the locations specified by Hamilton (1972). Travel-time residuals for the 14 Caltech stations

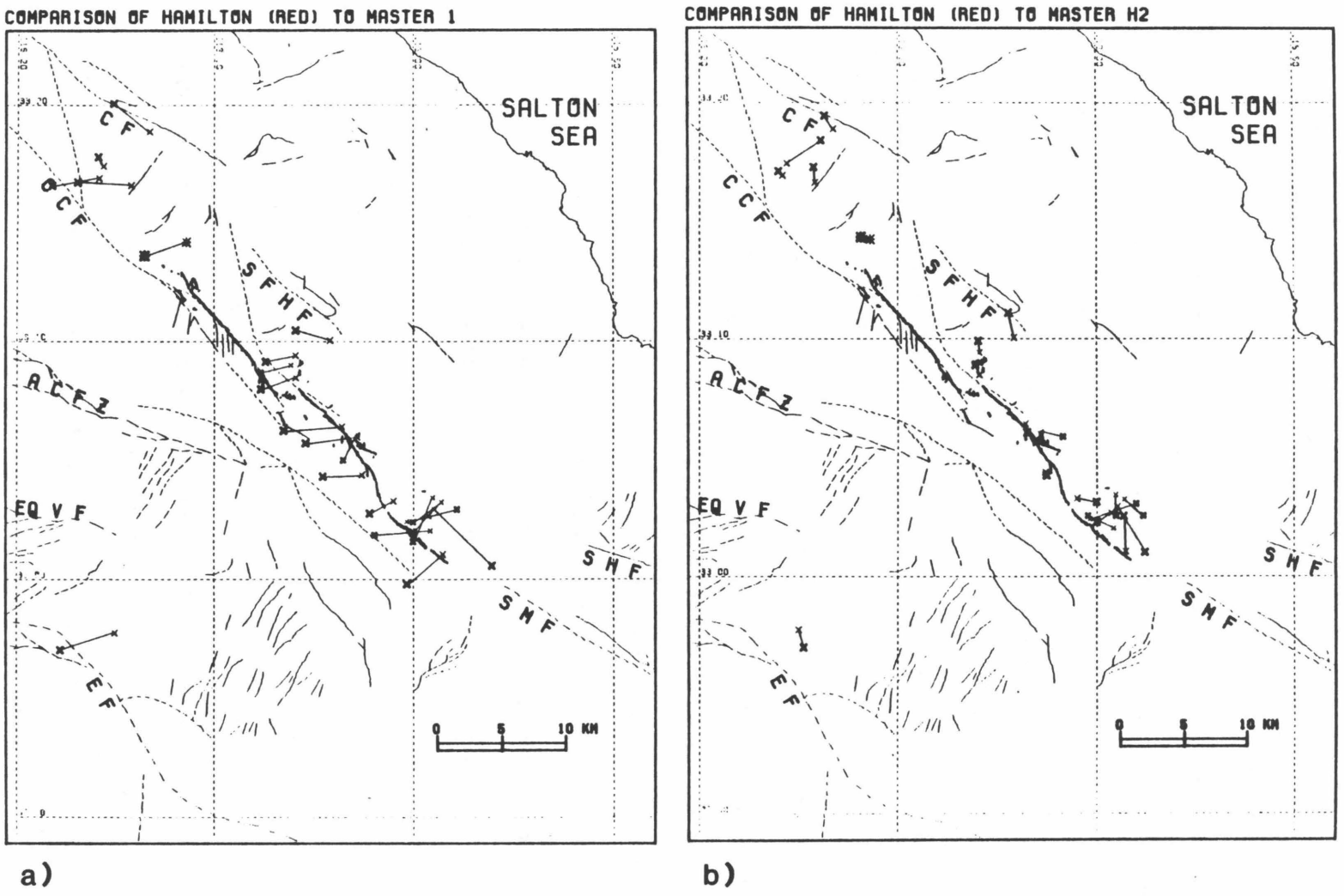

Figure 6-1. Comparison of locations of 22 aftershocks of the 1968 Borrego Mountain earthquake. Heavy symbols are locations with 14 Caltech stations. Light symbols are locations with dense local array (Hamilton, 1972). Lines between symbols are mislocation vectors for each event. a) Caltech locations with no station delays. b) Caltech locations with station delays derived from Hamilton's (1972) locations.

were calculated and analyzed statistically. Due to the chance of outliers skewing the averages, median values are considered to be a more robust estimator of "true" station corrections than average delays (Johnson, 1979). Consequently the median residuals were used as station corrections. The aftershocks were relocated with the new station-delay model, with the results shown in figure 6-1b. As can be seen, the mislocation vectors are reduced in length (1-2 km) and scattered in orientation. The only events that still show large mislocation vectors are at the extremities of the rupture zone, and also at the extremities of the USGS network in 1968. Thus they might represent mislocations by Hamilton (1972).

This technique was used successfully to relocate all the seismicity in the region from 1960 to 1968 (Corbett and McNally, 1979). This is not truly a master-event technique, but it demonstrates three points: 1) bias caused by data from distant stations can be eliminated with the proper station corrections, eliminating the need for distance weighting; 2) a dense seismic network can be used to locate precisely events that occurred years before the network was installed; 3) calibration can be achieved by using two independent data sets for the same events.

Santa Barbara--1978

The relocation of the Santa Barbara earthquake and its aftershocks has been discussed in Chapter 2. This section will discuss lessons learned and mistakes made in that process. When the Santa Barbara activity first occurred, the routine locations exhibited the pattern shown in Figure 6-2a. As can be seen, the aftershock zone appears to be quite broad, and the mainshock is located 7 km southeast of the aftershock zone. In a subsequent study (Corbett and Johnson, 1978), one of the aftershocks was used as a master event, with the locations shown in Figure 6-2b. As shown, the aftershock zone was now tightly clustered and located offshore, several

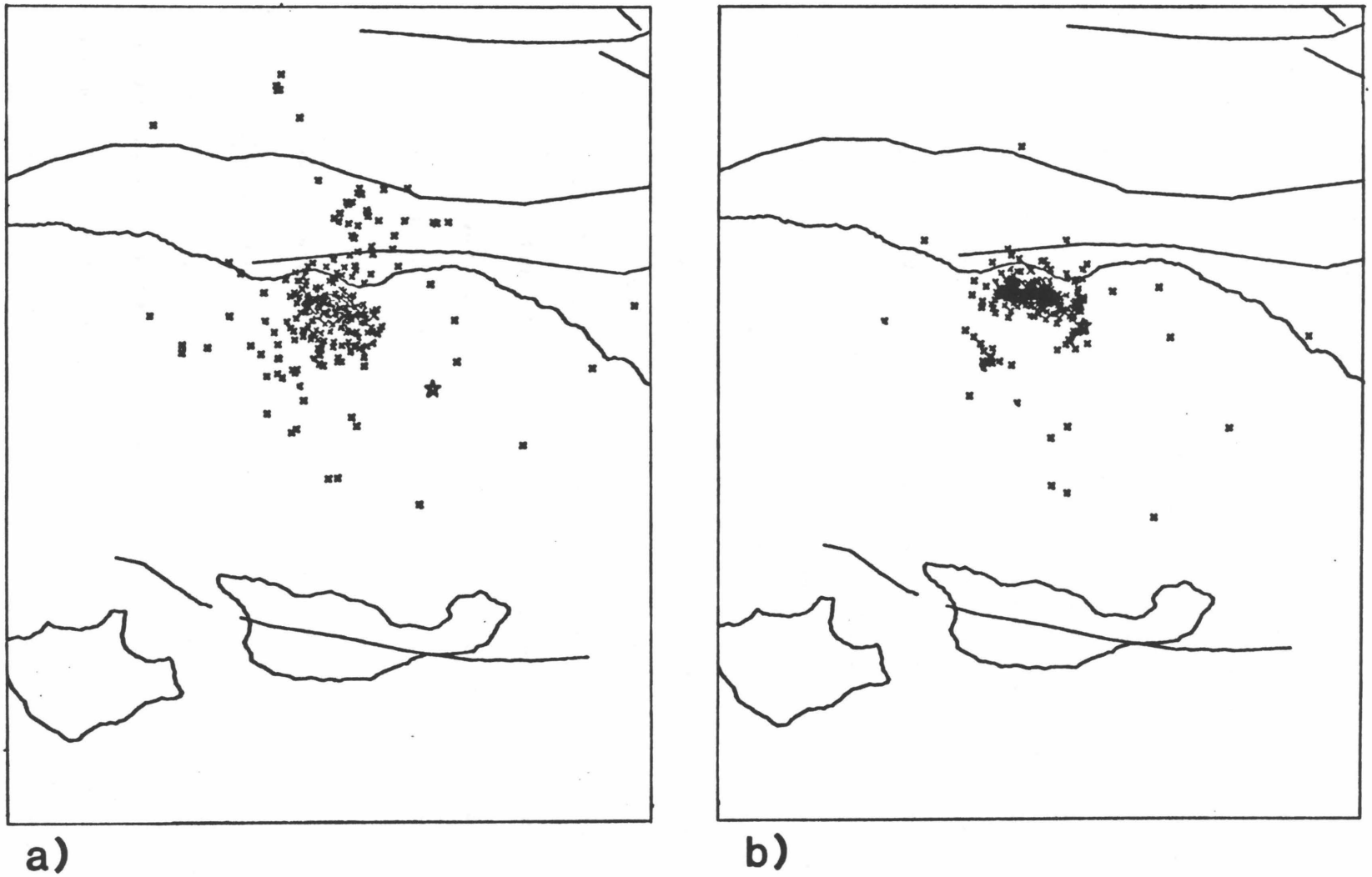

Figure 6-2. Mislocations of the 1978 Santa Barbara earthquake and aftershocks. a) routine catalog locations. b) master event relocations.

kilometers south of Santa Barbara.

The improved locations were the result of three systematic properties of the master event: 1) the same set of stations were used for all locations; 2) the same starting location was used for each event; 3) an aftershock was used that was about the same magnitude as all the other aftershocks. The larger mainshock had been "pulled away" from the aftershock zone because it was recorded on many more stations, all of which were located to the east and southeast. The importance of using the same starting location for each event cannot be overemphasized. Most location programs, including HYPO71 and QED1, automatically start at the first-arrival station, which may vary from event to event. Due to the capricious nature of weighting algorithms, different starting locations cause these programs to weight the data differently as the iterations progress.

This study was reported on as the "Santa Barbara Channel" earthquake by Corbett and Johnson (1978). Subsequently, explosions detonated in the channel were used to calibrate the master event, as discussed in Chapter 2. This led to even better absolute locations of the Santa Barbara activity, depicted in figure 6-3. It is clear that the activity was actually located under the city of Santa Barbara, and the authors found it necessary to change the title of their study (Corbett and Johnson, 1982).

The work in chapter 2 surmounted the two disadvantages of the master event technique (Pavlis, 1982). The four nearest stations were usable in spite of the fact that they were not operating when the "master" explosions occurred. They were calibrated by locating the first 24 hours of aftershocks with the four stations not controlling the solutions. Median residuals from the best-located events provided stations delays. The tenuousness of basing station corrections on a single data point was overcome by carefully comparing potential master events for internal

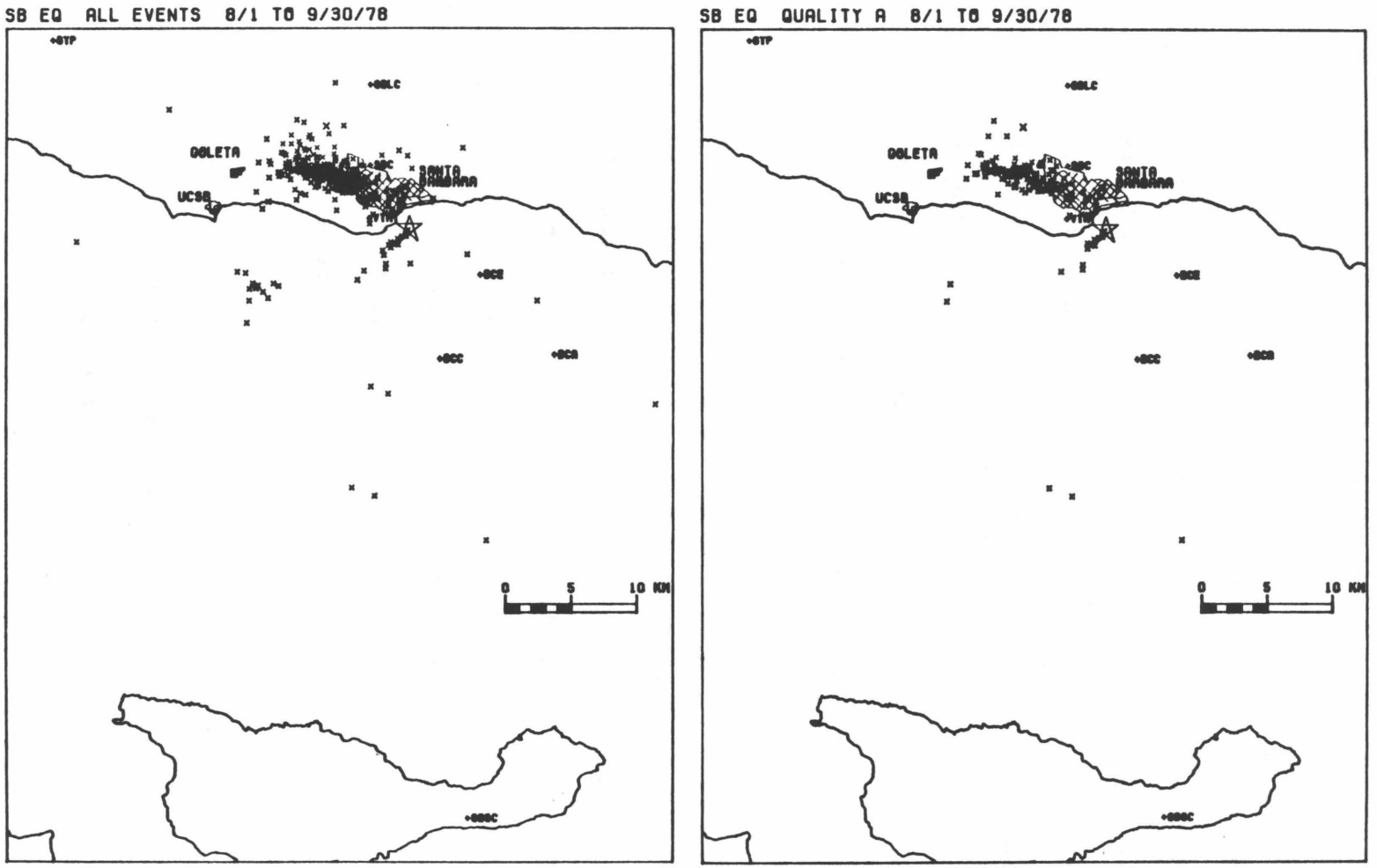

Figure 6-3. Locations of 1978 Santa Barbara earthquake and aftershocks calibrated with explosion data. a) all events. b) A-quality events only. Note northward translation of aftershock zone with little change in appearance compared to figure 6-2b.

consistency and consistency with median residuals for each station.

An interesting feature is the cluster of aftershocks 10 km southwest of the main body of aftershocks (fig. 6-3a) that disappears when only the higher quality data are considered (fig. 6-3b). Double checking the computer solution for the events revealed that they are an artifact of a peculiarity in the velocity model. Most of the events of this cluster are E-quality locations that were dominated by data from stations SBSM or PKM. These two stations are in opposite directions, but both are near the cross-over distance predicted by the model. This produces a double minimum in the travel-time differences between these two stations--one at the aftershock zone and one 10 km southwest. Evidently these two stations can trade off in the northeast-southwest direction if there aren't sufficient other data to prevent this.

The experience with the Santa Barbara earthquakes demonstrates several features of the master-event technique: 1) when properly used, a master event greatly reduces scatter in locations; 2) uncalibrated stations may be calibrated from independently derived locations; 3) systematic velocity gradients can cause large (5-10 km) absolute mislocations in spite of good station distribution; 4) changes in absolute location have little effect on the pattern of relative locations (compare figs. 6-2b and 6-3a); 5) master-event locations must still be filtered to remove systematically bad locations.

Santa Barbara Island--1981--Precision vs. Accuracy

In chapter 5, several different location procedures were tested on the first 24 hours of activity to see what kind of biases they could produce. These tests are summarized in figure 6-4, which shows the 7 different mainshock locations that result from the different methods tested. Location 1 is from the previous attempt by

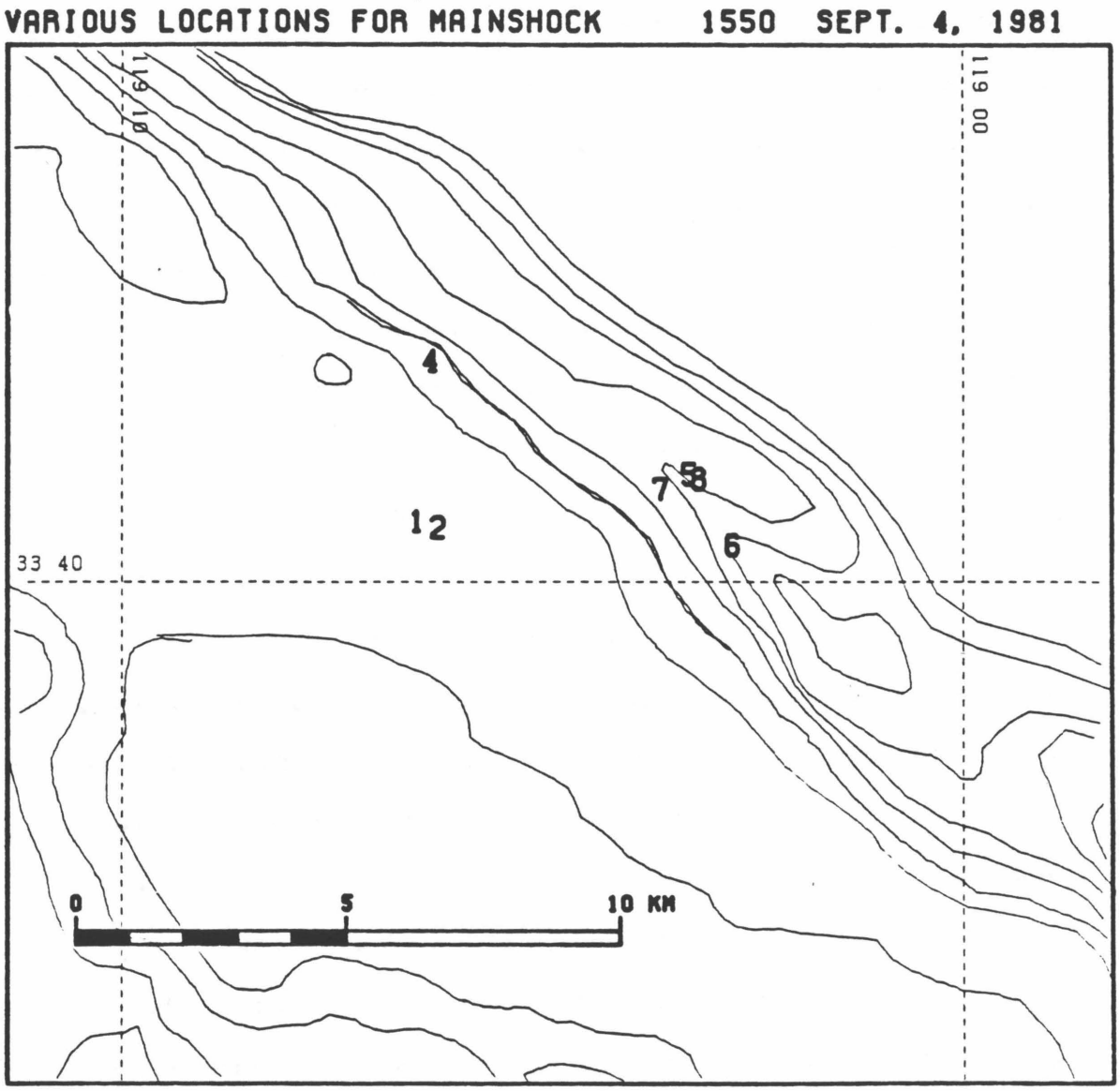

Figure 6-4. Various locations of the 1981 Santa Barbara earthquake resulting from differing velocity model, station delays, stations used, and starting location. Details in text.

Corbett and Piper (1981). Location 2 is the result of using the velocity model VM1, derived in Chapter 4, but with no station delays. We may use the Catalina quarry blast as a master event by fixing its location and calculating subsequent P-residuals (stations delays). Starting the locations at the same point for which the station delays are derived is one of the regimens of the master-event technique. Location 3 is the result of starting at the quarry with VM1 and the derived P-delays. In this case, it has the unfortunate result that most of the tested earthquakes failed to iterate away from the quarry (fig. 6-5). Only seven events located correctly in the true aftershock zone. These are larger events that are constrained by data from many stations. To alleviate this problem, the master-event technique was violated by allowing the location to start at the first station, i.e., SBI. This resulted in location 5. The difference between 3 and 5 demonstrates that changing starting location had a negligible effect in this case.

Locations 4, 5, and 6 were all derived with the freed starting location, and demonstrate the result of different assumptions about the station delay at the critical station SBI. A problem with the SBI record was that for the Catalina blast, two arrivals were observed: the first was low amplitude and emergent; and the second was large and impulsive. For reasons discussed in chapter 4, the second arrival is taken as the "correct" one, which results in location 5. If we had, however, used the weak first arrival at SBI to define the station delay, the mainshock would plot at location 4. On another hand, we might take the complication at SBI as justification for doubting both arrivals. Thus we might choose to locate the mainshock without the data from SBI, using only the surrounding, more distant stations. This results in location 6. This assumption had the disadvantage that most of the smaller events do not locate well without data from SBI. In addition, there is little reason to doubt that the second arrival at SBI is the correct one to use. Consequently the method associated

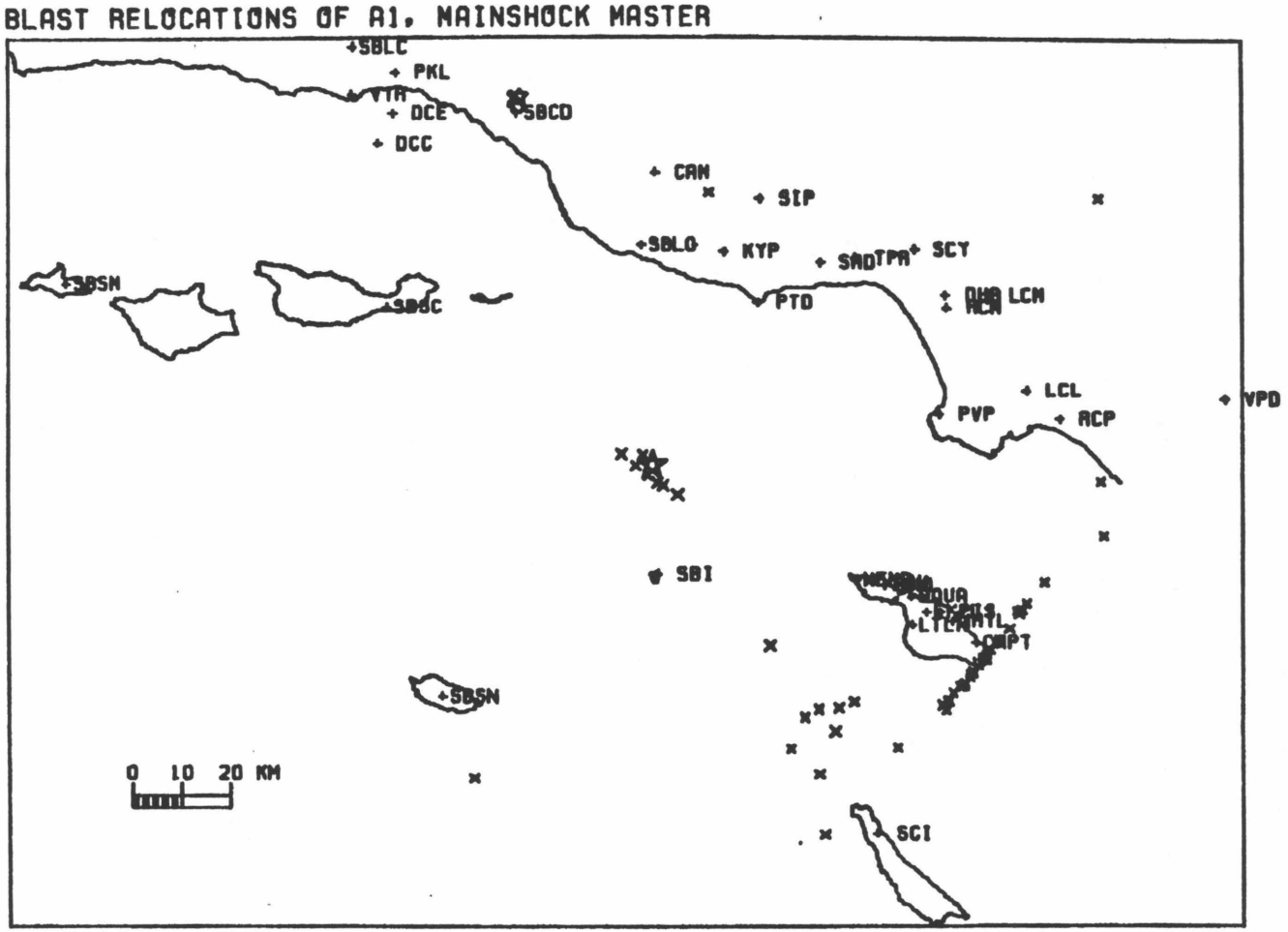

Figure 6-5. Mislocations of the 1981 Santa Barbara Island aftershocks resulting from using Catalina Quarry as starting location. The few correctly located events are the 7 largest. The smaller events scatter in a direction dictated by network geometry.

with location 5 is thought to be the most reasonable and was used for the Phase I relocations in chapter 5. Subsequently it was desirable to relocate the activity in the aftershock zone itself with a master event chosen from the aftershocks. An aftershock is probably more appropriate because it is proximate to the seismicity, and it has comparable depth. An aftershock also has the advantage of permitting the use of S-delays, which improves the location of small events and constrains depth. Using the master event resulted in location 7 for the mainshock (figure 6-4). Use of the master event did not significantly improve the location of the mainshock, but it greatly increased the number of well-located aftershocks.

At this point it is best to summarize the implications of these different locations. The distance from 1 to 2 represents the result of changing velocity model alone, which is quite small. The distance from 1 and 2 to 5, or from 4 to 5 is about 5 km and represents the systematic bias which can result from using incorrect station delays. The distance from 5 to 6 is about 1.5 km and represents the uncertainity in the absolute location of the mainshock. This is analogous to the accuracy of location. The difference between 5 and 7 is 0.5 km and represents the uncertainity resulting from which event is chosen as the master event. This is analogous to the precision of the location.

CONCLUSIONS

Definition of CME technique

It would be misleading to give a precise procedure for doing CME locations since the techniques employed depend on the data set invloved. Individual workers must determine the best approach to the specialized set of conditions they are faced with. However, I have learned some guidelines for achieving precise earthquake locations.

Choosing a Master Event. First, the best possible velocity model for the area should be used. All station corrections determined will be relative to this model. The best candidate for a master event is a single well-recorded earthquake that has a magnitude comparable to and has a hypocenter near to the events it is to be used to locate. It should have clear impulsive arrivals at the maximum number of stations near the hypocenter, with azimuthal control also a consideration. The master event should be chosen carefully after comparison with other events in the area.

Using a Master Event. The master event should be calibrated by data independent of the earthquakes it will be used to locate, preferably by explosion data. A station that does not record the master event cannot be used (i.e. do not assume zero residual at these stations). Stations that did not record the calibration event may be usable if they can be calibrated independently. The residuals for the calibrated master event become the station corrections to be used in relocations. The master-event hypocenter should be used as the starting location for the relocated earthquakes. Since this last step may cause poorly constrained events to "locate" at the starting location, the relocations should be filtered for quality.

Testing a Master Event. The master event itself should be included in the relocations. It should "relocate" at the same hypocenter as before, with 0.00 rms error. The master-event relocations should greatly reduce the station residuals and rms error for most of the relocated events. Failure to do so may indicate that there is a station with an incorrect delay. An effective test is to plot rms vs. distance of hypocenters from the master event. The rms should be low near the master event, and increase with distance, as lateral velocity variations reduce the applicability of the master event with distance.

BIBLIOGRAPHY

Aki, K. (1973). Scattering of P waves under the Montana LASA, *J. Geophys. Res.* **78**, 1334-1346.

Allen, C.R. (1957). San Andreas fault zone in San Gorgonio Pass, southern California, *Geol. Soc. Amer. Bull.* **68**, 315-350.

Allen, C.R., L.T. Silver, and F.G. Stehli (1960). The Agua Blanca fault -- A major transverse structure of northern Baja California, Mexico, *Geol. Soc. Amer. Bull.* **71**, 457-482.

Alpha, T.R. (1981). Oblique map of the southern California inner Continental Borderland, *U.S. Geol. Survey Open-File Report 81-1312*, 1 sheet, scale 1:340,000.

Anderson, J.G. (1983?). The September 4, 1981, Santa Barbara Island, California, earthquake: Interpretation of strong-motion data, *pre-print*.

Anderson, K.A. (1981). Epicentral location using arrival time order, *Bull. Seis. Soc. Amer.* **71**, 541-545.

Arnal, R.E. (1976). Miocene paleobathymetric changes of the Santa Rosa-Cortes Ridge area, California Continental Borderland, *Amer. Assoc. Petro. Geol. Pacific Section, Misc. Pub 24*, 60-79.

Atwater, T. (1970). Implications of plate tectonics for the tectonic evolution of western North America, *Geol. Soc. Amer. Bull.* **81**, 3515-3536.

Barrows, A.G. (1974). A review of the geology and the earthquake history of the Newport-Inglewood structural zone, southern California, *Calif. Div. Mines and*

Geology Spec. Rpt. 114, 115p.

Beyer, L.A. (1980). Offshore southern California, *in* Oliver, H.W. (ed.). Interpretation of the gravity map of California and its continental margin, *Calif. Div. Mines and Geology Bull. 205*, 8-14.

Beyer, L.A. (1982). Bouger gravity map of California, Long Beach sheet, *Calif. Div. Mines and Geology*, scale 1:250,000.

Blake, M.C. Jr., and 7 others (1978). Neogene basin formation in relation to plate-tectonic evolution of the San Andreas fault system, *Amer. Assoc. Petro. Geol. Bull.* **62**, 344-372.

Bogaert, B., M. Reichle, W. Prothero, and S. Zelikovitz (1978). Aftershock study of the August 13, 1978 Santa Barbara, California earthquake, *Trans. Amer. Geophys. Union* **59**, 1130.

Bromery, R.W., K.O. Emery, and J.R. Balsey, Jr. (1960). Reconnaissance airborne magnetometer survey off southern California, *U.S. Geol. Survey Map GP-211*, 1 sheet, scale 1:1,000,000.

Campbell, R.H., R.F. Yerkes, and C.M. Wentworth (1966). Detachment faults in the central Santa Monica Mountains, California, *U.S. Geol. Survey Prof. Paper 550-C*, C1-C11.

Castle, R.O., J.P. Church, and M.R. Elliot (1976). Aseismic uplift in southern California, *Science* **192**, 251-253.

Clements, T. and K.O. Emery (1947). Seismic activity and topography of the sea-floor of southern California, *Bull. Seis. Soc. Amer.* **37**, 309-313.

Cole, M.R. (1975). Poway clasts, sandstone petrology, and palinspastic reconstruction of the southern California Borderland, *Geol. Soc. Amer. abs. w/programs* **7**, 305.

Corbett, E.J. (1983). Velocity structure of southern California Continental Borderland as seen from Catalina Island, *Earthquake Notes* **54(1)**, 67-68.

Corbett, E.J. and T.M. Hearn (1981). The depth of the seismic zone in the Transverse Ranges of southern California, presented at the John Muir Geophysical Society meeting, Oct. 7-9, 1981, Lake Arrowhead, California.

Corbett, E.J. and C.E. Johnson (1978). The Santa Barbara Channel earthquake of August 13, 1978, *Trans. Amer. Geophys. Union* **59**, 1130.

Corbett, E.J. and C.E. Johnson (1980). Evidence for mid-crustal shearing in the western Transverse Ranges, California, *Trans. Amer. Geophys. Union* **61**, 1043.

Corbett, E.J. and C.E. Johnson (1982). The Santa Barbara, California, earthquake of 13 August 1978, *Bull. Seis. Soc. Amer.* **72**, 2201-2226.

Corbett, E.J. and K.C. McNally (1978). Changes in stress indicated by "preshocks" to the 1968 Borrego Mountain earthquake, *Trans. Amer. Geophys. Union* **59**, 1127.

Corbett, E.J. and K.C. McNally (1979). Seismicity of the Borrego Mountain region 1960-1968, *Earthquake Notes* **50(4)**, 4.

Corbett, E.J. and K.A. Piper (1981). The Santa Barbara Island, California earthquake, September 4, 1981, *Trans. Amer. Geophys. Union* **62**, 958.

Crandall, G.J., B.P. Luyendyk, M.S. Reichle, and W.A. Prothero (1983). A marine seismic study of the Santa Barbara Channel, California, *Marine Geophys. Res.* **6**, 15-37.

Crandall, G., M. Reichle, B.P. Luyendyk, and W.A. Prothero (1979). Marine seismic refraction study of the Santa Barbara Channel (Southern California Borderlands), *Trans. Amer. Geophys. Union* **60**, 886.

Crouch, J.K. (1979). Neogene tectonic evolution of the California Continental Borderland and western Transverse Ranges, *Geol. Soc. Amer. Bull.* **90**, 338-345.

Crowell, J.C. (1974). Origin of late Cenozoic basins in southern California, *in* Dickinson, W.R. (ed.). Tectonics and Sedimentation, *Soc. Econ. Paleon. and Min., Spec. Pub. 22*, 190-204.

Davis, G.A. J.L. Anderson, E.G. Frost, and T.J. Shakelford (1980). Mylonitization and detachment faulting in the Whipple-Buckskin-Rawhide Mountains terrane, southeastern California and western Arizona, *Geol. Soc. Amer. Memior 153*, 79-129.

Dewey, J.W. (1971). Seismicity studies with the method of joint hypocentral determination, *Ph.D. thesis*, Univ. of California, Berkeley.

Dewey, J.W. (1972). Seismicity and tectonics of western Venezuela, *Bull. Seis. Soc. Amer.* **62**, 1711-1751.

Dibblee, T.W., Jr. (1975). Late Quatenary uplift of the San Bernardino Mountains on the San Andreas and related faults, *Calif. Div. Mines and Geology Spec. Rpt. 118*, 127-135.

Dickinson, W.R. and W.S. Snyder (1979). Geometry of triple junctions and subducted slabs related to the San Andreas transform, *J. Geophys. Res.* **84**, 561-572.

Douglas, A. (1967). Joint epicentre determination, *Nature* **215**, 47-48.

Ebel, J.E. (1980). Evidence for fault asperities from systematic time-domain modelling of teleseismic waveforms, *Ph.D.thesis*, Calif. Inst. Tech., Pasadena, 141p.

Ebel, J.E., D.V. Helmberger and T.C. Wallace (1980). Evidence for fault asperities from the analysis of near-field and teleseismic waveforms, *Trans. Amer. Geophys. Union* **61**, 1027.

Emery, K.O. (1954). General geology of the offshore area, southern California, *Calif. Div. Mines and Geology Bull. 170*, v. 1, chap. 2, 107-111.

Emery, K.O. (1958). Shallow submerged marine terraces of southern California, *Geol. Soc. Amer. Bull.* **69**, 39-60.

Emery, K.O. (1960). *The sea off southern California*, John Wiley and Sons, New York, 366p.

Emery, K.O. and F.P. Shepard (1945). Lithology of the sea floor off southern California, *Geol. Soc. Amer. Bull.* **56**, 431-478.

Ergas, R.A. and D.D. Jackson (1981). Spatial variations of crustal seismic velocities in southern California, *Bull. Seis. Soc. Amer.* **71**, 671-689.

Evernden, J.F. (1969). Identification of earthquakes and explosions by use of teleseismic data, *J. Geophys. Res.* **74**, 3828-3856.

Ford, G.A. and W.R. Normark (1980). Map showing a deep-tow geophysical study of the north end of the San Clemente fault, California borderland, *U.S. Geol. Survey Map MF-1230*, 1 sheet, scale 1:36,417.

Forman, J.A. (1970). Age of the Catalina Island pluton, California, *Geol. Soc. Amer. Spec. Paper 124*, 37-45.

Frost, E.G., T.E. Cameron, D. Krummenacher, and D.L. Martin (1981). Possible regional interaction of mid-Tertiary detachment faulting with the San Andreas fault and the Vincent-Orocopio thrust system, Arizona and California, *Geol. Soc. Amer. abs. w/programs* **13**, 455.

Frost, E.G. and D.L. Martin (eds.) (1982). *Mesozoic-Cenozoic tectonic evolution of the Colorado River region, California, Arizona, and Nevada*, Cordilleran Publishers, San Diego, 608p.

Fuis, G. and V. Lamanuzzi (1978). Seismicity of the eastern Transverse Ranges, southern California, *Trans. Amer. Geophys. Union* **59**, 1051.

Gardner, J.K. (1964). Earthquakes in the Walker Pass region, California, and their relation to the tectonics of the southern Sierra Nevada, *Ph.D.thesis*, Calif. Inst. Tech., Pasadena, 122p.

Geiger, L. (1912). Probability method for the determination of earthquake epicenters from arrival time only (translated from German), *Bull. St. Louis Univ.* **8(1)**, 56-71.

Given, D.D. and C.L. Koesterer (1983). Station arrival data for a quarry blast on Santa Catalina Island, California, *U.S. Geol. Survey Open-File Report 83-462*, 12p.

Green, S.M. (1983). Seismotectonic study of the San Andreas, Mission Creek, and Banning fault system, *M.S. thesis*, Univ. of Calif., Los Angeles, 52p.

Greene, H.G., K.A. Bailey, S.H. Clarke, J.I. Ziony, and M.P. Kennedy (1979). Implications of fault patterns of the inner Continental Borderland between San Pedro and San Diego, *in* Abbott, P.L. and W.J. Elliot (eds.), Earthquakes and other perils: San Diego region, *Geol. Soc. Amer. Annual meeting guidebook*, 21-27.

Greene, H.G., S.H. Clarke Jr., M.E. Field, F.I. Linker, and H.C. Wagner (1975). Preliminary report on the environmental geology of selected areas of the southern California Continental Borderland, *U.S. Geol. Survey Open-File Report 75-596*, 69p.

Gutenberg, B. (1941). Mechanism of faulting in southern California indicated by seismograms, *Bull. Seis. Soc. Amer.* **31**, 263-302.

Gutenberg, B. (1943). Earthquakes and structure in southern California, *Geol. Soc. Amer. Bull.* **54**, 499-526.

Gutenberg, B. (1951). Waves from blasts recorded in southern California, *Trans. Amer. Geophys. Union* **33**, 427-431.

Gutenberg, B. and C.F. Richter (1937). Materials for the study of deep-focus earthquakes (second paper), *Bull. Seis. Soc. Amer.* **27**, 157-183.

Gutenberg, B., C.F. Richter, and H.O. Wood (1932). The earthquake in Santa Monica Bay, California, on August 30, 1930, *Bull. Seis. Soc. Amer.* **22**, 138-154.

Hadley, D.M. (1978). Geophysical investigations of the structure and tectonics of southern California, *Ph.D. thesis*, Calif. Inst. Tech., Pasadena, 167p.

Hadley, D. and H. Kanamori (1978). Recent seismicity in the San Fernando region and tectonics in the west-central Transverse Ranges, California, *Bull. Seis. Soc. Amer.* **68**, 1449-1457.

Hadley, D. and H. Kanamori (1979). Regional S-wave structure for southern California from the analysis of teleseismic Rayleigh waves, *Geophys. J. R. Astr. Soc.* **58**, 655-666.

Hamilton, R.M. (1970). Time-term analysis of explosion data from the vicinity of the Borrego Mountain, California earthquake of 9 April 1968, *Bull. Seis. Soc. Amer.* **60**, 367-381.

Hamilton, R.M. (1972). Aftershocks of the Borrego Mountain earthquake from April 12 to June 12, 1968, *U.S. Geol. Survey Prof. Paper 787*, 31-54.

Hamilton, R.M., R.F. Yerkes, R.D. Brown Jr., R.O. Burford, and J.M. DeNoyer (1969). Seismicity and associated effects, Santa Barbara region, *U.S. Geol. Survey*

Prof. Paper 679, 47-68.

Harding, T.P (1973). Newport-Inglewood trend, California--an example of wrenching style of deformation, *Amer. Assoc. Petro. Geol. Bull.* **57**, 97-116.

Harrison, J.C., R.E. von Huene, and C.E. Corbato (1966). Bouger gravity anomalies and magnetic anomalies off the coast of southern California, *J. Geophys. Res.* **71**, 4921-4941.

Haxel, G. and J. Dillon (1978). The Pelona-Orocopia schist and Vincent-Chocolate Mountain thrust system, southern California, *in* D.G. Howell and K.A. McDougall (eds.), Mesozoic paleogeogaphy of the western United States, *Soc. Econ. Paleo. Min. Pacific Section*, 453-469.

Healy, J.H. (1963). Crustal structure along the coast of California from seismic-refraction measurements, *J. Geophys. Res.* **68**, 5777-5787.

Hearn, T.M. (in press). P_n Travel times in southern California, *J. Geophys. Res.*.

Henyey, T.L. (1976). Heat flow and tectonic patterns on the southern California Borderland, *Amer. Assoc. Petro. Geol. Pacific Section, Misc. Pub 24*, 427-448.

Henyey, T.L., J.K. McRaney, D.V. Manov, and T.L. Teng (1978). The 1978 Santa Barbara earthquake as recorded by an offshore seismic network, *Trans. Amer. Geophys. Union* **59**, 1130.

Hileman, J.A., C.R. Allen, and J.M. Nordquist (1973). Seismicity of the southern California region, 1932-1972, *Seismological Lab., Calif. Inst. Tech.*, contribution no. 2385, 487p.

Hill, R.L. and 8 others (1979). Earthquake hazards associated with faults in the greater Los Angeles metropolitan area, Los Angeles County, California, *Calif. Div. Mines and Geology Open-File Report 79-16 LA*, 202p.

Hill, R.T. (1928). Southern California geology and Los Angeles earthquakes, *So. Calif. Acad. Sci.*, 232p.

Howell, D.G. (ed.) (1976a). Aspects of the geologic history of the California Continental Borderland, *Pacific Section, Amer. Assoc. Petro. Geol. Misc. Pub 24*, 561p.

Howell, D.G. (1976b). Late-Miocene counterclockwise rotation of the south half of Santa Cruz Island, *Amer. Assoc. Petro. Geol. Pacific Section, Misc. Pub 24*, 449-454.

Howell, D.G., C.J. Stuart, J.P. Platt, and D.J. Hill (1974). Possible strike-slip faulting in the southern California borderland, *Geology* **2**, 93-98.

Howell, D.G., C.J. Stuart, J.P. Platt, and D.J. Hill (1975). Possible strike-slip faulting in the southern California borderland: Reply, *Geology* **3**, 3-4.

Howell, D.G. and J.G. Vedder (1981). Structural implications of stratigraphic discontinuities across the southern California Borderland, *in* Ernst, W.G. (ed.). *The Geotectonic Development of California*, Prentice-Hall Inc., Englewood Cliffs, N.J., 535-558.

Howell, D.G., and others (1978). General geology, petroleum appraisal, and the nature of environmental hazards, eastern Pacific shelf, latitude 28° to 38° north, *U.S. Geol. Survey Circular 786*, 29p.

Jennings, C.W. (1962). Geologic map of California, Long Beach sheet, *Calif. Div. Mines and Geology*, scale 1:250,000.

Jennings, C.W. (1975). Fault map of California, *Calif. Div. Mines and Geology, Geologic Data Map 1*, scale 1:750,000.

Jennings, C.W. and R.G. Strand (1969). Geologic map of California, Los Angeles sheet, *Calif. Div. Mines and Geology*, scale 1:250,000.

Johnson, C.E. (1979). CEDAR -- an approach to the computer automation of short-period local seismic networks, *Ph.D. thesis*, Calif. Inst. Tech., Pasadena, 332p.

Johnson, C.E. and D.M. Hadley (1976). Tectonic implications of the Brawley earthquake swarm, Imperial Valley, California, January 1975, *Bull. Seis. Soc. Amer.* **66**, 1133-1144.

Junger, A. (1975). Some thoughts on the structure of the Continental Borderland, southern California, *Geol. Soc. Amer. abs. w/programs* **7**, 331.

Junger, A. (1976). Tectonics of the southern California Borderland, *Amer. Assoc. Petro. Geol. Pacific Section, Misc. Pub 24*, 486-498.

Junger, A. (1979). Maps and seismic profiles showing geologic structure of the northern Channel Island platform, California Continental Borderland, *U.S. Geol. Survey Map MF-991*, 5 sheets, scale 1:250,000, 16p.

Junger, A. and H.C. Wagner (1977). Geology of the Santa Monica and San Pedro basins, California Continental Borderland, *U.S. Geol. Survey Map MF-820*, 5 sheets, scale 1:250,000, 10p.

Kamerling, M.J. and B.P. Luyendyk (1979). Tectonic rotations of the Santa Monica Mountains region, western Transverse Ranges, California, suggested by paleomagnetic vectors, *Geol. Soc. Amer. Bull. pt. I* **90**, 331-337.

Kamerling, M.J. and B.P. Luyendyk (1981). Paleomagnetism and tectonics of the islands of the southern California Continental Borderland, *Trans. Amer. Geophys. Union* **62**, 855.

Kanamori, H. (1978). Quantification of earthquakes, *Nature* **271**, 411-414.

Kanamori, H. (1981). The nature of seismicity patterns before large earthquakes, *in* Simpson, D. and P. Richards (eds.). *Earthquake Prediction–An*

International Review, Maurice Ewing Series 4, 1-19.

Kanamori, H. and D.L. Anderson (1975). Theoretical basis for some empirical relations in seismology, *Bull. Seis. Soc. Amer.* **65**, 1073-1095.

Keilis-Borok, V.I. (1959). On estimation of the displacement in an earthquake source and of source dimensions, *Ann. Geofis. (Rome)* **12**, 205-214.

Keller, B. (1983). P_n in the western Transverse Ranges, *pre-print*, Univ. of Calif., Santa Barbara.

Keller, B., W.A. Prothero, Jr., A.M. Trehu, and D.J. Stierman (1983). Ray trace model of the Santa Barbara, California, land-sea refraction experiment, *Geophy. Res. Letters* **10**, 933-936.

Kemnitzer, L.E. (1933). Geology of San Nicolas and Santa Barbara Island, southern California, *M.S. thesis*, Calif. Inst. Tech., Pasadena, 45p.

Klein, F.W. (1978). Hypocenter location program HYPOINVERSE, *U.S. Geol. Survey Open-File Report 78-694*, 113p.

Lee, W.H.K. and J.C. Lahr (1975). HYPO71 (revised): A computer program for determining hypocenter, magnitude, and first motion pattern of local earthquakes, *U.S. Geol. Survey Open-File Report 75-311*, 114p.

Lee, W.H.K. and J.G. Vedder (1973). Recent earthquake activity in the Santa Barbara Channel region, *Bull. Seis. Soc. Amer.* **63**, 1757-1773.

Lee, W.H.K., C.E. Johnson, T.L. Henyey, and R.F. Yerkes (1978). A preliminary study of the Santa Barbara, California earthquake of August 13, 1978 and its major aftershocks, *U.S. Geol. Survey Circular 797*, 11p.

Lee, W.H.K., R.F. Yerkes, and M. Simirenko (1979). Recent earthquake activity and focal mechanisms in the western Transverse Ranges, California, *U.S. Geol. Survey Circular 799*, 1-26.

Legg, M.R. (1980). Seismicity and tectonics of the inner Continental Borderland of southern California and northern Baja California, Mexico, *M.S. thesis*, Univ. of California, San Diego, 60p.

Legg, M.R. and M.P. Kennedy (1979). Faulting offshore San Diego and northern Baja California, *in* Abbott, P.L. and W.J. Elliot (eds.), Earthquakes and other perils: San Diego region, *Geol. Soc. Amer. Annual meeting guidebook*, 29-46.

Lonsdale, P. (1979). A deep-sea hydrothermal site on a strike-slip fault, *Nature* **281**, 531-534.

Luyendyk, B.P., J.S. Hornafius, M.J. Kamerling, and R.R. Terres (1982). Simple shear of southern California during the Neogene. *Trans. Amer. Geophys. Union* **63**, 914-915.

Luyendyk, B.P., M.J. Kamerling, and R. Terres (1980). Geometric model for Neogene crustal rotations in southern California, *Geol. Soc. Amer. Bull. pt. I* **91**, 211-217.

Matti, J.C. and D.M. Morton (1982). Geologic history of the Banning fault zone, southern California, *Geol. Soc. Amer. abs. w/programs* **14**, 184.

Matti, J.C. B.F. Cox, C.M. Obi, R.E. Powell, M.E. Hinkle, A. Griscom, and E.L. McHugh (1982). Mineral resource potential of the Whitewater Wilderness Study Area, Riverside and San Bernardino counties, California, *U.S. Geol. Survey Map MF-1478-A*, scale 1:24,000, 6p.

Meisling, K.E. and R.J. Weldon (1982). The late Cenozoic structure and stratigraphy of the western San Bernardino Mountains, *in* Geologic excursions in the Transverse Ranges, *Geol. Soc. Amer. Cordilleran section guidebook*, 75-81.

Meisling, K.E. (1983). Neotectonics of the north frontal fault system of the San Bernardino Mountains, southern California: Cajon Pass to Lucerne Valley, *Ph.D. thesis*, Calif. Inst. Tech., Pasadena, 394p.

Meissner, R. and J. Strehlau (1982) Limits of stresses in continental crusts and their relation to the depth-frequency distribution of shallow earthquakes. *Tectonics* **1**, 73-89.

Minch, J.A., K.N. Gibson, and G.L. Peterson (1976). Clast populations in Sespe and Poway conglomerates and their possible bearing on the tectonics of the southern California Borderland, *Amer. Assoc. Petro. Geol. Pacific Section, Misc. Pub 24*, 256-265.

Mogi, K. (1969). Some features of recent seismic activity in and near Japan, (2) Activity before and after great earthquakes, *Bull. Earthquake Res. Inst.* **47**, 395-417.

Moore, D.G. (1969). Reflection profiling studies of the California Continental Borderland: Structure and Quaternary turbidite basins, *Geol. Soc. Amer. Spec. Paper 107*, 142p.

Moore, G.W. (1976). Basin development in the California borderland of the Basin and Range province, *Amer. Assoc. Petro. Geol. Pacific Section, Misc. Pub 24*, 383-392.

Morton, D.M. and Miller, F.K. (1975). Geology of the San Andreas fault zone north of San Bernardino between Cajon Canyon and Santa Ana Wash, *Calif. Div. Mines and Geology Spec. Rpt. 118*, 136-146.

Nardin, T.R. (1981). Seismic stratigraphy of the Santa Monica and San Pedro basins, California Continental Borderland; late Neogene history of sedimentation and tectonics, *PhD. thesis*, Univ. Southern California, Los Angeles, 295 p.

Nardin, T.R. and T.L. Henyey (1978). Pliocene-Pleistocene diastrophism of Santa Monica and San Pedro shelves, California Continental Borderland, *Amer. Assoc. Petro. Geol. Bull.* **82**, 247-272.

NEIS (National Earthquake Information Service) (1981). Preliminary Determination of Epicenters, Sept. 1981, *U.S. Geol. Survey*, 23p.

Nicholson, C., P. Williams, L. Seeber, and L. Sykes (1983). San Andreas seismicity and fault tectonics through the eastern Transverse Ranges, *Trans. Amer. Geophys. Union* **64**, 768.

Nilsen, T.H. and S.H. Clarke (1975). Sedimentation and tectonics in the early Tertiary Continental Borderland of central California, *U.S. Geol. Survey Prof. Paper 925*, 64p.

Oliver, H.W. (1980). Transverse Ranges, *in* Oliver, H.W. (ed.). Interpretation of the gravity map of California and its continental margin, *Calif. Div. Mines and Geology Bull. 205*, 15-16.

Patterson, R.H. (1978). Neotectonics of the Santa Cruz Island Fault, California, *Earthquake Notes* **49(1)**, 21.

Pavlis, G.L. (1982). Progressive Inversion, *Ph.D. thesis*, Univ. of Wash., Seattle, 296p.

Pechmann, J.C. (1983). The relationship of small earthquakes to strain accumulation along major faults in southern California, *Ph.D. thesis*, Calif. Inst. Tech., Pasadena, 175p.

Pilger, R.H. Jr. (1978). Structure of Santa Cruz-Catalina ridge, California borderland: Implications for the Neogene tectonics of southern California, *Trans. Amer. Geophys. Union* **59**, 1211.

Pilger, R.H. Jr. (1976). Structure of Santa Cruz-Catalina ridge and adjacent areas, southern California Continental Borderland, from reflection and magnetic profiling: Implications for late Cenozoic tectonics of southern California, *PhD. thesis*, Univ. Southern California, Los Angeles, 159p.

Platt, J.P. (1976). The significance of the Catalina Schist in the history of the southern California borderland, *Amer. Assoc. Petro. Geol. Pacific Section, Misc. Pub 24*, 47-52.

Plawman (1978). Crustal structure of the Continental Borderland and adjacent portions of Baja California between latitudes 30° N. and 33° N., *M.S. thesis*, Oregon State Univ., Corvallis, 72p.

Powell, R.E. (1981). Geology of the crystalline basement complex, eastern Transverse Ranges, southern California: Constraints on regional tectonic interpretation, *Ph.D. thesis*, Calif. Inst. Tech., Pasadena, 441p.

Press, F. (1956). Determination of crustal structure from phase velocity of Rayleigh waves, Part I: Southern California, *Geol. Soc. Amer. Bull.* **67**, 1647-1658.

Real, C.R. (in press). Seismicity and tectonics of the Santa Monica-Hollywood-Raymond Hill fault zone and northern Los Angeles basin, Los Angeles County, California, *in* Transverse Ranges, *U.S. Geol. Survey Prof. Paper.*

Richter, C.F. (1958). *Elementary Seismology*, W.H. Freeman and Co., San Francisco, 768p.

Ridlon, J.B. (1972). Pleistocene-Holocene deformation of the San Clemente Island crustal block, California, *Geol. Soc. Amer. Bull.* **83**, 1831-1844.

Rogers, T.H. (1967). Geologic map of California, San Bernardino sheet, *Calif. Div. Mines and Geology*, scale 1:250,000.

Roller, J.H. and J.H. Healy (1963). Seismic-refraction measurements of crustal structure between Santa Monica Bay and Lake Mead, *J. Geophys. Res.* **68**, 5837-5849.

Rundle, J.B. (1978). Gravity changes and the Palmdale uplift, *Geophys. Res. Letters* **5**, 41-44.

Rundle, J.B. and W. Thatcher (1980). Speculations on the nature of the southern California uplift, *Bull. Seis. Soc. Amer.* **70**, 1869-1886.

Sadler, P.M. (1982). An introduction to the San Bernardino Mountains as the product of young orogenesis, *in* Geologic excursions in the Transverse Ranges, *Geol. Soc. Amer. Cordilleran section guidebook*, 57-65.

Sadler, P.M. (1982). Provenance and structure of late Cenozoic sediments in the northeast San Bernardino Mountains, *in* Geologic excursions in the Transverse Ranges, *Geol. Soc. Amer. Cordilleran section guidebook*, 83-91.

Savage, J.C., W.H. Prescott, M. Lisowski, and N.E. King (1981). Rapid aseismic strain change observed on the San Andreas Fault near Palmdale, California, *Science* **211**, 56-58.

Sharp, R.V. (ed.) (1972). The Borrego Mountain earthquake of April 9, 1968, *U.S. Geol. Survey Prof. Paper 787*, 207p.

Shedlock, K.M. and S.W. Roecker (1983). A method of determining *in situ* velocity and relative hypocenter relocations using refracted waves, *Earthquake Notes* **54(1)**, 28.

Shepard, F.P., and K.O. Emery (1941). Submarine topography off the California coast: Canyons and tectonic interpretations, *Geol. Soc. Amer. Spec. Paper 31*, 171p.

Shor, G.G. Jr., and R.W. Raitt (1958a). Seismic studies in the southern California Borderland, *Proceedings XX International Geologic Congress*, Mexico, 1956, Section IX, 243-259.

Shor, G.G. Jr., and R.W. Raitt (1958b). Seismic studies in the southern California Continental Borderland, *Marine Physical Lab., Scripps Instit. of Oceanography, Report 58-78*, 17p.

Shor, G.G., R.W. Raitt, and D.D. McGowan (1976). Seismic refraction studies in the southern California Borderland, *Marine Physical Lab., Scripps Instit. of Oceanography, Report 76-13*, 70p.

Sibson, R.H. (1982). Fault zone models, heat flow, and the depth distribution of earthquakes in the continental crust of the United States, *Bull. Seis. Soc. Amer.* **72**, 151-163.

Slemmons, D.B. and D.H. Chung (1982). Maximum credible earthquake magnitudes for the Calaveras and Hayward fault zones, California, *Calif. Div. Mines and Geology Spec. Pub. 62*, 115-124.

Smith, W.S.T. (1900). A topographic study of the islands of southern California, *Calif. Univ. Pubs. in Geol.* **2(7)**, 179-230.

Stierman, D.J. and W. Ellsworth (1976). Aftershocks of the February 21, 1973, Pt. Mugu, California earthquake, *Bull. Seis. Soc. Amer.* **66**, 1931-1952.

Stewart, R. and J. Peselnick (1978). Systematic behavior of compressional velocities in Franciscan rocks at high pressure and temperature, *J. Geophys. Res.* **83**, 831-839.

Sylvester, A.G., S.W. Smith, and C.H. Scholz (1970). Earthquake swarm in the Santa Barbara Channel, California, 1968, *Bull. Seis. Soc. Amer.* **60**, 1047-1060.

Taylor, J.C. (1976). Geologic appraisal of the petroleum potential of offshore southern California: The borderland compared to onshore coastal basins, *U.S. Geol. Survey Circular 730*, 43p.

Thatcher, W. (1976). Episodic strain accumulation in southern California, *Science* **194**, 691-695.

Toppozada, T.R., C.R. Real, and D.L. Parke (1981). Preparation of isoseismal maps and summaries of reported effects for pre-1900 California earthquakes, *Calif. Div. Mines and Geology Open-File Report 81-11 SAC*, 179p.

Townley and Allen (1939). Descriptive catalog of earthquakes of the Pacific coast of the United States, 1769-1928, *Bull. Seis. Soc. Amer.* **29**, 1-297.

Vedder, J.G. (1976). Precursors and evolution of the name California Continental Borderland, *Amer. Assoc. Petro. Geol. Pacific Section, Misc. Pub 24*, 6-11.

Vedder, J.G., L.A. Beyer, A. Junger, G.W. Moore, A.E. Roberts, J.C. Taylor, and H.C. Wagner (1974). Preliminary report on the geology of the Continental Borderland of southern California, *U.S. Geol. Survey Map MF-624*, 9 sheets, 34p.

Vedder, J.G. and D.G. Howell (1976). Review of the distribution and tectonic implication of Miocene debris from the Catalina schist, California Continental Borderland and adjacent coastal areas, *Amer. Assoc. Petro. Geol. Pacific Section, Misc. Pub 24*, 326-342.

Vedder, J.G. and R.M. Norris (1963). Geology of San Nicolas Island, California, *U.S. Geol. Survey Prof. Paper 369*, 65p.

Vedder, J.G., J.C. Taylor, R.E. Arnal, and D. Bukry (1976). Maps showing the locations of selected pre-Quaternary rock samples from the California Continental Borderland, *U.S. Geol. Survey Map MF-737*, 3 sheets.

Vedder, J.G. and M.I. Toth (1976). Proposed new geographic names for features in the California Continental Borderland, *Amer. Assoc. Petro. Geol. Pacific Section, Misc. Pub 24*, 12-14.

Vedder, J.G. and others (1976). Miocene rocks and their relation to older strata and basement, Santa Catalina Island, California, *in* Armantrout, J. and others (eds.). *Cenozoic Paleogeography of the Western United States*, Pacific Section Soc. Econ. Paleo. and Min., Pacific Coast Paleogeography Symposium **3**, 239-256.

Vedder, J.G., H.C. Wagner and J.E. Schoellhamer (1969). Geological framework of the Santa Barbara Channel region, *U.S. Geol. Survey Prof. Paper 679*, 1-12.

Wallace, T.C., D.V. Helmberger, and J.E. Ebel (1981). A broad-band study of the August 13, 1978 Santa Barbara earthquake, *Bull. Seis. Soc. Amer.* **71**, 1701-1718.

Weaver, D.W., D.P. Doerner and B. Nolf (1969). Geology of the Northern Channel Islands, *Special Pub: Am. Assoc. Petrol. Geol. and Soc. Econ. Paleo. Min., Pacific sections*, 200p.

Whitcomb, J.H. (1973). The 1971 San Fernando earthquake series, focal mechanisms and tectonics, *Ph.D. thesis*, Calif. Inst. Tech., Pasadena, 443p.

Whitcomb, J.H. and L.K. Hutton (1978). On the magnitude of the August 13, 1978, Santa Barbara, California earthquake, *Trans. Amer. Geophys. Union* **59**, 1130.

Whitcomb, J.H., C.R. Allen, and 9 others (1979). Caltech-U.S. Geol. Survey monthly preliminary epicenters from March 1978 to January 1979, *Seismological Laboratory Report*, Calif. Inst. Tech., Pasadena.

Wiggins, R.A. (1972). The general inverse problem: implication of surface waves and free oscillations for earth structure, *Rev. of Geophys. and Space Phys.* **10**, 251-285.

Wilcox, R.E., T.P. Harding, and D.R. Seeley (1973). Basic wrench tectonics, *Amer. Assoc. Petro. Geol. Bull.* **57**, 74-96.

Wood, H.O. (1947). Earthquakes in southern California with geologic relations, *Bull. Seis. Soc. Amer.* **37**, 107-217.

Wyss, M. (1979). Estimating maximum expectable magnitude of earthquakes from fault dimensions, *Geology* **7**, 336-340.

Yeats, R.S. (1968a). Rifting and rafting in the southern California borderland, *Stanford Univ. Pubs., Geol. Sci.* **11**, 307-322.

Yeats, R.S. (1968b). Southern California structure, sea-floor spreading and the history of the Pacific basin, *Geol. Soc. Amer. Bull.* **79**, 1693-1702.

Yeats, R.S. (1973). Newport-Inglewood fault zone, Los Angeles basin, California, *Amer. Assoc. Petro. Geol. Bull.* **57**, 117-135.

Yeats, R.S. (1976). Extension versus strike-slip origin of the southern California borderland, *Amer. Assoc. Petro. Geol. Pacific Section, Misc. Pub 24*, 455-485.

Yeats, R.S. (1978). Neogene acceleration of subsidence rates in southern California, *Geology* **6**, 456-460.

Yeats, R.S. (1981). Quaternary flake tectonics of the California Transverse Ranges, *Geology* **9**, 16-20.

Yeats, R.S. (1983). Large-scale Quaternary detachments in Ventura Basin, southern California, *J. Geophys. Res.* **88**, 569-583.

Yeats, R.S., M.R. Cole, W.R. Merschat, and R.M. Parsley (1974). Poway fan and submarine cone and rifting of the inner southern California Borderland, *Geol. Soc. Amer. Bull.* **85**, 293-302.

Yelin, T.S. and R.S. Crosson (1982). A note on the south Puget Sound basin magnitude 4.6 earthquake of 11 March 1978 and its aftershocks, *Bull. Seis. Soc. Amer.* **72**, 1033-1038.

Yerkes, R.F. and W.H.K. Lee (1979). Late Quaternary deformation in the western Transverse Ranges, California, *U.S. Geol. Survey Circular 799*, 27-37.

Yerkes, R.F., H.G. Greene, J.C. Tinsley and K.R. Lajoie (1980). Seismotectonic setting of the Santa Barbara Channel area, southern California, *U.S. Geol. Survey Open File Report 80-299.*

Yerkes, R.F., T.H. McCulloh, J.E. Schoellhamer, and J.G. Vedder (1965). Geology of the Los Angeles Basin, California--An Introduction, *U.S. Geol. Survey Prof. Paper 420-A*, 57p.

Ziony, J.I., C.M. Wentworth, J.M. Buchanan-Banks, and H.C. Wagner (1974). Preliminary map showing recency of faulting in coastal southern California, *U.S. Geol. Survey Map MF-585*, 3 sheets, scale 1:250,000, 15p.

APPENDIX

Felt Report of the Santa Barbara Island Earthquake of September 4, 1981

The following is from the log book of Ranger Ken Giles who was based on Santa Barbara Island on the day of the earthquake.

> About 8:50 A.M. Labor Day weekend got off to a roaring start--earthquake!!! There was a roar and then a shaking, then another roar and the shaking became severe. Things starting to fall over. I headed for the door. Then, just as suddenly as it had begun it was over. No more than 5 seconds duration. It was as though a giant cockeyed ball bearing had rolled beneath the island and then out to sea. A foot inspection of the northern half of the island yielded no evidence of structural changes and only occasional single boulder rockfalls have been spotted--one small boulder dislodged from the Arch Point scattering most of the birds on the rocks. They spent the day sitting in the Kelp beds.

The following is from the official Case Incident Report filed by Ranger Ken Giles on Sept. 6:

> On Friday morning Sept. 4 1981 Ranger Giles was in the kitchen of the Santa Barbara Island Quonset Hut awaiting the Morning Report. At 0850 a loud roaring sound could be heard that seemed to be coming from a long way off. Coincident with the sound, a gentle shaking was felt that set dishes and glasses rattling in the cabinets. The initial gentle vibration was followed by a much stronger shock that shook the island causing things to fall from the walls and doors to open. Ranger Giles abandoned the Quonset Hut and ran to a position where Arch Point could be observed. At that time the tremors ceased. The duration of the event was no more than 8-10 seconds. Ranger Giles immediately called HQ and learned that the earthquake was also felt there. Then he made a visual inspection of the water lines, gas lines, and general integrity of the living quarters. No damage was found. No tsunami was observed. The mild and strong tremors may have corresponded to earthquake "s" and "p" waves. Birds roosting on Arch Point abandoned the island and sat in the sea the rest of the day 50-300 yards to the east.
>
> A check of the island by foot revealed no significant structural damage. Isolated boulders at Arch Point and Landing Cove were dislodged but they were of very small size. Interviews of boaters who had sailed around the island later in the day indicated no new rock slides or other apparent damage.

TABLE I. Phase I Locations. Santa Barbara Island Earthquakes 1981-1982.

YEAR MO DA HR MN SEC LATITUDE LONGITUDE DEPTH MAG GAP NSTA Q RMS ERH ERZ

YEAR	MO	DA	HR	MN	SEC	LATITUDE	LONGITUDE	DEPTH	MAG	GAP	NSTA	Q	RMS	ERH	ERZ
1981	2	23	0	7	34.46	34 3.12	118 50.04	6.94		134	7	E	0.02	99.0	99.0
1981	2	24	20	49	34.75	33 56.83	118 38.98	5.00	2.4	115	47	C	0.19	1.2	99.0
1981	2	25	0	25	4.40	34 11.00	118 59.18	3.89		111	9	C	0.29	2.9	3.6
1981	2	26	19	33	10.30	33 47.66	118 37.05	5.00		156	20	C	0.13	1.6	99.0
1981	2	26	22	31	56.27	33 58.22	119 13.68	5.05	1.9	145	20	C	0.20	2.8	99.0
1981	2	27	15	11	12.78	34 10.66	118 34.87	6.13	3.5	51	80	C	0.30	3.0	99.0
1981	3	7	6	35	16.35	34 2.24	118 55.93	8.99		160	10	B	0.09	1.4	3.0
1981	3	10	14	57	31.48	34 10.44	118 59.68	5.69	1.6	77	36	D	0.50	8.0	99.0
1981	3	11	16	47	47.59	33 56.97	119 7.74	5.00	1.4	300	8	E	0.10	99.0	99.0
1981	3	11	20	10	48.40	34 10.63	118 59.26	4.74		109	15	C	0.28	2.9	2.9
1981	3	25	13	53	33.75	34 0.94	119 0.26	5.21	0.0	239	8	D	0.13	11.8	7.9
1981	3	26	5	19	34.33	33 58.75	118 42.82	5.75	0.9	213	12	D	0.05	27.5	99.0
1981	3	26	14	52	53.11	34 4.53	118 57.29	6.95		173	6	E	0.00	99.0	99.0
1981	3	28	0	57	12.93	33 57.61	118 42.25	14.88	2.2	142	39	B	0.10	1.1	0.8
1981	3	31	11	36	31.02	34 1.99	118 59.80	15.89	2.4	166	21	B	0.16	1.3	1.0
1981	4	3	0	31	1.38	34 7.86	118 59.29	8.95		109	11	B	0.11	1.3	2.3
1981	4	4	22	5	21.90	34 15.16	118 49.49	5.00	2.0	74	17	C	0.31	1.8	99.0
1981	4	4	22	5	23.50	34 14.87	118 49.30	5.00	2.0	60	16	C	0.37	2.5	99.0
1981	4	13	4	33	29.85	34 7.48	119 18.35	5.00	2.0	97	22	C	0.28	2.0	99.0
1981	4	20	20	44	28.82	34 22.71	119 21.21	5.00		290	4	E	0.00	99.0	99.0
1981	4	21	12	44	32.53	33 57.31	118 31.51	4.98		234	11	E	0.04	99.0	99.0
1981	4	22	23	41	4.41	34 10.42	118 59.28	4.55		89	14	C	0.33	2.8	2.4
1981	4	23	2	44	19.33	34 14.68	119 29.58	5.01		119	11	E	0.03	99.0	99.0
1981	4	24	19	53	14.43	34 6.96	119 32.01	5.00	2.5	125	31	C	0.22	1.5	99.0
1981	4	24	19	56	13.62	34 8.82	119 31.18	5.00		123	17	C	0.18	3.1	99.0
1981	4	28	1	41	42.89	34 6.56	118 56.66	4.98		175	7	E	0.00	99.0	99.0
1981	4	28	19	32	20.73	34 16.18	118 32.26	5.00		182	8	E	0.00	99.0	99.0
1981	4	29	11	29	53.99	33 53.89	118 39.50	5.00		158	9	E	0.09	99.0	99.0
1981	4	29	18	3	21.32	33 59.56	118 42.36	4.93		257	6	E	0.03	99.0	99.0
1981	4	29	18	54	10.64	34 14.99	119 27.14	5.02	2.1	98	20	C	0.25	2.3	99.0
1981	4	29	19	15	41.12	34 14.83	119 27.78	5.01		111	13	C	0.20	2.6	99.0
1981	5	1	19	14	43.66	33 47.23	118 50.32	5.60		304	8	E	0.06	99.0	99.0
1981	5	4	23	10	1.09	34 12.94	119 8.59	5.67		154	11	C	0.14	2.7	99.0
1981	5	7	0	8	57.73	34 10.46	118 59.71	3.12		104	17	C	0.34	2.6	3.0
1981	5	7	10	6	7.62	33 55.01	118 39.18	5.00		142	15	C	0.13	1.4	99.0
1981	5	11	17	24	2.60	33 59.69	118 42.82	4.81		244	12	D	0.11	7.1	1.9
1981	5	20	8	12	2.42	34 21.98	119 29.15	5.00		231	10	C	0.04	1.5	99.0
1981	5	22	3	45	12.49	33 5.46	118 33.48	5.00	1.9	207	19	E	0.00	99.0	99.0
1981	5	28	18	36	18.94	34 12.67	118 38.34	5.43	1.6	95	21	C	0.21	1.2	99.0
1981	5	30	0	25	54.19	34 15.61	119 36.27	5.00		154	13	C	0.11	2.4	99.0
1981	5	30	22	59	18.66	34 8.21	119 4.00	4.71		252	8	E	0.17	99.0	99.0
1981	6	1	5	55	33.83	33 59.11	118 52.86	4.44		288	16	E	0.12	99.0	99.0
1981	6	3	6	6	16.52	33 59.72	118 37.71	4.99	2.0	192	19	D	0.15	10.5	99.0
1981	6	3	23	20	31.35	34 7.02	118 38.81	5.05	1.9	136	12	E	0.42	99.0	99.0
1981	6	4	10	59	4.97	34 5.77	118 58.08	4.97		197	8	E	0.02	99.0	99.0
1981	6	5	6	5	51.98	34 1.45	118 45.83	5.04		185	8	E	0.05	99.0	99.0
1981	6	6	22	24	59.08	33 56.26	119 2.59	5.00		300	11	E	0.36	99.0	99.0
1981	6	7	16	23	18.99	33 56.33	118 46.55	5.00	1.6	299	6	E	0.19	99.0	5.3
1981	6	9	14	31	52.07	33 59.02	118 40.63	9.92		129	14	A	0.05	1.0	1.6
1981	6	9	17	1	29.10	34 0.85	118 46.53	4.85		174	9	C	0.12	4.0	2.4
1981	6	13	23	29	18.89	33 58.38	118 41.46	5.15		258	10	E	0.00	99.0	99.0
1981	6	15	21	18	20.27	34 0.77	118 42.90	5.35		233	6	E	0.00	99.0	99.0
1981	6	17	0	18	14.53	34 7.26	119 0.76	2.46		161	7	E	0.67	99.0	27.0
1981	6	17	11	9	45.71	34 7.33	119 2.37	5.30		151	4	E	0.00	99.0	99.0
1981	6	17	11	20	6.07	34 7.63	119 2.04	4.93		142	3	E	0.00	99.0	99.0
1981	6	18	5	31	12.90	33 56.10	118 39.03	5.00	2.6	139	19	C	0.12	1.1	99.0
1981	6	18	8	0	25.56	33 56.53	118 40.99	5.62	2.2	273	12	D	0.05	5.4	99.0
1981	6	20	22	44	58.72	34 6.61	118 59.87	12.31		178	10	A	0.04	0.9	1.2
1981	6	20	22	52	1.95	34 10.47	118 59.11	3.70		105	8	C	0.32	3.8	3.8
1981	6	23	4	17	52.92	34 0.93	118 44.79	5.37		211	5	E	0.00	99.0	99.0
1981	6	24	20	48	6.11	33 29.30	119 5.98	5.00	2.7	137	36	C	0.14	2.3	99.0
1981	6	24	23	55	8.68	34 10.58	118 59.55	4.84		113	15	C	0.32	3.2	5.2
1981	6	26	0	37	16.51	34 10.71	118 59.99	3.80		120	9	C	0.30	3.3	4.6
1981	6	30	0	26	51.11	34 10.72	118 59.63	5.33		115	10	D	0.27	10.2	11.5
1981	6	30	6	57	6.25	34 2.64	118 59.34	2.76		213	8	E	0.01	99.0	99.0
1981	7	2	17	16	17.57	34 11.41	118 58.88	4.09		112	9	A	0.03	0.4	0.5
1981	7	3	23	56	48.10	33 57.94	118 41.51	5.34		281	10	E	0.00	99.0	99.0
1981	7	3	23	57	42.86	33 56.76	118 40.95	5.18		271	10	E	0.04	99.0	99.0
1981	7	4	7	4	12.01	33 55.03	118 39.53	5.01	2.7	193	72	C	0.18	2.3	99.0
1981	7	5	9	48	36.45	33 57.37	118 41.48	4.98		287	9	E	0.06	99.0	99.0
1981	7	8	0	6	33.84	34 11.31	118 58.85	1.17		117	5	D	0.31	6.7	7.8
1981	7	8	3	6	42.75	33 58.39	118 38.68	3.93		312	3	E	0.00	99.0	99.0
1981	7	9	7	46	8.41	34 14.02	119 23.71	5.00		116	18	E	0.08	99.0	99.0
1981	7	9	7	51	30.22	34 13.62	119 23.80	5.03		172	17	E	0.10	99.0	99.0
1981	7	9	8	34	16.97	34 17.34	119 24.35	5.00		187	17	C	0.04	1.1	99.0
1981	7	9	8	42	19.90	34 16.61	119 24.27	5.00		256	13	E	0.02	99.0	99.0
1981	7	9	21	36	52.31	34 20.57	119 25.35	5.00		285	10	E	0.03	99.0	99.0
1981	7	9	23	44	24.06	34 13.69	119 22.83	5.02		210	11	E	0.04	99.0	99.0
1981	7	9	23	51	34.53	34 14.05	119 23.89	5.00		206	11	C	0.01	0.8	99.0
1981	7	9	23	59	40.30	34 18.40	119 24.72	5.00		247	11	E	0.03	99.0	99.0
1981	7	10	0	0	55.43	34 17.05	119 24.47	5.00		190	19	C	0.08	2.5	99.0
1981	7	10	22	10	23.80	34 11.33	118 58.73	2.68		171	7	E	0.04	99.0	99.0
1981	7	12	13	33	47.61	33 59.36	118 42.66	4.93		258	10	E	0.04	99.0	99.0
1981	7	15	0	16	39.69	34 11.37	118 59.34	1.87		115	5	D	0.23	13.0	13.5
1981	7	15	23	2	3.25	34 10.85	118 59.50	4.91		113	8	C	0.28	2.9	4.2
1981	7	20	15	49	24.06	34 16.55	119 26.63	5.00		198	10	E	0.07	99.0	99.0
1981	7	20	16	16	38.30	34 16.69	119 27.43	5.00		183	15	D	0.18	20.9	99.0
1981	7	21	13	42	28.29	34 2.88	118 56.73	18.43		154	29	B	0.17	1.9	1.0
1981	7	22	22	46	35.49	34 15.32	119 31.63	5.00		108	22	C	0.22	2.0	99.0
1981	7	23	23	35	2.22	34 6.93	119 6.24	3.90		248	9	D	0.08	5.5	1.2
1981	7	24	19	1	59.91	34 11.36	118 59.04	4.69		106	8	A	0.04	0.4	0.5
1981	7	29	23	37	49.51	33 50.23	118 43.05	5.01	3.5	80	47	C	0.29	2.8	99.0
1981	7	29	23	39	57.28	33 48.48	118 41.63	5.00	3.9	82	65	C	0.19	1.0	99.0
1981	7	29	23	41	13.21	33 55.13	118 44.57	5.00	2.9	266	10	E	0.41	99.0	99.0
1981	7	29	23	57	3.70	33 50.12	118 39.71	5.00	1.8	172	8	E	0.29	99.0	99.0
1981	7	30	0	14	58.72	33 53.12	118 45.59	5.00	1.8	285	8	E	0.30	99.0	99.0
1981	7	30	0	29	47.89	33 50.00	118 39.97	5.00	1.7	327	4	E	0.81	99.0	0.0
1981	7	30	0	55	36.60	33 51.39	118 42.52	5.01	2.7	135	43	C	0.27	3.6	99.0
1981	7	30	1	10	27.22	33 52.20	118 43.59	5.01	1.6	158	19	C	0.14	4.2	99.0
1981	7	30	1	56	55.31	33 48.71	118 41.83	5.03	3.7	97	85	C	0.16	1.1	99.0
1981	7	30	7	32	25.31	33 49.81	118 46.82	5.00	1.9	200	15	E	0.30	99.0	99.0
1981	7	30	8	51	8.34	33 52.82	118 43.46	0.00	2.4	257	29	D	0.19	5.2	2.9
1981	7	30	11	56	0.99	33 48.58	118 42.20	5.00	3.6	85	69	C	0.24	1.3	99.0
1981	8	1	6	42	15.04	33 48.88	118 42.57	4.99	3.2	165	25	C	0.24	3.2	99.0
1981	8	1	6	55	42.06	33 53.32	118 43.40	2.43	2.4	210	11	B	0.10	2.1	1.1
1981	8	1	15	3	18.36	33 48.14	118 41.79	5.01	2.8	136	42	C	0.17	1.6	99.0
1981	8	2	3	40	16.51	33 54.71	118 39.43	5.00		318	6	E	0.06	99.0	99.0
1981	8	2	9	23	45.27	33 51.29	118 42.45	5.02	2.4	161	26	C	0.22	4.0	99.0
1981	8	2	9	37	43.24	33 54.95	118 43.96	4.81	2.0	205	19	C	0.15	3.0	2.4
1981	8	2	18	43	48.16	33 51.31	118 43.03	5.00	1.8	181	8	E	0.22	99.0	99.0
1981	8	3	20	10	2.07	34 6.10	119 4.86	6.12		225	9	D	0.39	12.1	5.6
1981	8	4	13	58	54.39	34 4.29	118 40.27	4.41	1.9	175	8	B	0.12	1.8	1.2
1981	8	6	6	59	16.92	33 52.96	119 17.83	5.00	2.0	97	15	C	0.14	1.8	99.0
1981	8	7	1	43	40.21	33 57.86	118 42.64	5.41		279	8	E	0.00	99.0	99.0
1981	8	8	0	38	24.97	34 2.04	118 41.25	5.00		271	6	E	0.19	99.0	0.0
1981	8	12	22	58	34.86	34 8.23	118 36.98	4.26	2.7	119	80	B	0.21	1.2	1.3
1981	8	14	1	9	33.89	33 58.33	118 34.51	5.00	3.4	106	75	C	0.26	1.2	99.0
1981	8	15	12	31	12.04	33 59.46	119 11.10	5.02	2.2	119	14	C	0.17	2.8	99.0
1981	8	16	0	11	23.50	34 2.70	119 0.04	15.09		161	11	B	0.09	1.4	2.0
1981	8	18	9	23	54.69	33 48.43	118 42.21	5.00	3.5	59	71	C	0.23	1.5	99.0
1981	8	18	13	16	7.00	33 48.99	118 47.58	5.00		205	7	E	0.00	99.0	99.0
1981	8	20	19	16	15.58	33 47.62	119 32.51	5.00		162	10	E	0.15	99.0	99.0
1981	8	22	14	21	29.09	34 18.41	119 28.28	4.98	2.4	178	28	C	0.08	1.1	99.0
1981	8	22	14	27	24.07	34 19.17	119 28.54	4.99	1.8	196	14	C	0.05	2.5	99.0
1981	8	22	14	47	53.46	34 16.19	119 28.80	5.00	2.6	187	32	C	0.22	2.5	99.0
1981	8	22	15	8	40.57	34 0.64	118 42.73	4.92		236	6	E	0.03	99.0	99.0
1981	8	22	21	39	48.96	34 16.13	119 29.09	4.99	2.4	187	28	C	0.23	2.6	99.0
1981	8	23	6	58	15.36	33 26.91	119 2.62	5.03	2.5	278	21	E	0.02	99.0	99.0
1981	8	23	22	23	58.60	34 4.31	118 50.32	4.56		153	8	E	0.00	99.0	99.0
1981	8	26	23	52	16.93	33 47.71	118 40.53	5.00		181	9	C	0.04	3.2	99.0
1981	8	29	1	57	34.66	33 57.73	118 30.37	5.00		194	18	D	0.28	5.4	99.0
1981	9	4	6	26	20.53	33 24.70	118 52.40	3.75		283	9	E	0.51	99.0	99.0
1981	9	4	15	5	43.78	34 5.55	118 40.09	5.00		217	6	E	0.00	99.0	99.0
1981	9	4	15	50	50.68	33 40.91	119 3.22	4.98	5.3	108	129	C	0.17	1.3	99.0
1981	9	4	15	57	43.14	33 39.18	119 1.02	5.00	3.6	134	56	C	0.11	0.8	99.0
1981	9	4	16	4	42.19	33 41.09	119 4.18	5.00	1.8	161	12	E	0.12	99.0	99.0
1981	9	4	16	7	2.80	33 39.98	119 2.43	5.00	2.2	200	14	E	0.02	99.0	99.0
1981	9	4	16	8	0.37	33 41.46	119 3.29	5.00		206	6	E	0.00	99.0	99.0
1981	9	4	16	9	59.24	33 39.12	119 0.79	5.00	2.5	174	33	C	0.03	0.6	99.0
1981	9	4	16	13	14.81	33 39.00	119 0.64	5.00	2.0	81	22	C	0.03	1.0	99.0
1981	9	4	16	16	45.42	33 40.30	119 2.41	5.00		200	9	E	0.00	99.0	99.0
1981	9	4	16	17	8.61	33 41.92	119 2.90	5.00		203	6	E	0.00	99.0	99.0
1981	9	4	16	17	52.98	33 40.21	119 2.75	5.00	2.3	135	24	C	0.11	1.3	99.0
1981	9	4	16	18	36.10	33 39.02	119 0.87	5.01		190	9	E	0.00	99.0	99.0
1981	9	4	16	19	51.15	33 44.47	119 8.27	5.00	1.8	116	14	E	0.09	99.0	99.0
1981	9	4	16	20	29.57	33 43.91	119 4.72	5.00		213	7	E	0.00	99.0	99.0
1981	9	4	16	25	45.99	33 40.00	119 2.11	5.00	1.8	134	16	C	0.10	1.4	99.0
1981	9	4	16	27	21.80	33 39.20	119 0.72	5.00	1.9	148	14	C	0.09	2.4	99.0
1981	9	4	16	32	43.81	33 38.30	118 59.30	5.00		179	11	E	0.01	99.0	99.0
1981	9	4	16	42	23.98	33 43.05	119 3.29	4.99	1.9	206	12	E	0.04	99.0	99.0
1981	9	4	16	46	17.68	33 40.00	119 2.39	5.00	2.1	154	29	C	0.09	1.2	99.0
1981	9	4	16	51	33.41	33 41.45	119 2.31	4.99	2.2	200	18	C	0.06	4.4	99.0
1981	9	4	16	58	4.10	33 42.21	119 5.49	5.00		167	11	E	0.07	99.0	99.0
1981	9	4	17	4	39.86	33 38.06	118 59.11	5.00	3.3	126	74	C	0.08	0.5	99.0
1981	9	4	17	17	4.64	33 39.97	119 2.28	5.00	1.8	134	12	C	0.10	2.8	99.0
1981	9	4	17	22	8.78	33 38.66	118 59.68	5.00	3.0	127	68	C	0.05	0.4	99.0
1981	9	4	17	46	40.09	33 39.53	119 0.22	5.00	1.9	147	14	C	0.04	1.8	99.0
1981	9	4	18	14	56.63	33 58.04	118 41.86	4.47		279	10	E	0.10	99.0	99.0
1981	9	4	18	29	49.72	33 39.92	119 1.26	5.00	1.8	132	13	C	0.09	3.1	99.0
1981	9	4	18	31	57.80	33 40.58	119 0.88	4.99	1.8	192	13	E	0.01	99.0	99.0
1981	9	4	18	59	30.15	33 39.87	119 3.02	5.00	1.9	94	14	C	0.14	2.5	99.0
1981	9	4	19	11	50.61	33 40.29	119 3.12	5.00	1.8	156	12	E	0.02	99.0	99.0
1981	9	4	19	35	39.43	33 42.82	119 5.36	5.01	1.9	143	22	E	0.16	99.0	99.0
1981	9	4	19	36	47.97	33 42.53	119 4.63	5.00	2.4	108	38	C	0.10	1.8	99.0
1981	9	4	19	43	38.28	33 39.97	119 2.41	5.00	2.5	122	31	C	0.07	0.7	99.0
1981	9	4	19	48	23.81	33 41.29	119 1.89	4.99	2.4	185	24	C	0.13	1.9	99.0
1981	9	4	19	52	18.37	33 58.81	118 41.53	5.53	2.0	210	17	C	0.08	1.4	99.0
1981	9	4	20	10	31.61	33 40.09	119 1.37	5.00	2.8	135	32	C	0.09	0.7	99.0
1981	9	4	20	14	47.04	33 37.46	119 0.72	5.00		187	6	E	0.00	99.0	99.0
1981	9	4	20	16	0.96	33 38.50	118 59.43	5.00	2.2	124	25	C	0.10	1.4	99.0
1981	9	4	20	22	11.76	33 39.09	119 2.22	5.00	2.3	122	31	C	0.08	1.0	99.0
1981	9	4	20	25	54.53	33 44.84	118 56.13	5.00	1.5	316	11	E	0.11	99.0	99.0
1981	9	4	20	26	29.53	33 40.30	119 1.93	5.00	1.9	153	16	C	0.07	2.7	99.0
1981	9	4	20	51	11.64	33 40.32	119 3.18	5.00	1.8	157	14	E	0.00	99.0	99.0
1981	9	4	20	51	43.37	33 41.48	119 4.88	5.00	2.9	108	56	C	0.10	0.8	99.0
1981	9	4	21	0	6.00	33 41.41	119 4.79	5.00	2.8	108	40	C	0.11	0.8	99.0
1981	9	4	21	33	28.15	33 38.29	118 59.32	5.00	2.0	84	15	C	0.13	1.1	99.0
1981	9	4	21	35	29.60	33 40.07	119 3.10	5.00	1.3	204	7	E	0.00	99.0	99.0
1981	9	4	22	2	13.61	33 40.24	119 1.38	5.00	1.5	175	8	E	0.28	99.0	99.0
1981	9	4	22	30	40.24	33 40.61	119 9.46	5.06	2.0	238	11	E	0.07	99.0	99.0
1981	9	4	22	30	51.43	34 0.73	118 45.79	4.91	2.0	207	6	A	0.00	0.0	0.0
1981	9	4	23	23	47.95	33 42.91	119 2.67	5.02	1.7	203	11	D	0.14	5.6	99.0
1981	9	5	0	0	47.46	33 39.49	119 0.64	5.00	2.6	133	42	C	0.06	0.7	99.0
1981	9	5	0	1	35.86	33 38.13	119 0.71	5.00		188	10	E	0.02	99.0	99.0
1981	9	5	0	39	11.66	33 40.31	119 0.05	5.00	1.9	183	12	D	0.05	8.9	99.0
1981	9	5	0	41	49.32	33 42.69	119 6.51	4.99	3.8	111	96	C	0.13	1.0	99.0
1981	9	5	0	54	59.71	33 42.71	119 4.74	5.00	1.6	213	14	E	0.01	99.0	99.0
1981	9	5	1	33	53.40	33 42.58	119 3.75	5.00	1.7	127	19	C	0.10	4.3	99.0
1981	9	5	1	48	26.68	33 42.25	119 6.38	5.00	2.0	137	12	E	0.08	99.0	99.0
1981	9	5	1	49	10.43	33 38.51	118 59.89	5.00	2.4	128	39	C	0.10	1.5	99.0
1981	9	5	2	33	51.78	33 42.24	119 5.89	5.00	2.4	110	38	C	0.03	0.4	99.0
1981	9	5	3	41	49.62	33 39.67	118 59.23	5.00	3.1	128	67	C	0.14	1.0	99.0
1981	9	5	4	2	58.13	33 42.73	119 6.24	4.98	3.6	111	94	C	0.14	1.0	99.0
1981	9	5	4	4	50.00	33 38.97	119 0.68	5.00		170	7	E	0.17	99.0	99.0
1981	9	5	4	12	13.35	33 40.54	119 2.38	5.01		155	10	E	0.10	99.0	99.0
1981	9	5	4	17	36.05	33 38.59	118 58.49	5.00	2.1	86	19	C	0.09	1.9	99.0
1981	9	5	4	18	48.08	33 39.43	119 1.76	5.00	3.1	102	71	C	0.09	0.8	99.0
1981	9	5	4	21	37.06	33 39.81	119 2.09	5.00	2.1	153	24	C	0.07	0.9	99.0
1981	9	5	4	26	26.21	33 41.33	119 4.71	4.99	2.6	108	55	C	0.12	1.0	99.0
1981	9	5	4	29	49.94	33 39.01	118 59.86	5.00		183	20	E	0.03	99.0	99.0
1981	9	5	4	59	23.99	33 42.24	119 6.10	5.00	2.2	121	23	C	0.07	1.9	99.0
1981	9	5	5	1	34.66	33 41.39	119 5.74	5.00		139	11	E	0.08	99.0	99.0
1981	9	5	5	8	41.50	33 40.18	119 2.45	5.00	1.9	156	23	C	0.10	3.1	99.0
1981	9	5	5	20	15.71	33 40.31	119 1.42	5.00	1.6	152	17	E	0.15	99.0	99.0
1981	9	5	5	33	15.37	33 40.03	119 3.33	5.00	1.9	157	24	C	0.07	1.8	99.0
1981	9	5	5	34	5.38	33 46.83	118 44.56	5.02		186	11	E	0.11	99.0	99.0
1981	9	5	6	41	40.29	33 38.92	118 59.99	5.00	2.0	130	22	C	0.10	1.3	99.0
1981	9	5	7	2	38.39	33 40.06	119 1.17	5.00	2.5	132	41	C	0.09	0.9	99.0
1981	9	5	8	33	22.73	33 39.71	119 1.80	5.00	2.1	152	21	C	0.05	1.0	99.0
1981	9	5	8	34	1.20	33 43.52	119 10.43	5.05		239	10	E	0.16	99.0	99.0
1981	9	5	8	55	50.66	33 39.94	119 2.81	5.00	2.3	138	37	C	0.07	0.7	99.0
1981	9	5	9	25	19.69	33 42.49	119 6.64	5.00	1.8	112	13	C	0.10	1.8	99.0
1981	9	5	9	42	59.04	33 38.73	119 0.55	5.00		187	12	E	0.10	99.0	99.0
1981	9	5	10	13	3.37	33 40.03	119 2.46	5.00	2.0	103	23	C	0.10	0.9	99.0
1981	9	5	11	50	34.05	33 39.51	119 0.62	5.00	2.6	133	44	C	0.08	0.8	99.0
1981	9	5	13	16	4.19	33 39.54	119 0.80	5.00	2.1	133	17	C	0.07	0.8	99.0
1981	9	5	13	36	40.89	33 39.70	119 2.21	5.00	2.2	154	40	C	0.08	0.7	99.0
1981	9	5	14	35	45.28	33 41.70	119 3.56	5.00	1.8	160	18	C	0.00	0.0	99.0
1981	9	5	16	17	11.12	33 38.97	119 0.86	5.00		81	14	C	0.05	1.7	99.0
1981	9	5	16	26	1.59	33 40.86	119 4.09	5.00	1.9	107	16	C	0.12	2.4	99.0
1981	9	5	20	18	39.78	33 44.31	119 11.61	5.00		153	13	E	0.24	99.0	99.0
1981	9	5	21	9	53.98	33 42.73	119 4.53	5.01		141	11	E	0.06	99.0	99.0
1981	9	5	21	21	6.61	33 38.46	118 59.07	5.00	2.4	126	35	C	0.10	0.9	99.0
1981	9	5	21	22	59.04	33 38.33	118 58.33	5.00		124	11	E	0.17	99.0	99.0
1981	9	5	21	36	40.09	33 38.98	118 59.15	5.01		127	15	D	0.12	5.6	99.0
1981	9	5	21	57	38.45	33 42.60	119 6.20	5.00	2.1	111	12	D	0.13	5.2	99.0
1981	9	6	1	54	4.50	33 39.03	119 0.87	5.00	2.1	148	23	C	0.09	1.7	99.0
1981	9	6	2	59	28.27	33 38.61	118 59.78	5.00	1.7	112	14	C	0.05	1.7	99.0
1981	9	6	6	18	56.50	33 38.64	118 59.29	5.00	2.0	128	22	C	0.03	1.5	99.0
1981	9	6	6	20	41.86	33 40.02	119 2.64	5.00	2.1	138	25	C	0.08	1.0	99.0
1981	9	6	9	17	0.44	33 44.35	119 8.02	4.98	3.7	116	50	C	0.18	1.0	99.0
1981	9	6	9	27	37.38	33 51.40	118 42.75	5.00	1.7	176	14	C	0.14	4.0	99.0
1981	9	6	9	30	28.51	33 39.41	119 0.58	5.00	1.9	133	23	C	0.09	1.5	99.0
1981	9	6	9	49	58.74	33 41.08	118 59.04	5.00	2.5	75	39	C	0.09	0.8	99.0
1981	9	6	11	23	44.73	33 38.44	118 59.72	5.01		145	13	E	0.12	99.0	99.0
1981	9	6	12	20	0.70	33 43.42	119 10.61	5.01	2.2	153	27	C	0.12	2.2	99.0
1981	9	6	13	41	48.78	33 39.74	119 0.93	5.00	1.9	149	14	E	0.09	99.0	99.0
1981	9	6	15	37	20.11	34 15.24	119 29.12	5.00		117	12	E	0.10	99.0	99.0
1981	9	6	18	30	31.33	33 40.79	119 2.29	5.00	3.1	104	48	C	0.08	0.6	99.0
1981	9	6	20	6	55.16	34 14.71	119 28.09	5.00	2.0	103	20	C	0.16	1.3	99.0
1981	9	6	21	58	25.26	33 40.97	119 1.69	5.00		153	12	E	0.07	99.0	99.0
1981	9	7	3	46	47.78	33 42.56	119 5.87	4.99	2.0	143	13	E	0.08	99.0	99.0
1981	9	7	5	26	0.65	34 16.23	119 27.72	5.00		208	12	E	0.06	99.0	99.0
1981	9	7	12	43	55.86	33 46.11	119 10.82	5.00	1.6	143	13	E	0.04	99.0	99.0
1981	9	7	12	44	53.51	33 45.58	119 8.81	5.00	1.8	183	12	E	0.08	99.0	99.0
1981	9	7	12	47	53.22	34 14.50	119 25.77	5.01		199	12	E	0.03	99.0	99.0
1981	9	7	15	21	31.55	33 40.01	119 1.10	5.00	2.3	132	38	C	0.12	1.3	99.0
1981	9	7	16	19	57.02	33 40.00	119 2.12	5.00	1.6	134	15	C	0.12	4.5	99.0
1981	9	7	18	58	49.51	33 38.88	119 0.42	5.00	1.9	147	19	C	0.08	1.2	99.0
1981	9	7	19	10	26.90	33 43.39	119 6.36	5.00	1.8	119	17	C	0.11	3.1	99.0
1981	9	7	19	42	40.65	33 39.72	119 2.10	5.00	2.2	102	26	C	0.09	0.9	99.0
1981	9	7	21	42	12.51	34 11.46	118 53.61	13.24		126	8	E	0.13	99.0	99.0
1981	9	8	1	22	7.33	33 41.69	118 57.89	5.00	1.8	145	7	E	0.06	99.0	99.0
1981	9	8	4	25	4.62	33 41.19	118 58.96	5.00	1.8	147	20	C	0.09	1.5	99.0
1981	9	8	5	27	25.91	33 39.16	119 0.16	5.00	2.0	83	22	C	0.03	0.5	99.0
1981	9	8	10	31	0.29	33 45.45	119 9.69	5.00	2.0	106	23	C	0.07	0.9	99.0
1981	9	8	10	36	41.61	33 39.51	119 0.33	5.00	2.8	132	46	C	0.09	0.9	99.0
1981	9	8	11	33	30.01	33 42.68	119 3.56	4.99	2.0	162	22	C	0.13	2.1	99.0
1981	9	8	15	43	13.60	33 42.01	119 4.66	5.00	2.0	88	18	E	0.16	99.0	99.0
1981	9	8	20	8	58.76	33 39.83	119 2.32	4.99	2.1	86	22	C	0.17	2.5	99.0
1981	9	9	4	30	29.99	33 45.28	118 59.99	5.00		309	13	E	0.12	99.0	99.0
1981	9	9	6	24	17.72	33 38.55	118 58.92	5.00	2.0	177	10	E	0.05	99.0	99.0
1981	9	9	6	26	19.27	33 39.38	119 1.40	5.01		175	8	E	0.02	99.0	99.0
1981	9	9	6	33	15.57	33 39.72	119 2.33	5.00	2.8	122	61	C	0.11	0.8	99.0
1981	9	9	7	17	32.33	34 14.76	119 27.81	5.00		111	13	E	0.21	99.0	99.0
1981	9	9	9	25	3.00	33 43.22	119 4.93	5.01		167	11	C	0.06	2.6	99.0
1981	9	9	19	57	18.76	33 37.91	118 59.37	5.00		161	10	E	0.08	99.0	99.0
1981	9	9	23	36	15.23	33 38.87	119 2.11	5.00		191	12	D	0.13	9.7	99.0
1981	9	10	0	50	38.95	33 44.11	118 58.26	5.00	1.9	312	15	E	0.12	99.0	99.0
1981	9	10	1	53	55.50	33 39.41	119 0.26	5.00	2.2	128	31	C	0.08	0.9	99.0
1981	9	10	1	58	5.15	33 40.01	119 2.45	5.00	2.2	135	29	C	0.09	0.8	99.0
1981	9	10	5	43	55.81	33 41.81	119 5.29	4.99	3.4	109	65	C	0.15	1.0	99.0
1981	9	10	8	14	45.40	33 41.46	119 5.12	5.00	2.2	86	32	C	0.16	1.7	99.0
1981	9	10	9	44	20.77	33 44.68	119 7.74	5.00	2.3	156	27	C	0.18	2.0	99.0
1981	9	10	13	36	38.23	33 37.99	118 58.64	5.00	2.5	122	44	C	0.09	0.7	99.0
1981	9	10	16	8	1.85	33 41.48	119 4.88	5.00	3.2	108	48	C	0.11	0.9	99.0
1981	9	11	3	10	17.21	33 41.47	119 2.69	5.00	1.7	158	10	C	0.07	4.8	99.0
1981	9	11	3	30	32.41	33 48.12	119 9.34	5.00	2.0	118	19	C	0.10	1.9	99.0
1981	9	11	5	58	24.41	33 44.48	119 8.58	4.98	3.9	116	65	C	0.16	1.0	99.0
1981	9	11	6	50	12.98	33 39.03	119 2.07	5.00		179	18	C	0.04	1.8	99.0
1981	9	11	9	58	24.26	33 44.75	119 8.33	5.00	2.4	158	24	C	0.11	1.2	99.0
1981	9	11	10	40	11.73	33 38.93	118 59.90	5.00	2.4	126	36	C	0.11	1.1	99.0
1981	9	11	11	46	5.36	33 57.72	118 38.99	4.96		216	16	B	0.06	2.4	0.5
1981	9	11	17	31	39.12	33 44.00	119 6.79	5.00	2.4	113	20	C	0.13	1.8	99.0
1981	9	11	20	53	35.57	33 41.87	119 6.02	5.00	2.3	131	28	C	0.11	1.3	99.0
1981	9	11	22	49	29.95	33 40.28	119 3.20	5.00	2.1	137	19	C	0.10	0.9	99.0
1981	9	12	5	34	1.58	33 40.28	119 3.81	5.00	2.1	137	23	C	0.10	0.8	99.0
1981	9	12	6	26	25.32	33 41.37	119 4.61	5.00	2.1	108	31	C	0.14	1.3	99.0
1981	9	12	12	23	49.40	33 41.47	119 3.93	5.00		209	9	E	0.03	99.0	99.0
1981	9	12	13	57	33.93	34 5.90	118 53.79	5.00		321	5	E	0.00	99.0	99.0
1981	9	12	15	35	19.58	33 41.62	119 5.11	5.00	1.8	144	16	C	0.12	1.5	99.0
1981	9	12	16	19	41.55	33 40.16	119 2.67	5.00	2.2	136	19	C	0.08	0.7	99.0
1981	9	12	17	32	26.05	33 40.06	119 3.09	5.00	2.4	137	23	C	0.08	0.8	99.0
1981	9	12	18	17	15.59	33 41.51	118 59.28	5.00	2.0	127	9	E	0.05	99.0	99.0
1981	9	12	20	29	48.10	33 41.80	118 59.00	5.00	1.9	127	11	E	0.08	99.0	99.0
1981	9	12	23	14	32.60	33 38.93	118 58.94	5.00	2.4	124	26	C	0.11	0.9	99.0
1981	9	13	0	6	9.42	33 39.09	118 59.63	5.00	2.7	126	48	C	0.11	0.9	99.0
1981	9	13	23	36	10.61	33 39.11	119 1.32	5.00	2.4	131	34	C	0.10	0.7	99.0
1981	9	14	17	30	50.00	34 0.70	118 57.64	12.93	2.2	82	21	B	0.16	2.0	2.2
1981	9	15	10	47	7.89	33 40.10	119 2.79	5.00		203	11	C	0.03	0.6	99.0
1981	9	15	19	5	24.11	33 39.26	118 59.71	5.01		168	18	C	0.04	0.9	99.0
1981	9	15	19	56	12.49	33 38.07	118 59.07	5.00	3.2	124	60	C	0.11	0.6	99.0
1981	9	15	20	37	46.31	33 40.67	119 2.24	5.00	2.9	135	40	C	0.08	0.6	99.0
1981	9	15	22	21	45.16	34 8.34	118 54.66	5.00		179	8	E	0.75	99.0	99.0
1981	9	16	0	34	59.27	33 36.97	119 8.98	5.00		277	9	E	0.13	99.0	99.0
1981	9	16	1	16	59.96	33 36.47	118 56.66	5.00	3.2	116	89	C	0.10	0.7	99.0
1981	9	16	1	19	11.55	33 36.47	118 56.72	5.00	3.5	117	70	C	0.10	0.6	99.0
1981	9	16	6	29	8.07	33 40.57	119 2.18	4.99	2.8	103	42	C	0.08	0.6	99.0
1981	9	16	22	45	28.84	33 40.89	118 58.53	5.01	2.3	193	27	C	0.03	1.8	99.0
1981	9	17	21	5	46.98	33 38.71	119 0.80	5.01	2.1	129	18	C	0.11	1.4	99.0
1981	9	18	11	5	9.35	33 40.22	119 3.79	5.00	0.0	139	14	C	0.07	0.9	99.0
1981	9	18	11	53	14.83	33 42.06	119 4.17	5.00		211	12	E	0.06	99.0	99.0
1981	9	18	16	34	29.13	33 41.54	119 5.22	5.00	1.9	148	14	C	0.08	1.2	99.0
1981	9	19	3	4	32.48	33 58.56	118 39.66	4.70		172	10	E	0.07	99.0	99.0
1981	9	19	8	59	17.03	33 40.56	119 2.41	5.00	1.7	123	22	D	0.14	7.3	99.0
1981	9	19	12	15	47.42	33 33.70	118 57.86	2.63	2.8	132	19	A	0.09	0.8	1.3
1981	9	19	13	43	2.81	33 33.28	118 58.72	4.95	1.8	159	13	E	0.10	99.0	99.0
1981	9	20	3	14	21.97	33 40.10	119 1.67	5.00	1.8	80	18	C	0.14	2.5	99.0
1981	9	20	11	32	6.62	33 45.46	119 9.05	5.00	1.8	91	18	E	0.12	99.0	99.0
1981	9	20	17	52	2.68	33 59.66	118 43.56	5.02		248	10	E	0.03	99.0	99.0
1981	9	21	4	49	10.92	33 40.70	119 2.22	5.00	1.7	199	12	E	0.21	99.0	99.0
1981	9	21	10	8	8.51	33 38.89	119 0.51	5.00	3.1	128	67	C	0.11	0.6	99.0
1981	9	21	22	38	23.25	33 39.76	119 0.23	5.01	1.7	167	17	D	0.10	8.5	99.0
1981	9	22	0	11	4.79	33 41.13	119 3.10	5.00	2.1	138	18	C	0.09	1.3	99.0
1981	9	22	17	53	0.20	33 38.42	119 0.88	5.00		190	10	E	0.03	99.0	99.0
1981	9	23	13	52	43.45	33 38.07	118 58.97	5.00	2.2	123	21	C	0.10	0.9	99.0
1981	9	23	19	11	1.57	33 40.01	119 2.70	5.00	2.1	182	14	C	0.10	1.7	99.0
1981	9	23	19	54	22.15	33 38.78	118 59.70	5.00	2.4	84	30	C	0.11	1.0	99.0

TABLE I. Phase I Locations. Santa Barbara Island Earthquakes 1981-1982.

YEAR	MO	DA	HR	MN	SEC	LATITUDE	LONGITUDE	DEPTH	MAG	GAP	NSTA	Q	RMS	ERH	ERZ
1981	9	24	2	36	56.01	33 58.70	118 45.57	10.38	2.0	137	20	A	0.07	1.0	1.0
1981	9	25	5	45	33.36	33 43.08	118 54.15	5.00		232	7	E	0.15	99.0	99.0
1981	9	25	16	52	17.94	34 7.01	118 49.75	5.00		360	5	E	0.10	99.0	0.0
1981	9	25	16	52	30.59	34 7.16	118 48.85	5.00		215	5	E	0.00	99.0	99.0
1981	9	25	16	53	45.52	33 57.39	118 33.83	5.01		262	10	E	0.07	99.0	99.0
1981	9	25	16	54	15.10	33 59.15	118 51.22	4.13		290	8	E	0.00	99.0	99.0
1981	9	25	17	0	4.11	33 59.76	118 51.02	3.81	1.3	286	5	E	0.00	99.0	99.0
1981	9	25	22	3	33.14	33 46.77	118 28.12	5.08		200	9	E	0.03	99.0	99.0
1981	9	26	5	58	25.24	33 40.15	119 4.02	5.00		139	10	C	0.02	0.6	99.0
1981	9	26	6	58	54.14	33 40.81	119 0.42	5.00	2.2	83	23	C	0.07	0.7	99.0
1981	9	26	7	50	10.08	33 40.84	119 0.49	5.00	2.3	83	21	C	0.09	1.0	99.0
1981	9	26	16	53	30.73	33 40.06	119 3.80	5.01		208	9	E	0.02	99.0	99.0
1981	9	27	8	19	50.81	33 39.40	119 7.19	5.00	2.4	144	31	C	0.11	1.2	99.0
1981	9	27	14	33	27.46	33 39.58	119 7.02	5.00	2.5	111	43	C	0.13	0.9	99.0
1981	9	27	20	59	33.81	33 57.48	118 33.30	5.00	1.9	102	33	C	0.20	2.3	99.0
1981	9	27	22	52	57.15	33 32.89	119 14.99	5.02		153	12	E	0.12	99.0	99.0
1981	9	28	9	46	25.24	33 46.01	119 9.44	5.00	1.9	164	13	C	0.08	2.9	99.0
1981	9	28	13	34	7.54	34 4.71	118 59.28	4.73		228	9	E	0.03	99.0	99.0
1981	9	28	22	42	6.52	34 9.73	118 46.15	6.71		164	8	E	0.10	99.0	99.0
1981	9	29	18	12	28.96	33 38.67	119 0.73	5.00	2.5	82	28	C	0.11	0.9	99.0
1981	9	29	21	33	8.10	33 39.04	118 59.78	5.01	2.1	164	21	C	0.10	1.8	99.0
1981	9	30	0	24	52.96	33 46.03	119 12.97	5.00		152	14	D	0.17	6.3	99.0
1981	9	30	1	37	10.38	33 42.65	119 4.51	5.00	1.9	143	14	C	0.34	0.7	0.7
1981	9	30	20	13	43.31	33 59.26	119 34.71	4.42	2.1	191	33	C	0.17	4.8	3.4
1981	10	1	6	37	52.73	33 35.68	119 3.83	5.00		360	2	E	0.00	99.0	99.0
1981	10	1	9	25	37.38	33 41.08	119 4.43	5.00	1.9	141	19	C	0.09	0.7	99.0
1981	10	2	8	13	42.72	33 38.66	119 1.06	5.00	1.5	172	10	E	0.11	99.0	99.0
1981	10	2	21	13	14.52	33 38.61	118 58.58	5.00	2.3	88	21	B	0.16	0.4	0.4
1981	10	2	23	52	48.57	33 58.33	118 40.32	3.98		304	5	E	0.06	99.0	99.0
1981	10	3	9	34	12.26	33 26.95	118 54.20	4.44		191	8	E	0.11	99.0	99.0
1981	10	3	15	0	43.62	33 40.08	119 3.20	5.00	1.8	136	16	C	0.09	1.4	99.0
1981	10	3	17	59	39.76	33 44.98	119 8.83	5.00		138	11	E	0.02	99.0	99.0
1981	10	3	21	15	15.17	33 40.59	119 1.30	5.00	1.9	132	21	C	0.03	0.8	99.0
1981	10	5	2	9	45.38	33 39.43	118 59.09	5.00	1.7	109	17	C	0.11	2.0	99.0
1981	10	5	20	31	2.86	33 47.97	119 14.54	5.00	2.8	99	33	C	0.21	1.3	99.0
1981	10	5	23	44	38.62	34 15.28	119 25.49	5.01		207	11	C	0.06	2.5	99.0
1981	10	5	23	47	16.03	34 9.63	118 45.89	4.97		167	8	E	0.00	99.0	99.0
1981	10	6	0	31	31.27	33 39.06	118 59.27	5.00	2.0	144	14	E	0.07	99.0	99.0
1981	10	6	4	52	11.14	33 56.83	118 39.18	4.99	1.6	124	22	C	0.13	1.2	99.0
1981	10	6	7	6	18.90	33 38.89	119 0.62	5.00		170	12	E	0.02	99.0	99.0
1981	10	6	9	14	9.66	33 38.88	119 0.79	5.00	1.6	190	13	E	0.04	99.0	99.0
1981	10	6	11	2	13.67	33 40.13	118 59.17	5.00	2.2	126	18	C	0.05	0.6	99.0
1981	10	6	20	33	52.53	33 43.82	118 30.50	5.00	2.3	83	42	C	0.18	1.5	99.0
1981	10	6	20	36	42.68	33 42.83	118 31.76	5.00	1.8	128	23	C	0.25	4.3	99.0
1981	10	6	20	38	18.96	33 42.39	118 33.52	5.00	1.6	147	15	E	0.11	99.0	99.0
1981	10	7	9	41	56.24	33 47.24	119 11.37	5.00	1.7	211	10	E	0.07	99.0	99.0
1981	10	7	13	42	30.43	34 0.62	118 42.87	4.87		238	11	E	0.01	99.0	99.0
1981	10	7	17	29	56.33	33 40.29	119 3.48	5.01	0.0	206	12	E	0.02	99.0	99.0
1981	10	7	22	34	48.89	33 30.82	119 7.16	5.00	1.8	327	15	E	0.17	99.0	99.0
1981	10	7	22	44	46.71	34 9.58	118 45.99	5.14		164	4	E	0.00	99.0	99.0
1981	10	9	4	1	59.58	33 44.85	119 9.09	4.99	2.2	139	21	C	0.09	1.0	99.0
1981	10	9	12	1	51.87	33 19.58	119 21.24	5.00	1.9	154	17	C	0.24	4.0	99.0
1981	10	9	17	27	51.88	33 40.77	118 58.11	5.00		229	9	E	0.06	99.0	99.0
1981	10	9	21	27	31.29	33 20.46	119 23.11	5.00	0.0	147	18	E	0.05	99.0	99.0
1981	10	11	3	59	28.18	33 47.53	119 17.73	5.00		162	12	E	0.23	99.0	99.0
1981	10	11	7	25	20.50	33 41.53	119 2.69	5.00		181	11	D	0.06	9.3	99.0
1981	10	11	18	10	12.79	33 39.65	119 1.02	5.00	3.7	100	99	C	0.10	0.6	99.0
1981	10	12	6	57	36.62	34 9.70	119 0.06	2.28	1.7	107	19	D	0.38	9.3	9.3
1981	10	12	7	29	33.67	33 39.23	118 59.38	5.00	2.0	128	10	E	0.15	99.0	99.0
1981	10	12	12	13	17.21	33 40.04	119 1.57	5.00	2.4	132	44	C	0.12	1.8	99.0
1981	10	12	23	33	40.43	34 9.81	118 46.00	4.95		163	4	E	0.00	99.0	99.0
1981	10	12	23	34	54.35	34 9.82	118 45.94	5.03		164	4	E	0.02	99.0	99.0
1981	10	13	1	55	5.52	33 40.79	118 59.98	5.00		129	8	E	0.04	99.0	99.0
1981	10	13	1	55	7.67	33 41.16	119 1.14	5.01		153	7	E	0.09	99.0	99.0
1981	10	13	19	9	20.89	33 58.27	118 42.43	5.00		274	12	E	0.10	99.0	12.6
1981	10	14	1	53	22.60	33 40.00	119 3.60	5.01	1.8	136	13	C	0.11	3.0	99.0
1981	10	14	3	7	15.19	34 6.25	118 58.07	5.12		126	15	E	0.09	99.0	99.0
1981	10	14	8	21	35.07	33 39.93	119 2.49	5.00	1.8	138	14	C	0.09	0.9	99.0
1981	10	14	20	9	3.86	33 58.50	118 37.28	4.53	0.0	118	17	D	0.19	5.5	3.6
1981	10	15	4	16	3.00	33 40.07	119 2.73	5.00	1.7	135	10	C	0.11	2.7	99.0
1981	10	16	12	30	20.12	34 14.92	119 35.39	5.00	1.6	123	21	C	0.26	2.6	99.0
1981	10	17	0	53	34.26	33 37.99	118 59.55	5.00	2.5	125	35	C	0.10	0.7	99.0
1981	10	17	7	4	47.44	33 39.89	119 1.63	5.00	2.0	80	22	C	0.09	0.6	99.0
1981	10	17	13	35	48.97	33 38.38	118 59.22	5.00	1.8	143	20	C	0.09	1.3	99.0
1981	10	17	13	42	3.71	34 8.15	118 59.11	5.00		219	8	E	0.00	99.0	99.0
1981	10	18	20	20	34.71	33 38.83	118 59.77	5.00		127	12	C	0.17	1.8	99.0
1981	10	20	11	16	43.09	33 35.37	118 55.77	5.00		148	9	E	0.02	99.0	99.0
1981	10	20	23	24	33.31	33 43.04	119 6.70	5.01		172	10	E	0.01	99.0	99.0
1981	10	21	9	12	58.25	33 45.04	119 7.29	5.00		184	13	E	0.10	99.0	99.0
1981	10	21	10	59	39.51	33 43.52	118 57.84	5.06		246	8	E	0.07	99.0	99.0
1981	10	22	16	43	12.79	33 42.47	118 59.29	5.00	2.5	128	20	C	0.09	1.7	99.0
1981	10	23	3	36	26.91	33 56.64	118 34.03	5.01	0.0	231	19	E	0.36	99.0	99.0
1981	10	23	5	49	13.35	33 30.29	118 54.43	5.12		154	10	E	0.07	99.0	99.0
1981	10	23	17	28	17.08	33 38.23	118 58.99	5.00	4.6	124	108	C	0.12	0.6	99.0
1981	10	23	17	34	47.90	33 38.16	119 0.42	5.01	1.8	118	15	E	0.08	99.0	99.0
1981	10	23	17	46	8.03	33 37.63	118 58.57	5.00	2.8	122	39	C	0.13	0.8	99.0
1981	10	23	19	15	52.51	33 37.81	118 58.79	5.00	4.6	123	93	C	0.13	0.7	99.0
1981	10	23	19	28	54.30	33 37.74	119 0.22	5.01		126	11	C	0.09	2.1	99.0
1981	10	23	21	32	6.83	33 38.57	118 59.93	5.00	1.8	83	14	C	0.10	1.4	99.0
1981	10	23	22	58	16.56	33 38.24	118 58.73	5.00	2.1	123	24	C	0.09	1.0	99.0
1981	10	24	5	11	45.98	33 37.79	118 59.80	5.00	1.5	182	11	C	0.07	1.3	99.0
1981	10	24	6	29	29.25	33 39.37	118 57.36	5.00	1.7	230	16	C	0.14	4.8	99.0
1981	10	24	9	1	43.65	33 38.63	118 56.95	5.00	1.8	122	20	D	0.13	5.7	99.0
1981	10	24	10	26	30.36	33 37.59	118 58.17	5.00	2.3	121	32	C	0.13	1.4	99.0
1981	10	24	12	25	47.86	33 37.21	118 58.94	5.00	1.8	122	11	E	0.14	99.0	99.0
1981	10	24	13	53	33.71	33 37.86	118 59.39	5.00	2.4	125	28	C	0.10	0.7	99.0
1981	10	24	15	23	56.89	34 12.10	118 39.46	4.72		165	8	E	0.00	99.0	99.0
1981	10	25	6	28	38.09	33 38.67	119 0.62	5.00	2.9	129	40	C	0.10	0.6	99.0
1981	10	25	18	53	58.13	33 37.34	118 57.81	5.00	1.7	167	9	E	0.08	99.0	99.0
1981	10	25	22	9	21.80	33 38.19	119 0.42	5.01		167	9	E	0.07	99.0	99.0
1981	10	26	0	3	3.28	34 2.72	118 50.18	4.98		179	8	E	0.02	99.0	99.0
1981	10	26	0	3	38.11	34 2.34	118 50.23	5.00		187	7	E	0.02	99.0	99.0
1981	10	26	6	51	31.46	33 38.62	118 59.83	5.00		164	13	E	0.04	99.0	99.0
1981	10	26	9	44	50.03	33 38.13	118 58.57	5.00	1.7	122	14	C	0.11	1.2	99.0
1981	10	27	23	18	6.07	33 43.38	119 3.83	5.00		152	10	E	0.11	99.0	99.0
1981	10	28	17	44	26.62	34 11.67	118 58.92	5.07		148	7	A	0.00	0.0	0.0
1981	10	29	6	15	36.33	33 38.83	119 0.56	5.03	2.0	168	21	C	0.13	2.0	99.0
1981	10	30	17	7	25.76	33 37.49	118 58.62	5.00	3.7	122	81	C	0.11	0.6	99.0
1981	10	30	17	48	55.82	33 38.40	119 0.32	5.00		118	8	E	0.08	99.0	99.0
1981	10	30	18	27	43.04	33 49.22	118 34.19	5.00	0.0	140	15	E	0.16	99.0	99.0
1981	10	31	15	51	28.95	33 39.41	118 59.14	5.00	2.3	144	21	C	0.09	2.6	99.0
1981	10	31	23	14	33.06	33 39.95	119 2.52	5.00	3.3	103	88	C	0.08	0.5	99.0
1981	11	2	5	8	6.02	33 38.17	118 58.13	5.00	3.1	153	22	C	0.11	1.8	99.0
1981	11	3	6	29	56.90	33 38.36	118 58.33	5.00		237	7	E	0.26	99.0	0.0
1981	11	3	12	5	36.74	34 11.83	118 39.97	4.78		266	6	E	0.00	99.0	99.0
1981	11	3	22	36	49.74	34 11.44	118 58.80	4.52		148	8	A	0.00	0.0	0.0
1981	11	4	11	54	55.90	33 55.13	118 36.80	5.01	2.7	79	31	C	0.19	0.9	99.0
1981	11	4	14	18	43.91	33 38.83	119 1.10	5.00		172	11	E	0.02	99.0	99.0
1981	11	4	14	18	45.93	33 38.89	119 1.22	5.00		149	9	E	0.15	99.0	99.0
1981	11	4	14	19	14.68	34 4.09	118 57.55	8.80		148	12	E	0.00	99.0	99.0
1981	11	4	18	46	54.85	34 3.00	118 57.42	10.24		136	10	E	0.01	99.0	99.0
1981	11	6	14	12	23.75	34 12.79	118 38.37	4.64	1.5	152	17	A	0.13	1.0	0.8
1981	11	6	23	52	28.21	34 11.35	118 58.84	4.12		146	6	E	0.00	99.0	99.0
1981	11	10	7	13	20.95	33 37.92	118 58.54	5.00		141	11	E	0.12	99.0	99.0
1981	11	10	7	29	58.13	33 40.14	119 3.26	5.00	1.9	136	16	C	0.10	1.0	99.0
1981	11	10	20	3	39.17	34 10.52	118 59.53	3.53		112	10	C	0.34	2.9	3.6
1981	11	11	14	26	0.25	33 37.28	118 58.50	5.00	1.7	155	11	E	0.13	99.0	99.0
1981	11	12	14	21	56.54	33 41.64	119 3.46	5.00	2.1	106	22	C	0.07	0.7	99.0
1981	11	14	0	8	34.41	34 11.28	118 59.02	3.05		111	10	B	0.19	2.2	3.8
1981	11	16	6	5	23.48	33 39.67	118 56.01	5.00	1.8	236	22	E	0.12	99.0	99.0
1981	11	16	14	47	25.25	33 59.89	118 51.61	9.87	0.0	150	18	B	0.11	1.8	2.2
1981	11	16	22	44	41.44	33 42.88	119 7.28	5.00	2.2	152	20	C	0.08	1.1	99.0
1981	11	17	2	53	40.76	33 42.38	119 5.90	5.00	3.1	110	91	C	0.13	0.8	99.0
1981	11	17	16	59	22.60	34 1.09	118 44.93	5.30	0.0	189	15	B	0.09	2.4	1.2
1981	11	17	16	59	51.59	34 2.09	118 45.38	3.73	0.0	175	6	E	0.02	99.0	99.0
1981	11	19	22	0	18.07	34 10.91	118 58.90	0.49		103	9	D	0.40	5.5	99.0
1981	11	19	22	10	10.37	33 42.45	119 6.36	5.00	2.0	112	11	C	0.07	0.9	99.0
1981	11	23	8	9	23.77	33 58.30	118 41.36	5.36		157	11	E	0.01	99.0	99.0
1981	11	23	12	39	59.84	33 54.40	118 41.51	5.00	1.8	90	23	C	0.16	1.7	99.0
1981	11	24	0	13	4.34	34 6.81	118 59.33	9.81		174	12	B	0.01	1.4	1.9
1981	11	24	17	54	44.00	33 39.73	119 1.66	5.00		196	12	C	0.12	2.0	99.0
1981	11	25	20	16	54.18	34 7.30	118 59.01	5.98		161	5	E	0.03	99.0	99.0
1981	11	26	14	13	14.54	33 38.08	118 59.94	5.00	1.8	165	10	C	0.11	1.5	99.0
1981	11	26	19	48	41.73	33 38.13	119 0.12	5.00		184	6	E	0.09	99.0	99.0
1981	11	30	15	47	16.45	33 26.91	119 4.81	9.55	1.8	146	9	E	0.08	99.0	99.0
1981	11	30	23	3	38.31	34 5.39	119 3.44	7.07	0.0	190	12	D	0.24	6.7	7.8
1981	12	1	18	5	37.60	33 43.86	119 8.41	5.02		189	10	C	0.19	2.8	99.0
1981	12	2	19	22	45.99	34 9.15	118 57.36	5.60		181	5	E	0.05	99.0	99.0
1981	12	2	21	50	9.11	34 9.63	118 46.39	5.35		157	7	E	0.00	99.0	99.0
1981	12	3	23	18	41.39	34 10.96	118 59.73	0.01		78	16	B	0.27	1.7	4.8
1981	12	4	1	25	29.08	34 17.77	119 24.37	5.00		250	11	E	0.04	99.0	99.0
1981	12	4	9	37	45.50	33 38.20	118 58.78	5.00	2.0	123	43	C	0.10	1.2	99.0
1981	12	5	3	34	13.33	33 40.20	119 3.64	5.00		207	11	E	0.02	99.0	99.0
1981	12	5	11	56	24.97	33 41.80	119 5.75	5.00	2.7	110	89	C	0.10	0.6	99.0
1981	12	5	22	48	47.57	34 18.45	119 24.19	5.00		246	10	E	0.03	99.0	99.0
1981	12	6	5	37	33.43	34 14.61	119 23.56	5.01		206	12	E	0.04	99.0	99.0
1981	12	8	14	17	17.14	33 39.00	119 0.99	5.00	2.2	129	23	C	0.08	0.7	99.0
1981	12	8	16	16	2.69	34 11.46	118 58.90	6.04		114	11	D	0.04	12.4	99.0
1981	12	8	19	41	17.63	33 35.58	119 27.19	5.01	0.0	153	17	E	0.25	99.0	99.0
1981	12	8	19	42	47.46	33 35.78	119 25.71	5.00	0.0	146	15	E	0.30	99.0	99.0
1981	12	9	10	6	33.41	33 37.16	119 5.30	5.00		157	9	E	0.05	99.0	99.0
1981	12	9	17	24	16.69	34 8.31	118 44.36	3.79		170	9	E	0.00	99.0	99.0
1981	12	9	22	58	23.45	33 41.55	119 5.01	5.00	3.5	109	99	C	0.12	0.7	99.0
1981	12	10	9	11	42.27	33 41.63	119 5.41	5.00	2.5	109	44	C	0.11	1.1	99.0
1981	12	10	15	11	26.29	34 3.42	118 47.58	4.01		115	8	E	0.08	99.0	99.0
1981	12	11	15	17	56.49	33 27.04	118 28.95	5.00	1.7	161	17	E	0.07	99.0	99.0
1981	12	11	18	42	19.73	33 41.52	119 4.90	4.99	2.8	108	30	C	0.09	1.1	99.0
1981	12	14	11	32	59.76	33 42.66	119 6.32	5.00	3.9	111	106	C	0.13	0.7	99.0
1981	12	14	14	1	5.81	33 42.86	119 6.65	5.00		202	13	E	0.10	99.0	99.0
1981	12	14	14	35	37.62	33 42.83	119 6.97	5.00		224	8	E	0.09	99.0	99.0
1981	12	14	23	32	49.69	34 11.40	118 58.75	5.23		147	13	A	0.02	0.5	0.6
1981	12	15	11	4	15.85	33 39.53	118 59.73	5.00		164	9	E	0.09	99.0	99.0
1981	12	15	21	30	47.66	33 56.23	118 39.99	5.00	2.4	86	34	C	0.24	1.6	99.0
1981	12	16	12	43	10.23	33 58.88	118 37.84	11.06		127	10	E	0.18	99.0	99.0
1981	12	16	23	14	38.92	34 11.48	118 58.91	4.57		147	6	A	0.01	0.2	0.8
1981	12	17	21	16	20.16	33 39.36	119 0.69	5.00		189	8	C	0.10	3.4	99.0
1981	12	19	2	28	5.74	33 37.97	118 59.75	5.00	2.4	82	36	C	0.16	1.6	99.0
1981	12	23	16	32	8.60	34 11.35	118 58.80	4.73		118	10	B	0.10	1.5	1.9
1981	12	23	23	32	37.06	33 46.81	119 9.38	4.97	2.2	118	22	D	0.12	7.6	99.0
1981	12	24	18	40	14.46	33 45.84	119 6.10	5.00	1.9	279	17	E	0.14	99.0	99.0
1981	12	29	7	35	57.99	33 42.00	119 6.05	5.01	1.9	212	14	E	0.06	99.0	99.0
1981	12	29	20	22	5.39	33 45.89	119 9.26	5.00	2.1	253	14	E	0.06	99.0	99.0
1981	12	30	5	10	55.43	34 14.47	119 23.42	5.00	1.9	186	30	C	0.12	2.8	99.0
1981	12	30	10	10	1.14	34 1.25	118 46.07	3.49		188	11	E	0.06	99.0	99.0
1981	12	31	14	15	25.96	34 13.89	119 25.10	5.03	2.0	105	32	C	0.24	1.9	99.0
1981	12	31	20	51	24.21	34 15.82	119 23.28	5.00		204	12	C	0.02	0.6	99.0
1982	1	1	3	37	0.87	34 16.11	119 24.55	5.00	1.9	181	33	C	0.21	2.6	99.0
1982	1	1	3	45	18.34	34 14.03	119 24.94	5.01	2.0	85	36	C	0.21	1.6	99.0
1982	1	1	3	48	56.43	34 20.72	119 25.67	5.00		284	9	E	0.02	99.0	99.0
1982	1	1	6	38	40.09	34 2.26	118 56.89	5.80		203	14	D	0.13	6.2	99.0
1982	1	1	22	7	42.76	33 35.58	118 56.95	5.00		254	7	E	0.04	99.0	99.0
1982	1	2	11	17	52.02	33 45.21	118 59.96	5.00	1.4	268	19	E	0.13	99.0	99.0
1982	1	6	11	17	16.53	33 46.48	118 41.92	5.01	2.0	189	14	C	0.11	2.6	99.0
1982	1	6	11	51	41.22	33 37.72	119 3.09	5.02	1.6	248	13	C	0.10	4.2	99.0
1982	1	6	16	38	5.69	33 44.27	118 59.43	5.00	1.9	313	14	E	0.11	99.0	99.0
1982	1	8	22	18	46.72	34 18.65	119 24.68	5.00		291	9	E	0.04	99.0	99.0
1982	1	10	3	58	24.05	33 49.53	118 36.82	5.01	2.1	181	21	C	0.15	1.6	99.0
1982	1	10	4	40	9.83	33 49.76	118 36.89	5.00	2.4	79	38	C	0.20	1.8	99.0
1982	1	10	21	15	4.19	33 53.97	118 36.30	5.00	2.0	202	35	C	0.19	3.0	99.0
1982	1	11	14	48	26.29	33 49.92	118 35.76	5.01	2.2	147	34	C	0.20	2.2	99.0
1982	1	11	23	18	58.15	33 46.44	119 1.43	5.00	0.0	278	18	E	0.15	99.0	99.0
1982	1	12	8	34	46.78	34 14.47	119 25.64	5.02	0.0	108	17	C	0.08	2.6	99.0
1982	1	14	23	3	55.12	34 11.24	118 59.00	4.08		105	9	B	0.10	1.8	1.6
1982	1	15	12	25	54.98	34 0.09	119 7.99	6.12	3.1	69	104	C	0.24	3.8	99.0
1982	1	15	12	27	19.25	34 3.47	119 5.54	12.53	1.8	202	17	C	0.13	2.9	1.3
1982	1	15	12	37	9.51	34 2.62	119 6.84	10.38	1.8	127	20	C	0.22	2.8	2.7
1982	1	15	16	57	54.82	34 11.38	118 58.94	5.85		169	7	E	0.03	99.0	99.0
1982	1	17	12	9	34.65	33 57.58	118 46.86	12.15	1.6	244	18	B	0.07	2.0	1.1
1982	1	17	13	15	30.10	34 10.85	118 59.60	5.52		105	17	C	0.38	3.6	99.0
1982	1	19	0	41	19.01	33 39.43	119 2.31	5.00	2.5	133	43	C	0.11	1.7	99.0
1982	1	20	9	38	26.94	34 15.82	118 34.22	5.01		122	19	C	0.20	1.6	99.0
1982	1	20	21	48	31.93	34 16.87	119 37.90	5.01		166	20	C	0.10	3.3	99.0
1982	1	20	23	46	32.61	34 15.18	119 26.86	5.00	0.0	98	19	C	0.16	2.6	99.0
1982	1	23	11	10	24.38	33 53.71	119 5.57	7.99		282	13	E	0.21	99.0	99.0
1982	1	24	1	9	46.86	33 53.57	118 31.37	5.00	0.0	230	22	E	0.07	99.0	99.0
1982	1	25	10	43	39.81	33 37.49	119 0.22	5.00	1.9	241	12	C	0.10	3.7	99.0
1982	1	25	22	50	17.26	34 14.43	119 27.03	5.00	0.0	106	26	C	0.16	1.9	99.0
1982	1	26	9	45	41.22	33 55.83	119 23.48	5.01	1.7	112	23	C	0.08	1.9	99.0
1982	1	27	9	12	44.91	33 57.54	118 42.02	8.00		141	15	A	0.08	0.9	1.9
1982	1	28	2	33	54.76	33 36.25	118 55.28	5.00	1.7	120	22	D	0.14	7.6	99.0
1982	1	28	15	58	0.49	34 16.41	119 26.42	5.00		222	12	C	0.10	1.7	99.0
1982	1	29	10	51	33.98	33 48.33	118 56.92	5.00	2.1	302	11	E	0.10	99.0	99.0
1982	1	29	10	52	34.62	33 38.19	118 59.06	5.00	2.2	124	12	E	0.03	99.0	99.0
1982	1	29	22	24	45.43	33 40.57	118 58.24	5.00	2.3	181	9	E	0.10	99.0	99.0
1982	1	31	8	15	0.97	33 54.43	118 45.13	13.33	2.3	240	36	B	0.11	2.0	1.0
1982	2	1	0	0	30.41	33 59.86	118 51.04	9.58		223	8	A	0.00	0.0	0.0
1982	2	1	6	45	44.22	34 9.03	119 14.64	5.00		250	13	B	0.21	0.8	0.7
1982	2	1	14	21	50.31	33 52.09	118 42.09	5.00	0.0	156	21	C	0.06	0.7	99.0
1982	2	2	18	0	5.02	33 46.79	119 13.05	5.00	3.6	98	43	C	0.32	1.9	99.0
1982	2	3	15	9	34.53	33 40.31	119 2.80	5.01	0.0	156	25	E	0.07	99.0	99.0
1982	2	3	21	8	23.00	34 10.80	119 9.50	7.49		211	9	E	0.25	99.0	99.0
1982	2	6	21	45	28.72	34 7.55	118 57.73	4.88		133	13	E	0.11	99.0	99.0
1982	2	7	20	39	16.20	33 39.22	119 0.25	5.00	2.4	128	49	C	0.13	1.5	99.0
1982	2	8	13	7	3.93	34 12.29	118 38.74	4.69	1.8	112	30	B	0.22	1.4	1.4
1982	2	8	13	8	28.01	33 58.21	118 52.81	16.79	2.4	162	42	B	0.12	1.5	0.6
1982	2	9	23	52	16.66	34 17.35	119 24.47	5.00		252	9	C	0.02	1.3	99.0
1982	2	10	0	42	2.20	34 15.09	118 34.25	5.00		311	12	E	0.06	99.0	99.0
1982	2	10	1	5	54.92	34 15.17	119 23.27	5.00		189	11	C	0.03	0.5	99.0
1982	2	10	1	7	6.48	34 14.09	119 24.23	5.04	0.0	112	22	C	0.14	1.4	99.0
1982	2	10	4	0	18.69	34 13.68	119 23.92	5.01	0.0	114	17	C	0.19	4.0	99.0
1982	2	10	4	11	23.30	34 14.19	119 23.50	5.00		110	10	E	0.23	99.0	99.0
1982	2	10	4	11	31.38	34 21.35	119 24.88	5.00		310	5	E	0.00	99.0	99.0
1982	2	11	1	39	17.10	34 1.30	118 54.89	5.46		206	8	A	0.00	0.0	0.0
1982	2	11	15	48	38.00	33 52.43	118 45.68	5.00		293	10	E	0.15	99.0	99.0
1982	2	11	23	9	51.85	34 7.24	119 17.55	5.00	2.4	86	47	C	0.42	2.6	99.0
1982	2	13	13	58	20.70	33 52.67	118 41.95	5.01		274	11	E	0.04	99.0	99.0
1982	2	15	7	26	57.51	33 27.71	118 52.73	5.00	1.9	262	11	E	0.03	99.0	99.0
1982	2	16	20	3	25.61	33 51.82	118 34.35	5.00		326	4	E	0.60	99.0	0.0
1982	2	17	5	9	30.67	34 1.90	118 47.76	4.72	1.9	118	18	B	0.17	2.8	1.9
1982	2	19	5	49	24.58	33 26.80	118 52.79	5.00	2.5	153	29	C	0.09	1.9	99.0
1982	2	19	8	59	59.99	33 58.58	119 26.36	5.00		190	15	E	0.26	99.0	99.0
1982	2	19	11	3	30.10	33 39.70	118 59.02	5.00	1.4	234	11	E	0.10	99.0	99.0
1982	2	19	14	53	43.46	33 26.93	118 52.84	5.00	2.7	183	36	C	0.08	0.8	99.0
1982	2	19	15	2	49.53	33 24.65	118 56.87	5.00	2.1	161	15	E	0.12	99.0	99.0
1982	2	19	19	11	23.42	33 27.22	118 52.99	5.00	2.4	99	39	C	0.12	1.2	99.0
1982	2	19	19	51	49.21	33 27.25	118 52.95	5.00	2.3	151	22	D	0.13	5.9	99.0
1982	2	19	22	1	30.69	33 27.14	118 53.31	5.00	2.5	182	28	C	0.09	1.3	99.0
1982	2	20	1	58	40.56	33 27.34	118 52.63	5.00	1.7	151	11	E	0.02	99.0	99.0
1982	2	20	4	50	6.96	33 27.24	118 53.01	5.00	2.4	99	21	C	0.08	1.0	99.0
1982	2	20	5	28	7.01	33 27.23	118 53.14	5.00	1.8	152	11	C	0.05	1.6	99.0
1982	2	21	18	4	0.25	33 46.41	119 1.75	5.00	1.6	310	10	E	0.09	99.0	99.0
1982	2	21	18	56	14.27	33 26.87	118 52.89	5.00	3.2	100	88	C	0.11	0.8	99.0
1982	2	22	6	49	27.91	33 38.94	119 0.88	5.00	2.8	129	46	C	0.08	0.9	99.0
1982	2	23	12	28	51.24	33 27.25	118 52.90	5.00	2.9	99	39	C	0.09	0.8	99.0
1982	2	23	12	29	55.47	33 27.27	118 52.93	5.00	2.3	181	12	C	0.03	1.8	99.0
1982	2	23	18	54	0.63	33 27.14	118 52.83	5.00	2.9	133	29	C	0.05	0.4	99.0
1982	2	23	22	40	9.03	34 3.13	118 41.19	4.12		259	9	E	0.00	99.0	99.0
1982	2	24	8	26	51.96	33 50.78	118 47.78	5.00	2.2	245	16	E	0.11	99.0	99.0
1982	2	24	17	9	20.58	33 27.19	118 53.11	5.00	2.5	99	31	C	0.07	0.9	99.0
1982	2	24	17	14	16.76	33 27.26	118 52.97	5.00	2.9	99	23	C	0.08	0.8	99.0
1982	2	25	0	49	42.24	34 11.73	119 9.66	4.54	2.0	168	26	C	0.25	2.6	1.9
1982	2	26	1	3	21.83	33 57.07	118 40.25	6.02	1.9	137	22	C	0.09	3.5	99.0
1982	2	26	5	15	41.55	33 44.00	119 6.82	5.00		280	12	E	0.11	99.0	99.0
1982	2	26	6	9	18.79	33 27.75	118 52.83	5.00	2.2	262	16	D	0.09	11.2	99.0
1982	2	26	11	21	30.89	33 26.99	118 54.06	5.00	2.1	252	23	D	0.07	8.3	99.0
1982	2	26	13	30	15.91	33 27.22	118 53.04	5.00	3.5	99	80	C	0.08	0.6	99.0
1982	2	26	14	27	57.68	33 59.80	118 49.08	4.48		248	10	E	0.00	99.0	99.0
1982	2	26	18	9	10.34	34 7.33	118 40.87	4.78		212	12	E	0.02	99.0	99.0
1982	2	26	22	36	42.13	33 59.52	118 43.23	4.98		253	6	E	0.04	99.0	99.0
1982	2	26	23	12	33.12	33 56.63	118 39.56	5.00	1.8	235	17	C	0.12	3.0	99.0
1982	2	28	8	4	28.00	33 32.68	118 44.74	5.00	1.8	129	11	E	0.03	99.0	99.0
1982	2	28	14	8	19.67	34 11.87	119 8.98	5.38		163	14	C	0.20	2.8	99.0
1982	3	4	17	57	50.17	33 42.65	119 4.63	5.00		189	10	E	0.15	99.0	99.0
1982	3	5	22	19	47.38	33 40.80	119 3.09	4.99	2.5	105	45	C	0.09	0.9	99.0
1982	3	7	9	2	20.43	33 26.29	118 55.43	5.12	1.7	202	11	E	0.05	99.0	99.0
1982	3	7	9	57	23.92	33 26.89	118 55.28	4.74	2.2	195	12	E	0.07	99.0	99.0
1982	3	8	4	14	16.26	33 27.12	118 53.58	0.86	2.4	100	41	B	0.14	1.1	2.1
1982	3	9	7	48	23.96	33 38.52	118 54.59	5.00	1.8	112	15	C	0.19	3.8	99.0
1982	3	9	14	55	52.56	33 27.84	118 53.77	3.52	1.7	149	11	D	0.27	9.6	12.5
1982	3	9	23	18	33.01	33 59.88	118 43.62	5.96		244	9	E	0.00	99.0	99.0
1982	3	10	10	45	9.58	33 26.29	118 55.32	5.66	1.7	202	12	D	0.08	5.8	99.0
1982	3	11	14	36	8.73	34 1.64	118 58.34	6.23		171	15	D	0.21	7.2	99.0
1982	3	12	12	45	33.09	33 27.07	118 53.10	0.63	3.5	100	56	B	0.16	1.0	2.1
1982	3	12	13	8	26.21	33 28.29	118 55.01	5.10	1.8	210	9	E	0.02	99.0	99.0
1982	3	12	13	14	51.33	33 31.12	119 2.17	5.00	1.2	202	8	E	0.07	99.0	99.0
1982	3	12	23	37	53.95	33 38.71	118 59.02	5.00		178	6	E	0.01	99.0	99.0
1982	3	13	18	54	49.06	33 25.87	118 54.50	3.08	2.1	203	21	C	0.10	3.5	4.0
1982	3	13	19	4	11.55	33 27.01	118 53.66	3.83	2.4	152	28	D	0.26	5.4	5.7
1982	3	13	23	0	53.64	33 27.08	118 53.41	1.26	1.6	152	20	B	0.13	2.2	3.4
1982	3	14	18	35	40.27	33 27.13	118 55.42	5.00	1.8	192	11	E	0.20	99.0	0.0
1982	3	19	20	24	9.20	33 43.84	119 4.80	5.00	1.7	143	13	E	0.05	99.0	99.0
1982	3	20	4	44	50.77	33 43.09	119 6.16	5.00	2.8	145	28	C	0.11	1.1	99.0
1982	3	24	5	35	19.08	34 11.82	118 39.98	4.55		189	11	E	0.00	99.0	99.0
1982	3	24	16	30	53.23	33 56.81	118 40.08	5.34		138	14	E	0.06	99.0	99.0
1982	3	28	18	42	31.76	34 15.01	119 31.93	5.00		109	16	C	0.06	1.2	99.0
1982	4	2	7	21	29.51	33 25.74	118 54.92	4.34	1.9	206	14	E	0.10	99.0	99.0
1982	4	2	16	59	42.14	34 13.08	118 37.64	5.01	0.0	116	23	C	0.19	1.3	99.0
1982	4	3	23	5	20.96	33 56.04	118 44.00	5.70		158	9	E	0.02	99.0	99.0
1982	4	4	8	37	49.79	33 56.26	118 37.48	5.00		307	13	E	0.15	99.0	99.0
1982	4	4	17	38	58.20	33 34.19	118 55.55	4.98		140	13	E	0.06	99.0	99.0
1982	4	4	22	51	5.46	33 34.16	118 55.47	4.95	2.6	118	22	E	0.10	99.0	99.0
1982	4	4	22	52	21.26	33 30.54	119 3.06	5.00		274	7	E	0.14	99.0	99.0
1982	4	5	0	52	24.49	33 34.16	118 55.56	5.03	2.3	140	25	E	0.07	99.0	99.0
1982	4	5	0	52	55.93	33 34.67	118 55.38	4.94		142	6	E	0.01	99.0	99.0
1982	4	5	0	53	47.13	33 34.49	118 58.07	5.00		202	5	E	0.00	99.0	99.0
1982	4	5	1	14	55.00	33 34.49	118 54.06	5.00	4.0	115	92	C	0.13	0.7	99.0
1982	4	5	1	35	8.81	33 34.23	118 55.86	5.03		143	9	E	0.02	99.0	99.0
1982	4	5	2	12	33.17	33 34.55	118 54.82	2.35	3.0	114	33	A	0.10	0.8	1.5
1982	4	5	2	36	7.74	33 34.33	118 55.90	4.98		143	6	E	0.04	99.0	99.0
1982	4	5	2	41	36.22	33 34.59	118 54.61	2.10	2.7	114	34	B	0.09	1.7	3.5
1982	4	5	2	46	42.20	33 34.71	118 54.59	1.81	2.3	127	19	B	0.06	1.4	3.0
1982	4	5	3	46	28.05	33 34.18	118 55.37	4.93	2.5	123	33	E	0.06	99.0	99.0
1982	4	5	5	43	46.84	33 33.95	118 55.48	5.06	1.9	130	19	E	0.03	99.0	99.0
1982	4	5	6	39	41.44	33 34.13	118 55.49	5.02		139	9	E	0.03	99.0	99.0
1982	4	5	11	13	37.09	33 34.18	118 55.43	4.96	3.4	123	55	E	0.11	99.0	99.0
1982	4	5	12	14	18.79	33 34.70	118 54.14	5.00	2.4	234	20	E	0.09	99.0	99.0
1982	4	5	13	10	13.55	33 34.13	118 55.24	4.82	2.9	122	45	E	0.11	99.0	99.0
1982	4	5	13	13	40.38	33 35.30	118 52.95	5.00	2.5	115	27	C	0.14	3.2	99.0
1982	4	5	13	58	4.41	33 34.24	118 55.37	5.00	1.8	139	7	E	0.09	99.0	99.0
1982	4	5	14	23	47.22	33 33.95	118 55.36	5.02	1.8	138	6	E	0.06	99.0	99.0

TABLE I. Phase I Locations. Santa Barbara Island Earthquakes 1981-1982.

YEAR	MO	DA	HR	MN	SEC	LATITUDE	LONGITUDE	DEPTH	MAG	GAP	NSTA	Q	RMS	ERH	ERZ
1982	4	5	17	28	56.76	33 35.08	118 52.89	5.00	2.2	230	12	C	0.11	2.6	99.0
1982	4	5	20	12	24.68	33 34.39	118 54.22	1.37	2.1	117	20	B	0.08	2.0	4.3
1982	4	5	20	40	17.69	33 34.08	118 53.47	4.94	1.7	139	10	E	0.03	99.0	99.0
1982	4	6	10	20	17.07	33 51.53	118 30.81	5.00		291	9	E	0.22	99.0	99.0
1982	4	6	17	39	51.17	33 34.48	118 55.84	5.00		144	12	E	0.13	99.0	99.0
1982	4	6	21	53	24.77	33 33.78	118 55.14	5.01	2.1	120	10	E	0.09	99.0	99.0
1982	4	8	15	3	3.92	34 11.71	118 38.34	5.00	2.6	74	40	C	0.24	1.1	99.0
1982	4	9	14	27	37.10	33 56.99	118 40.31	5.23	2.3	72	36	C	0.10	0.5	99.0
1982	4	9	20	28	13.05	33 33.72	118 55.25	5.27		123	8	E	0.05	99.0	99.0
1982	4	9	22	2	48.93	33 25.99	118 55.07	4.92	2.0	204	7	E	0.07	99.0	99.0
1982	4	10	6	22	53.03	33 27.06	118 55.37	3.63		191	9	E	0.17	99.0	99.0
1982	4	10	7	16	41.24	33 38.57	118 59.78	5.00	1.4	145	10	E	0.03	99.0	99.0
1982	4	11	4	37	2.80	33 26.93	118 53.42	0.87	2.9	153	33	B	0.14	1.5	2.5
1982	4	11	8	27	43.98	34 12.00	118 38.54	5.44	1.7	92	26	C	0.23	1.7	99.0
1982	4	13	11	2	12.16	34 4.33	118 57.57	14.56	4.0	76	90	B	0.23	1.1	0.8
1982	4	13	12	57	59.98	34 3.50	118 58.24	5.52		194	10	C	0.03	3.3	99.0
1982	4	13	13	5	54.69	34 3.22	118 59.26	10.14		206	10	D	0.13	5.0	7.5
1982	4	14	1	20	34.30	34 2.69	118 48.47	4.00		119	9	E	0.00	99.0	99.0
1982	4	14	11	55	26.32	33 38.36	119 0.74	5.00		241	12	D	0.12	8.0	99.0
1982	4	15	4	44	16.84	34 2.99	118 58.87	12.44	1.7	170	16	B	0.12	1.8	1.8
1982	4	15	17	15	17.68	33 34.76	118 55.23	5.00	2.4	238	7	E	0.11	99.0	99.0
1982	4	15	18	49	32.29	33 35.08	118 54.93	5.00		252	7	E	0.02	99.0	99.0
1982	4	17	12	47	16.83	33 12.13	118 42.59	5.01	1.8	214	15	E	0.09	99.0	99.0
1982	4	18	20	44	38.65	34 3.92	118 59.11	11.60		114	16	B	0.14	1.3	1.3
1982	4	19	9	55	40.70	33 34.42	118 55.29	5.00	2.8	125	22	C	0.09	1.0	99.0
1982	4	19	9	59	5.15	33 52.08	118 42.16	5.00	1.8	168	15	C	0.06	1.2	99.0
1982	4	19	21	56	42.72	33 34.72	118 54.98	5.00	2.5	124	22	C	0.12	1.4	99.0
1982	4	20	0	22	46.71	33 58.98	118 39.78	11.86	2.3	121	39	B	0.11	1.2	1.1
1982	4	20	5	24	25.37	33 35.27	118 54.18	5.00	2.5	123	28	C	0.09	2.1	99.0
1982	4	20	6	53	8.53	34 2.33	118 58.87	15.91	2.3	215	14	C	0.16	3.5	4.7
1982	4	21	16	54	7.74	33 51.93	119 6.10	5.00	0.0	283	18	E	0.14	99.0	99.0
1982	4	23	1	45	53.80	33 26.84	118 54.25	4.99	2.3	153	16	C	0.05	0.7	99.0
1982	4	23	2	1	52.05	33 28.05	118 54.90	5.27	1.6	271	9	E	0.34	99.0	99.0
1982	4	23	8	12	59.14	34 15.35	119 40.08	5.00	1.6	143	28	C	0.23	2.4	99.0
1982	4	24	5	34	56.84	34 14.56	119 23.02	5.01	0.0	162	16	C	0.08	2.5	99.0
1982	4	24	8	26	48.60	34 17.73	119 23.92	5.00		194	12	E	0.09	99.0	99.0
1982	4	24	16	24	44.99	33 25.85	118 54.62	4.09		204	11	E	0.08	99.0	99.0
1982	4	24	18	36	50.36	34 7.41	118 58.33	4.06	0.0	157	19	D	0.17	5.9	4.3
1982	4	26	10	24	40.86	33 57.63	118 42.59	9.87		134	10	E	0.05	99.0	99.0
1982	4	26	10	25	22.23	34 0.35	118 43.85	5.00		228	5	E	0.00	99.0	99.0
1982	4	26	10	28	12.58	33 59.85	118 43.80	4.89		243	8	E	0.01	99.0	99.0
1982	4	26	13	5	59.58	34 16.99	119 23.74	5.00		196	14	C	0.10	2.4	99.0
1982	4	27	13	32	32.84	34 4.11	118 58.54	12.09	1.9	118	30	B	0.17	1.1	1.4
1982	4	28	2	59	48.07	33 39.96	119 0.77	5.00		190	8	E	0.01	99.0	99.0
1982	4	28	15	4	41.78	33 26.60	118 52.75	0.51	2.2	155	13	B	0.09	1.8	3.1
1982	4	29	7	46	24.23	34 7.37	119 18.39	5.00		250	15	E	0.29	99.0	99.0
1982	4	29	15	33	45.24	33 34.27	118 54.68	2.72	3.9	116	74	A	0.11	0.7	1.3
1982	4	29	16	0	40.87	33 33.79	118 55.19	5.16	1.5	136	10	E	0.05	99.0	99.0
1982	4	29	16	1	39.23	33 35.70	119 2.81	5.00		203	4	E	0.00	99.0	99.0
1982	4	29	16	2	37.44	33 34.92	118 54.06	0.17	1.6	114	15	B	0.11	1.3	2.2
1982	4	29	17	37	30.98	33 34.49	118 54.64	2.46	2.6	115	29	B	0.13	1.5	3.0
1982	4	29	19	5	42.32	33 34.30	118 55.51	5.04	1.8	140	10	E	0.04	99.0	99.0
1982	4	29	22	14	42.41	34 3.24	118 59.69	6.13	1.9	56	22	C	0.15	4.8	99.0
1982	4	29	23	14	34.71	33 34.50	118 55.99	4.95	2.1	148	11	E	0.02	99.0	99.0
1982	4	30	0	24	36.19	33 34.58	118 54.35	1.93	2.4	115	23	A	0.07	1.0	1.9
1982	5	1	9	53	1.89	33 34.73	118 54.87	2.47	2.3	112	21	B	0.07	2.0	8.9
1982	5	1	11	32	25.88	33 30.12	119 2.84	5.00		273	7	E	0.18	99.0	99.0
1982	5	1	15	29	18.48	33 34.76	118 54.33	0.09	2.3	114	29	C	0.12	2.3	5.3
1982	5	1	17	59	21.25	33 34.28	118 54.75	2.69	2.7	116	32	A	0.08	0.7	1.4
1982	5	1	18	5	28.54	33 34.83	118 56.69	5.39		151	10	E	0.06	99.0	99.0
1982	5	1	20	1	37.80	33 34.76	118 54.87	2.60	2.9	112	35	A	0.10	0.7	1.4
1982	5	2	3	3	8.67	33 34.49	118 55.77	4.94	1.8	144	9	E	0.06	99.0	99.0
1982	5	2	11	38	29.39	34 15.93	119 37.98	5.00	2.4	133	40	C	0.18	1.2	99.0
1982	5	2	11	39	54.64	34 16.03	119 37.74	5.00	2.2	131	16	C	0.12	1.2	99.0
1982	5	3	3	8	42.13	34 15.81	118 34.82	5.00	2.3	94	37	C	0.27	1.3	99.0
1982	5	3	8	23	58.91	33 57.43	118 44.10	13.94	3.2	93	33	B	0.20	1.1	1.1
1982	5	5	4	4	15.06	34 4.30	118 46.42	3.82		155	7	E	0.00	99.0	99.0
1982	5	5	7	34	27.99	33 43.06	119 7.37	5.01	1.5	200	10	E	0.03	99.0	99.0
1982	5	5	15	2	21.86	33 34.36	118 55.66	4.97	1.9	141	11	E	0.05	99.0	99.0
1982	5	9	0	54	31.83	33 34.84	118 55.50	5.00	2.1	127	15	C	0.02	0.5	99.0
1982	5	9	1	1	36.04	33 34.82	118 54.71	2.27	2.3	113	37	B	0.11	1.2	2.3
1982	5	9	3	54	34.23	33 34.86	118 54.68	2.21	2.3	113	33	B	0.09	1.0	2.1
1982	5	9	10	38	3.35	33 34.46	118 55.55	5.04	2.2	130	15	E	0.07	99.0	99.0
1982	5	9	18	2	34.14	33 34.56	118 55.80	5.00		144	7	E	0.03	99.0	99.0
1982	5	9	19	8	0.91	33 39.54	119 0.79	5.00	2.3	130	18	C	0.07	1.3	99.0
1982	5	9	21	28	54.83	33 57.73	118 40.84	5.99		151	10	C	0.13	5.0	99.0
1982	5	10	7	46	31.31	33 39.59	118 58.71	5.00	2.2	158	18	B	0.22	0.6	0.5
1982	5	13	17	54	33.90	33 34.28	118 55.56	5.00		140	6	E	0.05	99.0	99.0
1982	5	14	21	41	39.76	33 39.99	119 2.74	5.00	2.3	134	28	C	0.09	0.9	99.0
1982	5	18	1	3	50.58	34 1.85	118 50.09	4.92		194	11	E	0.08	99.0	99.0
1982	5	20	4	21	9.60	33 38.86	119 0.93	5.00	2.1	129	15	C	0.10	1.0	99.0
1982	5	22	11	52	21.03	33 42.84	119 7.60	5.00	2.2	153	13	C	0.08	1.5	99.0
1982	5	23	7	38	48.60	33 45.83	119 9.43	5.00	2.0	162	13	C	0.04	1.0	99.0
1982	5	25	17	20	4.57	33 37.99	118 58.75	5.00	2.0	123	11	C	0.13	1.3	99.0
1982	5	27	8	53	53.01	33 27.66	118 56.39	5.00		265	7	E	0.14	99.0	0.0
1982	5	27	19	33	47.98	33 59.40	118 51.09	5.49		246	8	E	0.12	99.0	99.0
1982	5	31	16	33	29.15	33 57.07	118 39.81	5.73		86	19	C	0.09	1.7	99.0
1982	6	1	5	15	49.25	33 42.59	118 57.37	5.00	1.9	221	12	C	0.13	3.8	99.0
1982	6	1	14	26	38.42	33 40.00	119 2.84	5.00	2.2	186	12	C	0.04	1.1	99.0
1982	6	3	15	9	34.27	33 38.46	118 58.72	5.00		164	15	C	0.10	1.4	99.0
1982	6	3	18	34	28.98	34 12.16	118 39.25	5.02		112	18	A	0.08	0.8	0.7
1982	6	4	5	25	14.46	34 0.31	118 43.65	5.12		235	8	E	0.04	99.0	99.0
1982	6	5	16	58	7.26	33 38.72	119 0.46	5.00	1.9	129	12	C	0.10	1.1	99.0
1982	6	7	3	25	21.46	33 42.40	119 1.65	5.01	2.1	135	14	C	0.04	0.6	99.0
1982	6	9	7	0	26.53	33 40.62	119 1.27	5.00		132	9	C	0.16	3.1	99.0
1982	6	11	23	19	5.05	33 50.33	118 41.81	5.00	0.0	144	12	E	0.23	99.0	99.0
1982	6	12	6	38	47.74	33 42.02	119 5.10	5.00		165	16	E	0.02	99.0	99.0
1982	6	14	3	25	41.97	33 40.99	118 58.06	5.00	1.7	155	9	D	0.18	6.6	99.0
1982	6	15	16	31	31.14	34 16.80	119 27.88	5.00		297	11	E	0.03	99.0	99.0
1982	6	16	12	37	0.37	34 3.29	118 58.39	13.73	1.6	79	27	B	0.23	1.6	1.6
1982	6	16	20	40	43.93	34 0.21	118 44.01	11.05		128	10	A	0.04	0.6	1.0
1982	6	17	7	19	8.68	34 7.98	118 59.30	5.47		124	12	C	0.18	4.5	11.4
1982	6	18	15	24	2.54	33 38.61	119 0.39	5.00	2.2	129	25	C	0.11	1.1	99.0
1982	6	22	18	49	44.68	33 26.22	118 54.02	5.00	1.6	135	8	C	0.18	4.6	6.8
1982	6	27	11	46	31.83	34 11.88	119 11.05	5.04		213	13	D	0.27	10.6	99.0
1982	7	2	19	22	58.47	34 10.93	118 58.93	3.18	0.0	101	17	B	0.28	2.4	3.3
1982	7	3	4	19	44.87	33 56.36	118 38.85	5.00	1.8	101	24	C	0.14	1.1	99.0
1982	7	5	18	49	0.64	33 35.56	118 53.85	5.00		131	9	B	0.22	0.8	0.8
1982	7	6	15	48	57.77	33 57.81	118 34.20	5.95		176	13	D	0.19	7.6	99.0
1982	7	7	6	32	41.37	33 57.58	118 41.15	5.64		127	13	C	0.07	1.7	99.0
1982	7	10	11	11	5.90	33 39.36	119 0.14	5.00	1.9	128	17	C	0.11	1.2	99.0
1982	7	11	2	28	56.69	33 53.52	118 40.33	5.00	2.4	87	34	C	0.19	1.0	99.0
1982	7	14	10	22	26.31	34 0.39	118 40.68	8.17		100	14	A	0.06	0.6	1.2
1982	7	21	10	30	34.44	34 13.91	118 36.56	5.00	0.0	94	22	C	0.28	1.9	99.0
1982	7	21	16	30	53.61	34 4.10	118 56.94	15.69	2.0	77	23	B	0.09	1.2	0.7
1982	7	22	5	22	19.20	33 46.72	119 9.95	5.00		142	13	D	0.11	8.5	99.0
1982	7	25	9	21	54.67	33 39.27	118 59.74	5.00	1.8	146	22	D	0.15	5.3	99.0
1982	7	27	5	32	43.08	33 41.94	119 1.25	5.00	2.4	78	39	C	0.10	0.8	99.0
1982	7	28	9	54	29.45	34 1.13	118 43.07	8.72	0.0	89	26	A	0.09	0.7	1.2
1982	7	28	16	42	49.74	34 15.30	118 32.44	5.00	2.5	48	74	C	0.31	1.2	99.0
1982	7	29	2	15	28.44	34 6.05	119 0.77	16.12	3.0	107	52	B	0.19	1.2	0.9
1982	7	29	5	50	8.56	33 57.10	118 41.02	5.29	3.2	57	54	C	0.26	1.0	99.0
1982	7	29	5	59	20.02	33 58.25	118 42.66	4.92		146	10	B	0.05	1.1	0.7
1982	7	29	7	13	44.75	33 58.05	118 42.83	5.35		275	6	E	0.03	99.0	99.0
1982	7	30	2	46	26.57	33 57.76	118 42.45	5.64	0.0	88	22	C	0.12	1.5	99.0
1982	8	5	3	52	47.42	34 2.64	118 58.66	14.02	2.1	81	35	B	0.18	1.3	1.0
1982	8	5	4	6	13.08	33 57.67	118 54.23	6.12		127	14	D	0.16	2.0	4.8
1982	8	8	21	56	38.88	33 59.43	118 48.45	4.84		279	9	E	0.17	99.0	29.1
1982	8	9	4	42	39.01	34 15.99	118 38.82	5.00	0.0	101	18	C	0.10	0.8	99.0
1982	8	16	22	45	48.62	34 10.92	118 59.91	6.31	1.2	119	8	D	0.26	17.6	99.0
1982	8	17	4	23	37.16	34 0.80	119 9.10	5.76	0.0	147	23	C	0.20	2.3	99.0
1982	8	21	1	19	35.77	33 37.84	119 24.59	5.00	2.3	218	10	D	0.15	7.2	99.0
1982	8	23	18	54	34.17	33 40.65	119 1.49	5.00	0.0	194	18	C	0.11	2.8	99.0
1982	8	24	18	59	31.90	33 39.80	119 1.07	5.00		192	9	E	0.02	99.0	99.0
1982	8	25	10	20	13.46	33 39.76	119 1.99	5.00		197	8	E	0.02	99.0	99.0
1982	8	26	17	59	51.04	34 2.55	118 46.75	3.14		142	5	E	0.14	99.0	99.0
1982	8	26	23	13	36.32	34 11.42	118 58.86	5.01		147	7	E	0.00	99.0	99.0
1982	8	29	19	32	14.68	33 6.38	118 54.55	5.01	0.0	290	11	E	0.02	99.0	99.0
1982	8	30	10	16	38.29	33 40.09	118 59.14	5.00	2.3	182	25	C	0.11	1.0	99.0
1982	8	31	23	37	48.93	33 58.70	118 32.76	5.00		244	12	D	0.25	9.3	99.0
1982	9	3	22	30	29.16	34 8.86	118 50.71	4.48		134	6	E	0.00	99.0	99.0
1982	9	4	8	43	0.62	33 58.82	118 54.05	16.19	2.2	165	30	A	0.13	1.0	0.5
1982	9	5	21	12	21.83	34 7.23	119 0.03	8.13		162	9	E	0.20	99.0	99.0
1982	9	10	17	47	5.58	33 39.10	118 59.38	5.00	3.1	161	53	C	0.12	1.5	99.0
1982	9	14	8	53	8.92	33 55.06	118 39.81	4.99		168	7	E	0.01	99.0	99.0
1982	9	14	13	47	2.49	33 54.51	118 39.28	5.01	0.0	132	20	C	0.20	4.4	99.0
1982	9	16	9	29	0.65	33 39.17	118 59.85	5.00	2.3	114	28	C	0.09	0.8	99.0
1982	9	16	9	37	51.90	33 38.42	119 0.04	5.00		166	8	C	0.04	1.8	99.0
1982	9	16	18	36	16.63	33 43.83	119 6.34	5.00		199	7	E	0.05	99.0	99.0
1982	9	18	0	49	21.00	33 39.37	119 0.37	5.01		187	10	C	0.05	2.0	99.0
1982	9	19	0	42	21.90	33 38.12	119 12.74	5.00		232	11	E	0.11	99.0	99.0
1982	9	20	18	20	23.26	34 0.68	118 45.73	5.33		210	7	E	0.00	99.0	99.0
1982	9	22	22	32	45.73	33 38.70	118 59.89	5.00		164	12	D	0.04	6.8	99.0
1982	9	25	2	58	34.64	34 2.81	118 58.22	16.85	2.2	204	25	B	0.17	1.8	1.0
1982	9	26	11	25	9.39	33 48.95	118 32.42	5.00		151	8	E	0.10	99.0	99.0
1982	9	27	9	43	58.72	34 16.33	119 36.65	5.00	2.6	126	36	C	0.20	1.3	99.0
1982	10	2	10	5	19.73	33 53.55	119 23.17	5.00	2.1	152	30	C	0.23	2.9	99.0
1982	10	4	4	11	26.50	33 38.96	118 59.69	5.00	1.8	163	14	E	0.11	99.0	99.0
1982	10	4	22	35	46.57	34 9.51	118 58.93	3.40		101	11	C	0.22	2.9	3.9
1982	10	5	2	51	49.00	34 7.31	118 59.35	4.83		161	7	E	0.01	99.0	99.0
1982	10	5	13	29	12.22	34 7.94	118 59.22	5.00		125	12	C	0.43	2.2	3.2
1982	10	5	16	10	10.50	33 59.08	118 50.27	7.47	2.1	129	21	C	0.33	3.9	3.1
1982	10	9	5	8	28.74	34 3.78	118 58.00	13.52	1.9	152	26	B	0.23	2.2	1.6
1982	10	9	11	27	21.41	33 58.94	118 54.78	12.54		166	15	C	0.13	3.2	4.9
1982	10	14	0	51	32.15	34 11.54	118 37.77	5.79	2.3	79	24	C	0.27	2.4	99.0
1982	10	15	9	57	20.17	34 12.74	118 38.05	3.24	3.3	74	41	B	0.28	1.0	1.6
1982	10	16	15	58	32.12	33 40.12	119 2.80	5.00	2.5	171	22	C	0.10	1.2	99.0
1982	10	18	23	17	7.47	34 15.64	119 37.37	5.00		245	12	E	0.06	99.0	99.0
1982	10	19	9	6	27.28	33 56.75	118 57.14	6.10		267	10	D	0.17	6.2	99.0
1982	10	19	22	37	12.84	33 58.99	118 54.10	14.42		139	18	B	0.15	2.0	1.5
1982	10	20	8	37	42.57	33 45.82	119 7.69	5.00	0.0	205	9	E	0.03	99.0	99.0
1982	10	20	17	39	6.18	34 6.87	118 59.54	11.57	0.0	172	9	E	0.02	99.0	99.0
1982	10	22	4	25	14.24	33 59.50	118 49.97	4.78		284	9	E	0.00	99.0	99.0
1982	10	24	19	23	18.98	34 5.77	119 13.90	5.01	3.8	88	42	C	0.28	1.5	99.0
1982	10	25	20	6	52.33	33 45.31	119 8.25	4.99		208	6	E	0.01	99.0	99.0
1982	10	26	23	17	17.93	33 38.26	118 59.57	5.00		180	7	E	0.00	99.0	99.0
1982	10	27	23	32	21.83	34 2.11	118 44.12	4.10		190	5	E	0.00	99.0	99.0
1982	11	1	0	30	46.64	33 38.59	119 0.85	5.02		171	13	E	0.09	99.0	99.0
1982	11	10	8	18	38.51	33 55.15	118 40.75	5.08	2.2	206	56	C	0.18	2.8	99.0
1982	11	11	22	36	59.47	34 3.12	118 48.81	4.39		139	12	E	0.04	99.0	99.0
1982	11	12	2	48	45.37	34 0.30	118 55.39	11.42		169	15	A	0.01	0.3	0.6
1982	11	12	5	44	47.03	34 1.22	118 45.03	5.97		113	9	A	0.00	0.0	0.0
1982	11	12	21	14	25.04	34 1.01	118 42.36	5.10		139	10	B	0.03	1.7	3.0
1982	11	13	15	42	28.39	34 2.21	118 46.68	3.01		151	5	E	0.07	99.0	99.0
1982	11	13	22	40	42.85	33 55.59	119 19.57	5.00	2.3	134	37	C	0.13	1.0	99.0
1982	11	14	2	13	45.24	33 55.32	119 19.98	5.00	2.0	136	10	E	0.13	99.0	99.0
1982	11	16	20	34	33.82	34 14.84	119 0.92	5.00		128	12	C	0.44	1.3	1.3
1982	11	17	10	16	41.75	33 40.47	119 1.63	5.00		143	14	E	0.06	99.0	99.0
1982	11	21	15	59	0.31	33 32.32	118 33.11	7.41		163	9	E	0.03	99.0	99.0
1982	11	21	16	2	24.98	34 11.91	118 38.18	5.48	2.3	69	43	C	0.24	1.4	99.0
1982	11	22	5	19	4.41	34 16.70	118 35.16	5.00		324	5	E	0.00	99.0	99.0
1982	11	25	8	47	37.23	33 57.95	118 57.23	5.00	0.0	264	12	C	0.04	2.3	99.0
1982	11	25	8	49	5.39	33 57.67	118 57.35	5.21		266	7	E	0.02	99.0	99.0
1982	11	25	12	40	40.27	33 47.50	119 5.62	5.00	1.9	309	11	E	0.14	99.0	99.0
1982	11	26	9	14	13.68	34 16.88	119 24.81	5.00		211	14	C	0.03	1.9	99.0
1982	11	26	14	39	53.89	34 14.03	119 25.55	5.04		228	15	E	0.09	99.0	99.0
1982	11	26	16	43	52.63	34 20.48	119 25.62	5.00		288	7	E	0.01	99.0	99.0
1982	11	29	2	26	20.55	34 1.80	118 46.06	3.34		172	8	E	0.05	99.0	99.0
1982	11	29	2	58	17.12	33 38.91	119 1.36	5.01	2.0	122	18	C	0.18	1.3	99.0
1982	12	2	18	30	51.68	33 28.65	119 5.03	4.92	2.0	270	8	E	0.04	99.0	99.0

TABLE II. Phase II Locations. Santa Barbara Island Earthquakes 1981-1982.

YEAR MO DA HR MN SEC LATITUDE LONGITUDE DEPTH MAG GAP NSTA Q RMS ERH ERZ

YEAR	MO	DA	HR	MN	SEC	LATITUDE	LONGITUDE	DEPTH	MAG	GAP	NSTA	Q	RMS	ERH	ERZ
1981	5	1	19	14	40.49	33 36.50	118 53.36	10.68		339	8	E	0.04	99.0	99.0
1981	6	24	20	48	6.12	33 29.70	119 6.63	11.75	2.7	135	36	A	0.06	0.8	1.7
1981	8	23	6	58	18.57	33 37.60	118 59.15	13.69	2.5	302	21	E	0.04	99.0	99.0
1981	9	4	6	26	19.73	33 20.39	119 3.52	15.66		346	9	D	0.46	41.7	11.5
1981	9	4	15	50	50.68	33 40.92	119 3.60	11.48	5.3	105	129	A	0.07	0.5	0.9
1981	9	4	15	57	43.18	33 39.29	119 1.58	10.32	3.6	134	86	A	0.03	0.3	0.6
1981	9	4	16	4	42.14	33 40.20	119 2.81	10.63	1.8	184	12	E	0.06	99.0	99.0
1981	9	4	16	7	2.78	33 39.91	119 3.20	10.59	2.2	204	14	E	0.01	99.0	99.0
1981	9	4	16	8	0.33	33 41.47	119 5.85	10.65		209	6	E	0.07	99.0	99.0
1981	9	4	16	9	59.24	33 39.02	119 1.35	10.13	2.3	177	33	A	0.01	0.3	0.9
1981	9	4	16	13	14.83	33 38.89	119 0.90	10.00	2.0	148	22	A	0.02	0.4	1.2
1981	9	4	16	16	45.32	33 40.20	119 3.14	11.93		156	9	E	0.03	99.0	99.0
1981	9	4	16	17	8.59	33 42.08	119 5.56	10.82		207	6	E	0.10	99.0	99.0
1981	9	4	16	17	52.90	33 40.23	119 3.29	11.12	2.3	82	24	B	0.08	0.7	2.3
1981	9	4	16	18	36.13	33 38.88	119 0.67	9.47		170	9	E	0.02	99.0	99.0
1981	9	4	16	19	51.05	33 44.17	119 7.85	16.15	1.8	89	14	B	0.10	1.8	4.3
1981	9	4	16	20	29.15	33 44.43	119 9.68	10.63		183	7	E	0.04	99.0	99.0
1981	9	4	16	25	45.98	33 39.87	119 2.38	11.58	1.8	81	16	A	0.05	0.5	1.0
1981	9	4	16	27	21.80	33 39.08	119 0.91	9.80	1.9	148	16	B	0.06	0.9	3.1
1981	9	4	16	32	43.69	33 38.11	119 0.20	12.49		184	11	E	0.03	99.0	99.0
1981	9	4	16	42	23.60	33 42.94	119 5.37	16.32	1.9	167	12	E	0.05	99.0	99.0
1981	9	4	16	46	17.64	33 39.91	119 2.69	12.12	2.1	103	29	A	0.03	0.3	0.9
1981	9	4	16	51	33.22	33 41.32	119 3.87	13.39	2.2	106	18	A	0.04	0.6	1.6
1981	9	4	16	58	4.09	33 42.22	119 5.68	10.82		123	11	E	0.04	99.0	99.0
1981	9	4	17	4	59.93	33 38.15	118 59.46	6.85	3.3	126	74	C	0.04	3.7	99.0
1981	9	4	17	17	4.59	33 39.96	119 2.37	11.09	1.5	134	12	A	0.04	0.7	1.8
1981	9	4	17	22	8.86	33 38.68	118 59.97	6.73	3.0	130	68	C	0.04	2.7	99.0
1981	9	4	17	46	48.16	33 39.50	119 0.52	8.61	1.9	130	14	D	0.04	11.1	99.0
1981	9	4	18	29	49.66	33 40.01	119 2.10	10.66	1.8	179	13	D	0.03	22.4	99.0
1981	9	4	18	31	57.78	33 40.49	119 1.54	10.63	1.8	198	13	E	0.03	99.0	99.0
1981	9	4	18	59	30.08	33 40.02	119 3.36	11.52	1.9	124	14	A	0.05	0.7	0.9
1981	9	4	19	11	50.65	33 40.39	119 3.47	10.69	1.8	158	12	E	0.02	99.0	99.0
1981	9	4	19	35	39.36	33 42.50	119 5.14	14.10	1.9	130	22	D	0.17	5.4	8.7
1981	9	4	19	36	47.91	33 42.54	119 4.54	12.48	2.4	84	38	B	0.07	0.9	2.6
1981	9	4	19	43	38.25	33 39.88	119 2.69	12.42	2.5	81	31	A	0.02	0.2	0.6
1981	9	4	19	48	23.76	33 41.36	119 2.67	10.68	2.4	126	24	D	0.07	19.9	99.0
1981	9	4	20	10	31.65	33 40.15	119 1.72	9.22	2.8	80	32	C	0.03	4.3	99.0
1981	9	4	20	14	46.21	33 40.43	119 3.18	11.11		184	6	E	0.19	99.0	99.0
1981	9	4	20	16	1.00	33 38.74	119 0.19	8.17	2.2	82	25	D	0.03	10.8	99.0
1981	9	4	20	22	11.72	33 39.86	119 2.87	12.06	2.3	81	31	A	0.03	0.3	0.8
1981	9	4	20	25	52.67	33 39.04	118 59.94	10.62	1.5	155	11	D	0.06	21.4	99.0
1981	9	4	20	26	29.53	33 40.16	119 1.68	10.64	1.9	80	16	D	0.05	23.1	99.0
1981	9	4	20	51	43.25	33 41.29	119 5.06	15.09	2.9	108	86	A	0.05	0.5	0.6
1981	9	4	20	51	11.65	33 40.16	119 2.91	10.62	1.8	157	14	E	0.01	99.0	99.0
1981	9	4	21	0	5.90	33 41.24	119 4.68	14.66	2.8	108	40	A	0.04	0.3	0.4
1981	9	4	21	33	28.12	33 38.59	119 0.46	10.63	2.0	128	15	E	0.06	99.0	99.0
1981	9	4	21	35	29.54	33 40.01	119 3.93	10.77	1.3	209	7	E	0.03	99.0	99.0
1981	9	4	22	2	13.50	33 40.37	119 2.69	10.62	1.5	181	8	D	0.22	22.3	99.0
1981	9	4	22	50	40.38	33 40.45	119 9.02	10.53	2.0	198	11	D	0.19	29.2	99.0
1981	9	4	23	23	47.92	33 43.02	119 3.20	10.52	1.7	170	11	D	0.12	10.1	99.0
1981	9	5	0	0	47.53	33 39.58	119 0.94	6.93	2.6	81	42	C	0.02	2.2	99.0
1981	9	5	0	1	35.82	33 37.98	119 1.17	10.59		191	10	E	0.04	99.0	99.0
1981	9	5	0	39	11.63	33 40.38	119 1.69	10.55	1.9	196	12	D	0.00	18.0	99.0
1981	9	5	0	41	49.23	33 42.92	119 7.15	12.00	3.8	101	96	A	0.11	0.7	1.9
1981	9	5	0	54	59.69	33 42.73	119 5.26	10.31	1.6	216	14	E	0.02	99.0	99.0
1981	9	5	1	33	53.43	33 42.66	119 4.05	8.82	1.7	128	19	D	0.06	10.2	99.0
1981	9	5	1	48	26.76	33 42.14	119 5.62	10.50	2.0	143	12	E	0.05	99.0	99.0
1981	9	5	1	49	10.36	33 38.67	119 0.52	10.63	2.4	82	39	D	0.03	8.4	99.0
1981	9	5	2	33	51.72	33 42.40	119 6.86	12.19	2.4	88	38	B	0.10	1.1	3.1
1981	9	5	3	41	49.49	33 39.47	119 0.87	10.55	3.1	118	67	D	0.07	14.5	99.0
1981	9	5	4	2	58.02	33 42.63	119 6.37	15.92	3.6	111	94	A	0.05	0.3	0.5
1981	9	5	4	4	49.90	33 38.91	118 58.88	10.49		182	7	E	0.05	99.0	99.0
1981	9	5	4	12	13.34	33 40.60	119 2.63	10.06		156	10	E	0.05	99.0	99.0
1981	9	5	4	17	35.80	33 38.02	119 0.36	10.15	2.1	168	19	D	0.03	22.8	99.0
1981	9	5	4	18	48.11	33 39.55	119 2.24	9.31	3.1	80	71	D	0.07	9.5	99.0
1981	9	5	4	21	37.12	33 39.80	119 2.34	8.62	2.1	154	24	D	0.03	5.7	99.0
1981	9	5	4	26	26.08	33 41.36	119 5.14	14.33	2.6	85	55	A	0.06	0.4	1.6
1981	9	5	4	29	49.83	33 38.93	119 0.85	11.78		148	20	B	0.04	1.3	3.5
1981	9	5	4	59	25.99	33 42.24	119 6.08	10.59	2.2	121	23	D	0.03	21.2	99.0
1981	9	5	5	1	34.86	33 41.00	119 4.13	10.63		133	11	E	0.07	99.0	99.0
1981	9	5	5	8	41.48	33 40.13	119 3.02	11.35	1.9	156	23	B	0.05	0.9	3.3
1981	9	5	5	20	15.84	33 40.51	119 2.00	9.67	1.6	184	17	D	0.20	9.6	42.9
1981	9	5	5	33	15.37	33 39.98	119 3.41	10.88	1.9	82	24	B	0.03	0.5	2.3
1981	9	5	6	41	48.35	33 39.06	119 0.26	6.68	2.0	83	22	C	0.06	3.2	99.0
1981	9	5	7	2	38.43	33 40.17	119 1.87	8.26	2.5	81	41	C	0.06	4.4	99.0
1981	9	5	8	33	22.72	33 39.64	119 2.19	10.53	2.1	152	21	A	0.03	0.4	1.5
1981	9	5	8	34	1.81	33 43.71	119 7.59	10.59		176	10	E	0.29	99.0	99.0
1981	9	5	8	55	50.69	33 39.97	119 2.70	9.62	2.3	81	37	A	0.04	0.3	1.8
1981	9	5	9	25	19.67	33 42.70	119 6.99	10.63	1.8	172	13	C	0.05	1.8	99.0
1981	9	5	9	42	58.97	33 38.80	119 1.21	10.63		192	12	D	0.04	30.4	99.0
1981	9	5	10	13	3.34	33 40.02	119 2.77	11.60	2.0	81	23	A	0.04	0.3	1.2
1981	9	5	11	50	34.10	33 39.63	119 0.87	8.88	2.6	78	46	C	0.03	4.3	99.0
1981	9	5	13	16	4.21	33 39.43	119 0.92	10.78	2.1	131	17	A	0.01	0.2	0.5
1981	9	5	13	36	40.94	33 39.81	119 2.59	7.52	2.2	81	40	C	0.02	2.8	99.0
1981	9	5	14	35	45.34	33 41.60	119 3.76	10.63	1.8	160	18	C	0.06	1.9	99.0
1981	9	5	16	17	11.06	33 38.97	119 1.78	10.57		195	14	D	0.04	25.8	99.0
1981	9	5	16	26	1.54	33 40.80	119 4.16	12.71	1.9	107	16	A	0.03	0.5	1.6
1981	9	5	20	18	39.95	33 44.68	119 10.26	13.33		147	13	E	0.15	99.0	99.0
1981	9	5	21	9	53.90	33 42.26	119 4.34	16.30		141	11	E	0.15	99.0	99.0
1981	9	5	21	21	6.66	33 38.69	118 59.24	6.28	2.4	76	35	C	0.05	2.4	99.0
1981	9	5	21	22	58.96	33 38.53	118 59.71	9.84		164	11	E	0.07	99.0	99.0
1981	9	5	21	36	40.06	33 39.26	119 0.84	10.63		130	15	D	0.04	14.1	99.0
1981	9	5	21	57	38.36	33 42.69	119 7.00	11.15	2.1	88	12	B	0.07	2.0	4.4
1981	9	6	1	54	4.46	33 38.93	119 1.26	11.57	2.1	150	23	A	0.01	0.3	0.8
1981	9	6	2	59	28.30	33 38.65	119 0.07	10.63	1.7	130	14	C	0.02	2.3	99.0
1981	9	6	6	18	56.57	33 38.55	118 59.53	9.15	2.0	130	22	B	0.03	0.8	4.1
1981	9	6	6	20	41.90	33 40.13	119 3.02	8.41	2.1	82	25	C	0.03	4.7	99.0
1981	9	6	9	17	0.32	33 44.83	119 8.89	13.11	3.7	91	50	A	0.13	0.7	1.4
1981	9	6	9	30	28.63	33 39.65	119 0.86	7.32	1.9	81	23	C	0.03	0.6	99.0
1981	9	6	9	49	58.80	33 41.17	118 59.36	8.72	2.8	131	39	C	0.06	3.8	99.0
1981	9	6	11	23	44.97	33 39.39	119 1.01	5.73		149	13	C	0.09	2.0	99.0
1981	9	6	12	20	1.21	33 43.69	119 8.07	8.57	2.2	90	27	C	0.26	4.3	99.0
1981	9	6	13	41	48.79	33 39.76	119 1.13	10.63	1.9	81	14	C	0.04	3.6	16.3
1981	9	6	18	30	31.34	33 40.89	119 2.78	10.01	3.1	81	48	A	0.08	0.5	1.4
1981	9	6	21	58	25.24	33 41.04	119 1.86	10.70		198	12	E	0.02	99.0	99.0
1981	9	7	3	46	47.64	33 42.80	119 7.14	11.07	2.0	133	13	E	0.06	99.0	99.0
1981	9	7	12	43	55.96	33 45.87	119 10.04	10.59	1.6	186	13	E	0.07	99.0	99.0
1981	9	7	12	44	53.52	33 45.64	119 8.99	10.62	1.8	183	12	E	0.05	99.0	99.0
1981	9	7	18	21	31.57	33 40.23	119 1.72	8.31	2.3	81	38	D	0.07	6.6	99.0
1981	9	7	16	19	56.87	33 39.92	119 3.21	12.23	1.6	136	15	B	0.07	1.7	2.4
1981	9	7	18	58	49.58	33 38.99	119 0.80	7.10	1.9	148	19	C	0.02	4.4	99.0
1981	9	7	19	10	26.75	33 43.37	119 6.31	16.79	1.8	146	17	B	0.04	1.1	1.8
1981	9	7	19	42	40.63	33 39.78	119 2.42	11.72	2.2	81	36	A	0.02	0.2	0.9
1981	9	8	1	22	7.40	33 41.65	118 58.10	10.63	1.8	145	7	E	0.09	99.0	99.0
1981	9	8	4	23	4.64	33 41.30	118 59.36	10.63	1.8	86	20	C	0.04	4.0	99.0
1981	9	8	5	27	25.93	33 38.97	119 0.59	10.63	2.0	147	22	D	0.06	18.2	99.0
1981	9	8	10	31	0.30	33 44.85	119 8.09	15.66	2.0	89	23	B	0.11	1.1	1.7
1981	9	8	10	36	41.66	33 39.57	119 0.77	9.00	2.8	133	46	B	0.03	5.7	99.0
1981	9	8	11	33	30.02	33 42.80	119 4.08	9.27	2.0	83	22	C	0.12	3.1	99.0
1981	9	8	15	43	13.70	33 41.40	119 3.24	10.63	2.0	81	18	D	0.04	10.8	99.0
1981	9	8	20	8	58.80	33 39.71	119 1.90	10.66	2.1	87	22	B	0.09	1.1	4.8
1981	9	9	4	30	28.28	33 39.48	119 1.42	10.62		175	13	E	0.01	99.0	99.0
1981	9	9	6	24	17.72	33 38.45	118 59.46	10.63	2.0	180	10	E	0.07	99.0	99.0
1981	9	9	6	26	19.27	33 39.38	119 1.90	9.51		178	8	E	0.02	99.0	99.0
1981	9	9	6	33	15.47	33 39.58	119 2.66	12.81	2.8	104	61	A	0.05	0.4	0.6
1981	9	9	9	25	3.06	33 43.05	119 5.22	10.64		167	11	B	0.12	6.3	99.0
1981	9	9	19	57	15.63	33 38.14	119 0.63	10.59		169	10	E	0.03	99.0	99.0
1981	9	9	23	36	15.16	33 38.87	119 2.99	9.39		248	12	B	0.09	11.9	99.0
1981	9	10	0	50	37.53	33 39.14	118 59.86	10.63	1.9	187	15	C	0.06	4.5	99.0
1981	9	10	1	53	55.56	33 39.61	119 0.74	10.63	2.2	109	31	C	0.02	1.7	99.0
1981	9	10	1	58	5.10	33 39.99	119 2.84	12.55	2.2	81	29	A	0.03	0.3	1.2
1981	9	10	5	45	55.65	33 41.58	119 5.08	15.35	3.4	86	65	A	0.08	0.5	0.8
1981	9	10	8	54	45.48	33 41.28	119 4.39	10.63	2.2	84	32	D	0.11	5.8	99.0
1981	9	10	9	44	20.74	33 44.81	119 8.32	10.63	2.3	89	27	C	0.11	2.9	99.0
1981	9	10	13	56	38.28	33 37.85	118 58.38	7.40	2.5	82	44	C	0.04	4.7	99.0
1981	9	10	18	8	1.84	33 41.59	119 5.14	11.70	3.2	144	45	B	0.07	0.6	3.0
1981	9	11	3	10	17.28	33 41.37	119 2.63	7.24	1.7	157	10	C	0.02	3.2	99.0
1981	9	11	3	30	32.49	33 44.82	119 8.93	10.61	2.0	181	19	C	0.08	3.4	99.0
1981	9	11	5	56	24.25	33 44.55	119 9.11	15.62	3.9	91	65	A	0.11	0.6	0.8
1981	9	11	6	50	12.95	33 38.84	119 1.58	10.65		175	15	D	0.03	24.1	99.0
1981	9	11	9	58	24.27	33 44.82	119 8.36	10.63	2.4	158	24	C	0.08	0.7	99.0
1981	9	11	10	40	11.68	33 38.66	118 59.96	10.63	2.4	164	36	B	0.02	19.8	99.0
1981	9	11	17	31	39.03	33 43.91	119 6.88	14.50	2.4	87	20	A	0.05	0.6	1.1
1981	9	11	20	53	38.44	33 41.79	119 5.68	14.06	2.3	90	28	A	0.04	0.5	0.7
1981	9	11	22	49	29.94	33 40.06	119 2.82	10.59	2.1	82	19	A	0.03	0.3	1.2
1981	9	12	5	34	1.55	33 40.16	119 3.00	11.02	2.1	136	23	A	0.03	0.2	0.9
1981	9	12	6	26	25.30	33 41.31	119 4.58	11.72	2.1	88	31	B	0.08	0.7	2.5
1981	9	12	12	23	49.37	33 41.43	119 4.42	10.64		211	9	E	0.03	99.0	99.0
1981	9	12	15	35	19.59	33 41.49	119 4.80	10.63	1.8	84	16	C	0.09	3.6	99.0
1981	9	12	16	19	41.54	33 40.09	119 2.71	10.69	2.2	81	19	A	0.03	0.2	1.2
1981	9	12	17	32	26.00	33 39.88	119 2.64	11.22	2.4	81	23	A	0.02	0.2	0.9
1981	9	12	18	17	15.57	33 41.35	118 59.76	10.61	2.0	165	9	E	0.05	99.0	99.0
1981	9	12	20	29	47.87	33 41.23	119 0.14	10.63	1.9	167	11	E	0.06	99.0	99.0
1981	9	12	23	14	32.65	33 39.01	118 59.04	7.13	2.4	84	26	C	0.06	2.6	99.0
1981	9	13	0	6	9.35	33 38.78	118 59.89	10.63	2.7	77	48	D	0.07	6.0	99.0
1981	9	13	23	36	10.64	33 39.03	119 1.12	8.47	2.4	79	34	D	0.01	5.4	99.0
1981	9	15	10	47	7.92	33 39.82	119 1.97	10.64		197	11	D	0.03	21.4	99.0
1981	9	15	19	5	24.10	33 38.92	118 59.02	10.63		161	15	D	0.07	19.3	99.0
1981	9	15	19	56	12.40	33 37.79	118 59.41	11.19	3.2	83	60	A	0.04	0.3	0.6
1981	9	15	20	37	46.34	33 40.47	119 2.02	9.89	2.9	80	40	A	0.05	0.3	1.0
1981	9	16	0	35	0.52	33 39.11	119 1.47	10.63		241	9	E	0.04	99.0	99.0
1981	9	16	1	16	59.88	33 36.11	118 56.79	10.72	3.2	97	89	A	0.04	0.3	1.0
1981	9	16	1	19	11.48	33 36.11	118 57.06	11.42	3.8	97	70	A	0.04	0.3	0.6
1981	9	16	6	29	8.09	33 40.42	119 2.08	10.11	2.8	80	42	A	0.04	0.3	1.8
1981	9	16	22	45	28.94	33 41.23	118 59.38	10.63	2.3	127	27	C	0.04	3.0	99.0
1981	9	17	21	5	46.94	33 38.35	119 0.77	10.62	2.1	170	18	D	0.02	25.4	99.0
1981	9	18	11	8	9.46	33 39.92	119 3.26	13.46	0.0	137	14	A	0.03	0.3	1.1
1981	9	18	11	53	14.80	33 42.06	119 4.53	10.64		212	12	E	0.05	99.0	99.0
1981	9	18	16	34	29.05	33 41.48	119 5.24	13.54	1.9	86	14	A	0.03	0.4	1.6
1981	9	19	8	59	17.06	33 40.59	119 1.78	8.68	1.7	122	22	C	0.08	1.9	7.7
1981	9	19	12	15	47.67	33 33.47	118 57.68	10.63	2.3	131	19	C	0.04	2.8	99.0
1981	9	19	13	43	2.30	33 32.62	118 59.59	10.61	1.8	168	13	D	0.02	44.6	99.0
1981	9	20	5	14	21.82	33 40.02	119 2.72	11.22	1.8	134	18	B	0.06	1.8	4.3
1981	9	20	11	32	6.76	33 45.32	119 7.75	13.71	1.8	88	18	E	0.14	99.0	99.0
1981	9	21	4	49	10.75	33 41.15	119 0.41	0.02	1.7	189	12	E	0.14	99.0	99.0
1981	9	21	10	8	8.50	33 38.79	119 0.56	10.68	3.1	78	67	A	0.00	0.0	0.0
1981	9	21	22	38	22.99	33 38.93	119 1.38	10.63	1.7	174	17	D	0.05	23.1	99.0
1981	9	22	0	11	4.75	33 40.95	119 2.48	11.90	2.1	86	18	A	0.04	0.5	1.8
1981	9	22	17	53	0.19	33 38.36	119 0.47	9.46		187	10	E	0.05	99.0	99.0
1981	9	23	13	52	43.49	33 37.96	118 58.83	7.96	2.2	88	21	D	0.07	5.5	99.0
1981	9	23	19	11	1.44	33 39.75	119 2.74	13.11	2.1	128	14	A	0.03	0.5	1.3
1981	9	23	19	54	22.20	33 38.61	118 59.34	8.44	2.4	124	30	D	0.09	7.9	99.0
1981	9	25	5	45	32.03	33 39.95	119 2.99	10.62		203	7	E	0.04	99.0	99.0
1981	9	26	5	58	25.28	33 39.91	119 3.17	10.63		136	10	D	0.01	16.5	99.0
1981	9	26	6	58	54.19	33 40.83	119 0.71	8.70	2.2	130	23	C	0.04	4.1	99.0
1981	9	26	7	50	10.11	33 40.82	119 0.52	9.41	2.3	130	21	A	0.04	0.4	1.3
1981	9	26	16	53	30.77	33 39.85	119 2.84	10.63		182	9	E	0.02	99.0	99.0
1981	9	27	8	19	50.74	33 39.24	119 7.50	10.61	2.4	106	31	C	0.09	1.4	99.0
1981	9	27	14	33	27.34	33 39.33	119 6.87	14.82	2.5	89	43	A	0.06	0.4	0.8
1981	9	27	22	52	37.14	33 31.96	119 14.17	13.68		149	12	D	0.18	13.1	26.7
1981	9	28	9	46	25.23	33 46.08	119 9.54	10.63	1.9	164	13	D	0.05	10.1	99.0
1981	9	29	18	12	28.90	33 38.43	119 0.72	10.58	2.5	170	28	D	0.02	22.9	99.0
1981	9	29	21	33	8.00	33 38.82	118 59.76	10.63	2.1	164	21	D	0.04	22.8	99.0
1981	9	30	0	24	53.24	33 46.17	119 10.85	10.63		148	14	D	0.08	8.5	99.0
1981	9	30	1	37	10.38	33 42.55	119 4.24	10.63	1.9	143	14	B	0.26	5.9	99.0
1981	10	1	6	37	51.97	33 33.25	119 0.56	10.63		197	2	E	0.00	99.0	99.0
1981	10	1	9	28	37.34	33 40.99	119 4.23	11.06	1.9	126	19	A	0.06	0.5	1.6
1981	10	2	8	13	42.69	33 38.50	119 1.05	10.63	1.5	172	10	E	0.02	99.0	99.0
1981	10	2	21	13	14.27	33 38.07	118 59.52	10.49	2.3	125	21	A	0.07	0.7	1.0
1981	10	3	9	34	12.24	33 26.70	118 54.60	7.87		195	8	E	0.15	99.0	99.0
1981	10	3	15	0	43.63	33 39.85	119 2.44	10.63	1.8	135	16	D	0.04	16.8	99.0
1981	10	3	17	59	39.80	33 44.86	119 9.16	10.64		139	11	E	0.08	99.0	99.0
1981	10	3	21	15	15.15	33 40.22	119 0.62	11.74	1.9	130	21	B	0.08	0.8	3.4
1981	10	5	2	9	45.02	33 38.26	119 0.65	10.63	1.7	170	17	D	0.06	21.8	99.0
1981	10	5	20	31	3.10	33 47.70	119 12.80	11.38	2.8	96	33	B	0.11	0.7	2.9
1981	10	6	0	31	31.20	33 38.78	118 59.19	10.63	2.0	144	14	E	0.03	99.0	99.0
1981	10	6	7	6	18.87	33 38.76	119 1.09	10.63		172	12	E	0.02	99.0	99.0
1981	10	6	9	14	9.69	33 38.79	119 0.96	9.26	1.6	172	13	D	0.02	20.9	99.0
1981	10	6	11	2	13.70	33 40.17	118 59.46	10.63	2.2	126	15	C	0.04	3.0	99.0
1981	10	7	9	41	56.00	33 47.40	119 13.04	10.63	1.7	148	10	E	0.07	99.0	99.0
1981	10	7	17	29	56.33	33 40.15	119 3.42	10.63	0.0	185	12	E	0.03	99.0	99.0
1981	10	7	22	34	32.19	33 41.22	119 2.21	10.61	1.8	135	15	D	0.11	8.2	99.0
1981	10	9	4	1	59.61	33 44.83	119 8.89	10.63	2.2	91	21	C	0.09	3.8	99.0
1981	10	9	17	27	51.19	33 38.90	119 1.51	10.63		178	9	E	0.02	99.0	99.0
1981	10	11	3	59	28.76	33 47.51	119 14.44	10.63		152	12	D	0.19	5.2	99.0
1981	10	11	7	25	20.40	33 41.62	119 4.16	10.63		188	11	D	0.03	14.7	99.0
1981	10	11	18	10	12.81	33 39.55	119 1.00	9.34	3.7	78	39	A	0.04	0.2	1.0
1981	10	12	7	24	33.62	33 39.25	119 0.03	10.63	2.0	127	10	E	0.08	99.0	99.0
1981	10	12	12	13	17.24	33 40.11	119 1.45	8.26	2.4	81	44	B	0.09	0.8	3.9
1981	10	13	1	55	5.55	33 40.78	119 0.30	9.95		130	8	E	0.06	99.0	99.0
1981	10	13	1	55	7.63	33 41.07	119 0.62	10.63		151	7	E	0.05	99.0	99.0
1981	10	14	1	53	22.55	33 39.89	119 3.40	10.63	1.8	136	13	C	0.05	3.4	99.0
1981	10	14	0	21	35.07	33 39.82	119 2.39	10.40	1.8	134	14	A	0.02	0.2	0.8
1981	10	15	4	16	3.01	33 40.02	119 2.35	9.69	1.7	134	10	C	0.07	1.3	6.9
1981	10	17	0	53	34.31	33 37.80	118 59.29	7.18	2.5	79	35	C	0.04	3.8	99.0
1981	10	17	7	4	47.47	33 39.70	119 1.29	7.44	2.0	132	22	C	0.03	2.0	99.0
1981	10	17	13	35	49.03	33 38.18	118 59.00	7.66	1.8	84	20	C	0.04	3.9	99.0
1981	10	18	20	20	34.64	33 38.58	119 0.00	9.61		167	12	D	0.05	19.5	99.0
1981	10	20	11	16	43.07	33 34.95	118 55.40	9.65		145	9	D	0.04	23.8	99.0
1981	10	20	23	24	33.37	33 42.72	119 6.42	10.63		170	10	E	0.09	99.0	99.0
1981	10	21	9	12	58.42	33 45.14	119 6.69	10.50		223	13	E	0.08	99.0	99.0
1981	10	21	10	59	38.53	33 41.55	119 4.08	10.48		210	8	E	0.09	99.0	99.0
1981	10	22	16	43	12.80	33 42.51	118 59.43	10.63	2.5	128	30	C	0.05	2.4	99.0
1981	10	23	5	49	13.20	33 29.70	118 54.87	10.64		161	10	D	0.05	34.7	99.0
1981	10	23	17	28	16.98	33 37.87	118 59.66	10.54	4.6	162	108	A	0.02	0.1	0.3
1981	10	23	17	34	47.88	33 37.87	119 0.03	10.09	1.8	166	15	D	0.05	25.0	99.0
1981	10	23	17	46	8.06	33 37.80	118 58.40	7.49	2.8	83	30	C	0.08	3.6	99.0
1981	10	23	19	15	52.48	33 37.60	118 59.04	10.37	4.6	123	93	A	0.06	0.4	0.8
1981	10	23	19	28	54.33	33 37.56	118 54.60	10.59		124	11	C	0.12	2.2	8.8
1981	10	23	21	32	6.87	33 38.46	118 59.40	7.94	1.8	125	14	D	0.06	6.1	99.0
1981	10	23	22	58	16.55	33 38.20	118 58.59	10.62	2.1	113	34	C	0.03	2.4	99.0
1981	10	24	5	11	45.97	33 37.37	118 59.86	10.63	1.5	179	11	D	0.03	25.2	99.0
1981	10	24	6	29	28.80	33 38.14	118 59.81	10.65	1.7	163	16	A	0.05	0.7	1.2
1981	10	24	9	1	43.20	33 37.36	118 58.95	8.82	1.8	189	20	D	0.04	17.2	99.0
1981	10	24	10	26	30.42	33 37.75	118 58.61	6.97	2.3	85	32	C	0.06	4.8	99.0
1981	10	24	12	25	47.72	33 37.34	118 59.43	9.97	1.8	160	11	E	0.02	99.0	99.0
1981	10	24	15	53	33.77	33 37.78	118 59.21	5.95	2.4	123	28	C	0.03	1.7	99.0
1981	10	25	6	28	38.09	33 38.53	119 0.65	9.51	2.9	78	40	A	0.02	0.1	0.5
1981	10	25	18	53	58.15	33 37.09	118 57.70	9.59	1.7	151	9	E	0.03	99.0	99.0
1981	10	25	22	9	21.81	33 37.99	118 59.93	9.75		166	9	E	0.04	99.0	99.0
1981	10	26	6	51	31.42	33 38.50	119 0.58	10.78		128	13	E	0.04	99.0	99.0
1981	10	26	9	44	50.06	33 37.96	118 58.25	10.63	1.7	114	14	C	0.05	2.2	99.0
1981	10	27	20	10	5.98	33 43.29	119 3.97	12.75		152	10	E	0.15	99.0	99.0
1981	10	29	6	15	36.24	33 38.74	119 0.72	10.63	2.0	170	21	D	0.04	18.0	99.0
1981	10	30	17	7	28.78	33 37.86	118 58.52	11.45	3.7	116	81	A	0.04	0.2	0.4
1981	10	30	17	40	55.81	33 38.26	119 0.17	9.70		167	8	E	0.02	99.0	99.0
1981	10	31	15	51	29.04	33 39.24	118 58.86	6.36	2.3	144	21	C	0.04	2.3	99.0
1981	10	31	23	14	33.03	33 39.80	119 2.22	10.96	3.3	81	88	A	0.03	0.2	0.8
1981	11	2	5	8	5.73	33 37.29	118 59.41	10.69	3.1	160	22	A	0.03	0.3	0.9
1981	11	3	6	29	56.40	33 37.54	118 59.28	10.04		240	7	E	0.01	99.0	99.0
1981	11	4	14	18	48.73	33 37.69	118 59.71	10.61		143	9	E	0.08	99.0	99.0
1981	11	4	14	18	43.88	33 38.58	119 0.58	10.63		168	11	E	0.03	99.0	99.0
1981	11	10	7	13	21.18	33 38.16	118 58.07	7.68		140	11	E	0.19	99.0	99.0
1981	11	10	7	29	58.04	33 40.09	119 2.91	12.00	1.9	124	16	A	0.01	0.1	0.2
1981	11	11	14	26	0.24	33 37.41	118 58.80	8.80	1.7	158	11	E	0.05	99.0	99.0
1981	11	12	14	21	56.49	33 41.45	119 2.83	12.25	2.1	105	22	A	0.07	0.6	1.9
1981	11	16	6	5	23.04	33 38.62	118 58.52	9.52	1.8	138	22	E	0.04	99.0	99.0
1981	11	16	22	44	41.44	33 42.76	119 6.81	10.63	2.2	88	20	C	0.06	3.5	99.0
1981	11	17	2	53	40.67	33 42.25	119 5.76	14.14	3.1	110	91	A	0.07	0.5	1.1
1981	11	19	22	10	10.31	33 42.37	119 6.10	12.66	2.0	132	11	A	0.04	0.5	1.9
1981	11	24	17	34	43.98	33 39.64	119 1.56	10.63		194	12	D	0.03	22.2	99.0
1981	11	26	14	13	14.50	33 37.90	119 0.01	10.63	1.8	165	10	D	0.04	25.3	99.0
1981	11	26	19	48	41.69	33 37.92	119 0.11	10.63		186	6	D	0.01	27.2	99.0
1981	11	30	15	47	16.44	33 26.60	119 4.50	10.01	1.8	147	9	E	0.03	99.0	99.0
1981	12	1	18	5	37.57	33 43.76	119 8.46	10.55		169	10	B	0.08	1.3	2.6
1981	12	4	9	37	45.55	33 38.21	118 58.65	9.90	2.0	122	48	C	0.06	2.7	99.0
1981	12	5	3	34	13.35	33 40.10	119 3.45	10.56		206	11	E	0.05	99.0	99.0
1981	12	5	11	56	24.84	33 41.61	119 5.20	14.33	2.7	109	59	A	0.07	0.5	0.7
1981	12	8	14	17	17.15	33 38.87	119 0.70	9.43	2.2	129	33	D	0.04	8.2	99.0
1981	12	9	10	6	34.29	33 39.00	119 0.00	10.63		257	9	D	0.10	5.9	99.0
1981	12	9	22	58	23.32	33 41.38	119 4.86	15.15	3.5	100	99	A	0.07	0.4	0.8
1981	12	10	9	11	42.85	33 41.76	119 5.54	10.62	2.5	86	44	D	0.08	5.2	99.0
1981	12	11	18	42	19.59	33 41.37	119 4.96	14.08	2.8	85	30	A	0.05	0.5	0.9
1981	12	14	11	32	59.63	33 42.50	119 6.19	15.55	3.9	111	106	A	0.07	0.4	0.4
1981	12	14	14	1	5.05	33 42.78	119 6.28	10.62		200	13	E	0.04	99.0	99.0
1981	12	14	14	35	37.70	33 42.77	119 5.90	10.61		219	8	E	0.04	99.0	99.0
1981	12	15	11	4	15.83	33 39.34	118 59.75	10.63		164	9	D	0.05	23.1	99.0
1981	12	17	21	16	20.14	33 39.19	119 0.61	10.63		189	8	D	0.01	23.3	99.0
1981	12	19	2	28	5.88	33 37.86	118 58.66	6.07	2.4	81	36	C	0.11	3.0	99.0
1981	12	23	23	32	37.05	33 47.14	119 9.80	10.93	2.2	166	22	C	0.07	3.0	3.9
1981	12	24	18	40	13.46	33 42.85	119 7.22	10.60	1.9	211	17	E	0.06	99.0	99.0
1981	12	29	7	35	57.97	33 42.11	119 6.53	10.67	1.9	212	14	E	0.02	99.0	99.0
1981	12	29	20	22	5.33	33 45.98	119 10.05	10.25	2.1	258	14	E	0.03	99.0	99.0
1982	1	1	22	7	43.27	33 37.00	118 54.33	10.63		247	7	E	0.00	99.0	99.0
1982	1	2	11	17	50.05	33 38.12	119 1.66	10.63	1.4	243	19	C	0.12	4.6	99.0
1982	1	6	11	51	41.18	33 37.66	119 4.52	10.65	1.6	250	13	C	0.10	4.0	99.0
1982	1	6	16	38	4.02	33 38.67	119 1.44	10.63	1.9	131	14	C	0.04	2.6	99.0
1982	1	11	23	18	56.28	33 39.98	119 3.00	10.22	0.0	191	18	B	0.02	2.0	3.8
1982	1	19	0	41	19.04	33 39.78	119 2.83	10.63	2.5	108	43	C	0.06	1.3	99.0
1982	1	25	10	43	39.82	33 37.55	119 0.63	10.63	1.9	242	12	C	0.07	3.6	99.0
1982	1	28	2	33	54.80	33 36.29	118 55.48	9.92	1.7	120	22	B	0.08	1.3	3.6
1982	1	29	10	51	31.00	33 38.11	118 59.39	10.63	2.1	238	11	E	0.02	99.0	99.0
1982	1	29	10	52	34.64	33 38.21	118 59.37	10.63	2.2	125	12	C	0.02	3.7	99.0
1982	1	29	22	26	45.23	33 40.26	118 59.84	10.63	2.3	235	8	D	0.06	18.6	99.0
1982	2	2	18	0	5.07	33 46.88	119 12.26	15.95	3.6	96	43	A	0.08	0.5	0.4
1982	2	3	18	9	34.59	33 40.22	119 3.02	10.63	0.0	136	28	C	0.03	2.0	99.0
1982	2	7	20	39	16.23	33 39.50	119 0.78	10.63	2.4	109	49	C	0.08	1.5	99.0
1982	2	18	7	26	57.35	33 26.99	118 53.83	10.54	1.9	265	11	E	0.01	99.0	99.0
1982	2	19	3	49	24.70	33 27.22	118 53.47	10.63	2.5	152	29	C	0.03	1.4	99.0
1982	2	19	11	3	29.75	33 38.96	119 1.55	10.63	1.4	241	11	E	0.06	99.0	99.0
1982	2	19	14	53	43.40	33 26.91	118 52.95	12.36	2.7	153	36	A	0.03	0.3	0.8
1982	2	19	15	2	49.57	33 24.75	118 57.08	10.59	2.1	159	15	E	0.07	99.0	99.0
1982	2	19	19	11	23.45	33 27.10	118 53.11	8.89	2.4	153	39	C	0.05	2.5	99.0
1982	2	19	19	51	49.23	33 27.24	118 53.28	11.16	2.3	152	22	B	0.03	0.9	2.8
1982	2	19	22	1	30.75	33 27.11	118 53.43	10.86	2.5	152	38	A	0.01	0.1	0.3
1982	2	20	1	58	40.61	33 27.29	118 52.76	10.64	1.7	151	11	E	0.03	99.0	99.0
1982	2	20	4	50	7.01	33 27.23	118 53.16	10.63	2.4	152	21	C	0.03	3.7	99.0
1982	2	20	5	28	7.06	33 27.19	118 53.32	10.63	1.8	152	11	E	0.02	99.0	99.0
1982	2	21	15	3	58.78	33 42.15	119 5.44	10.64	1.6	246	10	E	0.02	99.0	99.0
1982	2	21	15	56	14.27	33 26.81	118 53.01	12.30	3.2	153	55	A	0.05	0.4	1.0
1982	2	22	6	49	27.93	33 39.04	119 1.24	10.63	2.8	110	46	C	0.03	1.4	99.0
1982	2	23	12	28	51.27	33 27.29	118 53.06	10.63	2.9	151	39	C	0.03	4.0	99.0
1982	2	23	12	29	55.51	33 27.08	118 53.17	10.63	2.3	153	12	C	0.04	4.3	99.0
1982	2	23	18	54	0.68	33 27.02	118 52.97	10.63	2.9	153	29	C	0.03	4.0	99.0
1982	2	24	17	9	20.70	33 27.29	118 53.24	8.99	2.5	151	31	C	0.04	2.6	99.0
1982	2	24	17	14	16.79	33 27.25	118 53.13	10.63	2.9	151	23	C	0.02	4.0	99.0
1982	2	26	5	15	41.95	33 45.86	119 5.98	16.28		164	12	E	0.06	99.0	99.0
1982	2	26	6	9	18.52	33 26.89	118 54.37	10.62	2.2	267	16	D	0.03	7.5	99.0

TABLE II. Phase II Locations. Santa Barbara Island Earthquakes 1981-1982.

YEAR	MO	DA	HR	MN	SEC	LATITUDE	LONGITUDE	DEPTH	MAG	GAP	RMS	Q	MAG	ERH	ERZ
1982	2	26	11	21	30.41	33 25.37	118 56.47	10.63	2.1	188	23	C	0.04	3.8	99.0
1982	2	26	13	30	16.20	33 28.31	118 54.87	10.63	3.6	204	58	C	0.07	1.4	99.0
1982	3	4	17	37	50.16	33 42.43	119 4.22	10.68		186	10	E	0.07	99.0	99.0
1982	3	5	22	19	47.39	33 40.36	119 2.48	10.16	2.8	81	45	B	0.07	0.5	2.9
1982	3	7	9	2	20.20	33 25.47	118 56.51	10.68	1.7	216	11	E	0.05	99.0	99.0
1982	3	7	9	57	23.53	33 25.29	118 56.04	10.85	2.2	215	12	E	0.03	99.0	99.0
1982	3	8	4	14	16.81	33 27.29	118 53.16	10.74	2.4	151	41	A	0.00	0.5	1.6
1982	3	9	7	48	23.47	33 37.15	118 57.36	8.34	1.8	144	18	D	0.11	13.3	99.0
1982	3	9	14	55	53.14	33 27.99	118 53.36	3.49	1.7	149	11	D	0.52	8.5	99.0
1982	3	10	10	45	9.78	33 26.82	118 54.61	7.84	1.7	196	12	D	0.22	8.9	14.8
1982	3	12	12	45	33.64	33 26.97	118 52.88	12.36	3.8	153	84	A	0.06	0.4	0.6
1982	3	12	13	8	26.83	33 24.44	118 56.00	10.78	1.8	221	9	E	0.02	99.0	99.0
1982	3	12	13	14	49.91	33 23.97	118 56.36	9.44	1.2	229	8	E	0.14	99.0	99.0
1982	3	12	23	37	33.92	33 38.68	118 59.48	10.63		178	6	E	0.02	99.0	99.0
1982	3	13	18	54	48.87	33 24.71	118 55.92	9.86	2.1	219	21	D	0.11	47.8	99.0
1982	3	13	19	4	11.52	33 28.98	118 54.72	10.65	2.4	186	28	D	0.27	7.0	14.0
1982	3	13	23	8	53.64	33 28.64	118 54.82	6.98	1.6	206	28	D	0.13	11.7	99.0
1982	3	14	18	35	39.61	33 24.73	118 55.67	10.38	1.8	218	11	E	0.04	99.0	99.0
1982	3	19	20	24	9.31	33 44.27	119 4.61	10.61	1.7	179	13	E	0.03	99.0	99.0
1982	3	20	4	44	38.77	33 43.18	119 4.48	10.63	2.3	166	28	C	0.06	1.7	99.0
1982	4	2	7	21	29.57	33 25.98	118 54.67	10.85	1.9	187	14	C	0.23	3.7	7.7
1982	4	4	17	38	58.14	33 33.67	118 55.71	10.88		122	13	D	0.07	26.8	99.0
1982	4	5	17	28	56.25	33 33.44	118 55.32	10.87	2.2	136	12	D	0.03	25.3	99.0
1982	4	6	22	51	0.46	33 33.69	118 55.68	10.89	2.6	122	22	E	0.04	99.0	99.0
1982	4	6	22	52	22.83	33 33.46	118 55.57	10.62		134	7	E	0.04	99.0	99.0
1982	4	8	0	52	24.48	33 33.61	118 55.57	10.62	2.3	124	23	D	0.06	26.7	99.0
1982	4	8	0	52	55.86	33 33.97	118 55.28	10.63		137	6	E	0.07	99.0	99.0
1982	4	8	0	53	44.88	33 33.36	118 53.28	10.65		208	8	E	0.08	99.0	99.0
1982	4	8	1	14	55.98	33 34.38	118 54.89	10.83	4.0	126	92	A	0.04	0.2	0.6
1982	4	8	1	35	8.76	33 33.68	118 55.72	10.71		137	9	E	0.04	99.0	99.0
1982	4	8	2	12	33.39	33 34.11	118 55.93	6.84	2.8	117	33	D	0.09	6.1	99.0
1982	4	8	2	36	7.64	33 33.69	118 55.76	10.64		138	6	E	0.04	99.0	99.0
1982	4	8	2	41	36.39	33 33.86	118 55.26	8.39	2.7	117	34	D	0.05	18.0	99.0
1982	4	8	20	12	24.82	33 33.43	118 55.42	10.41	2.1	120	20	D	0.06	26.4	99.0
1982	4	8	20	49	17.61	33 33.41	118 55.31	10.63	1.7	134	10	D	0.03	26.2	99.0
1982	4	6	21	53	24.78	33 33.30	118 55.33	10.88	2.1	134	10	D	0.05	28.1	99.0
1982	4	8	2	46	42.28	33 33.67	118 55.43	10.87	2.3	123	19	D	0.04	28.6	99.0
1982	4	8	3	46	27.97	33 33.84	118 55.26	10.65	2.8	129	53	D	0.05	24.0	99.0
1982	4	8	5	43	46.89	33 33.80	118 55.28	6.82	1.9	123	19	E	0.02	99.0	99.0
1982	4	8	6	39	41.37	33 33.71	118 55.77	10.64		138	9	D	0.04	28.7	99.0
1982	4	8	11	13	37.18	33 34.68	118 55.38	7.97	3.4	118	86	A	0.04	0.3	0.8
1982	4	8	12	14	18.65	33 34.67	118 55.36	7.88	2.6	122	20	D	0.04	42.0	99.0
1982	4	8	13	10	13.87	33 33.96	118 55.21	8.03	2.9	117	48	A	0.04	0.3	1.0
1982	4	8	13	13	39.84	33 33.63	118 55.88	10.61	2.8	121	27	D	0.05	27.2	99.0
1982	4	8	13	58	4.54	33 33.88	118 55.53	10.61	1.8	138	7	E	0.02	99.0	99.0
1982	4	8	14	23	47.18	33 33.44	118 55.53	10.62	1.8	136	6	E	0.02	99.0	99.0
1982	4	6	18	28	11.76	33 33.36	118 55.89	10.71		287	9	E	0.06	99.0	99.0
1982	4	6	17	39	51.16	33 34.23	118 55.09	8.83		143	12	D	0.11	20.7	99.0
1982	4	9	20	28	13.16	33 33.69	118 55.27	7.93		123	8	E	0.03	99.0	99.0
1982	4	9	22	2	48.63	33 24.85	118 56.77	10.35	2.0	218	7	E	0.06	99.0	99.0
1982	4	11	4	37	3.26	33 26.84	118 53.16	10.63	2.9	153	33	D	0.05	4.8	99.0
1982	4	10	7	16	41.28	33 38.37	118 59.68	8.64	1.4	143	10	E	0.01	99.0	99.0
1982	4	14	11	55	26.30	33 38.34	119 0.56	10.63		241	12	C	0.04	3.7	99.0
1982	4	15	17	13	17.41	33 33.74	118 56.22	10.63	2.4	240	7	D	0.07	14.5	99.0
1982	4	15	18	49	51.94	33 33.84	118 56.18	10.89		254	7	E	0.04	99.0	99.0
1982	4	19	21	54	42.68	33 34.39	118 54.71	10.31	2.8	126	22	B	0.06	5.8	99.0
1982	4	20	5	24	25.25	33 34.70	118 54.36	8.39	2.8	128	28	B	0.08	1.7	3.0
1982	4	19	9	55	48.73	33 34.27	118 55.15	10.64	2.8	126	22	C	0.05	4.2	99.0
1982	4	21	16	54	5.84	33 44.31	119 2.76	13.38	0.8	187	18	E	0.12	99.0	99.0
1982	4	23	1	45	53.78	33 26.12	118 53.58	10.62	2.3	156	16	B	0.02	0.6	99.0
1982	4	24	16	24	48.35	33 26.61	118 53.38	10.63		184	11	D	0.14	10.2	99.0
1982	4	28	2	59	48.85	33 39.88	119 1.43	10.63		194	8	E	0.03	99.0	99.0
1982	4	28	15	4	52.82	33 25.73	118 54.73	10.54	2.3	208	15	C	0.16	4.5	9.0
1982	4	29	15	33	45.48	33 34.18	118 54.52	9.63	3.9	126	74	A	0.04	0.3	0.9
1982	4	29	16	0	48.82	33 33.49	118 56.18	9.80	1.8	133	10	D	0.05	24.1	99.0
1982	4	29	16	1	39.18	33 33.84	119 1.32	10.62		198	6	E	0.02	99.0	99.0
1982	4	29	16	2	37.93	33 34.14	118 54.63	6.98	1.6	117	18	C	0.28	2.1	14.4
1982	4	29	17	37	31.17	33 33.49	118 55.88	6.61	2.6	117	29	D	0.11	8.8	99.0
1982	4	29	19	8	42.28	33 33.88	118 56.73	10.64	1.8	139	10	D	0.04	27.3	99.0
1982	4	29	23	14	34.62	33 33.84	118 55.76	10.56	2.1	139	11	D	0.04	28.4	99.0
1982	4	30	0	24	36.48	33 33.92	118 55.10	7.78	2.4	120	23	D	0.05	18.3	99.0
1982	5	1	18	29	18.83	33 33.94	118 56.08	10.58	2.3	118	29	C	0.19	2.7	9.1
1982	5	1	17	59	21.48	33 34.01	118 54.51	10.63	2.7	126	32	C	0.08	4.7	99.0
1982	5	1	18	5	25.14	33 34.79	118 57.99	10.49		168	10	E	0.12	99.0	99.0
1982	5	1	20	1	38.02	33 34.48	118 55.13	6.20	2.9	114	35	C	0.08	3.9	99.0
1982	5	1	9	53	2.93	33 34.19	118 56.04	6.79	2.3	118	21	B	0.05	8.9	99.0
1982	5	1	11	32	27.32	33 33.67	118 56.52	10.73		137	7	E	0.04	99.0	99.0
1982	5	2	3	3	8.67	33 34.36	118 55.48	10.58	1.8	128	9	C	0.15	4.1	13.0
1982	5	5	7	34	28.98	33 42.93	119 4.36	10.67	1.8	200	10	B	0.02	21.2	99.0
1982	5	5	18	2	21.98	33 24.12	118 55.62	7.74	1.9	127	11	D	0.06	16.9	99.0
1982	5	9	0	54	31.79	33 34.38	118 55.89	10.62	2.1	128	18	B	0.07	28.0	99.0
1982	5	9	1	1	34.22	33 34.26	118 55.40	7.77	2.3	124	37	B	0.04	15.4	99.0
1982	5	9	3	54	34.43	33 34.42	118 53.26	6.84	2.3	124	33	B	0.05	8.2	99.0
1982	5	9	10	38	3.28	33 34.10	118 55.72	10.63	2.3	129	13	D	0.03	26.0	99.0
1982	5	9	18	2	34.06	33 33.99	118 56.75	10.64		140	7	E	0.03	99.0	99.0
1982	5	9	19	8	9.98	33 39.68	119 1.97	7.44	2.3	136	18	C	0.04	4.4	99.0
1982	5	10	7	46	58.79	33 38.34	119 0.71	9.58	2.2	176	18	C	0.04	19.7	99.0
1982	5	13	17	54	33.83	33 33.83	118 58.73	10.63		139	6	E	0.08	99.0	99.0
1982	5	14	21	41	39.76	33 39.84	119 2.44	10.15	2.5	81	28	A	0.01	0.1	0.4
1982	5	20	4	21	9.62	33 38.82	119 0.57	9.77	2.1	128	18	B	0.04	0.4	2.1
1982	5	25	17	29	4.62	33 37.79	118 58.48	8.08	2.8	122	11	B	0.07	8.1	99.0
1982	5	27	8	53	52.96	33 24.29	118 56.04	10.59		224	7	E	0.06	99.0	99.0
1982	5	22	11	52	21.98	33 42.73	119 4.98	10.62	2.2	181	13	B	0.03	13.6	99.0
1982	5	23	7	38	48.63	33 43.29	119 5.38	10.62	2.6	162	13	C	0.08	2.2	99.0
1982	6	1	5	15	48.51	33 40.43	118 59.88	10.63	1.9	154	12	B	0.03	14.7	99.0
1982	6	1	14	24	38.43	33 39.82	119 2.72	10.62	2.2	154	12	B	0.05	16.7	99.0
1982	6	3	15	9	34.28	33 38.65	118 59.62	10.57		159	15	B	0.06	26.9	99.0
1982	6	8	16	58	7.27	33 38.69	119 0.52	9.17	1.9	128	12	B	0.04	18.7	99.0
1982	6	7	3	25	21.52	33 42.38	119 1.72	8.24	2.1	138	14	B	0.03	5.6	99.0
1982	6	9	7	9	26.52	33 40.47	119 1.03	10.88		131	9	C	0.12	2.6	12.1
1982	6	12	6	38	47.79	33 41.74	119 4.57	11.52		163	16	C	0.10	1.7	5.5
1982	6	14	3	25	41.52	33 39.85	119 0.13	10.62	1.7	166	9	D	0.04	19.5	99.0
1982	6	18	15	24	2.83	33 38.47	119 0.41	10.63	2.2	77	23	C	0.03	2.5	99.0
1982	6	22	18	49	44.83	33 26.34	118 53.29	9.28	1.6	186	8	C	0.03	4.8	99.0
1982	7	8	18	49	0.68	33 35.66	118 55.09	10.63		129	9	D	0.06	8.6	99.0
1982	7	10	11	11	3.85	33 39.98	119 0.06	10.63	1.9	127	17	D	0.04	15.1	99.0
1982	7	22	8	22	19.98	33 40.71	119 0.78	13.97		142	13	B	0.03	9.1	99.0
1982	7	28	9	21	54.68	33 39.93	118 59.98	10.62	1.8	148	22	B	0.11	19.5	99.0
1982	7	27	8	32	43.94	33 41.76	119 0.83	10.86	2.4	101	99	A	0.03	0.2	0.4
1982	8	23	18	54	34.18	33 40.49	119 1.38	10.62	0.8	194	18	B	0.02	18.9	99.0

YEAR	MO	DA	HR	MN	SEC	LATITUDE	LONGITUDE	DEPTH	MAG	GAP	RMS	Q	MAG	ERH	ERZ
1982	8	24	18	59	31.88	33 39.82	119 1.68	10.46		196	9	E	0.07	99.0	99.0
1982	8	25	10	20	13.48	33 39.61	119 1.89	10.63		197	8	E	0.02	99.0	99.0
1982	8	30	10	16	38.61	33 39.27	119 0.37	10.63	2.8	168	28	B	0.02	19.1	99.0
1982	9	10	17	47	5.35	33 38.39	119 0.49	10.36	2.1	168	83	A	0.02	0.2	0.4
1982	9	16	9	29	0.36	33 38.31	119 0.76	11.83	2.8	170	38	A	0.03	0.3	0.6
1982	9	16	9	37	51.87	33 38.34	119 0.68	10.63		170	8	B	0.02	28.8	99.0
1982	9	16	18	36	16.74	33 43.72	119 6.95	10.78		214	7	E	0.01	99.0	99.0
1982	9	18	0	49	29.97	33 39.27	119 0.88	10.63		172	10	B	0.03	23.4	99.0
1982	9	19	8	42	21.31	33 37.69	119 16.62	9.47		212	11	B	0.07	28.0	99.0
1982	9	22	22	32	45.70	33 38.46	118 59.28	10.63		168	12	B	0.01	21.6	99.0
1982	10	20	8	37	42.68	33 45.78	119 7.42	10.69	0.0	264	9	E	0.08	99.0	99.0
1982	10	4	4	11	24.45	33 38.94	118 59.89	10.63	1.8	163	14	E	0.04	99.0	99.0
1982	11	17	18	14	41.73	33 40.39	119 2.47	10.89		124	14	E	0.08	99.0	99.0
1982	12	2	10	30	55.61	33 38.91	119 1.08	10.63	2.9	321	8	E	0.47	99.0	99.0
1982	10	16	15	58	32.00	33 39.84	119 2.73	12.46	2.5	128	22	A	0.02	0.3	0.4
1982	10	28	20	6	52.44	33 45.18	119 6.91	10.88		202	6	E	0.02	99.0	99.0
1982	10	26	23	17	17.88	33 37.88	118 59.21	10.63		178	7	E	0.04	99.0	99.0
1982	11	1	0	20	44.64	33 38.68	119 1.67	9.87		172	10	E	0.04	99.0	99.0
1982	11	28	13	40	39.00	33 44.23	119 9.38	10.44	1.9	232	11	E	0.08	99.0	99.0
1982	11	29	2	56	17.03	33 38.09	119 1.47	10.63	2.0	178	18	B	0.02	22.1	99.0